Bitter taste receptors in the domestic dog (*Canis familiaris*)

Matthew Gibbs, BSc.

Thesis submitted to the University of Nottingham for the degree of Doctor of Philosophy

January 2021

Abstract

The sense of taste, or gustation, combines with olfactory and somatosensory cues to give the overall perception of flavour once a food is accepted into the mouth. The perception of bitter taste is thought to be primarily associated with rejection of a food, and protects animals from ingesting potentially toxic substances. Bitter taste is mediated through a group of G protein-coupled receptors known as the Taste type 2 receptors (Tas2rs) that are expressed in taste papillae on the tongue, and other surfaces in the oral cavity.

Bitter taste in the domestic dog is of interest for a number of reasons. Firstly, pet dogs are often fed a commercially prepared pet food. Any bitter taste from the raw materials used in the manufacture, or formed during the processing of the product has the potential to negatively impact on palatability. Secondly, bitter-tasting chemicals are sometimes used to deter pets from consuming substances that are harmful to them, such as automotive antifreeze and rodent poison.

In humans, bitter taste perception varies between individuals. Some of this variation is known to be related to gene sequence variation in some of the *TAS2Rs*. Whether this type of functional variation exists in dogs is not known. Dogs have been selectively bred, and now are one of the most phenotypically diverse of all species. If functional variation does exist in dog *Tas2rs* it may be associated with dog breed.

In order to understand the responses of dog Tas2rs and the impact of their variation, this project deorphanised dog bitter receptors, and characterised their receptive ranges. Equivalent human receptors were also tested so that, where possible, data for orthologous receptors from dog and human could be compared. A heterologous cell model was used, incorporating a novel $G_{\alpha16/gust/o}$ chimera. The performance of this model was compared to that of the frequently used $G_{\alpha16/gust44}$ chimera. Receptor sensitivity and breadth of tuning varied, showing both similarities and differences between orthologous dog and human receptors when tested with a library of 48 bitter compounds.

Gene expression data from dog fungiform taste papillae were also generated and used to confirm the expression of putative bitter receptors in the dog. Papillae were selected from different areas of the anterior portion of the tongue. RNA-seq analysis showed that Tas2r expression varied depending on location, with papillae from the front of the tongue showing significantly less Tas2r expression. Generally expression levels were very low, and not all dog Tas2rs could be confirmed as expressed from these samples.

Variation in sequence and functionality of dog bitter receptors between different dogs and different dog breeds was assessed, with dTas2r1 being studied as an example. A database of dog genomes was used to assess the levels of variation between dogs. Gene variants found in dTas2r1 were tested for functional impacts on receptor function and expression in the heterologous cell model. Only subtle effects on receptor function were seen. However, several rare variants caused a loss of cell-surface expression, presumably due to retention of the receptor intracellularly.

In summary, this study showed that species differences in the sensitivity and tuning of dog Tas2rs were found, when compared with their human orthologues. Ligands were identified for 7 of the 16 putative dog Tas2rs and this information was used to study the impacts of naturally occurring sequence variants in dog Tas2r1. Further work on variants occurring in other dog Tas2rs will confirm if any high impact variants might influence dog bitter taste perception, as is the case for humans.

Acknowledgements

I would like to thank my principal academic supervisor Dr Nicholas Holliday, for all his support and encouragement during the course of my studies. His positivity and understanding of my other work and family commitments were essential to me completing this thesis. I would also like to thank my second academic supervisor Dr Stephen Briddon for his support and guidance over the last four years.

My industrial supervisor and line manager Dr Scott McGrane has supported me over the entire length of this project, and for many years prior to that in my career at Mars, Inc. I would like to thank him for believing in me, and in my ability to complete this thesis, and for giving me the time I needed to balance this project with other work commitments. I would also like to thank Dr Darren Logan for his enthusiasm in getting this project up and running, and for his continued support throughout the course of my studies.

General thanks also go to lots of people at the Waltham Petcare Science Institute for their help and support. In particular I'd like to thank Ciaran O'Flynn for his support as I learnt about Linux shell scripting.

Thanks also to Dr Marcel Winnig and Dr Timo Vennegeerts of IMAX Discovery, who helped me with the high throughput screening I conducted at their laboratory in Milan. I would also like to thank Dr Jay Slack of Givaudan, for permission to use the $G_{\alpha16/gust44}$ cell line during this project.

Finally I would like to thank Mars, Inc. for supporting and funding this project. I have worked at Mars for the vast majority of my adult life, and during that time I have always received outstanding support to pursue my personal growth as a scientist. This support has helped me to achieve more than I previously though possible, and I appreciate it greatly.

Abbreviations

Amy2b	α-amylase 2B
Arsf	Arylsulfatase F
ATP	Adenosine triphosphate
BGH	Bovine growth hormone
cAMP	Cyclic adenosine monophosphate
cGMP	Cyclic guanosine monophosphate
CALHM1	Calcium homeostasis modulator 1
CCK	Cholecystokinin
CMV	Cytomegalovirus
DAG	Diacylglycerol
DMEM	Dulbecco's modified Eagle's medium
DNA	Deoxyribonucleic acid
D-PBS	Dulbecco's phosphate-buffered saline
DBVDC	Dog biomedical variant database consortium
EDTA	Ethylenediaminetetraacetic acid
ER	Endoplasmic reticulum
FBS	Foetal bovine serum
GDP	Guanosine diphosphate
GFP	Green fluorescent protein
GLAST	Glutamate aspartate transporter
GLP1	Glucagon-like peptide 1
GPCR	G protein-coupled receptor
GTP	Guanosine triphosphate
HEK	Human embryonic kidney
HEPES	4-(2-hydroxyethyl)-1-piperazineethanesulfonic acid
HPA axis	Hypothalamic–pituitary–adrenal axis
IP_3	Inositol 1,4,5-trisphosphate
IP_3R3	Inositol 1,4,5-trisphosphate receptor type 3
LB	Luria Bertani or lysogeny broth

LD	Linkage disequilibrium
LHR	Luteinising hormone receptor
Mgam	Maltase-glucoamylase
NGS	Next generation sequencing
ORF	Open reading frame
Otx1	Orthodenticle homeobox 1
PDE	Phosphodiesterase
PIP_2	Phosphatidylinositol 4,5-bisphosphate
PKA	Protein kinase A
PLCβ2	Phospholipase C β2
PROP	6-n-Propylthiouracil
PTC	Phenylthiocarbamide
qRT-PCR	Quantitative reverse transcription polymerase chain reaction
REEP	Receptor expression enhancing protein
RNA	Ribonucleic acid
RNA-seq	RNA-sequencing
ROMK channel	Renal outer medullary potassium channel
RTP1, RTP2, RTP1S	Receptor transporting protein 1, 2 and 1short
Ric8b	Resistance to inhibitors of cholinesterase 8 homolog B
SDS	Sodium dodecyl sulphate
SGLT	Sodium-glucose cotransporter
Sglt1	Sodium-glucose cotransporter 1
Smox	Spermine oxidase
SNP	Single-nucleotide polymorphism
Stxbp6	Syntaxin binding protein 6
TAS1R, Tas1r	Taste type 1 receptor
TAS2R, Tas2r	Taste type 2 receptor
Tm	Melting temperature
TM	Trans-membrane domain

TMM	Trimmed mean of M values
TRC	Taste receptor cell
TRPM5	Transient receptor potential cation channel subfamily M member 5
VGNC	Voltage gated sodium channels
WT	Wild type

Gene and Protein Naming Conventions

Throughout this thesis the following conventions for gene and protein naming are applied.

Gene names are *italicised* while protein names are not.

For humans all letters in the gene name are uppercase e.g. *TAS2R1*.

For other mammals the first letter of the gene name is in uppercase while remaining letters are in lower case e.g. *Tas2r119*.

In some cases, for clarity, a letter indicating the species for the gene or protein is added before the gene or protein name, e.g. d*Tas2r1* or dTas2r1 for a dog gene and protein.

Table of contents

Table of figures

Table of tables

Chapter 1. Introduction

1.1. Why study taste in dogs?

Dogs (*Canis familiaris*) are the most commonly-owned pet across many countries of the world (GfK, 2016). They were the first species ever to be domesticated by man (Thalmann *et al.*, 2013a) , and since that time have lived alongside humans (*Homo sapiens*). Due to the unique position dogs occupy within human society, it is perhaps not surprising that owners of dogs are often interested in how their pets perceive the world. How dogs see, smell, taste, touch and hear has shaped their relationship with humans, and given rise to numerous opinions about the senses of the dog.

Dogs belong to the family *Canidae*, which among others includes wolves (*Canis lupus*), coyotes (*Canis latrans*), jackals (*Canis adustus*, *Canis mesomelas* and *Canis aureus*) and foxes (all members of the *Vulpini* genus are referred to as "true foxes", but several other genera are included). After many years of discussion, it is now widely accepted that dogs are descended from wolves, although the exact location and timing of this event(s) is still under debate (Frantz *et al.*, 2016; Botigue *et al.*, 2017). Estimates of the timing of dog domestication vary, but fall between 20,000 and 40,000 years ago. This initial domestication event produced the first of two bottlenecks in dog evolution. The second occurred during the 1800s with the establishment of breed clubs, and an increased focus on selective breeding (Lindblad-Toh *et al.*, 2005). In the first of these two events, it appears that genetic variation actually increased in the dog genome as a result of a reduction in selective pressure associated with living alongside humans (Bjornerfeldt *et al.*, 2006). This is hypothesised to be the mechanism by which so much variation was introduced into the dog genome. During the second period of increased selective breeding in the 1800s, variation became segregated in the different dog breeds, and variation within breeds was drastically reduced (Ostrander *et al.*, 2005).

As dogs became domesticated, a number of changes occurred that separated them from their wolf ancestors. Their initial selection is thought to have been based on

tameness. Studies on the silver fox (a melanistic form of the red fox *Vulpes vulpes*) showed that selection for tameness also brought about polymorphic changes similar to some traits seen in the domestic dog (Trut *et al.*, 2009). Changes in coat colour (mostly loss of pigmentation resulting in white patches), along with the development of floppy ears and curved tails were all noted in the foxes. There is also genomic evidence that dogs adapted to a diet containing more carbohydrate (Axelsson *et al.*, 2013). This study identified changes in dogs relative to wolves in three genes related to the ability to digest and metabolise starch, namely α-amylase 2B (*Amy2b)*, maltase-glucoamylase (*Mgam*) and sodium-glucose transporter 1 (*Sglt1*).

However, there is no published research on how the dogs' sense of taste compares to that of the wolf. In the case of taste, general opinions among dog owners vary widely, and are sometimes related to the breed of dog in question. Some breeds might be perceived as greedy and indiscriminate in their sense of taste, while others might be thought of as fussy or discerning. Somewhat surprisingly, peer-reviewed research on the dog's sensitivity to tastes is rare.

Some of these observations have been found to have some scientific basis, while others remain unsubstantiated. Work on the Labrador Retriever breed revealed a 14bp deletion in the pre-opiomelanocortin (*Pomc*) gene (Raffan *et al.*, 2016). This was associated with increased body weight, adiposity, food motivation and was also found to be more common in dogs selected to become assistance dogs, presumably because of their performance in food reward-based training. The mutation was only found in Labradors, and the closely related Flat-Coat Retriever.

Although functional genetic variation in taste-related genes has not been previously described in dogs, it is well-known that such variation exists in humans, particularly in the bitter receptors (Bufe *et al.*, 2005; Soranzo *et al.*, 2005; Pronin *et al.*, 2007). It is intriguing to speculate that such variation may also exist in dogs, and that by way of selective breeding, may have become heterologous between dog breeds.

Scientific evaluation of these points would be of value to the pet food industry. The manufacture and sale of commercial pet food generated $22.62bn in retail sales for the US and $73.3bn worldwide in 2014 (PetFoodIndustry, accessed 2017). Product performance and palatability are key parameters for large companies producing pet food. A better understanding of the impact of bitter-tasting raw materials might help manufacturers avoid palatability problems or allow greater flexibility in the selection of ingredients, particularly where plant-based materials are concerned.

This information will also be of great interest to dog owners, particularly where bitter taste plays a role in animal safety. Accidental poisoning of pet dogs is not uncommon. Some products have become well-known for their involvement in cases of poisoning in pets. In particular automotive antifreeze, which may contain the toxin ethylene glycol, has been associated with pet poisonings. In one study (Rowland, 1987), the incidence of ethylene glycol poisoning in dogs and cats at Colorado State University Teaching Hospital between 1979 and 1986 was investigated. Of 104 cases, 56 were attributed to rodenticides and 30 to ethylene glycol, with ethylene glycol having the highest case-fatality rate of 43.3%, compared to 11.3% for rodenticides. Another study of phone calls made to the Kansas State Veterinary Diagnostic Laboratory found that 1,616 calls were made regarding exposure of cats and dogs to substances perceived as harmful by their caregivers during the three year period of 2009-2012 (Mahdi *et al.*, 2013). Of these 84.7% involved dogs, while 15.3% related to cats. The majority of calls were related to ingestion of drugs, but household chemicals, foods, pesticides and plants were also common. In the case of antifreeze, a sweet taste is sometimes attributed to it, and cited as the reason for its involvement in cases of dog poisoning. However, this has been shown not to be the case (Doty *et al.*, 2006), with ethylene glycol and antifreeze solutions having lower preference than water or a 20% sucrose solution (Marshall *et al.*, 1990).

Hazardous products, such as automotive antifreeze and rodenticides, are sometimes laced with the bitter-tasting (to humans) chemical denatonium benzoate (tradename Bitrex®). It is believed to deter unwanted, and potentially fatal ingestion by children

or pets (Berning *et al.*, 1982; Hansen *et al.*, 1993; Jackson *et al.*, 1995), although its efficacy for deterring ingestion by humans generally has been questioned (Jobson *et al.*, 2015). Understanding dogs' perception of denatonium benzoate, and other bitter chemicals, might help to confirm the appropriate level of inclusion for preventing ingestion, or identify chemicals that are more effective deterrents for dogs. *In vitro* testing of bitter receptors in cell-based models could help with predictions of what might taste most bitter to dogs, before moving to more expensive *in vivo* studies.

Dogs also engage in behaviours that would appear to show a disregard for the taste properties of objects, such as pica (ingestion of a non-food item) (Pirrone *et al.*, 2015) and coprophagia (ingestion of faeces) (Soave *et al.*, 1991). Coprophagia is known to play a vital role in nutrition for some species such as rabbits, but this has not been shown to be the case for the dog. Very little reliable information is available on what drives these phenomena. While behavioural traits and other senses, particularly olfaction, are likely to play a significant role in these incidences of seemingly inappropriate ingestion, it may be the case that bitter perception (or lack thereof) also plays a role, or is a useful deterrent.

1.2. Taste perception and taste receptors

The sensation of taste, or gustation, is sometimes assumed to be the complete range of sensory experiences when food is accepted into the mouth. However, gustation is only the component that is experienced through the action of specialised cells and anatomical structures that comprise the gustatory system. Other contributors such as smell, irritation (heat) and texture are experienced through other sensory systems such as the olfactory, chemesthetic and somatosensory systems.

Five taste modalities are widely accepted, namely sweet, bitter, salty, sour and umami (the savoury taste of meat). Other taste modalities may exist, such as starch taste (Sclafani, 2004), or the taste of fatty acids (Mattes, 2009), but in these cases some of the requirements for acceptance as a true taste modality are still to be met. In the case of the accepted taste modalities, receptors specific for each one have

been identified in the oral cavity. Sweet taste is mediated by the heterodimeric G protein-coupled receptors (GPCRs) Tas1r2 and Tas1r3 (Nelson *et al.*, 2001; Li *et al.*, 2002). Umami taste is also mediated by a heterodimeric GPCR and again Tas1r3 is involved, this time in combination with Tas1r1 (Li *et al.*, 2002; Nelson *et al.*, 2002). In both cases these are thought to be the primary mechanisms for sweet and umami taste perception, but they may not be the only ones. Alternative receptors for sweet taste perception have been proposed (Damak *et al.*, 2003), and it is now established that sodium-glucose cotransporters (SGLTs) are involved (Yasumatsu *et al.*, 2020). Sour taste was previously associated with members of the hyperpolarization activated cyclic nucleotide gated potassium channels (HCNs) (Stevens *et al.*, 2001) and the polycystic kidney disease (Pkd) gene family (Huang *et al.*, 2006; Ishimaru *et al.*, 2006), although more recent research attributes sour taste primarily to the proton-selective ion channel Otop1 (Teng *et al.*, 2019). The taste of salt is perhaps the least well understood of these 5 taste modalities, stimulating attraction in animals at low concentrations, but aversion at high concentrations. The attractive response has been shown to be mediated by the epithelial sodium channel ENaC (Stähler *et al.*, 2008; Yoshida *et al.*, 2009; Chandrashekar *et al.*, 2010), while the mechanism for aversion to high salt concentrations involves recruitment of the bitter and sour taste pathways (Oka *et al.*, 2013). Bitter taste is mediated through a family of GPCRs known as the Taste Type 2 Receptors or *Tas2rs*. First discovered in 2000 (Adler *et al.*, 2000; Chandrashekar *et al.*, 2000; Matsunami *et al.*, 2000), the *Tas2rs* are a family of receptors which often differ in number between species (see section 1.5).

1.3. Taste perception in the dog

Taste responses in dogs have been assessed by behavioural methods, and also with electrophysiological methods (Beidler *et al.*, 1955). Both bitter and sweet taste responses in dogs were confirmed in a two-pan choice test versus plain water (Grace *et al.*, 1969). In this study, dogs rejected the bitter alkaloid quinine, but preferred sucrose. Interestingly, dogs also rejected the artificial sweetener saccharin, which can give a bitter off-taste in humans (Kuhn *et al.*, 2004). Recording the activity of the

chorda tympani and the lingual branch of the glossopharyngeal nerve *in vivo* revealed that dogs responded to four classes of basic taste stimuli, namely sour, sweet, bitter and salty (Kitchell, 1963). Later work also confirmed specific responses in the chorda tympani to umami taste stimuli (Kumazawa *et al.*, 1991).
There is very little published information which details taste detection thresholds in dogs. In the case of bitter taste, dogs were shown to reject 0.01% (0.3mM) quinine (Grace *et al.*, 1969), but did not reject sucrose octaacetate, which is bitter-tasting to humans (Kare, 1971). Some electrophysiological studies have also shown responses to quinine at 20mM (Kitchell, 1963). However, these were not tested as minimum thresholds and merely represent a good starting point for further studies on comparative taste thresholds. In the case of denatonium benzoate, there is no published threshold data for dogs, but it has been shown that rodents (Davis *et al.*, 1988; Kaukeinen *et al.*, 1992) and pigs (Nelson *et al.*, 1997) do not perceive denatonium at as low a threshold as it is perceived by humans, a fact exploited in its use in rodenticides where the concentrations used are thought to be less aversive to rodents than to humans (Kaukeinen *et al.*, 1992).

1.4. GPCRs involved in taste and smell

GPCRs are involved with many biological processes such as vision, cardiac function and neurotransmission (Wolfe *et al.*, 2007). The GPCRs that mediate taste and smell form a varied group of receptors with some unique features. Three of the five basic tastes are mediated by GPCRs, namely sweet, umami and bitter. Bitter taste is mediated by a group of GPCRs (25 in humans), which show variation in the number of receptors present between species. Olfaction is also mediated by a family of GPCRs which can vary greatly in their number between different species (Niimura *et al.*, 2014). Humans have between 350-400 functional olfactory receptors (ORs) while dogs have around 800 and the African elephant almost 2000.

There are five major families of GPCRs found in mammals, class A (rhodopsin), class B (secretin and adhesion), class C (glutamate) and class F (frizzeled/taste2) (Fredriksson *et al.*, 2003; Davies *et al.*, 2008; Stevens *et al.*, 2013). All classes of GPCR

share a common structure within their transmembrane domains (TMs). The seven transmembrane helices are arranged in an anticlockwise formation, some of which are tilted in relation to the cell membrane (Unger *et al.*, 1995). The existence of three intracellular and three extracellular loops is also a conserved feature of all GPCRs. The largest family, the class A receptors, often have an eighth helix running parallel to the cell membrane at the cytoplasmic C-terminal region (Katragadda *et al.*, 2004; Rasmussen *et al.*, 2007). Other structural features of class A receptor TM regions include kinks in the transmembrane helices, particularly for TM7, and conserved sequences involved in receptor activation which are discussed in more detail in section 1.6.

In the class A receptors, which include all of the olfactory receptors, small molecule ligands normally interact with the pocket formed by the transmembrane helices, while larger peptide or protein ligands engage with the extra-cellular loops or N terminus in addition. In the case of class B receptors, the N-terminal domain is typically the site of ligand binding. Class C receptors, which include the *Tas1R* family responsible for the majority of sweet and umami taste perception, form dimers. They have large N-terminal domains, sometimes referred to as a "Venus flytrap". This contains the orthosteric binding site, although allosteric sites exist in the transmembrane region (Jiang *et al.*, 2005; Winnig *et al.*, 2007), and possibly the cysteine rich domain which links the transmembrane and N-terminal domains (Jiang *et al.*, 2004). Such features are shared with other class C GPCRs, such as the metabotropic glutamate receptors (Rondard *et al.*, 2015), where taste specific versions of the receptors have been implicated in umami taste perception (Chaudhari *et al.*, 2000; San Gabriel *et al.*, 2005; Yasumatsu *et al.*, 2015), and the calcium sensing receptor CaSR (Geng *et al.*, 2016), which has been implicated in the taste sensation known as kokumi (Ohsu *et al.*, 2010; Maruyama *et al.*, 2012).

The GPCRs are described as such due to their interaction with heterotrimeric G proteins, which consist of α, β and γ subunits. There are four families of G_{α} subunits, $G_{\alpha s}$, $G_{\alpha i/o}$, $G_{\alpha q}$ and $G_{\alpha 12}$ (Premont *et al.*, 2007). The $G_{\alpha s}$ family, which consists of $G_{\alpha s}$ and $G_{\alpha olf}$ derives its name from the ability to stimulate adenylyl cyclase, which causes

a rise in cyclic adenosine monophosphate (cAMP) and activation of protein kinase A (PKA). G_{olf}, was originally identified in olfactory sensory neurons (Jones *et al.*, 1987) and appears to be exclusively-expressed in these cells. The $G_{\alpha i/o}$ family is comprised of $G_{\alpha i}$, $G_{\alpha o}$, $G_{\alpha z}$, $G_{\alpha t}$, and $G_{\alpha gust}$. $G_{\alpha gust}$, forms part of gustducin (see Chapter 2), which is a G protein associated with the taste system (McLaughlin *et al.*, 1992). The $G_{\alpha i}$, $G_{\alpha o}$ and $G_{\alpha z}$ subunits act by inhibiting andenylyl cyclase, and thereby cAMP production. The $G_{\alpha t}$, and $G_{\alpha gust}$ subunits activate phosphodiesterases (PDEs) which increase hydrolysis of cyclic guanosine monophosphate (cGMP), and cAMP, respectively. The $G_{\alpha q}$ family, which consists of $G_{\alpha q}$ $G_{\alpha 11}$ $G_{\alpha 14}$ and $G_{\alpha 15}$ (formerly known as $G_{\alpha 16}$ in humans), are associated with a number of receptors including histamine, muscarinic and serotonin receptors. They activate the phospholipase C β family of enzymes (PLCβ), which increases production of inositol 1,4,5-trisphosphate (IP_3) and diacylglycerol (DAG). The $G_{\alpha 12}$ class, which is comprised of $G_{\alpha 12}$ and $G_{\alpha 13}$, has been associated with many different receptors, but in all cases the receptors signal through other G proteins in addition to $G_{\alpha 12}$ and/or $G_{\alpha 13}$. Signalling is primarily through the activation of the Rho GTPase family of monomeric signalling G proteins.

The βγ subunit of the G protein heterotrimer also consists of multiple members for each element. In the case of the G_{β} subunit a family of six members transcribed from five genes ($G_{\beta 1}$-$G_{\beta 6}$) have been identified. The G_{γ} family is more numerous, with 12 members reported (Downes *et al.*, 1999; Oldham *et al.*, 2008). Most G_{β} subunits can interact with most G_{γ} subunits but not all possible combinations occur (Clapham *et al.*, 1997). It is also possible for several $G_{\beta\gamma}$ dimers to interact with the same G_{α} subunit (Graf *et al.*, 1992).

Ligand binding induces conformational changes in the GPCR which in turn activates the G proteins, causing dissociation of the α-subunit from the βγ complex, and subsequent initiation of a cascade of downstream cellular signalling processes (Figure 1.2).

Tas2rs are closely related to the class A GPCRs (Di Pizio *et al.*, 2014), but are also closely related to the Frizzled family of GPCRs (Fredriksson *et al.*, 2003) and have

even been classified as a separate group (Horn *et al.*, 2003). The *Tas2rs* have the typical GPCR structure, with 7 transmembrane helices, three extracellular, and three intracellular loops. Ligand binding occurs at an orthosteric site within the transmembrane helices.

1.5. Tas2r evolution

Tas2r genes vary widely in number between different species (Conte *et al.*, 2003; Shi *et al.*, 2003; Go *et al.*, 2006; Dong *et al.*, 2009; Jiang *et al.*, 2012; Hu *et al.*, 2013; Shang *et al.*, 2017) from 0 in the bottlenose dolphin (*Tursiops truncates*) and several species of penguin (Zhao *et al.*, 2015) to 51 in the western clawed tree frog (*Xenopus tropicalis*) and 80 in the coelacanth (*Latimeria chalumnae*) (Syed *et al.*, 2014). Within mammals at least some of this variation is thought to be related to diet, and the likelihood of encountering plant materials carrying toxins (Shi *et al.*, 2006; Li *et al.*, 2014; Liu *et al.*, 2016; Shan *et al.*, 2018). In a broad analysis of 52 different vertebrate species, the ingestion of plant material was found to correlate with the size of the *Tas2r* repertoire (Li *et al.*, 2014). Further evidence of the link between dietary specialisation and *Tas2rs* was provided by an analysis of a superorder of placental mammals which includes the *Carnivora*, the *Laurasiatheria* (Liu *et al.*, 2016). This analysis also highlighted a link between animals that swallow their food whole and a reduced number of *Tas2r* genes.

Within the order *Carnivora* there are many other families besides the *Canidae*, some of which vary in their dietary habits. The order as a whole includes carnivores, herbivores and omnivores. The other families within the *Carnivora* are the *Pinnipedia* (seals), *Mephitidae* (skunks and stink badgers), *Procyonidae* (racoons, coatis and others), *Mustelidae* (weasels, badgers, otters, ferrets and others), *Hyaenidae* (Hyenas), *Eupleridae* (small group of mongoose-like carnivorans endemic to Madagascar), *Herpestidae* (mongooses), *Viverridae* (civets, genets and linsangs), *Nandiniidae* (African palm civets), *Prionodontidae* (banded and spotted linsangs), *Ursidae* (bears including giant pandas), *Ailuridae* (red pandas), and *Felidae* (lions and other big cats, ocelots, wild-cats, domestic cats and others) (Nyakatura *et al.*, 2012).

The *Tas2r* repertoires in the order *Carnivora* have been shown to be the smallest among terrestrial mammals, even where dietary adaptation to a herbivorous diet has taken place (Shan *et al.*, 2018). Herbivores and omnivores generally have larger *Tas2r* repertoires. (Hu *et al.*, 2013). In some cases, comparisons with more broadly omnivorous or herbivorous species reveal a lack of gene duplication in the *Carnivora*. Mice (*Mus musculus*) have a cluster of 5 genes in the orthologous group containing *dTas2r10* and *hTAS2R10* for example (Hu *et al.*, 2013) (Figure 1.3). Humans also show gene expansion events not seen in the *Carnivora*, such as that seen in the cluster of genes containing *hTAS2R43-50* (Figure 1.3).

Expansions in *Tas2r* repertoires in omnivores and herbivores are hypothesised to be related to the occurrence of bitter tasting toxins in the diet. However, the relationship between bitterness and toxicity is not clear. More toxic compounds do not necessarily have a stronger bitter taste (Glendinning, 1994) and small repertoires of bitter receptors can still detect a wide range of bitter compounds by being more broadly tuned (Behrens *et al.*, 2014). An alternative hypothesis exists whereby animals that encounter a high level of toxic compounds in their diet may in fact have a higher tolerance for bitter tastes, despite having more *Tas2rs*. Animals that rarely encounter such toxins may be more sensitive to them, and more likely to reject them because they can “afford” to do so, given that the majority of their diet does not contain such compounds (Glendinning, 1994).

Between humans and mice, there remains a reasonably large degree of similarity in the organisation and sequence of the *Tas2rs*. In humans, the *TAS2Rs* are split into two main clusters. One cluster on chromosome 7 consists of 9 *TAS2R* genes. The other main cluster is on chromosome 12 and consists of 15 *TAS2R* genes. One gene sits outside these clusters with *TAS2R1* on chromosome 5 (Conte *et al.*, 2003). In mice the *Tas2r*s are also organised in two main clusters, but both are on chromosome 6, separated by a region of approximately 70Mb. Cluster 1 contains the genes orthologous to those on human chromosome 7, while cluster 2 contains those orthologous to genes found on human chromosome 12. *Tas2r119* sits on mouse chromosome 15 and is orthologous to h*TAS2R1*. *Tas2r134* sits on mouse

chromosome 2 and has no functional orthologue in humans. The largest differences between mouse and human gene numbers are for those on human chromosome 12, and cluster 2 on mouse chromosome 6. Two expansion events appear to have occurred here for human *TAS2R* genes, while 3 expansion events occurred for mouse, giving rise to a large number of *Tas2rs* that do not have an orthologue in humans (Lossow *et al.*, 2016).

1.6. Tas2r Function and signalling.

The function of the Tas2rs differs from the closely-related class A GPCRs. Several key motifs conserved within the class A GPCRs are absent in the Tas2rs. The D/ERY motif in TM3, the CWxP motif in TM6 and the NPxxY motif in TM7 do not appear in the Tas2rs. The D/ERY motif plays a role in many, but not all, class A GPCRs in maintaining an inactive state by interacting with residues on TM6, and is referred to as the "ionic lock" (Rasmussen *et al.*, 2007; Schneider *et al.*, 2010). The CWxP motif is involved in switching between inactive and active states (Bhattacharya *et al.*, 2008; Nygaard *et al.*, 2009). The NPxxY motif constrains TM7 with TM1 and TM2 in the inactive conformation (Hofmann *et al.*, 2009). It appears that the Tas2rs may have activation mechanisms that differ to those of the other GPCR superfamily classes. A conserved LxxSL motif, which serves to stabilise the helical conformation of the cytoplasmic end of TM5, has been shown to be involved (Singh *et al.*, 2011), as has the third intracellular loop, particularly at the conserved His214 position which seems to be involved in the adoption of the inactive state (Pydi *et al.*, 2014). A comparison of class A GPCR conserved motifs and their counterparts in hTAS2Rs is shown in Table 1.1.

Table 1.1: A comparison of conserved motifs in class A GPCRs and their counterparts in hTAS2Rs reproduced from Di Pizio *et al.* (2016)
Residue numbering according to the Ballesteros-Weinstein numbering method (Ballesteros *et al.*, 1995), where the first number denotes the transmembrane helicies (1-7) and the second number is relative to the most conserved residue in that helix, which is arbitrarily numbered as 50.

Location	Class A GPCRs	TAS2Rs
TM1	**N**$^{1.50}$**xxV**$^{1.53}$	**N**$^{1.50}$**xxI**$^{1.53}$
TM2	**L**$^{2.46}$**xxxD**$^{2.50}$	**L**$^{2.46}$**xxxR**$^{2.50}$
TM3	**D(E)**$^{3.49}$**R**$^{3.50}$**Y**$^{3.51}$	**F**$^{3.49}$**Y**$^{3.50}$**xxK**$^{3.53}$
TM4	**W**$^{4.50}$	Position 4.50 is not conserved
TM5	**P**$^{5.50}$	**P**$^{5.50}$
TM6	**F**$^{6.44}$**xxxW**$^{6.48}$**xP**$^{6.50}$	**F**$^{6.44}$**xxxY**$^{6.48}$ Position 6.50 is not conserved
TM7	**N**$^{7.49}$**P**$^{7.50}$**xxY**$^{7.53}$	**H**$^{7.49}$**S**$^{7.50}$**xxL**$^{7.53}$

Alignment of TAS2Rs and non-olfactory GPCRs can influence the result of analysis relevant for the identification of conserved regulatory motifs. A further study by Topin *et al.* (2020) used 339 class II human olfactory receptors and manual curation of the alignment to identify conserved regions in human TAS2Rs, and non-olfactory GPCRs. Similar conserved regions were identified, although residues classed as conserved and residue numbering differed slightly (Figure 1.1).

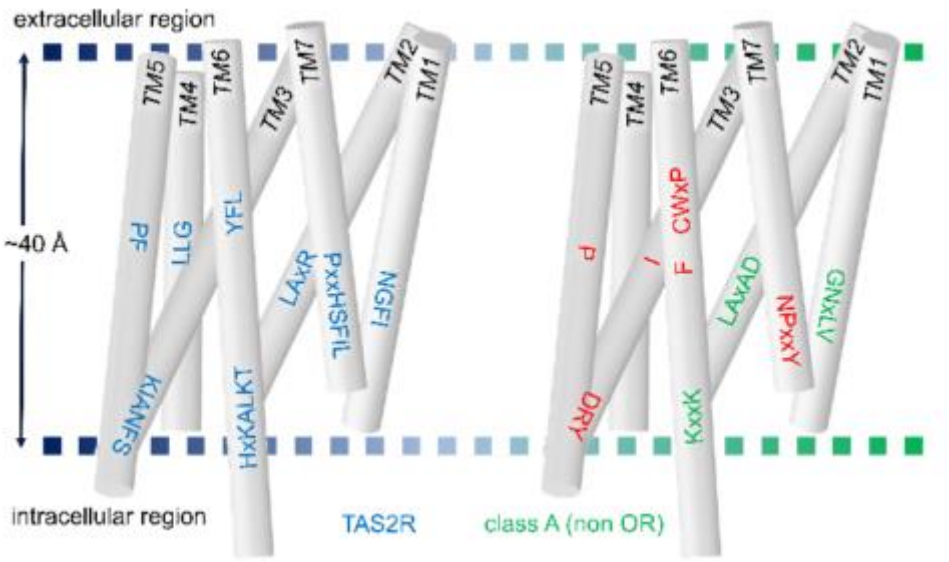

Figure 1.1: TAS2R and class A GPCR conserved motifs labelled on each transmembrane helix reproduced from Topin *et al.* (2020)
Functional regions in the class A GPCRs are highlighted in red.

Some Tas2rs may possess extracellular regions which serve to mediate access of ligands to the binding pocket (Brockhoff *et al.*, 2010; Sandal *et al.*, 2015). Such secondary or "vestibular" sites could be particularly relevant for broadly tuned receptors that recognise ligands from a variety of different chemical classes. The mechanism may provide a pre-screening authentication step, which allows ligand selection from a broader array of chemicals (Suku *et al.*, 2017). Similar mechanisms have also been described for other GPCRs. For example, molecular dynamics simulations of the binding of both antagonists and an agonist to the β1 and β2-adrenergic receptors showed the involvement of a vestibular site on the extracellular surface of the receptors (Dror *et al.*, 2011). This was also shown to be involved with the selectivity of norepinephrine for the β1-adrenergic receptor (Xu *et al.*, 2020).

The Tas2rs share many of the same signalling mechanisms as the receptors for sweet and umami stimuli, the Tas1rs. Although Tas1rs are class C GPCRs with a large extracellular domain, both Tas1rs and Tas2rs utilise the same heterotrimeric G protein complex as the starting point in their transduction mechanism, consisting of $G_{\alpha gust}$ (McLaughlin *et al.*, 1992), $G_{\beta 1}$ or $G_{\beta 3}$ (Huang *et al.*, 1999; Rossler, 2000) and $G_{\gamma 13}$ (Huang *et al.*, 1999) subunits. There is evidence that other G_{α} subunits may be

involved, as knockout of $G_{\alpha gust}$ in mice does not completely abolish responses to sweet, umami and bitter stimuli (Wong *et al.*, 1996; Ruiz *et al.*, 2003). In contrast the elimination of Trpm5 or Plcβ2 in mice does abolish responses to bitter, sweet and umami stimuli (Zhang *et al.*, 2003).

In the inactive state the G_{α} subunit is bound to guanosine diphosphate (GDP). Receptor activation leads to GDP exchange with guanosine triphosphate (GTP) and dissociation of the heterotrimeric G protein from the receptor and the α-subunit of the G protein from the βγ heterodimer (Figure 1.2).

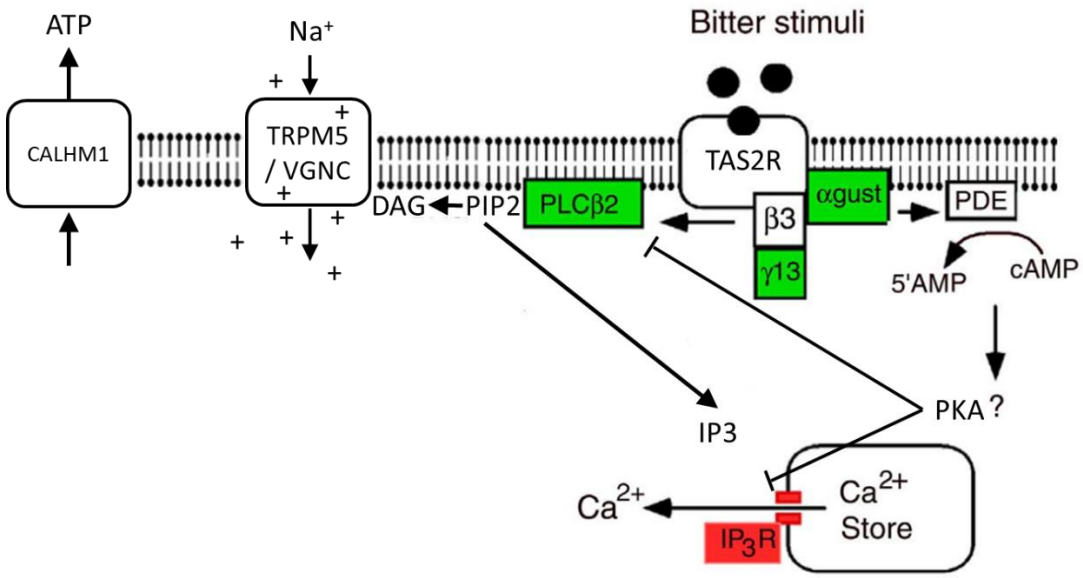

Figure 1.2: Transduction mechanism of Tas2rs
Bitter compounds stimulate Tas2rs on the apical membrane. $G_{\alpha gust}$ activates PDE. A proposed role of $G_{\alpha gust}$ is shown where conversion of cAMP to 5'AMP reduces activation of PKA, which phosphorylates both type 3 IP_3 receptor (IP_3R) and $PLC\beta_2$. This allows more robust Ca^{2+} release (Kinnamon, 2016). $G_{\beta 3\gamma 13}$ activates $PLC\beta_2$ which cleaves phosphatidylinositol 4, 5-bisphosphate (PIP_2) into diacylglycerol (DAG) and IP_3. IP_3 binds to its receptor on the endoplasmic reticulum (ER) causing calcium release, which activates transient receptor potential cation channel subfamily M member 5 (TRPM5). The resulting sodium influx activates voltage gated sodium channels (VGNC) and strong depolarisation of the membrane activates the voltage-gated adenosine triphosphate (ATP) release channel calcium homeostasis modulator 1 (CALHM1). ATP activates the purinergic receptors P2X2 and P2X3 on the afferent nerves (not shown). Figure adapted from Clapp *et al.* (2001) and Kinnamon (2016).

The $G_{\beta\gamma}$ heterodimer activates $PLC\beta_2$ (Rössler *et al.*, 1998) which cleaves PIP_2 into IP_3 and DAG. IP_3 activates IP_3R3 on the ER (Clapp *et al.*, 2001; Miyoshi, 2001) and Ca^{2+} is released from the cell stores in the ER. This leads to the activation of TRPM5 (Perez *et al.*, 2002) which causes an influx of Na^+, cell depolarisation, the generation of action potentials and the release of ATP via CALHM1 (Taruno *et al.*, 2013). The G_α subunit $G_{\alpha gust}$ also plays a role in bitter taste receptor signalling, activating PDEs to decrease intracellular cAMP levels (Yan *et al.*, 2001).

1.7. Molecular receptive ranges of Tas2rs

It has been estimated that there are many thousands of bitter-tasting molecules arising from plants and other sources. A current database of compounds activating human bitter receptors contains nearly 1,000 known bitter compounds, although in many cases the cognate human receptor is not known (Wiener *et al.*, 2012; Dagan-Wiener *et al.*, 2018). Also, bitter compounds can come from structurally-diverse chemical groups, including peptides, fatty acids, amino acids, esters, flavonoids and many others (Belitz *et al.*, 1985; Brockhoff *et al.*, 2007; Kohl *et al.*, 2013; Soares *et al.*, 2013). This variety in the potential source of bitter taste has resulted in the development of a repertoire of bitter taste receptors in most mammals.

The range of bitter compounds that can be detected by any mammal depends on two main variables. Firstly, the number of different bitter receptors the animal possesses as part of its taste mechanism, and secondly, the tuning breadth of these receptors, which can vary widely. Humans are currently thought to have 25 bitter taste receptors, of which all but 4 have been de-orphanised. The mouse has ~35 bitter receptors, of which 21 have been de-orphanised (Lossow *et al.*, 2016).

The tuning breadth of the receptors is determined with screening studies using libraries of compounds known to have a bitter taste in humans, and receptor expression in heterologous cell systems. This does bias the compound libraries for studies in any species other than human, as the compound selection is based on what activates human receptors and may not be optimal for determining the tuning breadth of receptors from other species. In humans three TAS2R receptors are thought of as broadly-tuned (TAS2R10, 14 and 46) (Behrens *et al.*, 2014). Some are thought of as narrowly-tuned (TAS2R3 and 5), while others have an intermediate breadth of tuning (TAS2R1, 4, 7, 30(47), 31(44), 39, 40, and 43) or are thought to be specific for certain classes of compounds (TAS2R16 and 38) (Meyerhof *et al.*, 2010). For the remaining receptors less data are available, but they can be classified based on the number of known ligands they have in the online resource BitterDB (Wiener *et al.*, 2012; Dagan-Wiener *et al.*, 2018) with TAS2R8, 9, 13, 20(49), 41, and 50 all

having between 1-3 known ligands and therefore being thought of as narrowly-tuned or at the lower end of the intermediately-tuned group. Four human receptors remain as orphans (TAS2R19, 42, 45, and 60). In the mouse 21 bitter taste receptors have been de-orphanised. Of these 4 (Tas2r105, 121, 135 and 144) are broadly-tuned, 10 (Tas2r108, 109, 110, 114, 117, 119, 123, 126, 137 and 140) are intermediate in their tuning breadth and 7 (Tas2r113, 115, 120, 122, 125, 138 and 139) are narrowly-tuned (Lossow *et al.*, 2016).

Tuning of receptors from other species has only been studied in a few cases. Chickens (*Gallus gallus*) and turkeys (*Meleagris gallopavo*) were found to have very small Tas2r repertoires with three and two functional receptors, respectively (Behrens *et al.*, 2014). However, all receptors in these two cases were broadly-tuned. The zebra finch (*Taeniopygia guttata*) and the western clawed tree frog were also included in this study. Three of the seven Tas2rs from the zebra finch were tested along with 6 of the 54 Tas2rs from the western clawed tree frog. The three zebra finch receptors were homologous to one chicken receptor Tas2r1, and it was shown that their combined tuning breadth was similar to that of the single Tas2r1 receptor in the chicken. This suggests that having more receptors that have been created by gene duplication events does not necessarily lead to a wider sensitivity to more compounds, but does allow the development of more specialised receptors.

In some other species, some limited functional characterisation has been performed. The Tas2r repertoire of the domestic cat (*Felis catus*) has been partially characterised (Lei *et al.*, 2015; Sandau *et al.*, 2015), as has that of some non-human primates (Imai *et al.*, 2012; Tsutsui *et al.*, 2016). No studies of Tas2r characterisation and tuning currently exist for the dog. Chapter 2 investigates the receptive ranges of dog Tas2rs.

1.8. Tas2r expression

Gustatory papillae contain bundles of specialised cells, referred to as taste buds. The expression of Tas2rs in the oral cavity is predominantly found in the taste buds of the circumvallate papillae, although expression is also found in the foliate, and more

occasionally in the fungiform papillae (Adler *et al.*, 2000; Matsunami *et al.*, 2000). Notably, all 25 human *TAS2Rs* have been shown to be expressed in gustatory papillae, indicating they all play a role in gustation despite their expression in other areas of the body (Behrens *et al.*, 2007). Some species differences in expression have been observed previously. Expression in the circumvallate papillae of rats was found to be largely homogeneous (Adler *et al.*, 2000), while that found in humans was more heterogeneous, with no more that 4-11 TAS2Rs expressed in any given taste receptor cell (Behrens *et al.*, 2007). No published data for expression of dog Tas2rs exists. Chapter 3 explores the expression of *Tas2rs* in dog fungiform papillae.

Tas2rs are also known to be expressed in other areas of the body, particularly in the airway and the gut. In the airway both the upper (Chen *et al.*, 2019), and lower (Liggett, 2013; Kim *et al.*, 2017) respiratory tract are sites of Tas2r expression. In the upper airway cilliated sinonasal airway epithelial cells express Tas2rs, and in particular TAS2R38 has been associated with patient sensitivity to respiratory infection (Lee *et al.*, 2012). In the lower airway expression of Tas2rs in smooth muscle cells plays a role in bronchodilation, a discovery that has led to research on the use of Tas2r agonists as a potential new class of bronchodilators (Nayak *et al.*, 2019). In the gut the role of Tas2rs is not as clear. Effects like delayed gastric emptying (Glendinning *et al.*, 2008), modulation of food intake (Janssen *et al.*, 2011) and anion secretion (Kaji *et al.*, 2009; Yang *et al.*, 2014) have been associated with intragastric infusion of Tas2r agonists. These effects may serve to protect the animal against the ingestion of toxic compounds, by retaining them in the stomach for longer or by washing them through the intestine. Effects on glucose homeostasis have also been reported (Dotson et al., 2008), which is in line with Tas2r mediated secretion of glucagon-like peptide 1 (GLP-1) and cholecystokinin (CCK) from enteroendocrine cells in response to Tas2r agonists (Jeon et al., 2011; Kim et al., 2014).

1.9. Tas2r variation

Domestication and selective breeding may have resulted in phenotypic diversity in dogs' feeding behaviours and sense of taste. Good evidence to support these suggestions is lacking, but it is not inconceivable that some diversity in the sense of taste may exist between dog breeds. This is particularly true in the multi-gene bitter receptor family, which is known to provide variation in bitter taste sensitivity in humans. Such variation may have originated as a protective measure, so that individuals might show different responses to novel, and potentially dangerous foodstuffs. It may also be related to unknown benefits of some of the variations related to non-taste roles of some *TAS2R*s. For example, the taster/non-taster haplotype of *TAS2R38* (Bufe *et al.*, 2005) influences taste sensitivity to the thiourea compounds 6-n-propylthiouracil (PROP) and phenylthiocarbamide (PTC), as well as other structurally related compounds that occur in foods, like goitrin (Wooding *et al.*, 2010). It has also been shown to be linked to the incidence of upper airway infection (Lee *et al.*, 2012). While this shows a benefit for those haplotypes associated with PROP/PTC sensitivity, it does not explain the continued existence of the less protective, non-taster haplotype. It may be that these haplotypes offer some, as yet undiscovered, advantage relating to other functions of *TAS2R38*.

In cases where a bitter compound activates a number of TAS2Rs, variation in the different receptors can interact with the overall haplotype, determining the level of perceived bitterness (Roudnitzky *et al.*, 2015). Cases where variation in different receptors for the same compound are all in the direction of increased sensitivity is strongly associated with phenotype. Where variations have opposing effects, genotype-phenotype associations are much weaker. Variation in the Tas2rs of the dog is explored in Chapter 4.

1.10. Tas2rs in dogs

The perception of bitter taste is widely distributed in many different species. From protozoa to primates aversion to bitter stimuli is common. In some cases, quinine for example, particular compounds are commonly avoided across a wide variety of different species (Garcia *et al.*, 1975). The number of *Tas2rs* in dogs has been

assessed several times using the available dog genome sequence at the time, and known *Tas2r* sequences from other species. The earliest example (Go *et al.*, 2006) used the known human (25) and mouse (35) intact Tas2r protein sequences and tblastn searches to look for genes in the dog and other species. A similar approach was taken in another study (Dong *et al.*, 2009). In both these studies, the number of intact *Tas2r* genes for dogs was considered to be 15. In another study (Hu *et al.*, 2013), the most recent assembly of the canine genome (CanFam3.1) was used, but only human TAS2R sequences were used for searches. Despite this 16 intact genes were reported. The most recent study (Shang *et al.*, 2017) reported 15 intact genes.

As part of this project a similar analysis was conducted to confirm the sequence of all putatively functional dog *Tas2r*s. Nucleotide and protein sequences for human and mouse *Tas2rs* were retrieved from Ensembl (www.ensembl.org) and used to perform blastn and tblastn searches on the dog genome (CanFam 3.1), respectively. Matching sequences were checked for an E value less than $1e^{-5}$ and an open reading frame of >800bp. Sequences were then used as queries for searches against the non-redundant database, and were discarded if the closest match was not a *Tas2r.* A summary of the reported dog *Tas2rs* is given in Table 1.2. This analysis revealed 16 putatively functional dog *Tas2r* genes, which is in agreement with other studies that identified either 15 or 16 putatively-functional receptor genes in dogs.

Table 1.2: Previously reported *Tas2rs* in the dog and those identified in this study
Alternative or previous gene numbering shown in brackets, (suffix p = pseudogene).

Go *et al.* (2006)	Dong *et al.* (2009)	Hu *et al.* (2013)	Shang *et al.* (2017)	This study (2017)
Tas2r1	*Tas2r1*	*Tas2r1*	*Tas2r1*	*Tas2r1*
Tas2r2	*Tas2r2*	*Tas2r2*	*Tas2r2*	*Tas2r2*
Tas2r3	*Tas2r3*	*Tas2r3*	*Tas2r3*	*Tas2r3*
Tas2r4		*Tas2r4 (16)*	*Tas2r4p*	*Tas2r4*
Tas2r5	*Tas2r5*	*Tas2r5*	*Tas2r5*	*Tas2r5*
Tas2r7	*Tas2r7*	*Tas2r7*	*Tas2r7*	*Tas2r7*
-	-	-	*Tas2r7 like 1p*	
-	-	-	*Tas2r7 like 2p*	
Tas2r8p	-	-	*Tas2r8p*	*Tas2r8p*
Tas2r9p	*Tas2r9*	*Tas2r9*	*Tas2r9p*	*Tas2r9p*
Tas2r10	*Tas2r10*	*Tas2r10*	*Tas2r10*	*Tas2r10*
Tas2r12	*Tas2r12*	*Tas2r12 (4)*	*Tas2r12*	*Tas2r12*
-	-	-	*Tas2r19p*	
Tas2r31p (44)	-	-	*Tas2r31p (44)*	*Tas2r31p (44)*
-	-	-	*Tas2r34*	
Tas2r38		*Tas2r38 (8)*	*Tas2r38*	*Tas2r38*
Tas2r39	*Tas2r39*	*Tas2r39 (11)*	*Tas2r39*	*Tas2r39*
Tas2r40	*Tas2r40*	*Tas2r40 (12)*	*Tas2r40*	*Tas2r40*
Tas2r41	*Tas2r41*	*Tas2r41 (13)*	*Tas2r41*	*Tas2r41*
Tas2r42 (55)	*Tas2r42 (55)*	*Tas2r42 (15)*	*Tas2r42*	*Tas2r42*
Tas2r43	*Tas2r43*	*Tas2r43 (14)*	*Tas2r43*	*Tas2r43*
Tas2r62p	*Tas2r62*	-	*Tas2r62p*	*Tas2r62*
Tas2r67	*Tas2r67*	*Tas2r67 (6)*	*Tas2r67*	*Tas2r67*
Totals (pseudogenes)				
15 (4)	15 (0)	16 (0)	15 (8)	16 (3)

To obtain the most relevant sequence for each gene to be synthesised, variation data from a database of dog whole genomes (The Dog Biomedical Variant Database Consortium or DBVDC) were checked in each instance. In cases where it was found that the reference genome sequence contained an infrequent variant that was likely to affect receptor function then the more common variant was used for gene synthesis and sub-cloning.

In the course of this analysis it was found that d*Tas2r4* was not a pseudogene despite the reference sequence showing a premature STOP codon at position 88 of the amino acid sequence. In all dogs in the DBVDC database, a cysteine residue was present at this position, giving a full length open reading frame (ORF) for this gene. Cloning and expression of the full receptor sequence showed that it was functional for some known ligands of the human TAS2R4 receptor (Chapter 2).

The gene sequence for d*Tas2r9* was found to be shorter that it's human orthologue. An earlier STOP codon at amino acid position 281 and a deletion of one amino acid residue at position 153 render the dog sequence 32 amino acids shorter than the human TAS2R9 protein sequence. This would relate to the loss of the C-terminal region and part of the seventh transmembrane helix based on a comparison with the human receptor. This may render the receptor non-functional, and it was designated as a pseudogene here, as is the case for most other studies (Table 1.2).

In the most recent study available (Shang *et al.*, 2017), d*Tas2r62* is listed as a pseudogene, while an entry is made for *dTas2r34*, a dog gene which was also identified in another publication (Li *et al.*, 2014). Both of the sequences given in the most recent publication map to the same area on dog chromosome 16 when used as queries in the BLASTN tool via the Ensembl portal. The sequence for d*Tas2r34* is found in the dog reference genome at position 16: 6261540-6262445(-). The sequence given for the d*Tas2r62* pseudogene only maps partially, with the largest section of nucleotides, 18-897 from a total of 906, mapping to the coordinates 16:6261658-6262537(-), where 788 residues are from an overlapping region with the coordinates for d*Tas2r34*. As it was not clear what the rationale was for inclusion of

this pseudogene sequence, or for naming this gene as d*Tas2r34*, the more often used d*Tas2r62* annotation was preferred.

Amino acid sequences were also aligned using CLC Sequence Viewer (Qiagen, Germany) and used to generate a phylogenetic tree using the Neighbour Joining method with the Jukes-Cantor protein distance measure and 1,000 bootstrap repetitions. The tree was later reformatted with iTOL (Figure 1.3) (Letunic *et al.*, 2019).

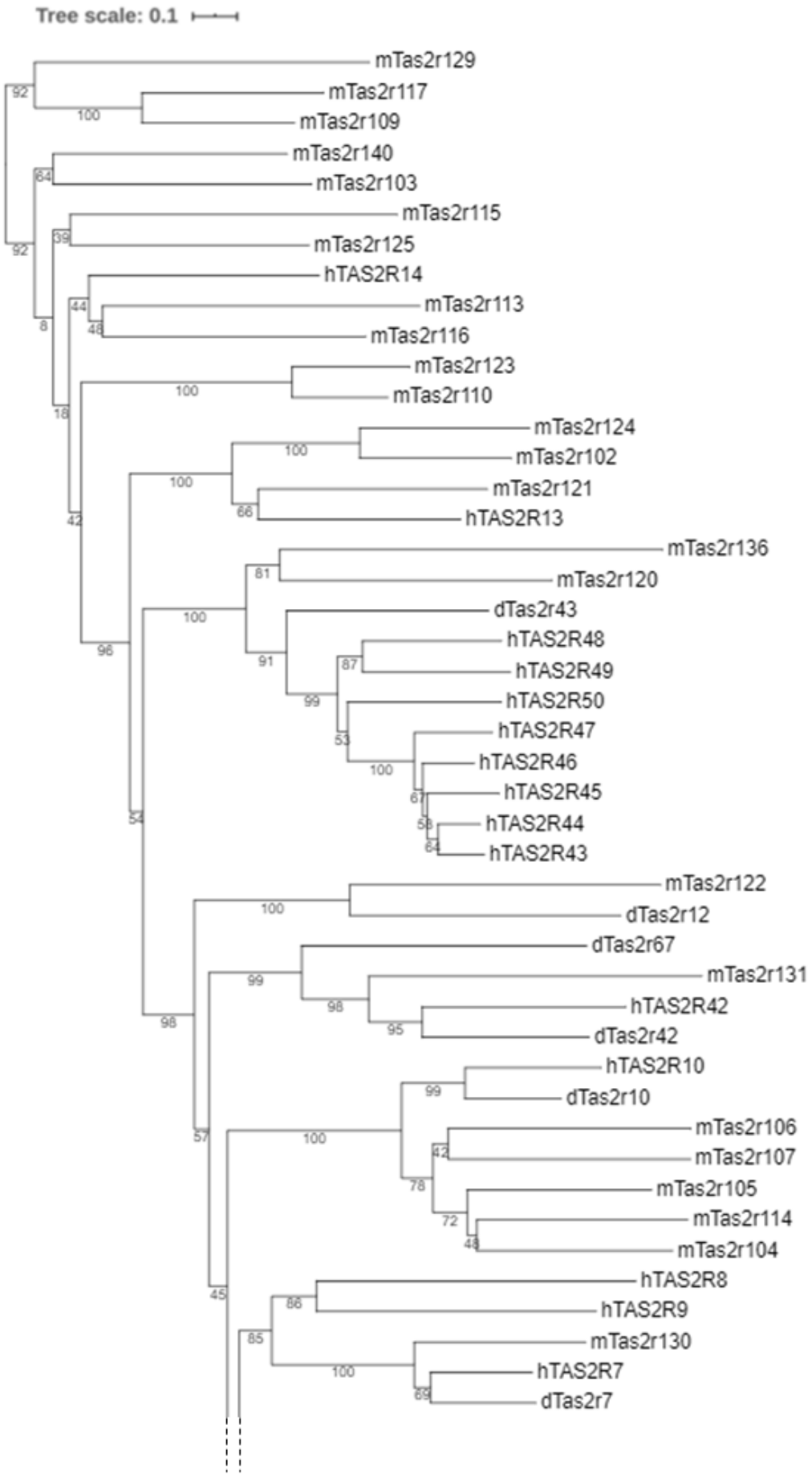
Tree scale: 0.1
mTas2r129
mTas2r117
mTas2r109
mTas2r140
mTas2r103
mTas2r115
mTas2r125
hTAS2R14
mTas2r113
mTas2r116
mTas2r123
mTas2r110
mTas2r124
mTas2r102
mTas2r121
hTAS2R13
mTas2r136
mTas2r120
dTas2r43
hTAS2R48
hTAS2R49
hTAS2R50
hTAS2R47
hTAS2R46
hTAS2R45
hTAS2R44
hTAS2R43
mTas2r122
dTas2r12
dTas2r67
mTas2r131
hTAS2R42
dTas2r42
hTAS2R10
dTas2r10
mTas2r106
mTas2r107
mTas2r105
mTas2r114
mTas2r104
hTAS2R8
hTAS2R9
mTas2r130
hTAS2R7
dTas2r7

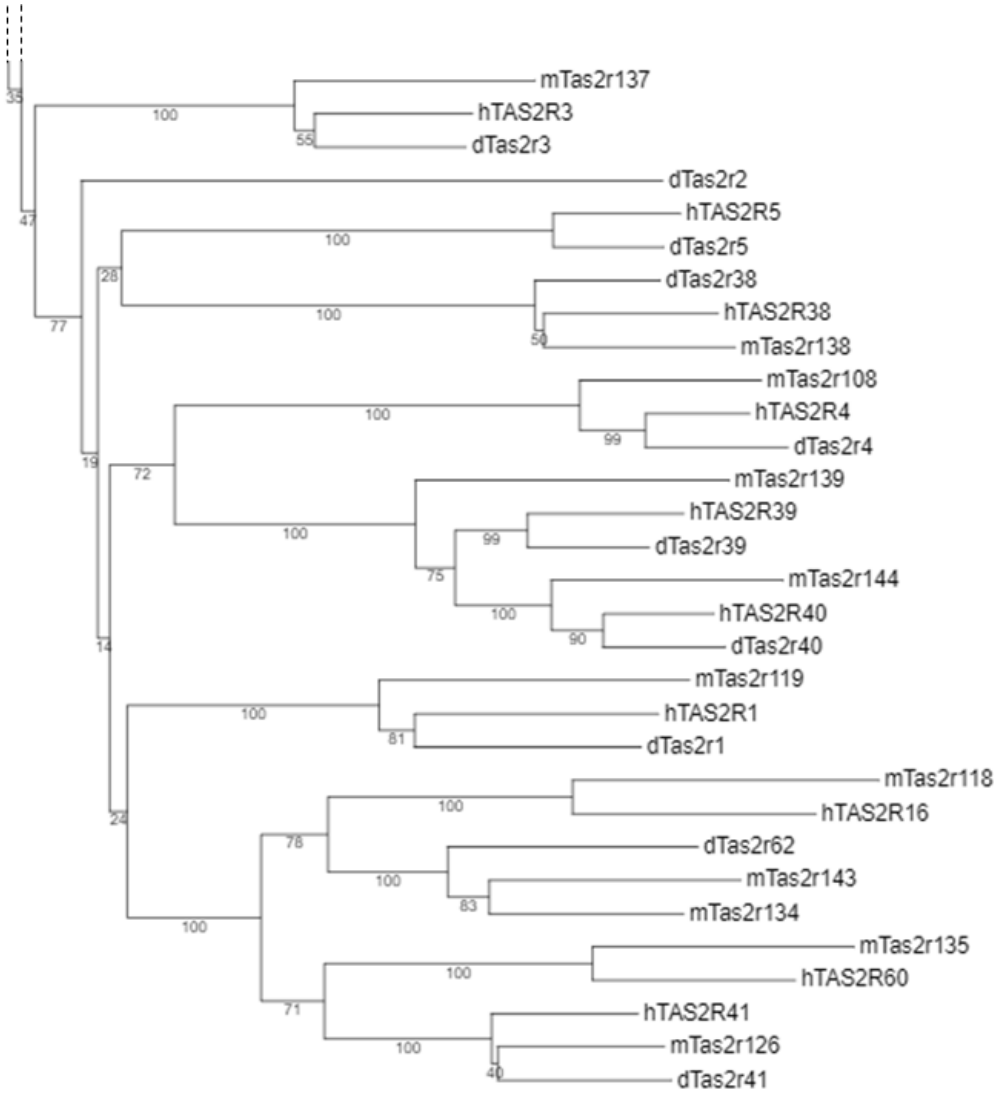

Figure 1.3: Phylogenetic tree of Tas2r amino acid sequences from three species
The tree was generated using the neighbour joining method with Jukes-Cantor protein distance measure and 1,000 bootstrap repetitions.

Dog *Tas2rs* are largely orthologous to human *TAS2Rs*, based on a definition of orthology where a phylogenetic clade that contains genes from two species and is supported by a >80% bootstrap value can be described as orthologous (Niimura *et al.*, 2005). The organisation of *Tas2rs* in the dog genome is similar to that found in humans. There are 2 main clusters of *Tas2r* genes on dog chromosomes 16 and 27, which contain genes orthologous to those found on human chromosomes 7 and 12, respectively. In humans, *hTAS2R1* is found on chromosome 5, while in dogs d*Tas2r1* is found on chromosome 34. One difference in chromosomal arrangement between

the two species appears for d*Tas2r2*, which is found on dog chromosome 14, whereas the human pseudogene is found on chromosome 7. Details of dog gene coordinates and their chromosomal positions are given in Table 1.3.

Table 1.3: Dog Tas2r gene coordinates and the chromosomal locations of dog and human genes (P = pseudogene)

Dog Gene	Coordinates	Human Gene (Chr)
d*Tas2r2*	14:27345807-27346718	*TAS2R2P* (7)
d*Tas2r3*	16:7435147-7436097	*TAS2R3* (7)
d*Tas2r4*	16:7424403-7425302	*TAS2R4* (7)
d*Tas2r5*	16:7406855-7407742	*TAS2R5* (7)
d*Tas2r38*	16:7224023-7225012	*TAS2R38* (7)
d*Tas2r39*	16:6465643-6466617	*TAS2R39* (7)
d*Tas2r40*	16:6439097-6440053	*TAS2R40* (7)
d*Tas2r41*	16:6230851-6231777	*TAS2R41* (7)
d*Tas2r62*	16:6261540-6262445	*TAS2R62P* (7)
d*Tas2r7*	27:34898964-34899902	*TAS2R7* (12)
d*Tas2r10*	27:34876090-34877058	*TAS2R10* (12)
d*Tas2r12*	27:34855685-34856629	*TAS2R12P* (12)
d*Tas2r42*	27:34739537-34740508	*TAS2R42* (12)
d*Tas2r43*	27:34792712-34793761	*TAS2R43-50* (12)
d*Tas2r67*	27:34748642-34749580	*TAS2R67P* (12)
d*Tas2r1*	34:4537632-4538525	*TAS2R1* (5)

While dogs show a reduced number (16) of putatively functional *Tas2r* genes when compared to humans (25) or mice (35), the number is not so low as to imply that the dog's sense of bitter taste is poor in comparison to that of these other species. This depends as much on the receptor breadth of tuning as it does on receptor repertoire. Other terrestrial members of the *Carnivora* show similar numbers of *Tas2rs* like the ferret (14), polar bear (15) and the giant panda (17), despite differences in their dietary habits. The walrus and Weddell seal, also members of the *Carnivora*, have only 4 and 5 *Tas2rs*, respectively, but they swallow their prey whole which contributes to a loss of *Tas2rs* in some species (Liu *et al.*, 2016).

1.11. Aims of this thesis

A better understanding of the perception of bitter taste by the dog would be of value to the pet food industry. It would enable more informed decisions to be made when looking at potential raw materials for inclusion in a diet. It would also be of use to companies involved with the development of pet repellents to reduce unwanted behaviours such as pica and coprophagia (potentially through micro-encapsulation of bitter deterrents), and to reduce the risk of ingestion of harmful substances such as antifreeze and rodenticides.

In Chapter 2, the receptive ranges of dog Tas2rs were explored using a cell-based model for Tas2r expression and screening. These data will help to explain species differences in the perception of bitter compounds between dogs and humans. The aim was to build an understanding of the overall sensitivity of dogs to bitter tastes, and to predict how dogs might respond to different bitter substances *in vivo*. A secondary aim was to allow the impact of naturally-occurring variations in the dog Tas2rs to be assessed, and to allow investigation of the impact selective breeding may have had on the taste sensitivity of different dog breeds.

While functionality *in vitro* indicates that Tas2r genes truly code for receptors that are activated by substances likely to be perceived as bitter, confirmation of expression in taste papillae further strengthens the case for their role in taste perception. In Chapter 3, dog fungiform papillae were tested to confirm the expression of Tas2rs. As a secondary aim, papillae were sampled across the anterior portion of the tongue, in order to examine spatial expression differences.

Dogs are unique in nature due to the influence humans have exerted on them through domestication and selective breeding. Numerous traits have become more or less common in different dog breeds as a result. Chapter 4 aimed to investigate if bitter taste perception may have been influenced by breeding, leading to differences in receptor sensitivity between breeds. If such variation exists in the Tas2rs, it suggests that breed-related differences in flavour perception could exist, which

would be a novel finding and of significant interest to dog owners and the pet food industry.

Chapter 2. Screening of dog Tas2rs with a library of bitter compounds

2.1. Introduction

2.1.1. Bitter compound selection

Many different naturally-occurring and synthetic compounds have been found to impart a bitter taste. Plants often produce bitter-tasting chemicals as a defence mechanism to deter ingestion by animals. For example, the naturally-occurring alkaloid strychnine is produced from the seeds of the *Strychnos nux-vomica* tree and was first identified in 1818. It was believed to have a variety of benefits when consumed as a tonic (Sandall, 1896), despite being poisonous. Modern drugs can also be found to have a bitter taste, which causes issues with compliance for prescribed medication. This is especially true in children where liquid formulations are required as opposed to pill formulations, making the bitter taste much more noticeable (Mennella *et al.*, 2013). Many of these taste observations have been compiled in the Merck Index (O'Neil, 2014), an encyclopaedia of chemicals published by the Royal Society of Chemistry.

The Merck Index and other sources have guided the selection of known bitter-tasting compounds for testing against heterologous cell models of human bitter receptors. For other species, the selection of compounds for testing is largely driven by what is known to taste bitter to humans and mice. An online repository for bitter taste receptor information called BitterDB (http://bitterdb.agri.huji.ac.il) is available (Wiener *et al.*, 2012; Dagan-Wiener *et al.*, 2018), and currently lists information for all human, mouse, cat and chicken Tas2rs and their associated ligands where available. Another major source of information not included in BitterDB is a patent from the American tastant development company, Senomyx (Li *et al.*, 2008). The patent lists 85 compounds tested against 23 human TAS2Rs.

In this work, both BitterDB and the Senomyx patent were used to select a panel of 48 compounds known to activate human TAS2Rs. Firstly, a known ligand for each human TAS2R that had a putative dog orthologue was selected where available.

There is no ligand listed for hTAS2R42 in either the BitterDB or the Senomyx patent. This information is shown in Table 2.1, where all ligands used from both the BitterDB and the Senomyx patent are listed against all human receptors having a dog orthologue.

Table 2.1: Known ligands for human TAS2Rs having a 1:1 orthologue in the dog that were used in this study

Human Receptor with 1:1 Dog Orthologue	Selected known ligands in the library based on BitterDB (threshold concentration/EC_{50} in µM where available)	Selected known ligands based on the Senomyx patent application[8] US20080038739A1 (test concentration in µM)	Number of Ligands
TAS2R1	Chloramphenicol (100[1]), Dextromethorphan (10[1]), Diphenidol (100[1]), Parthenolide (100[1]), Sucralose[4], Thiamine (1000[1]), Yohimbine (300[1])	Chloramphenicol (200), Chloroquine (10000), Methylprednisolone (50-100), 6-Nitrosaccharin (300), Oleuropein (2500), Omeprazole (250), Oxybutynin chloride (100), Oxyphenonium (HBr) (2500), Prednisone (250-500), Quinine-HCl (75)	16
TAS2R3	Chloroquine (10[1]/172[2])	Chloroquine (10000)	1
TAS2R4	Camphor (300[1]), Denatonium benzoate (300[1]), Colchicine (100[1]/1025[4]), Diphenidol (100[1]), Parthenolide (30[1]), Quinine (10[1]), Sucralose[2], Yohimbine (300[1])	4-Benzylpiperidine (250), Chloroquine (10000), Doxepin (150), Methylprednisolone (50-100), Oleuropein (2500), Omeprazole (250), Oxybutynin chloride (100), Oxyphenonium (HBr)	19

		(2500), Pirenzepine (2500), Quinine-HCl (75), Strychnine (2500), Trimethoprim (750)	
TAS2R5	1,10-phenanthroline (100^{1}), Sucralose[2]	Dimethylbiguanide (50000-100000), Oleuropein (2500)	4
TAS2R7	Chloroquine[3], Diphenidol (10^{1}), Papaverine (10^{1}), Quinine (10^{1}), Sucralose[2]	Chloroquine (10000), Ethylpyrazine (20000), Oxybutynin chloride (100), Oxyphenonium (HBr) (2500), Pirenzepine 2500), Quinine-HCl (75), Strychnine (2500), Trimethoprim (750)	11
TAS2R10	α-Thujone (100^{1}), Brucine (100^{1}), Camphor (300^{1}), Chloramphenicol(100^{1}), Chloroquine 10000^{1}), Cucurbitacin B (0.01^{1}), Cycloheximide (100^{1}) , Denatonium benzoate (3^{1}/120^{1}), Dextromethorphan (10^{1}), Diphenidol (30^{1}), N-(3-Oxooctanoyl)-L-homoserine lactone[2], Papaverine (10^{1}), Parthenolide (30^{1}), Quinine (10^{1}), Sucralose[2],	Brucine (250), 4-Benzylpiperidine (250), Chloramphenicol (200), Chloroquine (10000), Denatonium benzoate (1000), Doxepin (150), Ethylpyrazine (20000), Methylprednisolone (50-100), Oleuropein (2500), Omeprazole (250), Oxybutynin chloride (100)	24

	Strychnine (3[1]/21.8[4]), Yohimbine (300[1])		
TAS2R38	6-Nitrosaccharin (100[5]), Diphenidol (100[1]), Ethylpyrazine (300[1]), Propylthiouracil (0.11[1]), Phenylthiocarbamide (0.04[1]), Sinigrin (100[1]), Yohimbine (300[1])	Ethylpyrazine (20000), Oxybutynin chloride (100), Trimethoprim (750)	9
TAS2R39	Acetaminophen (3000[1]), Chloramphenicol (1000[1]), Chloroquine (100[1]), Colchicine (3000[1]), Denatonium benzoate (100[1]), Diphenidol (100[1]), Flavone (8[6]), Quinine (10[1]), Resveratrol (63[6]/109[6]), Sucralose[2], Thiamine (1000[1])	Acetaminophen (10000), Chloroquine (10000), Denatonium benzoate (1000), Oleuropein (2500), Omeprazole (250), Oxybutynin chloride (100), Oxyphenonium (HBr) (2500), Pirenzepine (2500), Strychnine (2500), Trimethoprim (750)	17
TAS2R40	Diphenidol (30[1]), Quinine (10[1])	Doxepin (150), Oxybutynin Chloride (100), Quinine-HCl (75), Strychnine (2500), Trimethoprim (750)	6
TAS2R41	Chloramphenicol (300-600[7]), Sucralose[2]	6-Nitrosaccharin (300)	3
TAS2R42	None identified	None identified	0
TAS2R43	Aloin (0.3[1]), Aristolochic acid (1100[1]), Chloramphenicol (100[1]), Denatonium benzoate	Aloin (500), Aristolochic acid (20), Chloramphenicol (200), Chloroquine (10000),	11

	(300[1]), Diphenidol (30[1]), Quinine (10[1])	Denatonium benzoate (1000), 6-Nitrosaccharin (300), Oxybutynin chloride (100), Oxyphenonium (HBr) (2500), Strychnine (2500)	

[1] *In vitro* cell-based calcium mobilisation assay (Meyerhof *et al.*, 2010).

[2] *In vitro* cell-based calcium mobilisation assay (Lossow *et al.*, 2016).

[3] *In vitro* preparation of cell membranes with receptor expression and purified G_{α} subunits, measuring receptor catalysed GDP/GTP[S] exchange (Sainz *et al.*, 2007).

[4] *In vitro* cell-based calcium mobilisation assay (Grassin-Delyle *et al.*, 2013).

[5] *In vitro* preparation of cell membranes with receptor expression and purified $G_{\alpha t}$, measuring receptor catalysed GDP/GTP[S] exchange (Pronin *et al.*, 2004).

[6] *In vitro* cell-based calcium mobilisation assay (Roland *et al.*, 2013).

[7] *In vitro* cell-based calcium mobilisation assay (Thalmann *et al.*, 2013b).

[8] *In vitro* cell-based calcium mobilisation assay (Li *et al.*, 2008)

The second criterion for test compound selection was to select a range of compounds to cover the potential ligand selectivity of dog orthologues for broadly-tuned human TAS2Rs. The human receptors TAS2R10, 14 and 46 are considered to be broadly-tuned (Behrens *et al.*, 2014), but only TAS2R10 has an orthologue in the dog. In total 24 compounds covering a range of structural pharmacophores were selected for dTas2r10, so that breadth of tuning might be compared between species in this case. Human TAS2R1, 4, 7, 39, 40 and 43, are considered to be intermediate in their tuning breadth. Multiple compounds were selected for the equivalent dog orthologues as detailed in Table 2.1. Human TAS2R3 and 5 are considered to be narrowly-tuned and 1 and 4 compounds were selected for the testing, respectively.

The compound library consists of approximately half naturally-occurring compounds and half synthetic compounds. Many of the compounds are drugs with a reported

bitter taste to humans. For example, the naturally-occurring compound quinine was used as an anti-malarial drug, but was limited in its supply. The development of synthetic alternatives like quinacrine and chloroquine greatly improved the availability of treatment for malaria (Krafts *et al.*, 2012). All three were included here as they are all reported to be bitter-tasting and share structural similarity (Figure 2.1). The available data for quinine and chloroquine show overlapping activation patterns of human TAS2Rs with both compounds active against hTAS2R3, 7, 10, 14, and 39, and quinine also active against hTAS2R31, 40, 43 and 46 (Sainz *et al.*, 2007; Meyerhof *et al.*, 2010). Quinacrine is listed as activating hTAS2R10 and 13 in the Senomyx patent US20080038739A1 (Li *et al.*, 2008).

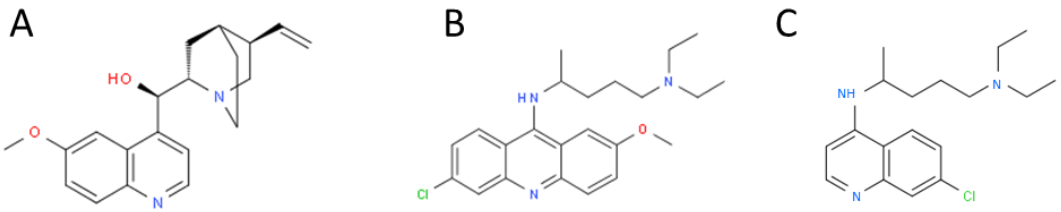

Figure 2.1: Chemical structures of A) quinine, B) quinacrine and C) chloroquine
All three are reported to taste bitter to humans.

In order to find as many active compounds for dog Tas2rs in the most efficient way, not all compound-receptor combinations were initially screened in a full concentration-response experiment. Instead, all compound-receptor combinations were tested in a pre-screen experiment where compounds were tested at the highest soluble concentration, then at 1/10 and 1/100 dilutions. Anything identified as a potential ligand from this screen was then tested in a full concentration–response experiment in two phases. The initial phase of testing was performed with a calcium mobilisation assay on the FlexStation instrument at the Waltham laboratory (n=1). Any receptor-compound combinations still showing evidence of specific activity were retested using the same assay setup and procedures, but with a Hamamatsu FDSS/µCELL system at the IMAX Discovery laboratory where 3 independent experiments were performed (n=3).

2.1.2. Identifying a heterologous expression system for Tas2rs.

Testing of Tas2rs in heterologous cell models has been performed for over 20 years. Native taste receptor cells can be cultured *in vitro* (Kishi *et al.*, 2001; Ozdener *et al.*, 2006), but may express multiple Tas2rs, which makes them less suitable for studies of specific receptor-ligand interactions. The first example of a Tas2r heterologous cell model used Tas2rs tagged with the first 39 amino acids of bovine rhodopsin at the N-terminus. The rhodopsin tag increased localisation to the plasma membrane in all the Tas2rs tested (Chandrashekar *et al.*, 2000). Later work identified a signal sequence consisting of the first 45 amino acids of the rat somatostatin type III receptor (rSstr3) (Ammon *et al.*, 2002) which has also been successfully, and more extensively, used for improving localisation of Tas2rs to the plasma membrane (Bufe *et al.*, 2002; Meyerhof *et al.*, 2010; Lossow *et al.*, 2016).

The expression of Tas2rs in the oral cavity has been shown to be exclusively associated with taste cells expressing the $G_{\alpha gust}$ subunit, a member of the $G_{i/o}$ family (Adler *et al.*, 2000) and to couple efficiently with $G_{\alpha gust}$, *in vitro* (Chandrashekar *et al.*, 2000). Gustducin was discovered in 1992 (McLaughlin *et al.*, 1992) and was first thought to be exclusively-expressed in taste papillae, but is now known to be expressed in the gastrointestinal (GI) tract as well (Hass *et al.*, 2007; Jang *et al.*, 2007). However, gustducin may not be the only G protein mediating Tas2r function. Mice lacking $G_{\alpha gust}$ show suppressed, but not completely abolished sensitivity to bitter compounds (Wong *et al.*, 1996). Caicedo *et al.* (2003) showed that $G_{\alpha i2}$ was also present in most bitter sensitive cells. Additionally, TAS2Rs in human airway smooth muscle have been shown to signal through $G_{\alpha i1}$, $G_{\alpha i2}$ and $G_{\alpha i3}$, while $G_{\alpha gust}$ is only expressed at trace levels in this tissue (Kim *et al.*, 2017).

The $G_{\alpha gust}$ subunit itself is not attractive for heterologous cell models. It does not couple readily with the βγ subunits that are endogenously-expressed in the HEK cell line (Slack *et al.*, 2005), whereas the promiscuous G_q class G_α subunit $G_{\alpha 16}$ does (Offermanns *et al.*, 1995). $G_{\alpha 16}$ also couples Tas2r activation in HEK cells to calcium

release by interacting directly with PLCβ and increasing production of IP_3 and DAG. However, $G_{\alpha16}$ failed to couple effectively with Tas2rs (Ueda *et al.*, 2003). A series of $G_{\alpha16/gust}$ chimeras were tested where different sections of the C-terminal of $G_{\alpha gust}$ were joined with the N-terminal of $G_{\alpha16}$. The C-terminal of the G_{α} subunit is known to be essential to GPCR-G protein interactions (Conklin *et al.*, 1993; Semack *et al.*, 2016). Of the tested $G_{\alpha16/gust}$ chimeras, two ($G_{\alpha16/gust37}$ and $G_{\alpha16/gust44}$) showed effective coupling for a mouse and human Tas2r, indicating that, using the crystal structure of related transducin ($G_{\alpha t1}$) as a basis, at least a β6 sheet, an α5 helix, and the extreme C-terminus of $G_{\alpha gust}$, are required for effective coupling (Ueda *et al.*, 2003). It was also shown that $G_{\alpha16/i2-44}$ and $G_{\alpha16/t2-44}$ chimeras were equally effective at coupling with Tas2rs which was not surprising given their near identical C-terminal regions when compared to $G_{\alpha gust}$ (Figure 2.2). However, the $G_{\alpha16/gust44}$ chimera was patented before being publicly disclosed (Slack *et al.*, 2005) and was not available at the start of this study. Therefore, an alternative commercially-available cell line was used (IMAX Discovery GmbH, Dortmund, Germany). This cell line stably expresses a $G_{\alpha16/gust/o}$ chimeric G-protein which, when tested with a limited number of human TAS2Rs and ligands, gave equivalent data to that published for the $G_{\alpha16/gust44}$ chimera. The last 44 amino acids of the chimera consist of $G_{\alpha gust1-6}$, $G_{\alpha o7-38}$ and $G_{\alpha gust39-44}$. The $G_{\alpha o}$ sequence is specific to GNAO1 isoform 1 in human, not the differently-spliced isoform 2. Sequence differences between the two chimeras are shown in Figures 2.2 and 2.3.

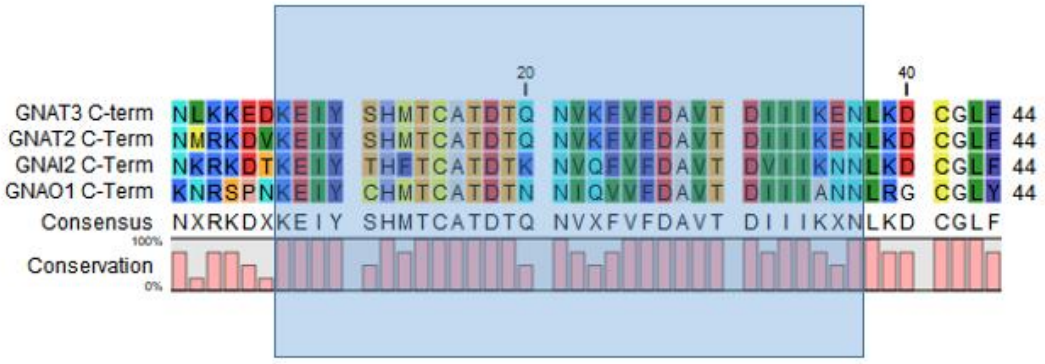

Figure 2.2: Alignment of the C-termini for the G_{α}subunits GNAT3 ($G_{\alpha gust}$), GNAT2 ($G_{\alpha t}$), GNAI2 and GNAO1

The 31 amino acid section of GNAO1 used in the $G_{\alpha 16/gust/o}$ chimera is highlighted.

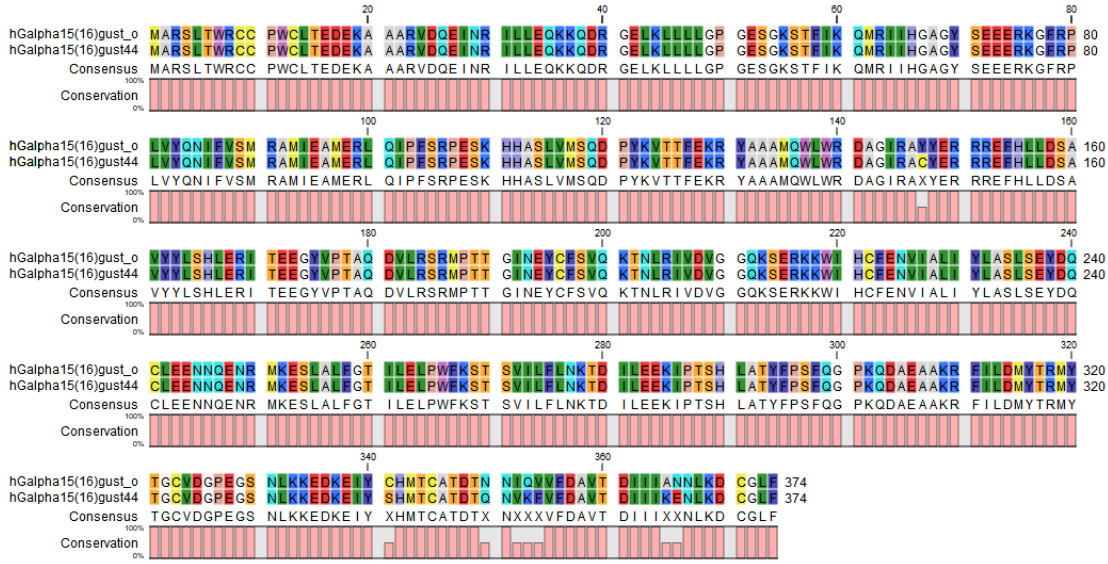

Figure 2.3: Alignment of the G protein chimera sequences for $G_{\alpha 16/gust44}$ and $G_{\alpha 16/gust/o}$

The $G_{\alpha 16/gust/o}$ chimera contains the $G_{\alpha 16}$ naturally-occurring variant rs310680 at position 147. Other differences are within the $G_{\alpha o7\text{-}38}$ sequence within the last 44 amino acid section.

Data provided by IMAX Discovery showed equivalent threshold sensitivity levels when compared to published data for $G_{\alpha 16/gust44}$ for the new chimera, with both hTAS2R10 with denatonium benzoate and hTAS2R14 with aristolochic acid.

2.1.3. Alternative heterologous expression systems for Tas2rs.

GPCR-G protein selectivity is determined by interactions between the intracellular side of the GPCR and the Gα, and to a lesser extent the Gβ, G protein subunits (Flock et al., 2017; Garcia-Nafria et al., 2019), but many other factors can exert an influence on this selectivity. In order to ascertain the impact of the novel G protein chimera used here, comparative work with the widely used $G_{\alpha16/gust44}$ chimera was desirable. Permission was sought to use the $G_{\alpha16/gust44}$ cell line from the patent holder Givaudan Inc., and was granted, with a cell line stably expressing $G_{\alpha16/gust44}$ being obtained. A limited programme of testing was performed using all compounds with dog and human Tas2r1 so that these responses could be compared between the two chimera expressing cell lines.

2.2. Aims of this Chapter

This Chapter aimed to identify as many compounds as possible with agonist activity against any of the dog Tas2rs. Compounds were selected based on known ligands for orthologous human receptors. Dog Tas2rs were expressed in a heterologous cell-based assay which utilised an N-terminal rSstr3 tag to facilitate correct localisation of Tas2rs to the plasma membrane. Two chimeric α G-protein subunits were tested and used to provide effective coupling from dog Tas2rs to an easily-measured signalling endpoint (calcium mobilisation), and retain the ability to interact with the endogenous βγ G-protein subunits expressed in the HEK cell line. Compounds were tested at three concentrations to provide an indication of potency and a shortlist for testing in a full concentration-response experiment.

2.3. Materials and methods

2.3.1. General molecular biology techniques

2.3.1.1. Polymerase chain reaction

Where polymerase chain reaction (PCR) was conducted, primers were designed using Primer-BLAST (Ye *et al.*, 2012) and synthesised by Eurofins (Ebersberg, Germany). Primers were typically used at a working concentration of 10μM with

0.5µL added per 25µL PCR to give a final concentration of 0.2µM. JumpStart™ *Taq* ReadyMix (Sigma-Aldrich, UK) was used for all general PCRs. This master mix contains an antibody which inactivates the *Taq* polymerase enzyme until a temperature above 70°C is reached, at which point the enzyme/antibody complex dissociates and full activity is restored. Such antibodies allow reactions to be prepared at room temperature and reduce or eliminate the formation of non-specific products and primer-dimers (Sharkey *et al.*, 1994). All reactions were prepared in 0.2mL thin-walled tubes. Thermal cycling was performed on a PCRmax AC-4 instrument (PCRmax, UK). Cycling parameters were set according to the manufacturer's recommendations for the master mix. An initial denaturation step of 94°C for two minutes was performed before a maximum of 35 cycles of amplification (Figure 2.4). Annealing temperatures of 1-2°C below the primer melting temperatures (Tm) were typically used. A final elongation step of 72°C for five minutes was performed to allow full extension of any incomplete products. Following completion of the thermal cycling, reactions were held at 4°C until they were collected and stored at -20°C.

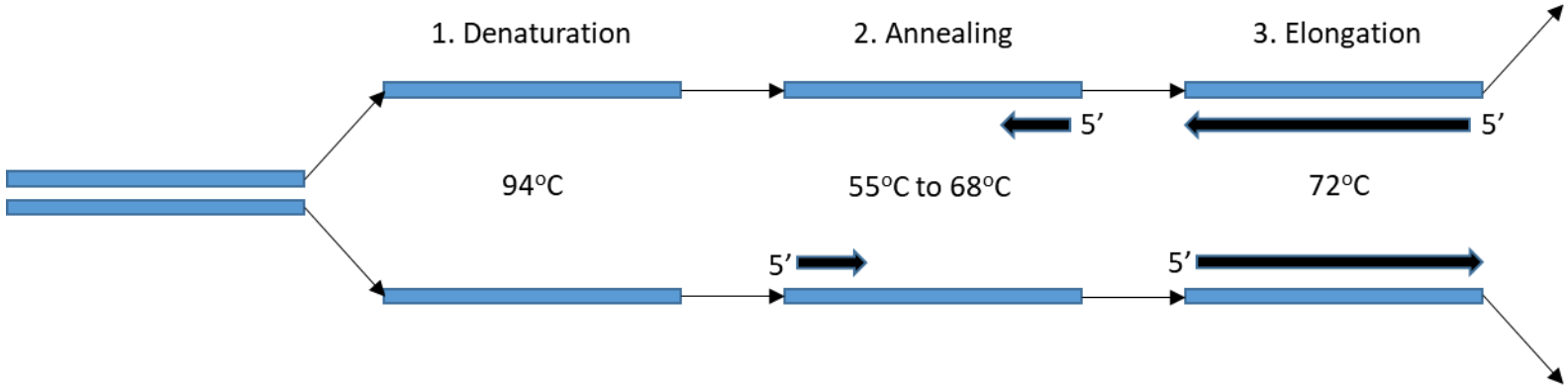

Figure 2.4: Polymerase chain reaction (PCR) amplifies specific double stranded DNA fragments. PCR starts with denaturation of the template DNA. Annealing of oligonucleotide primers follows as the temperature is reduced. Taq polymerase then extends the primers in a 5’ to 3’ direction during the elongation step. Further cycles of the same process cause a doubling of the number of template molecules at each cycle.

2.3.1.2. Gel electrophoresis

In order to check for the presence of PCR products of the correct size, and to separate DNA fragments from restriction digests for cloning, agarose gel electrophoresis was performed. Agarose gel electrophoresis uses an electric current passed through a porous agarose gel matrix to separate DNA fragments based on their size. Negatively charged DNA molecules migrate through the gel towards the positive electrode at different rates depending on their length. Here, 1% agarose gel was used routinely. Agarose (Thermo Fisher Scientific, UK) was weighed into a suitable flask and dissolved in buffer containing 40mM tris base, 20mM acetic acid and 1mM ethylenediaminetetraacetic acid (EDTA) (1X TAE buffer) (Sigma Aldrich, UK). The agarose was dissolved in the buffer by heating the mixture in a microwave oven. Once fully dissolved, the solution was allowed to cool for a few minutes before being poured into a gel frame with suitable gel combs inserted. The gel was allowed to cool and set completely before being transferred to an electrophoresis tank and submerged in 1X TAE buffer. Restriction digested DNA or PCR reaction products were mixed with 6X loading dye (Thermo Fisher Scientific, UK) before being loaded into the wells of the gel. A DNA size marker, 1kb Plus DNA Ladder (Thermo Fisher Scientific, UK), was also mixed with loading dye and water, and loaded into the gel in appropriate positions. Standard gels were 15cm x 15cm in size and 100V were applied for a period of 1.5 hours, or until sufficient separation was achieved to visualise individual fragments. Gels were then removed from the tray and post-stained with GelRed (Biotium, USA) for 45 minutes on a rocking platform before imaging with a UVP GelDoc-It system (Analytik Jena, Germany).

2.3.1.3. Gel extraction

In cases where recovery of a DNA fragment from a restriction digest was required for ligation, the gel was not visualised on the UVP GelDoc-It system, but on a blue light Safe Imager (Thermo Fisher Scientific, UK) to avoid exposure of laboratory personnel to UV light. DNA bands of interest were excised with a clean scalpel and weighed before DNA extraction with the QIAquick gel extraction kit (Qiagen, Germany). This

kit uses a silica membrane for binding DNA under high chaotropic salt conditions, and then eluting under low salt conditions. The gel slice was initially dissolved in 3 volumes of the high salt buffer at 50°C for 10 minutes. One volume of isopropanol was added to improve recovery of DNA fragments ≤500bp and ≥4 kb. An ethanol containing buffer was then used to wash the DNA before elution in a low salt buffer suitable for storage of the DNA.

2.3.1.4. Restriction digestion and ligation

For general restriction cloning, SuRE/Cut™ enzymes and buffers were purchased from Roche (Roche, UK). Typically, sub-cloning of *Tas2rs* was performed with EcoRI and XhoI, generating "sticky ends" for ease of ligation into the pcDNA5/FRT/TO expression vector containing the rSstr3 tag. Ligation was performed with T4 DNA Ligase (Thermo Fisher Scientific, UK). Restriction digestion was performed in thin-walled 0.2µL tubes as 50µL reactions. The required Roche buffer, in most cases buffer H, was used. Reagent volumes varied depending on the volume of DNA used, but generally 5µL of buffer H was used with 10 units of each enzyme, 10µg plasmid DNA and nuclease-free water (Qiagen, Germany) to a final volume of 50µL. Reactions were incubated at 37°C for 1 hour. Ligation was performed in 20µL reaction volumes with a 3:1 insert to vector molar ratio and 0.5 units of ligase. Reactions were incubated at room temperature for 1 hour.

2.3.1.5. Transformation

Transformation of plasmid DNA into *E.coli* was performed using One Shot TOP10 chemically-competent cells (Thermo Fisher Scientific, UK) using the standard heat shock protocol as indicated by the manufacturer. Aliquots of competent cells were thawed on ice before the addition of 5µL of ligation reaction or 10ng of plasmid DNA. Cells were then incubated on ice for 30 minutes to allow the DNA to associate with the cells. Cells were then heat-shocked at exactly 42°C for 30 seconds to allow entry of the DNA into the cells. This was followed by a 2 minute incubation on ice before the addition of 250µL of super-optimal broth with catabolite suppression

(SOC) media pre-warmed to 37°C. Cells were plated onto LB agar (Sigma Aldrich, UK) containing 100µg/mL ampicillin (Sigma Aldrich, UK) and incubated overnight at 37°C. The next day a single colony was re-streaked onto another selective agar plate and incubated overnight. The following day, a single colony was picked and used for plasmid DNA preparation with two different methods, depending on the application.

2.3.1.6. Plasmid DNA preparation

Plasmid DNA preparation was conducted with either the NucleoSpin Plasmid Mini kit (Machery Nagel, Germany) for small-scale preparations, or the Nucleobond Xtra Midi Plus kit for transfection-grade plasmid DNA in larger quantities (Machery Nagel, Germany).

For the NucleoSpin method, 5mL LB broth (Sigma Aldrich, UK) containing 50µg/mL ampicillin was inoculated from a single colony of transformed *E.coli*. Cultures were incubated overnight at 37°C with shaking at 225rpm. Cells were pelleted by centrifugation for 2 minutes at 11,000g. Cells were resuspended in a buffer containing RNase A to remove RNA. Cells were then lysed with a sodium dodecyl sulphate (SDS)/alkaline lysis buffer. SDS lyses the cell membrane and removes proteins from the plasmid DNA. The buffer also contains NaOH which denatures chromosomal DNA. A neutralising buffer was added which causes proteins and chromosomal DNA to precipitate, while plasmid DNA remains soluble. This buffer also contains chaotropic salts to create the conditions required for the plasmid DNA to bind to the silica column. The solution was then centrifuged for 5 minutes at 11,000g to pellet the precipitated debris. The supernatant was spun through the silica column and then the column was washed with an 80% EtOH buffer before being dried by centrifugation for 2 minutes at 11,000g. The plasmid DNA was then eluted from the column with 50µL of 5mM Tris/HCl, pH 8.5.

The NucleoBond Xtra Midi Plus kit employs many of the same reagents as the NucleoSpin Mini kit. A starter culture was prepared by inoculating 5mL of LB broth (Sigma Aldrich, UK) containing 50µg/mL ampicillin (Sigma Aldrich, UK) with a single

colony of transformed *E.coli*. This was incubated at 37°C with shaking at 225rpm for 8 hours before being used to inoculate 180mL of the same growth media in a 1L plastic Erlenmeyer flask with baffles and a vented lid (Corning, US). This larger culture was incubated at 37°C with shaking at 225rpm for 17 hours overnight. The next day a glycerol stock of the culture consisting of 500µl of culture and 500µl of 50% glycerol solution was prepared for long term storage at -80°C before the plasmid DNA was extracted. The extended protocol for extraction was used as provided by the manufacturer. Cultures were transferred to V-bottom 250mL centrifuge tubes (Corning, US) and centrifuged at 5,000g for 10 minutes at 4°C. The supernatant was discarded completely and the cell-pellet was re-suspended in buffer containing RNase A. Cells were then lysed with SDS/alkaline buffer containing a blue "LyseControl" agent. Addition of the neutralisation buffer and gentle inversion of the tube causes precipitation of the protein and chromosomal DNA. The blue colour disappears at this point and is designed to ensure proper mixing occurs. The binding columns were equilibrated with an ethanol/KCl buffer before the whole mixture was poured into the column filter and allowed to pass through the column under gravity. The filter was then washed with the same ethanol/KCl buffer used to equilibrate the column. The column filter was removed before washing the column with another ethanol-containing buffer to remove any residual contaminants. DNA was eluted in a low-salt buffer before the addition of isopropanol to precipitate the DNA. Next the DNA was loaded into a syringe and passed through a NucleoBond "Finaliser", which desalts and concentrates the DNA. The "Finaliser" is an alternative method to washing and drying of pelleted DNA. An ethanol wash was followed by drying of the "Finaliser" by forcing air through it 8-10 times or until no further liquid was expelled onto paper towel. DNA was eluted with 300µL 5mM Tris/HCl, pH 8.5. The eluate was passed through the "Finaliser" twice before being quantified with a Nanodrop spectrophotometer (Thermo Fisher, UK) and adjusted to 1µg/µL or as close to that concentration as possible. An absorbance ratio (260:280nm) of ~1.8 indicated pure DNA in all cases. Plasmid DNA was then aliquoted into 30µL volumes before being stored at -20°C. A sample of the plasmid DNA was sent for re-sequencing using the CMV forward primer and the BGH reverse primer. Results were checked to confirm the correct sequence before using the plasmid.

2.3.1.7. Sanger sequencing

Plasmid DNA for transfection, including that generated by site-directed mutagenesis (SDM), was re-sequenced before use. Sanger Sequencing (Sanger *et al.*, 1975; Sanger *et al.*, 1977) was carried-out using the Eurofins Mix2Seq service (Ebersberg, Germany). Mix2Seq tubes were prepared with 15µL of plasmid DNA at a concentration of 100ng/µL. Two microliters of the relevant sequencing primer (CMV forward or BGH reverse primer) at a concentration of 10µM was added to the tube.

2.3.1.8. Transfection

Introduction of plasmid DNA into the recipient HEK cell line was achieved using lipofection (Felgner *et al.*, 1987) with Lipofectamine 2000 reagent (Thermo Fisher Scientific, UK). Lipofection is achieved with cationic lipids which associate with negatively-charged nucleic acids and form lipid-DNA complexes having an overall positive charge. This allows the interaction of the complexes with the negatively-charged cell membrane, and uptake of the DNA into the cells, mainly through endocytosis (Chesnoy *et al.*, 2000). Subsequently, the DNA enters the nucleus where transcription can take place.

2.3.2. Cell lines

Upon receipt in the laboratory, cell lines were stored at around –191°C in a dry liquid nitrogen store (Custom Biogenic Systems, US). To resurrect the cells, one vial was removed from the store and thawed immediately by swirling the cryovial in a 37°C water bath, taking care not to submerge the tube more than halfway. The tube was sterilised with a 70% EtOH spray before being transferred to a laminar flow cabinet. The contents of the cryovial were quickly transferred to a 15mL polypropylene tube (Corning, US) containing 10mL of DMEM High-glucose (41956, Thermo Fisher Scientific, UK) with only 10% heat denatured FBS (16000, Thermo Fisher Scientific, UK) and 1% of a stock solution containing 10,000 units/mL penicillin and 10000ug/mL streptomycin (Thermo Fisher Scientific, UK) added. The tube was centrifuged slowly at 125 x g for 5 minutes. The supernatant was carefully removed

and the cells were re-suspended in 10mL fresh media before being plated into a T75 cell culture flask (Thermo Fisher Scientific, UK). All cell lines were tested for the presence of mycoplasma using the MycoAlert™ test kit (Lonza, Switzerland).

The screening experiments were performed using HEK293 PeakRapid cells stably-expressing $G_{\alpha16/gust/o}$ chimeric G protein and nat-Clytin, a calcium sensitive photoprotein (Axxam SpA, Milan, Italy). The cell line was maintained in the same medium as used for resurrection with the addition of 50µg/ml G418, 25µg/ml Hygromycin and 2.5µg/ml Blasticidin (Thermo Fisher Scientific, UK). Standard propagation conditions consisted of seeding 1.5 - 1.8x10^6 cells in a T75 flask twice a week, recovering about 10-15x10^6 cells at about 70% confluence. Larger T225 flasks were used when more cells were required for screening experiments. Some experiments were conducted using the $G_{\alpha16/gust44}$ expressing cell line and in these cases the culture media used consisted of the same DMEM high-glucose base with 10% heat denatured FBS, 1% Glutamax (35050-061, Thermo Fisher Scientific, UK), 1% of the same penicillin/streptomycin solution and 40µg/ml of G418 added.

2.3.3. Compound sourcing and preparation

Compounds were sourced from Sigma-Aldrich (Gillingham, UK) where possible. The exceptions were 6-nitrosaccharin from CarboSynth (Compton, UK) and diphenidol from Tokyo Chemical Industry (Oxford, UK). Compound details including supplier and product numbers are given in Appendix 2.1.

When testing compound-receptor combinations in a cell-based assay system there are two factors that often limit the concentration which may be tested, the solubility of the compound and the occurrence of responses that are not receptor-specific in the cells. Compounds were prepared in assay buffer, also referred to as Tyrode's buffer, which comprised 1mM magnesium chloride, 130mM sodium chloride, 5mM potassium chloride, 2mM calcium chloride, 5mM sodium bicarbonate and 20mM 4-(2-hydroxyethyl)-1-piperazineethanesulfonic acid (HEPES) with pH adjusted to 7.4

with 10M sodium hydroxide (Sigma-Aldrich, UK). To improve compound solubility, additional solvents are sometimes used with the most common choice being dimethyl sulfoxide (DMSO). However, DMSO itself can cause non-specific responses in the cells, so the sensitivity of the cell line to DMSO must first be established. The $G_{\alpha16/gust/o}$ cell line was tested for DMSO sensitivity and was found to tolerate a concentration of 1% DMSO without any response being recorded in the assay used here.

It is not guaranteed that using DMSO will improve solubility as compounds often precipitate when diluted at the appropriate concentration in assay buffer after being pre-dissolved at a higher concentration in DMSO. Based on the idea that it was only worth using DMSO if it improved solubility, all compounds were initially tested with DMSO to see if any significant improvement in solubility was seen by visual inspection. Final preparation details are shown in Table 2.2. If a compound was pre-dissolved in DMSO, assay buffer was supplemented with the same final concentration of DMSO so that all tests were representative, even when a vehicle only control was used.

Table 2.2: Preparation details for all compounds used in this study

Compound ID	**Compound**	**Solvent**	**Max (or2X) Solubility at RT**
C1	1, 10-Phenanthroline	Tyrode's buffer	20mM
C2	4-Benzylpiperidine	Tyrode's buffer	20mM
C3	6-Nitrosaccharin	Tyrode's buffer	20mM
C4	Acetaminophen	Tyrode's buffer	100mM
C5	6α-Methylprednisolone	Tyrode's buffer	1mM
C6	Aloin	Tyrode's buffer	1mM
C7	(-)-α-Thujone	Tyrode's buffer	12.5mM

C8	Aristolochic acid I	Tyrode's buffer	6.25/1mM
C9	Brucine sulphate salt hydrate	Tyrode's buffer	25mM
C10	(-)-Camphor	Tyrode's buffer	25mM
C11	Chloramphenicol	Tyrode's buffer	2.5mM
C12	Chlorhexidine	Tyrode's buffer	0.1mM
C13	Chloroquine diphosphate salt	Tyrode's buffer	200mM
C14	Colchicine	Tyrode's buffer	200/20mM
C15	Cucurbitacin B hydrate	Pre-dissolve in DMSO at 1000mM, use buffer +0.1% DMSO	1mM
C16	Cycloheximide	Tyrode's buffer	50mM
C17	Denatonium benzoate	Tyrode's buffer	100mM
C18	Dextromethorphan hydrobromide monohydrate	Tyrode's buffer	50mM
C19	1,1-Dimethylbiguanide hydrochloride	Tyrode's buffer	200mM
C20	1,1-Diphenyl-4-piperidino-1-butanol hydrochloride (Diphenidol)	Tyrode's buffer	6mM
C21	Doxepin hydrochloride	Tyrode's buffer	200mM
C22	Ethylpyrazine	Tyrode's buffer	200mM
C23	Flavone	Tyrode's buffer	0.4mM
C24	N-(3-Oxooctanoyl)-L-homoserine lactone	Tyrode's buffer	10mM
C25	Aurintricarboxylic acid	Tyrode's buffer	5mM
C26	L-Menthol	Tyrode's buffer	3.125mM
C27	Ofloxacin	Tyrode's buffer	12.5mM

C28	Oleuropein	Tyrode's buffer	100mM
C29	Omeprazole	Tyrode's buffer	1mM
C30	Oxybutynin chloride	Make 200mM DMSO stock then dilute in buffer +0.1% DMSO	200µM
C31	Oxyphenonium bromide	Tyrode's buffer	200mM
C32	Papaverine hydrochloride	Tyrode's buffer	10mM
C33	Parthenolide	Tyrode's buffer	400µM
C34	Picrotoxin	Tyrode's buffer	1mM
C35	Pirenzepine dihydrochloride	Tyrode's buffer	50mM
C36	Prednisone	Tyrode's buffer	1mM
C37	6-Propyl-2-thiouracil (PROP)	Pre-dissolve in DMSO at 2000mM, use buffer +0.23%	5mM
C38	N-Phenylthiourea (PTC)	Pre-dissolve in DMSO at 2000mM, use buffer +0.23%	5mM
C39	Quinacrine dihydrochloride	Tyrode's buffer	25mM
C40	Quinine hydrochloride dihydrate	Tyrode's buffer	12.5mM
C41	Resveratrol	Tyrode's buffer	1.5mM
C42	Sucralose	Tyrode's buffer	200mM
C43	D-(-)-Salicin	Tyrode's buffer	100mM
C44	Sinigrin hydrate	Tyrode's buffer	100mM
C45	Strychnine hydrochloride	Tyrode's buffer	6mM
C46	Thiamine hydrochloride	Tyrode's buffer	200mM
C47	Trimethoprim	Pre-dissolve in DMSO at 100mM, use buffer +0.1% DMSO	100µM

C48	Yohimbine	Pre-dissolve in DMSO at 100mM, use buffer +0.6% DMSO	600µM

2.3.4. Expression vector

Dog and human *Tas2r* gene sequences were sub-cloned into the pcDNA5/FRT/TO expression vector (Figure 2.5) downstream of the rSstr3 tag. An EcoRI sequence at the start of the *Tas2r* sequence and an XhoI sequence at the end facilitated easy cloning of multiple *Tas2r* sequences into the vector. Both EcoRI and XhoI are compatible with the same buffer for restriction digestion (Buffer H, Sigma-Aldrich, UK). *Tas2r* sequences were synthesised by Eurofins (Eurofins Genomics, Ebersberg, Germany) according to the sequences identified in Chapter 1.

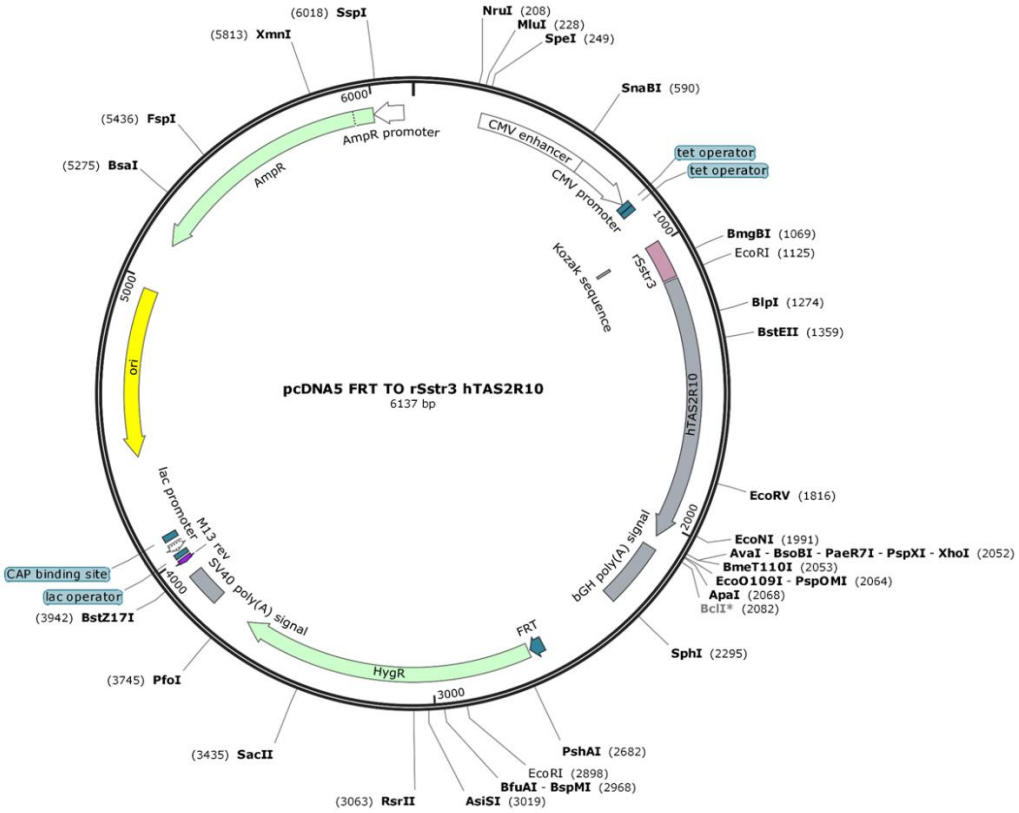

Figure 2.5: A plasmid map of the expression construct pcDNA5 FRT TO/rSstr3/hTAS2R10

All Tas2rs were cloned into this vector. Abbreviations not previously defined: Ampicillin Resistance (AmpR), Bovine Growth Hormone (bGH), Cytomegalovirus (CMV), Flp Recombination Target (FRT), Hygromycin Resistance (HygR), Origin of Replication (ori), Toposiomerase (TOPO), Tetracycline operator (tet operator). Inducible expression controlled with the tet operator was not used in these experiments.

2.3.5. Assay preparation and execution – Pre-screen

The calcium mobilisation assay was run over a two day period. On day one, culture media without selection antibiotics (Dulbecco's Modified Eagle's Medium + 4.5g/L D-Glucose + L-Glutamine - Pyruvate (DMEM), 10% Foetal Bovine Serum (FBS), 1% Penicillin/Streptomycin) (Thermo Fisher Scientific, UK), transfection media (DMEM) and trypsin (0.25% Trypsin) was brought to 37°C in a water bath. In a 2mL Eppendorf DNA Low-Bind tube (Eppendorf, UK) 10µL of Lipofectamine 2000 (Thermo Fisher Scientific, UK) was combined with 500µL DMEM and incubated at room temperature

for a minimum of 5 minutes. A separate 2mL tube was used to combine 3µg of expression plasmid DNA with 500µL of DMEM. The Lipofectamine and DNA mixes were then combined and incubated at room temperature for 30 minutes.

The cells were washed once with Phosphate Buffered Saline (PBS) (Thermo Fisher Scientific, UK). Trypsin was then gently washed over the cells before any excess trypsin was removed. Cells were returned to the incubator for a few minutes and then checked. A slight tap on the side of the flask was used to detach all cells and 10mL of culture media was used to re-suspend the cells. The cells were counted using the Nucleocounter (Chemometec, Allerod, Denmark) and the volume adjusted to give a suspension of $1.6x10^6$ cells/mL. One millilitre of cells was then added to each transfection mixture and mixed by inverting the tube several times before plating 25µL of the mixture into each well of a poly-D-lysine coated 384-well assay plate (354663, Corning, UK). Cells were returned to the incubator for 3 hours, after which 25µL/well of culture media was added to the cells and they were returned to the incubator overnight.

On day 2, a pre-prepared compound plate was removed from the -20^{o}C freezer and allowed to thaw at room temperature. Adenosine triphosphate (ATP) (Sigma-Aldrich, UK) was prepared with Tyrode's buffer at a concentration of 20µM and a dilution series was prepared at ½ concentrations. ATP stimulates the P2Y1 and P2Y2 receptors endogenously expressed in the HEK cell line (Schachter *et al.*, 1997), and was used here as a control for maximal stimulation. These were added to the plate according to the layout shown in Figure 2.6. Cal-520 dye (AAT Bioquest, Sunnyvale, USA) previously prepared in DMSO at a concentration of 500µM was added to Tyrode's buffer at 2µM with water soluble probenecid (Thermo Fisher Scientific, UK) at a concentration of 2.5mM. Cell plates were removed from the incubator and media was removed by flicking the plate onto paper towel. The dye solution was added to the plate at 20µL/well. The plate was then incubated at room temperature in the dark for 3 hours.

	1	2	3	4	5	6	7	8	9	10	11	12	13	14	15	16	17	18	19	20	21	22	23	24
A	ATP	ATP	C1	C1	C1	C1	C1	C1	C9	C9	C9	C9	C9	C9	C17	C17	C17	C17	C17	C17			ATP	ATP
B	ATP	Buffer	C1	C1	C1	C1	C1	C1	C9	C9	C9	C9	C9	C9	C17	C17	C17	C17	C17	C17			Buffer	ATP
C	ATP	ATP	C2	C2	C2	C2	C2	C2	C10	C10	C10	C10	C10	C10	C18	C18	C18	C18	C18	C18			ATP	ATP
D	ATP	Buffer	C2	C2	C2	C2	C2	C2	C10	C10	C10	C10	C10	C10	C18	C18	C18	C18	C18	C18			Buffer	ATP
E	ATP	ATP	C3	C3	C3	C3	C3	C3	C11	C11	C11	C11	C11	C11	C19	C19	C19	C19	C19	C19			ATP	ATP
F	ATP	Buffer	C3	C3	C3	C3	C3	C3	C11	C11	C11	C11	C11	C11	C19	C19	C19	C19	C19	C19			Buffer	ATP
G	ATP	ATP	C4	C4	C4	C4	C4	C4	C12	C12	C12	C12	C12	C12	C20	C20	C20	C20	C20	C20			ATP	ATP
H	ATP	Buffer	C4	C4	C4	C4	C4	C4	C12	C12	C12	C12	C12	C12	C20	C20	C20	C20	C20	C20			Buffer	ATP
I	ATP	ATP	C5	C5	C5	C5	C5	C5	C13	C13	C13	C13	C13	C13	C21	C21	C21	C21	C21	C21			ATP	ATP
J	ATP	Buffer	C5	C5	C5	C5	C5	C5	C13	C13	C13	C13	C13	C13	C21	C21	C21	C21	C21	C21			Buffer	ATP
K	ATP	ATP	C6	C6	C6	C6	C6	C6	C14	C14	C14	C14	C14	C14	C22	C22	C22	C22	C22	C22			ATP	ATP
L	ATP	Buffer	C6	C6	C6	C6	C6	C6	C14	C14	C14	C14	C14	C14	C22	C22	C22	C22	C22	C22			Buffer	ATP
M	ATP	ATP	C7	C7	C7	C7	C7	C7	C15	C15	C15	C15	C15	C15	C23	C23	C23	C23	C23	C23			ATP	ATP
N	ATP	Buffer	C7	C7	C7	C7	C7	C7	C15	C15	C15	C15	C15	C15	C23	C23	C23	C23	C23	C23			Buffer	ATP
O	ATP	ATP	C8	C8	C8	C8	C8	C8	C16	C16	C16	C16	C16	C16	C24	C24	C24	C24	C24	C24			ATP	ATP
P	ATP	Buffer	C8	C8	C8	C8	C8	C8	C16	C16	C16	C16	C16	C16	C24	C24	C24	C24	C24	C24			Buffer	ATP

	1	2	3	4	5	6	7	8	9	10	11	12	13	14	15	16	17	18	19	20	21	22	23	24
A	ATP	ATP	C25	C25	C25	C25	C25	C25	C33	C33	C33	C33	C33	C33	C41	C41	C41	C41	C41	C41			ATP	ATP
B	ATP	Buffer	C25	C25	C25	C25	C25	C25	C33	C33	C33	C33	C33	C33	C41	C41	C41	C41	C41	C41			Buffer	ATP
C	ATP	ATP	C26	C26	C26	C26	C26	C26	C34	C34	C34	C34	C34	C34	C42	C42	C42	C42	C42	C42			ATP	ATP
D	ATP	Buffer	C26	C26	C26	C26	C26	C26	C34	C34	C34	C34	C34	C34	C42	C42	C42	C42	C42	C42			Buffer	ATP
E	ATP	ATP	C27	C27	C27	C27	C27	C27	C35	C35	C35	C35	C35	C35	C43	C43	C43	C43	C43	C43			ATP	ATP
F	ATP	Buffer	C27	C27	C27	C27	C27	C27	C35	C35	C35	C35	C35	C35	C43	C43	C43	C43	C43	C43			Buffer	ATP
G	ATP	ATP	C28	C28	C28	C28	C28	C28	C36	C36	C36	C36	C36	C36	C44	C44	C44	C44	C44	C44			ATP	ATP
H	ATP	Buffer	C28	C28	C28	C28	C28	C28	C36	C36	C36	C36	C36	C36	C44	C44	C44	C44	C44	C44			Buffer	ATP
I	ATP	ATP	C29	C29	C29	C29	C29	C29	C37	C37	C37	C37	C37	C37	C45	C45	C45	C45	C45	C45			ATP	ATP
J	ATP	Buffer	C29	C29	C29	C29	C29	C29	C37	C37	C37	C37	C37	C37	C45	C45	C45	C45	C45	C45			Buffer	ATP
K	ATP	ATP	C30	C30	C30	C30	C30	C30	C38	C38	C38	C38	C38	C38	C46	C46	C46	C46	C46	C46			ATP	ATP
L	ATP	Buffer	C30	C30	C30	C30	C30	C30	C38	C38	C38	C38	C38	C38	C46	C46	C46	C46	C46	C46			Buffer	ATP
M	ATP	ATP	C31	C31	C31	C31	C31	C31	C39	C39	C39	C39	C39	C39	C47	C47	C47	C47	C47	C47			ATP	ATP
N	ATP	Buffer	C31	C31	C31	C31	C31	C31	C39	C39	C39	C39	C39	C39	C47	C47	C47	C47	C47	C47			Buffer	ATP
O	ATP	ATP	C32	C32	C32	C32	C32	C32	C40	C40	C40	C40	C40	C40	C48	C48	C48	C48	C48	C48			ATP	ATP
P	ATP	Buffer	C32	C32	C32	C32	C32	C32	C40	C40	C40	C40	C40	C40	C48	C48	C48	C48	C48	C48			Buffer	ATP

Figure 2.6: Layout of the compound library on the pre-screen plates
Compounds were tested at three concentrations represented as different shades of blue, with the darker shade representing the higher concentration. ATP control columns were added to the plates on the day of use, again colour relates to concentration with the darkest shade being the highest concentration.

After this incubation, the cell plate was washed on a plate washer (Asys Atlantis, Biochrom, UK) with 100µL of room temperature Tyrode's buffer. The buffer was then aspirated off and this was repeated. A final aspiration step left a volume of 25µL of buffer remaining. The plate was then incubated for a further 15 minutes in the dark before being transferred to the FlexStation along with the compound plate and a box of black 384-well FlexStation tips (Molecular Devices, 9000-0764).

Plates were read on the FlexStation with an excitation wavelength of 485nm and an emission wavelength of 525nm. The cut-off for emission was automatically set at 515nm. Total read time for each column was 90 seconds, with read intervals of 2

seconds. Test compound (25µL) was injected at 19 seconds into the run with a pipette height of 20µL and a rate setting of 5.

2.3.6. Data analysis – Pre-screen

Data were initially analysed in Softmax Pro v5.4.1 (Molecular Devices, USA). Responses were expressed as peak increase in fluorescence intensity, normalised to the baseline which was calculated as %baseline x 0.01. The peak increase was generally seen at around 10 seconds after compound injection. This resulted in data equivalent to ΔF/F(baseline) using the first 8 read points before compound injection to calculate the baseline. The baseline fluorescence was set at 0 by subtraction of 1 from all data; in the normalised data a value of 1 then represented a 100% increase over baseline. The following formula was applied to represent data as a percentage of the maximal response of the cells to the application of 10µM ATP.

$$Activity\ [\%] = 100 * \left(\frac{x - \langle VehicleControl \rangle}{\langle ATPControl \rangle - \langle VehicleControl \rangle} \right)$$

Where x is the calculated signal value of a well (ΔF/F).
< > indicate median of the calculated signal values (ΔF/F) for the vehicle control wells (min, buffer) and ATP control (max, 10µM ATP).

Data from individual experiments were expressed as mean ± SD of the replicates. Data charts and statistical analyses were produced in GraphPad Prism v8.2.1 (GraphPad Software, USA).

2.3.7. Statistical analysis and selection criteria for concentration-response testing

In order to select compounds for follow-up concentration-response testing, several criteria were applied. Initially, a two-way ANOVA was applied to the data. A 2-way ANOVA does not account for the direction of the concentration range. The data

could be in any order and the ANOVA output would be the same. Multiple comparisons were also generated to give more detail on which concentrations of compound gave significant differences. However, there are some cases where relying on the ANOVA alone could lead to erroneous conclusions, particularly where compounds give atypical responses in the cells. These can be from auto-fluorescence of the compounds or other kinds of artefact, particularly with higher concentrations. For all receptor-compound combinations yielding significant interaction in the ANOVA, the raw signal traces were also examined. A typical calcium response shows a rapid increase in fluorescence at the injection of the compound followed by a gradual return to baseline levels over the course of around 3 minutes. Auto-fluorescence of a compound is quite easily identified, as the fluorescence level increases immediately at compound injection, but then remains constant over the remaining read time. In some cases the maximum compound concentration stimulated the cells to such an extent that the signal exceeded the capacity of the FlexStation, resulting in signal saturation. This is also simple to identify from the signal trace and if this was the only evidence for a compound-receptor interaction then these combinations were not tested in the concentration-response phase.

Response traces were always examined in the context of the mock-transfected cell response for that compound. While auto-fluorescent artefacts are easier to see, artefacts from non-specific stimulation of the cells can look like legitimate calcium responses. In fact, they may well be the result of test compounds interacting with other cell surface receptors endogenous to the HEK cell line. Therefore, to proceed to the concentration-response phase of the testing, there needed to be at least one test concentration where the response was specific to the receptor-transfected cells.

In summary, the requirements for a receptor-compound combination to be tested in a full concentration-response experiment were significance in the ANOVA, evidence of a receptor-specific response and typical response characteristics in the raw signal traces.

2.3.8. Assay preparation and execution – concentration-response testing

Assays for concentration-response testing were carried-out in the same way as for the pre-screen testing. The plate layout used for the initial testing phase at Waltham was altered to that shown in Figure 2.7. The concentration-response curves for ATP were omitted in these experiments as they were not used in downstream analysis and it allowed one more compound to be tested per-plate.

	1	2	3	4	5	6	7	8	9	10	11	12	13	14	15	16	17	18	19	20	21	22	23	24
A	ATP	C1	C1	C2	C2	C3	C3	C4	C4	C5	C5	C6	C6	C7	C7	C8	C8	C9	C9	C10	C10	C11	C11	ATP
B	Buffer	C1	C1	C2	C2	C3	C3	C4	C4	C5	C5	C6	C6	C7	C7	C8	C8	C9	C9	C10	C10	C11	C11	Buffer
C	ATP	C1	C1	C2	C2	C3	C3	C4	C4	C5	C5	C6	C6	C7	C7	C8	C8	C9	C9	C10	C10	C11	C11	ATP
D	Buffer	C1	C1	C2	C2	C3	C3	C4	C4	C5	C5	C6	C6	C7	C7	C8	C8	C9	C9	C10	C10	C11	C11	Buffer
E	ATP	C1	C1	C2	C2	C3	C3	C4	C4	C5	C5	C6	C6	C7	C7	C8	C8	C9	C9	C10	C10	C11	C11	ATP
F	Buffer	C1	C1	C2	C2	C3	C3	C4	C4	C5	C5	C6	C6	C7	C7	C8	C8	C9	C9	C10	C10	C11	C11	Buffer
G	ATP	C1	C1	C2	C2	C3	C3	C4	C4	C5	C5	C6	C6	C7	C7	C8	C8	C9	C9	C10	C10	C11	C11	ATP
H	Buffer	C1	C1	C2	C2	C3	C3	C4	C4	C5	C5	C6	C6	C7	C7	C8	C8	C9	C9	C10	C10	C11	C11	Buffer
I	ATP	C1	C1	C2	C2	C3	C3	C4	C4	C5	C5	C6	C6	C7	C7	C8	C8	C9	C9	C10	C10	C11	C11	ATP
J	Buffer	C1	C1	C2	C2	C3	C3	C4	C4	C5	C5	C6	C6	C7	C7	C8	C8	C9	C9	C10	C10	C11	C11	Buffer
K	ATP	C1	C1	C2	C2	C3	C3	C4	C4	C5	C5	C6	C6	C7	C7	C8	C8	C9	C9	C10	C10	C11	C11	ATP
L	Buffer	C1	C1	C2	C2	C3	C3	C4	C4	C5	C5	C6	C6	C7	C7	C8	C8	C9	C9	C10	C10	C11	C11	Buffer
M	ATP	C1	C1	C2	C2	C3	C3	C4	C4	C5	C5	C6	C6	C7	C7	C8	C8	C9	C9	C10	C10	C11	C11	ATP
N	Buffer	C1	C1	C2	C2	C3	C3	C4	C4	C5	C5	C6	C6	C7	C7	C8	C8	C9	C9	C10	C10	C11	C11	Buffer
O	ATP	C1	C1	C2	C2	C3	C3	C4	C4	C5	C5	C6	C6	C7	C7	C8	C8	C9	C9	C10	C10	C11	C11	ATP
P	Buffer	C1	C1	C2	C2	C3	C3	C4	C4	C5	C5	C6	C6	C7	C7	C8	C8	C9	C9	C10	C10	C11	C11	Buffer

Figure 2.7: Plate layout for the initial phase of the concentration-response testing with the FlexStation
ATP max (10µM)/min (buffer) controls were included on these plates, but were not used in the analysis. The representation of C1-C11 is only an example. Compounds tested for each receptor were based on the results from the pre-screen.

In the later repeat-testing phase with the Hamamatsu FDSS/µCELL system the same layout was used with two minor differences. At this point in the work the decision had been made not to use the ATP data in the calculation as the responses had proved too variable between experiments (see Results section 2.4.1). This allowed one more compound to be tested per plate, but also meant there were no blank wells on the plate. To keep vehicle (injection of buffer only) wells available in the data, the dilution series in the repeat-testing phase had the last point as a blank, rather than as a sequential dilution point as shown in Figure 2.7.

Assay setup for this phase of testing was identical to that performed previously. The Hamamatsu FDSS/µCELL system was set up with a gain of x4 and a threshold setting of 10000. Dispense speed was set at 5µL/s and height at 1.5mm.

2.3.9. Data analysis – concentration-response testing

Data produced in the initial phase and repeat phase of concentration-response testing were analysed with Softmax Pro v5.4.1 and response curves were plotted in GraphPad Prism v8.2.1 (GraphPad Software, USA). Data were expressed as mean ± SD for the initial phase data (n=1) and mean ± SEM for the repeat phase data (n=3). Slope fitting was done using the Hill equation:

$$Response = Bottom + \frac{(Top\text{-}Bottom)}{1+10^{(LogEC_{50}\text{-}X)HillSlope}}$$

Where X = log concentration of the test compound.

In cases where enough data was available to indicate that the slope of the curve could be estimated a variable slope four parameter fit was used (top, bottom, EC_{50}, Hill Slope). In cases where it was not possible to estimate the slope from the data a three parameter fit was used with the Hill Slope set at 1.

Two-way ANOVA was also used here to identify threshold concentrations. Unfortunately, in most cases calculation of the EC_{50} value was not possible. Many compound-receptor combinations did not reach a maximum plateau in their signal, being limited by either compound solubility or the production of strong artefacts in the mock-transfected cells. A small number of EC_{50} values could be calculated and are included in the results summary table (Table 2.7).

2.4. Results

2.4.1. Pre-screen testing data

The pre-screen test data for dTas2r1 are presented here as a representative example. This receptor had one of the highest rates of positive compound selection for subsequent concentration-response testing, indicating it may be one of the more

broadly-tuned receptors in the dog. In total, 24 of the 48 compounds tested were selected for testing in the full dose-response Tas2r1 experiments. Here the data for dTas2r1 will be discussed in detail, but the same criteria were applied to all pre-screening data.

In all cases ATP was used as a control in the assay. Stimulation of the cells with 10µM ATP resulted in a peak response of approximately 3.5 fold over baseline fluorescence and an EC_{50} of 2.4µM (Figure 2.8). Negative controls consisted of the assay buffer. Where DMSO was used in the preparation of the compound, negative controls consisting of assay buffer with DMSO at the same concentration as used for the compound preparation were included.

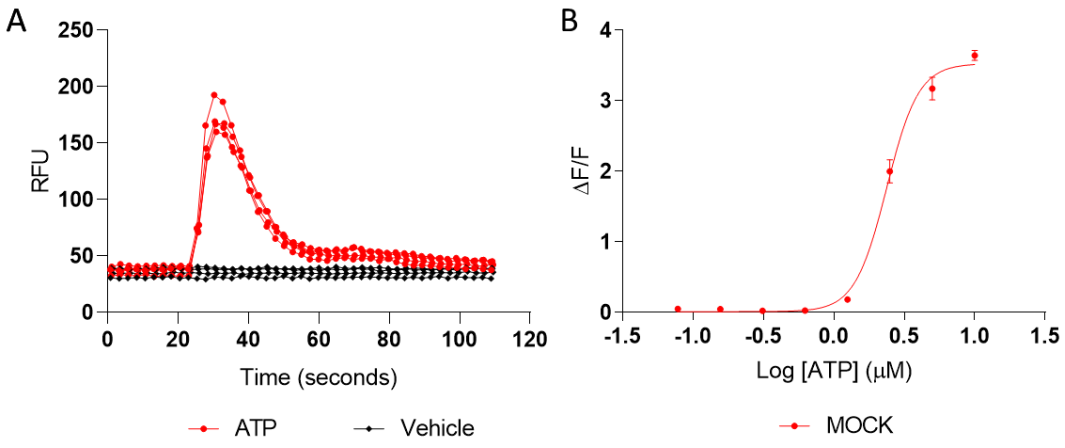

Figure 2.8: Response data for mock transfected cells when stimulated with 10µM ATP and a 2-fold dilution series
A) ATP (10µM) stimulates a transient calcium response in HEK293T cells. B) The response of HEK293T cells to ATP is concentration dependant. This was initially used to normalise data between experiments. However, ATP responses proved to be variable between experiments and this normalisation was not used in the final data analysis.

Use of a stimulator control like ATP is intended to help reduce variation between experiments by providing a maximal fluorescence reference point. In assays where there is little or no background fluorescence this can prove useful, as fluctuations in dye loading are accounted for in a way not possible with the ΔF/F method. However, in the assay used here baseline fluorescence was always well above zero. There was

variation in the level of baseline fluorescence depending on which Tas2r receptor had been transfected, but in all cases the level was most likely sufficient to at least partially account for any variation in dye loading. In addition to this, the level of fluorescence seen with the stimulation by 10µM ATP was quite variable between experiments. In particular, the washing of the cells seemed to effect this. This was quite noticeable because the plate washer used in these experiments washed column 1 of the plate first and then moved sequentially across the plate. This resulted in higher ATP responses in control column 24 when compared to column 1. Incubating the plate at room temperature for 15 minutes post-washing reduced this affect, but did not eliminate it. This might be caused by the mechanical effect of washing the cells resulting in ATP release, and subsequent activation of endogenous P2Y1 and P2Y2 receptors (Schachter *et al.*, 1997).

In light of these findings, normalisation to the ATP response was not used in the final data analysis. Instead the ΔF/F baseline (ΔF/F) method was used for all data.

2.4.1.1. dTas2r1: effect of 1,10-phenanthroline and 4-benzylpiperadine

An example of a receptor-compound combination that was selected for follow-up concentration-response testing was dTas2r1 with 1, 10-phenanthroline. As Figure 2.9 indicates, HEK293 cells transfected with either d*Tas2r1* plasmid, or empty vector (mock) were assessed for responses to this compound in the calcium mobilisation assay. 1, 10-Phenanthroline selectively induced responses in d*Tas2r1*-transfected cells at 1 and 10mM (Figure 2.8), with significant differences from the mock indicated by two way ANOVA. Time-course data (Figure 2.10) indicated a rapid peak response, within 20 seconds of compound addition, consistent with a receptor-mediated calcium mobilisation mechanism.

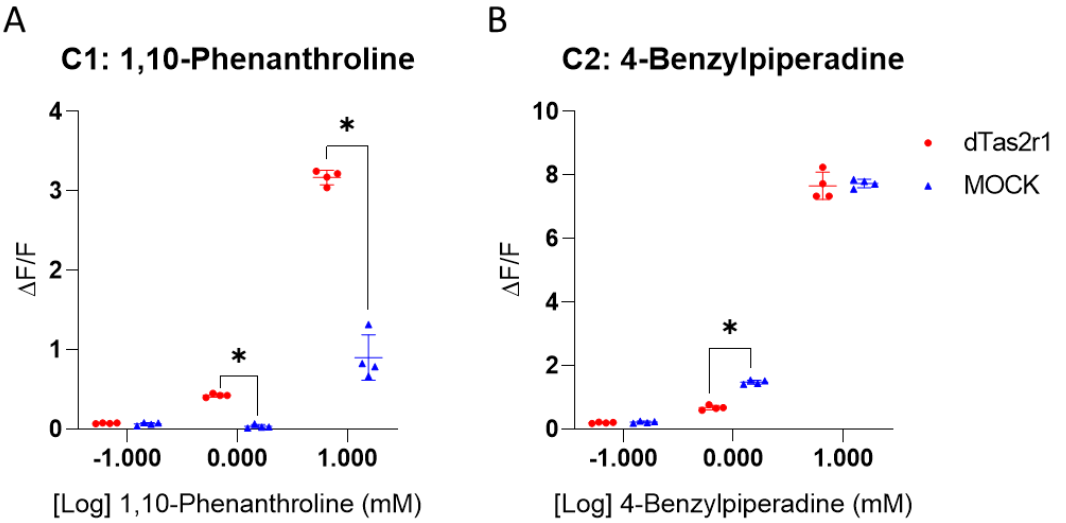

Figure 2.9: Pre-screening data for dTas2r1 and A) 1, 10-phenanthroline or B) 4-benzylpiperadine
Data are represented as change in fluorescence/initial baseline fluorescence against log test compound concentration. Error bars represent standard deviation (SD) of quadruplicate measurements from one experiment (n=1). * $p<0.05$ dTas2r1 vs mock transfected (two way ANOVA and Sidak's multiple comparisons test).

Examination of the raw data traces from the FlexStation show typical data for the d*Tas2r1*-transfected cells with evidence of dose-dependency. The mock-transfected cells do show a smaller response at the highest concentration however, there is no response at the following concentration indicating a receptor-specific response at this concentration (Figure 2.9 and 2.10).

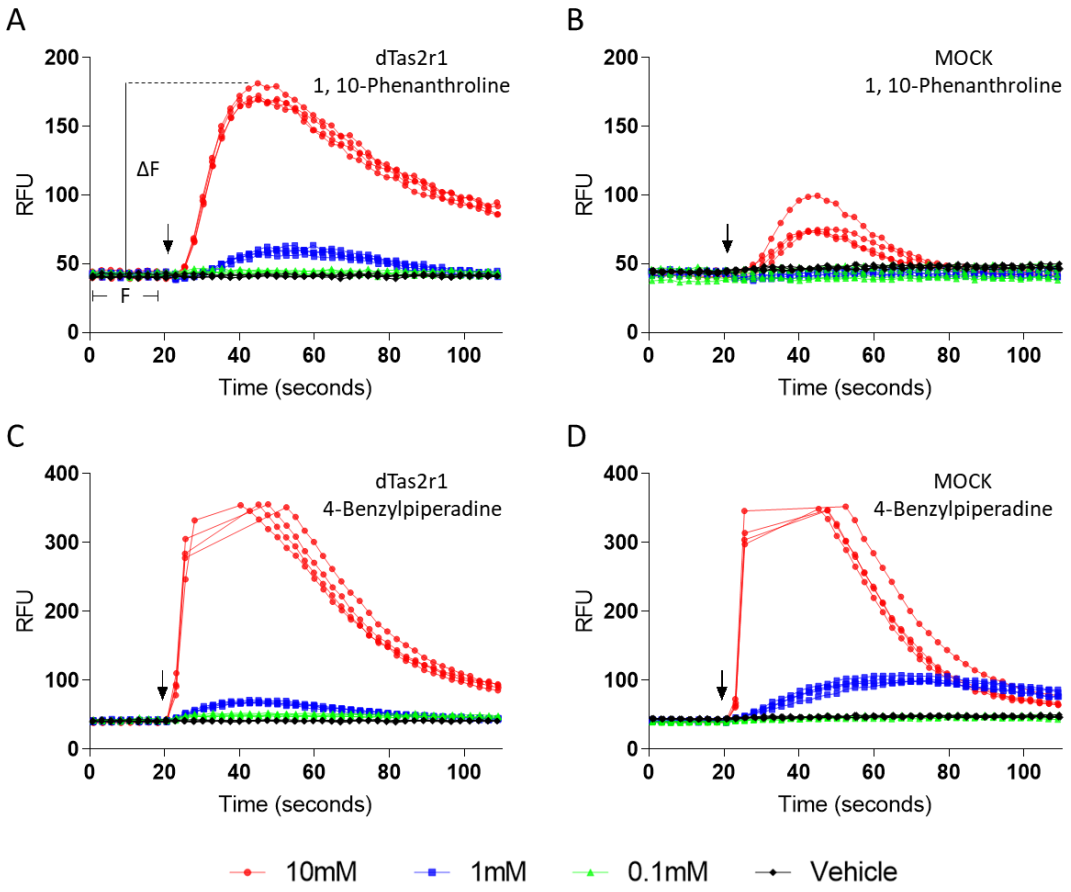

Figure 2.10: Raw data for responses of dTas2r1 and mock transfected cells to two test compounds
A) dTas2r1 with 1, 10-phenanthroline. Baseline fluorescence (F) was calculated as the mean of the first eight read points. Change in fluorescence (ΔF) was calculated as the peak reading minus the baseline. B) Mock with 1, 10-phenanthroline. C) dTas2r1 with 4-benzylpiperadine. D) Mock with 4-benzylpiperadine. The four individual replicates for each treatment are plotted, with data represented as relative fluorescent units (RFU). Arrows indicate timing of compound injection.

Based on this, a dose-response experiment for d*Tas2r1* transfected, and mock transfected cells with 1,10-phenanthroline would be expected to show specific responses with d*Tas2r1* transfected cells, or no activity with concentrations below 10mM.

An example of a receptor-compound combination that was not selected for dose-response testing was dTas2r1 with 4-benzylpiperadine. In this example there was no receptor specific response at any concentration (Figure 2.9).

The multiple comparison tests shows only the intermediate concentration test point to be significant while the second and third were not significant. However, the intermediate concentration shows a higher response in the mock-transfected cells.

Examination of the raw data traces showed that at the highest test concentration signal saturation occurred. Therefore, the data for the highest concentration could not be relied upon. Both d*Tas2r1* and mock-transfected cells responded at the intermediate concentration. There is no evidence of a receptor-specific activation of the cells and hence this compound would not be tested in a concentration-response experiment with dTas2r1 (Figure 2.10).

2.4.1.2. dTas2r1 pre-screening data

All pre-screen data for dTas2r1 are shown in Figures 2.11, 2.12, 2.13 and 2.14.

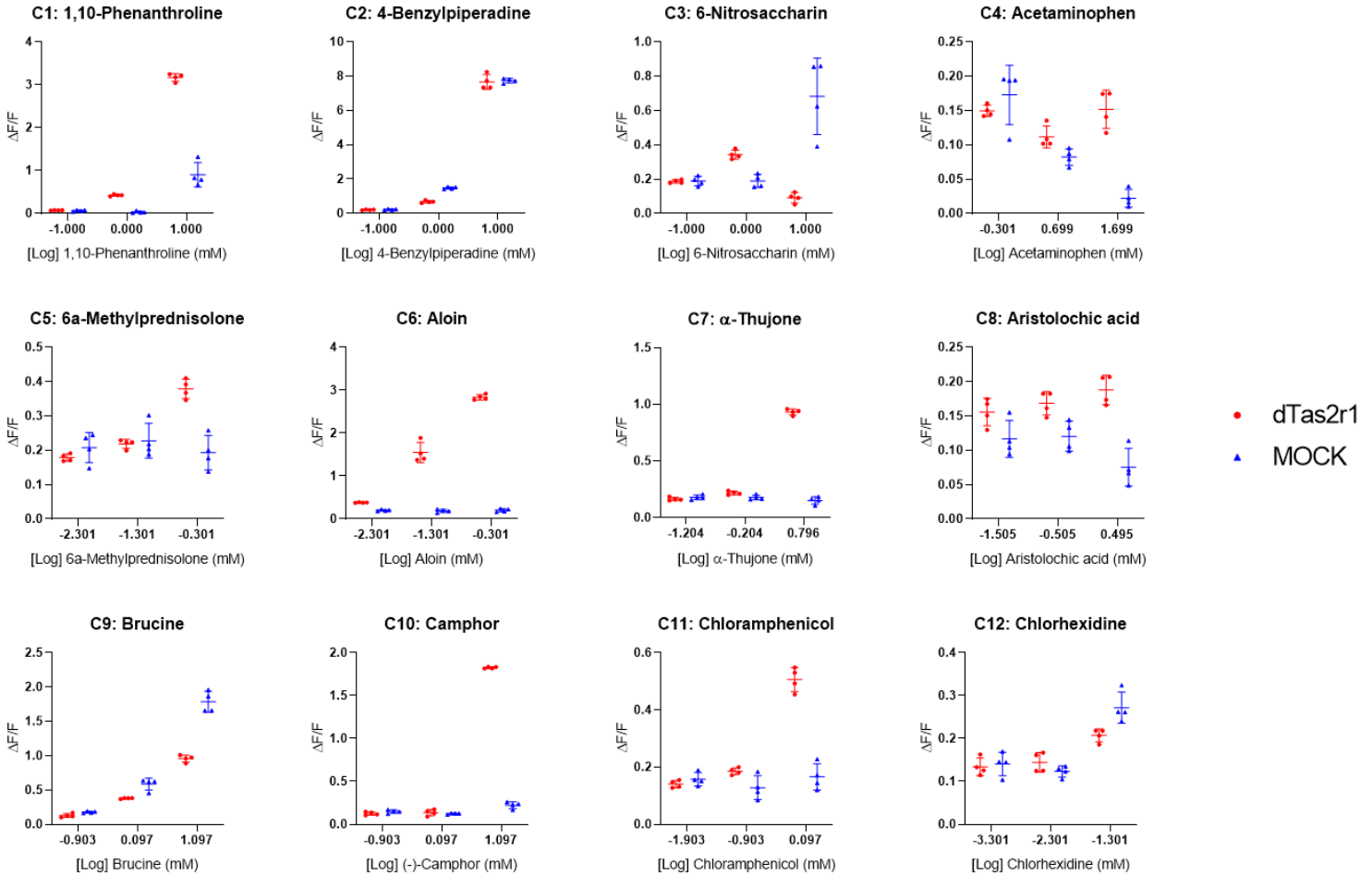

Figure 2.11: Pre-screening peak calcium response data for dTas2r1 and the first 12 compounds in the library
Data are represented as ΔF/F against log concentration. Mock cells are transfected with plasmid vector that does not contain a Tas2r. Error bars represent standard deviation (SD) of quadruplicate tests. Data are from 1 experiment (n=1).

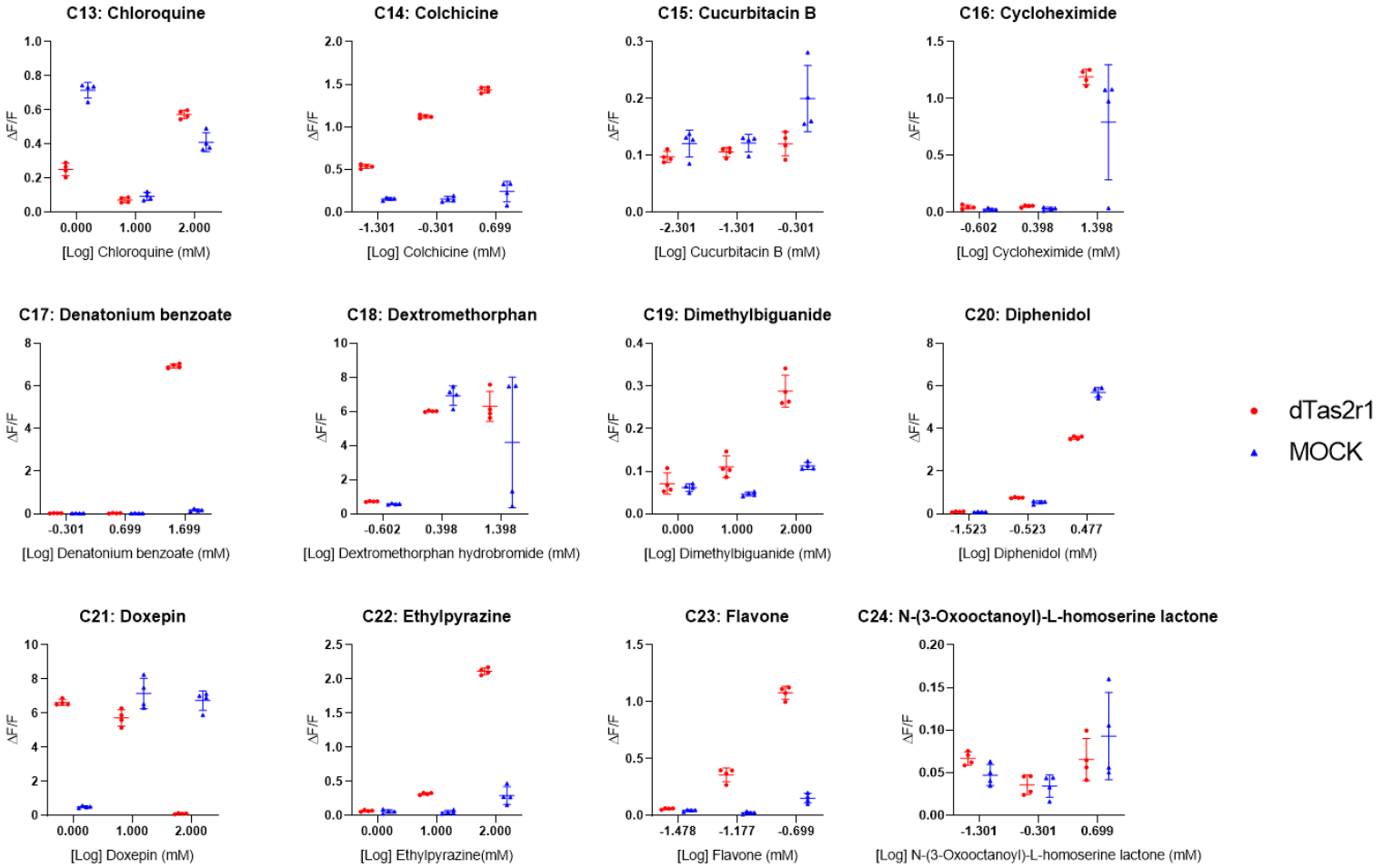

Figure 2.12: Pre-screening peak calcium response data for dTas2r1 and the second 12 compounds in the library
Data are represented as ΔF/F against log concentration. Mock cells are transfected with plasmid vector that does not contain a Tas2r. Error bars represent standard deviation (SD) of quadruplicate tests. Data are from 1 experiment (n=1).

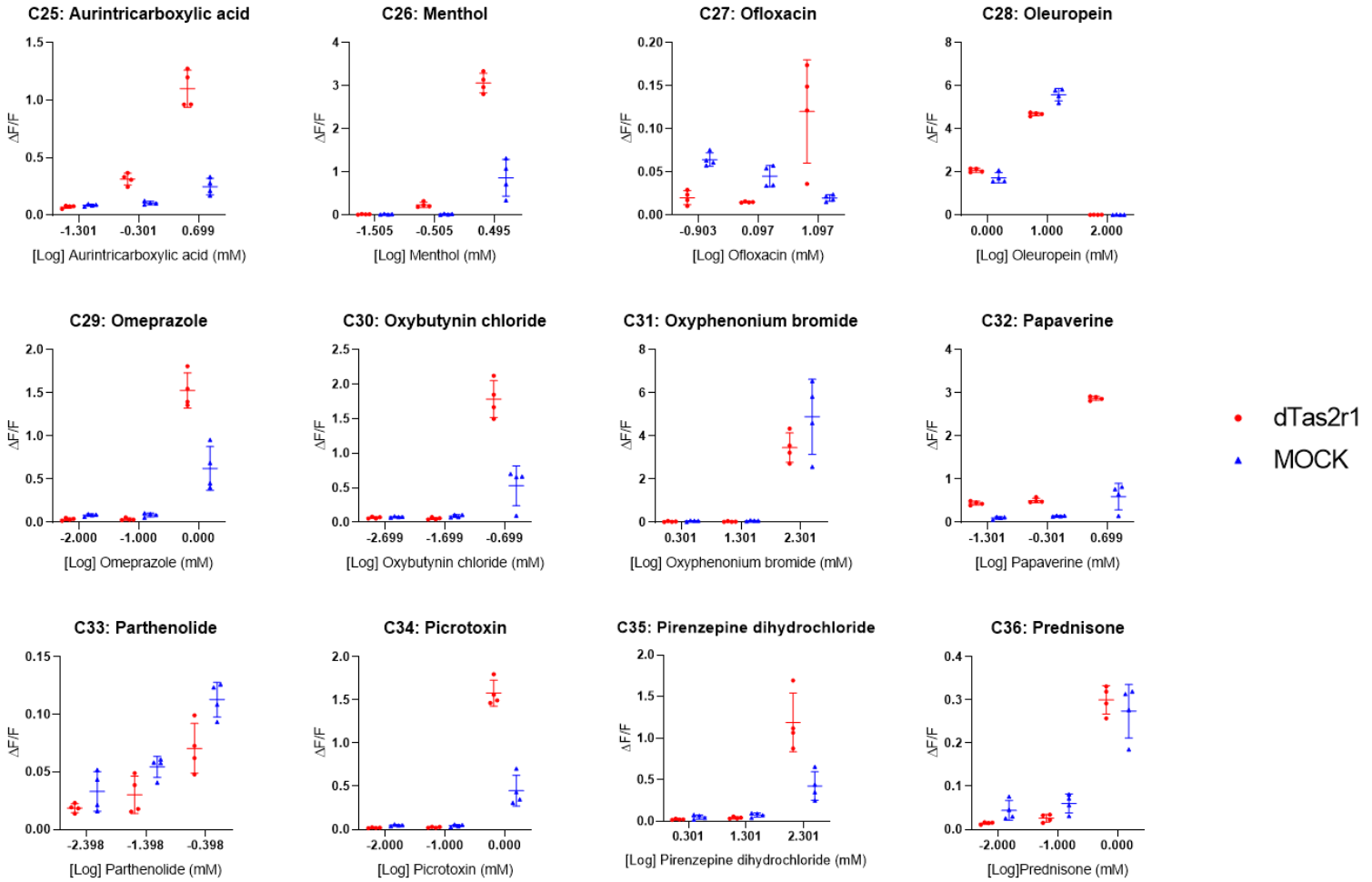

Figure 2.13: Pre-screening peak calcium response data for dTas2r1 and the third 12 compounds in the library
Data are represented as ΔF/F against log concentration. Mock cells are transfected with plasmid vector that does not contain a Tas2r. Error bars represent standard deviation (SD) of quadruplicate tests. Data are from 1 experiment (n=1).

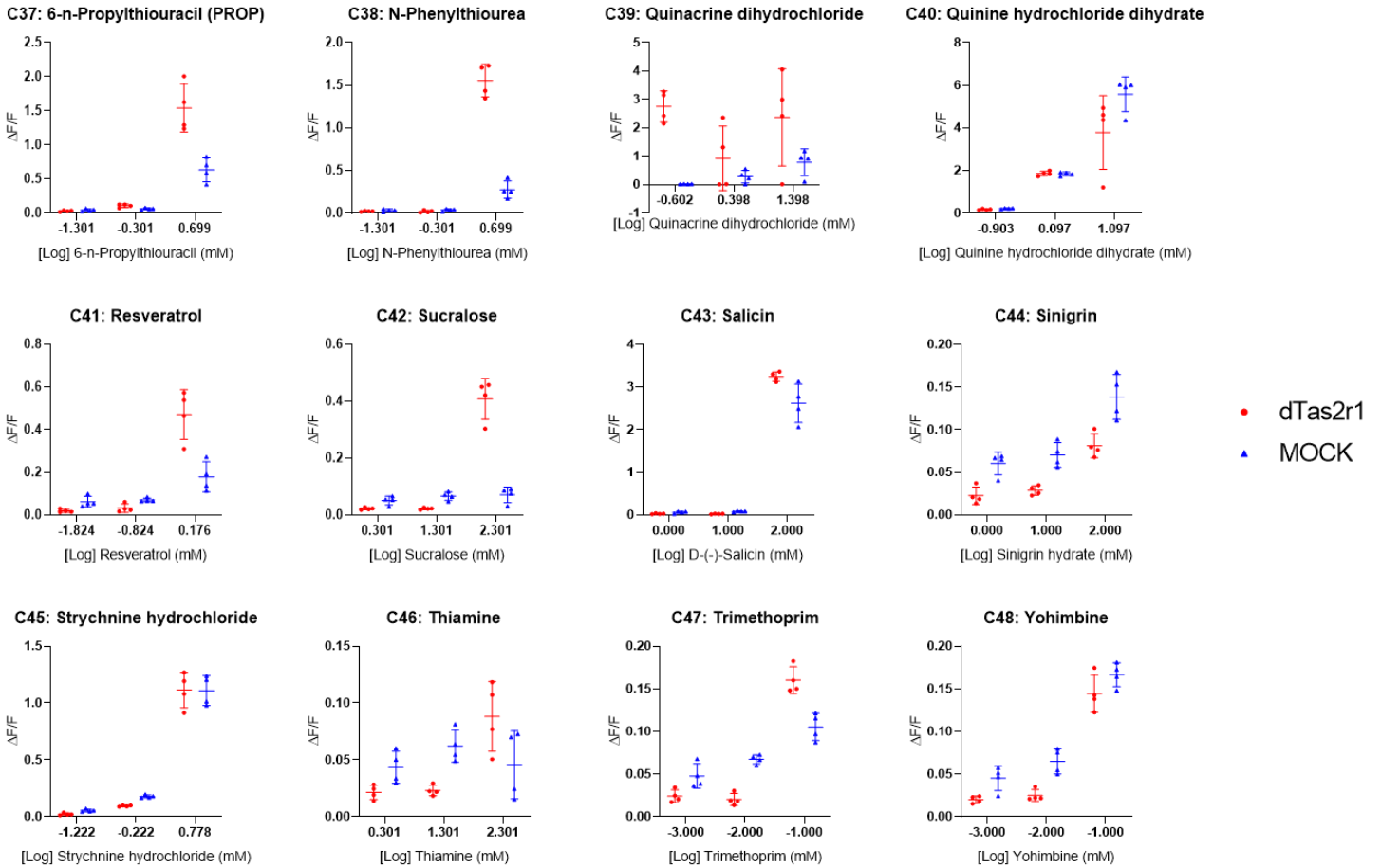

Figure 2.14: Pre-screening peak calcium response data for dTas2r1 and the last 12 compounds in the library
Data are represented as ΔF/F against log concentration. Mock cells are transfected with plasmid vector that does not contain a Tas2r. Error bars represent standard deviation (SD) of quadruplicate tests. Data are from 1 experiment (n=1).

All data for the dTas2rs were reviewed in this way to determine the selection of compounds that would proceed to the concentration-response testing phase.

In some cases, these preliminary results matched with ligands identified for the orthologous human receptor, but this was not always the case. For example, yohimbine stimulates 5 human TAS2Rs (TAS2R1, 4, 10, 38 and 46) (Meyerhof *et al.*, 2010), nearly all of which have an orthologue in the dog, hTAS2R46 being the exception. In this pre-screen, no potential responses with the dog Tas2rs were observed with this compound (Figure 2.14). In this and other similar cases, a test with the responding human receptors in the assay system would help to determine if this lack of activity in dog really is a species-specific difference, or a result of the differences between the assay system used here and that used in other laboratories. This comparison was conducted as part of the concentration-response testing.

With previously-identified ligands for human receptors, the concentration used is very important for identifying a positive result in comparison to controls. Diphenidol has been reported as the most prolific stimulator of human TAS2Rs with a total of 15 responsive receptors (Meyerhof *et al.*, 2010), 8 of which have an orthologue in the dog. In this pre-screen, diphenidol did not produce any specific responses. Responses in the receptor-expressing cells were always accompanied by similar responses in the mock-transfected cells (Figure 2.12 and 2.15). Previously, diphenidol was identified as being active with human TAS2Rs at a concentration of 0.1mM (Meyerhof *et al.*, 2010). However, this concentration falls between the test points used in this pre-screen of 3mM, 0.3mM and 0.03mM. Testing in a full concentration-response experiment would be appropriate in situations like this where, although there was no evidence of a specific response in this pre-screen, there was reason to believe that the compound would activate some dog Tas2rs.

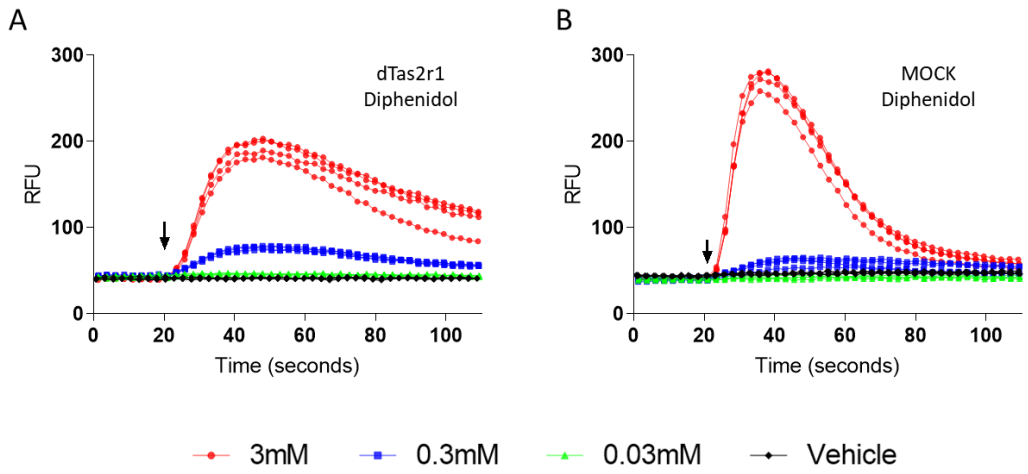

Figure 2.15: Raw data for responses of dTas2r1 to diphenidol
A) Raw data for dTas2r1-transfected cells. B) Raw data for mock transfected cells. The four individual replicates for each treatment are plotted, with data represented as relative fluorescent units (RFU). Arrows indicate timing of compound injection.

In the case of both yohimbine and diphenidol, there is reason to believe they should show some activity against dog Tas2rs given their prolific stimulation of human TAS2Rs. In these and similar cases, the compounds were listed for concentration-response testing despite lack of a positive response in the pre-screen. Table 2.3 contains the details of all the receptor-compound combinations that were still shortlisted for concentration-response testing despite the lack of a specific response in the pre-screen.

Table 2.3: Receptor-compound combinations shortlisted for dose-response testing despite the lack of a specific response in the pre-screen data

Compound	Responsive human orthologous receptors	Stimulating concentrations (μM)
Brucine	hTAS2R10	100
Dextromethorphan hydrobromide monohydrate	hTAS2R1	10
	hTAS2R10	10
Diphenidol	hTAS2R1	100
	hTAS2R4	100
	hTAS2R7	10
	hTAS2R10	30
	hTAS2R38	100
	hTAS2R39	100
	hTAS2R40	30
	hTAS2R43	30
Parthenolide	hTAS2R1	100
	hTAS2R4	30
	hTAS2R10	30
PROP	hTAS2R38	0.11
PTC	hTAS2R38	0.04
Sinigrin	hTAS2R38	100
Strychnine	hTAS2R10	3
Yohimbine	hTAS2R1	300
	hTAS2R4	300
	hTAS2R10	300
	hTAS2R38	300

A summary of all receptor-compound combinations selected for concentration-response testing is presented in Tables 2.4A and 2.4B.

Table 2.4: A. Summary of compounds 1-24 showing those selected for further testing

Compound-receptor combinations selected for follow-up testing in a concentration-response experiment have an asterisk in the corresponding cell.

	C1: 1, 10 Phenanthroline	C2: 4-Benzylpiperadine	C3: 6-Nitrosaccharin	C4: Acetominophen	C5: 6α-Methylprednisolone	C6: Aloin	C7: (−)-α-Thujone	C8: Aristolochic acid I	C9: Brucine sulphate salt hydrate	C10: (-)-Camphor	C11: Chloramphenicol	C12: Chlorhexidine
											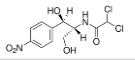	
dTas2r1	*		*		*	*	*			*	*	
dTas2r2	*											
dTas2r3			*		*		*	*		*	*	*
dTas2r4						*	*	*		*	*	*
dTas2r5	*				*	*	*			*	*	*
dTas2r7					*	*	*			*	*	*
dTas2r10							*	*		*	*	
dTas2r12											*	
dTas2r38						*	*			*	*	*
dTas2r39				*		*	*			*	*	
dTas2r40												
dTas2r41						*	*	*		*	*	
dTas2r42								*			*	
dTas2r43						*	*	*				
dTas2r62										*	*	*
dTas2r67												

	C13: Chloroquine diphosphate salt	C14: Colchicine	C15: Cucurbitacin B hydrate	C16: Cycloheximide	C17: Denatonium benzoate	C18: Dextromethorphan hydrobromide monohydrate	C19: Dimethylbiguanide hydrochloride	C20: Diphenidol	C21: Doxepin	C22: Ethylpyrazine	C23: Flavone	C24: N-(3-Oxooctanoyl)-L-homoserine lactone
	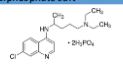	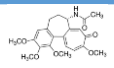	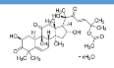		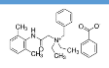		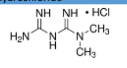			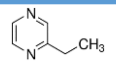		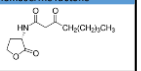
dTas2r1	*	*		*	*	*	*	*	*	*	*	
dTas2r2		*			*			*				
dTas2r3	*	*	*	*				*		*	*	*
dTas2r4		*	*	*	*			*			*	*
dTas2r5	*	*	*		*			*			*	*
dTas2r7	*	*	*	*	*			*		*	*	*
dTas2r10	*		*	*	*	*		*		*		
dTas2r12			*					*			*	
dTas2r38	*	*	*	*	*			*		*	*	*
dTas2r39	*	*			*			*		*	*	
dTas2r40			*					*		*	*	*
dTas2r41			*					*			*	*
dTas2r42			*					*				
dTas2r43					*			*				
dTas2r62			*	*	*			*				*
dTas2r67								*				

Table 2.4: B. Summary of compounds 25-48 showing those selected for further testing

Compound-receptor combinations selected for follow-up testing in a concentration-response experiment have an asterisk in the corresponding cell.

	C25: Aurintricarboxylic acid	C26: L-Menthol	C27: Ofloxacin	C28: Oleuropein	C29: Omeprazole	C30: Oxybutynin chloride	C31: Oxyphenonium bromide	C32: Papaverine hydrochloride	C33: Parthenolide	C34: Picrotoxin	C35: Pirenzepine dihydrochloride	C36: Prednisone
		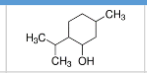	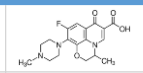	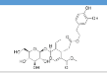	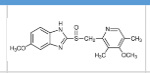	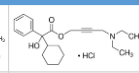	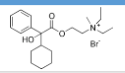	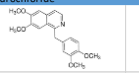		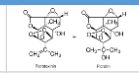		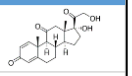
dTas2r1	*	*	*				*		*	*		
dTas2r2	*		*									
dTas2r3												
dTas2r4	*								*	*		*
dTas2r5							*					
dTas2r7	*						*	*				
dTas2r10						*	*	*	*	*	*	
dTas2r12												
dTas2r38												
dTas2r39												
dTas2r40			*									
dTas2r41			*				*					
dTas2r42												
dTas2r43												
dTas2r62		*	*									
dTas2r67		*										

	C37: 6-Propyl-2-thiouracil (PROP)	C38: N-Phenylthiourea (PTC)	C39: Quinacrine dihydrochloride	C40: Quinine hydrochloride dihydrate	C41: Resveratrol	C42: Sucralose	C43: D-(-)-Salicin	C44: Sinigrin hydrate	C45: Strychnine hydrochloride	C46: Thiamine	C47: Trimethoprim	C48: Yohimbine
		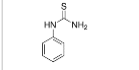	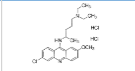	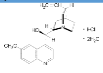	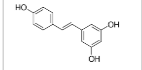	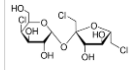	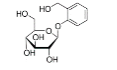	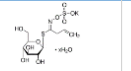		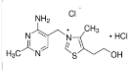	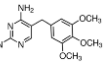	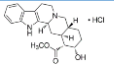
dTas2r1					*	*		*		*		*
dTas2r2												
dTas2r3	*											
dTas2r4				*	*	*						*
dTas2r5						*						
dTas2r7					*	*						
dTas2r10				*		*			*			*
dTas2r12												
dTas2r38	*	*						*				*
dTas2r39					*	*				*		
dTas2r40												
dTas2r41						*						
dTas2r42												
dTas2r43	*											
dTas2r62										*		
dTas2r67										*		

2.4.2. Concentration-response testing data

For each concentration-response test the experiment was performed once on the FlexStation at the Waltham laboratory (initial phase) then, if indication of a specific response was seen, repeated three times using the Hamamatsu FDSS/µCELL system (repeat phase) at the laboratories of IMAX Discovery (Milan, Italy). Data were compared between the different experiments and where possible an EC_{50} value was calculated. Data were also compared to published responses for human orthologous receptors.

2.4.2.1. Tas2r1 concentration-response testing

dTas2r1 had one of the highest selection rates for concentration-response testing. In total, 29 compounds were screened on the FlexStation at Waltham. Of these, 18 were selected for further confirmation using the FDSS/µCELL system at IMAX Discovery. Compounds with confirmed activity in the pre-screen and the concentration-response experiments with either dTas2r1, hTAS2R1 or both are shown here.

Some compounds, once screened in the initial concentration-response testing phase at Waltham, did not show any evidence of specific receptor activation. In many cases, similar responses in the mock-transfected cells meant no specific receptor activation could be seen. A summary of these compounds is given in Table 2.5, along with the reason for not following-up with repeated testing at the IMAX Discovery laboratory.

Table 2.5: Compounds failing to show specific responses in the initial phase concentration-response testing with Tas2r1
Selection is based on pre-screen results for dTas2r1 or because they were published hTAS2R1 ligands. These compounds were not retested as part of the repeat testing phase done at IMAX Discovery.

Compound	Reason for discontinuation of testing	Published activating concentration for hTAS2R1 (mM)	Reference
Aloin	No specific response	Not published	NA
Chloroquine	No specific response	Not published	NA
Cycloheximide	No specific response	Not published	NA
Denatonium Benzoate	No specific response	Not published	NA
Dextromethorphan hydrobromide	No specific responses	0.01	Meyerhof *et al.* (2010)
Dimethylbiguanide	No response	Not published	NA
Diphenidol	No specific response	0.1	Meyerhof *et al.* (2010)
Doxepin	No specific response	Not published	NA
Ofloxacin	No specific response	Not published	NA
Parthenolide	No response	0.1	Meyerhof *et al.* (2010)
Picrotoxin/Picrotoxinin	No response	1.0 (Picrotoxinin)	Meyerhof *et al.* (2010)
Sinigrin	No specific response	Not published	NA

In the case of Picrotoxin, a small response was seen with dTas2r1 at a concentration of 0.5mM. However, Picrotoxin is an equimolar mixture of Picrotoxinin and Picrotin. Of these two compounds Picrotoxinin has been shown to be more active with hTAS2R14 (Behrens *et al.*, 2004) and was also shown to be active against hTAS2R1 at a concentration of 1mM (Meyerhof *et al.*, 2010). Here, the maximum soluble concentration of picrotoxinin that could be achieved was 0.5mM. With no response in hTAS2R1 to either compound, and only a small, not completely specific response in dTas2r1 to Picrotoxin these compounds were not retested at IMAX Discovery.

2.4.2.1.1. Selective responses of dTas2r1 in concentration-response tests

In many cases dTas2r1 showed activity with compounds that did not activate hTAS2R1. Some differences in ligand binding profiles between orthologous receptors were expected, but the situation was most marked for this receptor, with a combination of results showing dog specific agonists, human specific agonists and some agonists common to both receptors.

The heterocyclic organic compound 1, 10 phenanthroline is not a known ligand of hTAS2R1, being found to stimulate only hTAS2R5 when previously used at concentrations up to 1mM (Meyerhof et al., 2010). However, it was found to stimulate dTas2r1 in this study. In Figure 2.16 concentration-response testing data from the initial phase and repeat phase testing is shown. The data collected in the initial phase showed larger responses than that collected from the repeat phase. Also, sensitivity was higher with thresholds of 0.37mM and 3.33mM in the initial phase and repeat phase, respectively.

Colchicine was not previously found to activate hTAS2R1 (Meyerhof et al., 2010), but did activate dTas2r1 in this study. The compound was highly soluble and could be tested at concentrations of 11.1mM with no activation in the mock-transfected cells. Higher concentrations of 200mM and 66.6mM were initially soluble, but precipitated out of solution after 1-2 minutes at room temperature. The higher concentrations

also caused responses in the mock-transfected cells. The threshold for activation was 1.2mM (Figure 2.16).

The highly odorous food and flavour-related compound ethylpyrazine was previously shown to activate hTAS2R38, but not hTAS2R1, when a maximum test concentration of 3mM was used (Meyerhof et al., 2010). In this study dTas2r1 was activated, but not hTAS2R1. Specific activity for dTas2r1 was seen at a similar concentration to that of hTAS2R38 at 3.7mM in the initial phase of testing (Figure 2.16).

Flavone was previously shown to activate hTAS2R14 and hTAS2R39, with a low threshold of 8µM (Roland et al., 2011). In the initial phase experiments, dTas2r1 was also activated at a low threshold of 2.5µM while hTAS2R1 was inactive. While this pattern of specific activation for dog, but not human, Tas2r1 was preserved in the data generated in the repeat phase, the threshold for dTas2r1 was much higher, with specific responses being seen with 66µM (Figure 2.16). The reasons for this difference are not clear, but are most likely related to the reduced overall sensitivity seen in the data from the experiments run on the FDSS/µCELL system.

Aurintricarboxylic acid is not a previously identified hTAS2R1 ligand, but did give some activity in the initial phase data with dTas2r1, and a threshold concentration of 62µM. Higher concentrations showed low levels of activation in the mock transfected cells, but this was largely caused by slight autofluorescence of the compound. The data from the repeat phase of testing showed some evidence of a response in dTas2r1, but the response was not clear, with some activation in the other test conditions also (Figure 2.16).

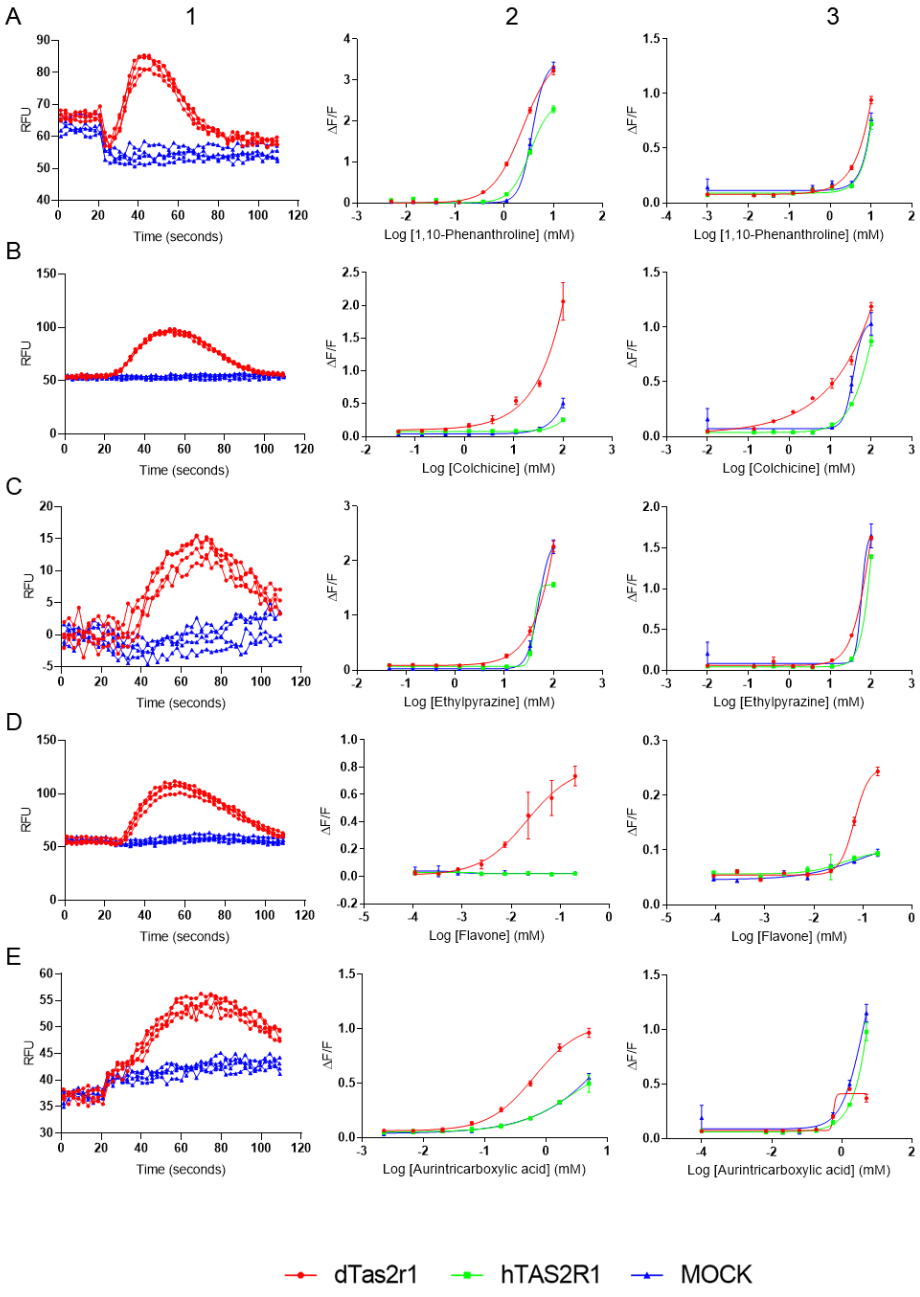

Figure 2.16: Compounds showing specific activity for dTas2r1, but not hTAS2R1
Rows A-E each show data from one of the five compounds A) 1, 10-phenanthroline, B) Colchicine, C) Ethylpyrazine, D) Flavone, E) Aurintricarboxylic acid. Column 1 shows raw data for the highest concentration where a specific response was seen with dTas2r1. Column 2 shows full concentration-response data for the initial phase testing. Column 3 shows concentration-response data from the repeat phase. The initial phase includes FlexStation data produced at the Waltham laboratory (n=1, error bars=SD). The repeat phase includes data produced at the IMAX Discovery laboratory with the Hamamatsu FDSS/µCELL system (n=3, error bars=SEM).

2.4.2.1.2. Selective responses of hTAS2R1 in concentration response tests

The corticosteroid 6α-methylprednisolone was previously found to activate hTAS2R1, with a test concentration of 0.05 or 0.1mM (Li et al., 2008). In this study, some evidence of activation was seen for hTAS2R1 but not for dTas2r1. This was only seen in the initial phase, and the response was not confirmed in the repeat phase. This may be related to the reduced sensitivity observed in the experiments performed at IMAX Discovery, as the responses observed at Waltham were small, at around 0.3 ΔF/F for the maximum test concentration of 0.5mM (Figure 2.17A).

Chloramphenicol caused specific activation of hTAS2R1, while dTas2r1 did not show specific activation (Figure 2.17A). Activation of hTAS2R1 by chloramphenicol is in-line with published data, previously being shown to be active at 0.1mM (Meyerhof et al., 2010), although here the activating concentration was higher at 0.28mM in the initial phase data and 0.83mM in the repeat phase.

The antimuscarinic drug oxyphenonium bromide was previously identified as a hTAS2R1 agonist at a test concentration of 2.5mM (Li et al., 2008). This was confirmed here, with a threshold concentration of 3.7mM in the initial phase data and a lower threshold of 0.41mM in the repeat phase data generated with the FDSS/µCELL system. However, the dog orthologue of the receptor was unresponsive to this compound (Figure 2.17A).

Resveratrol was previously shown to activate hTAS2R14 and hTAS2R39 (Roland *et al.*, 2013) at 16µM and 63µM respectively. Some activity was seen here for the human TAS2R1 receptor, but only at elevated concentrations. The initial phase data showed activation at 27µM, but increasing concentrations gave no further increases in signal. This finding was not replicated in the FDSS/µCELL data where only the highest concentration of 750µM gave an indication of a specific response in both the human and dog receptors (Figure 2.17B). This was not considered as good evidence of dTas2r1 activation due to the high concentration and lack of concentration-dependent responses.

Sucralose activates a wide range of both human and mouse Tas2rs including hTAS2R1 (Lossow *et al.*, 2016). Here activation was seen for hTAS2R1 only at very high concentrations of 11.1mM and above. A smaller response for dTas2r1 was seen in the initial phase data, but this was not evident in the replicated data from the FDSS/µCELL system, most likely due to the reduced sensitivity in this experiment (Figure 2.17B). Based on this data sucralose was not considered a hit for dTas2r1.

Thiamine also gave rather weak activation at elevated concentrations only. Previously it was shown to stimulate hTAS2R1 and hTAS2R39 at a 1mM concentration (Meyerhof *et al.*, 2010). Here stimulation of hTAS2R1 was seen with concentrations of 3.7mM, but not at the next lowest concentration of 1.2mM. The data from the repeat phase was slightly more difficult to interpret due to a large drop in baseline signal at the point of injection. Inspection of the response curves show a clear difference between hTAS2R1 and the mock-transfected cell line. The responses for dTas2r1 are not clear. There was a statistically significant increase in signal for dTas2r1 at second and third concentrations of 33.3mM and 11.1mM but there was no evidence of this signal being dose-dependent (Figure 2.17B). This was not considered to be sufficient evidence of dTas2r1 activation.

Yohimbine is an indoloquinolizidine alkaloid and was previously reported to stimulate a number of human TAS2Rs, including hTAS2R1 at a concentration of 0.3mM (Meyerhof *et al.*, 2010). In this study activation of hTAS2R1 with a test concentration of 0.3mM was seen in the initial phase data, but this was not evident in the repeated experiments with the FDSS/µCell system (Figure 2.17B).

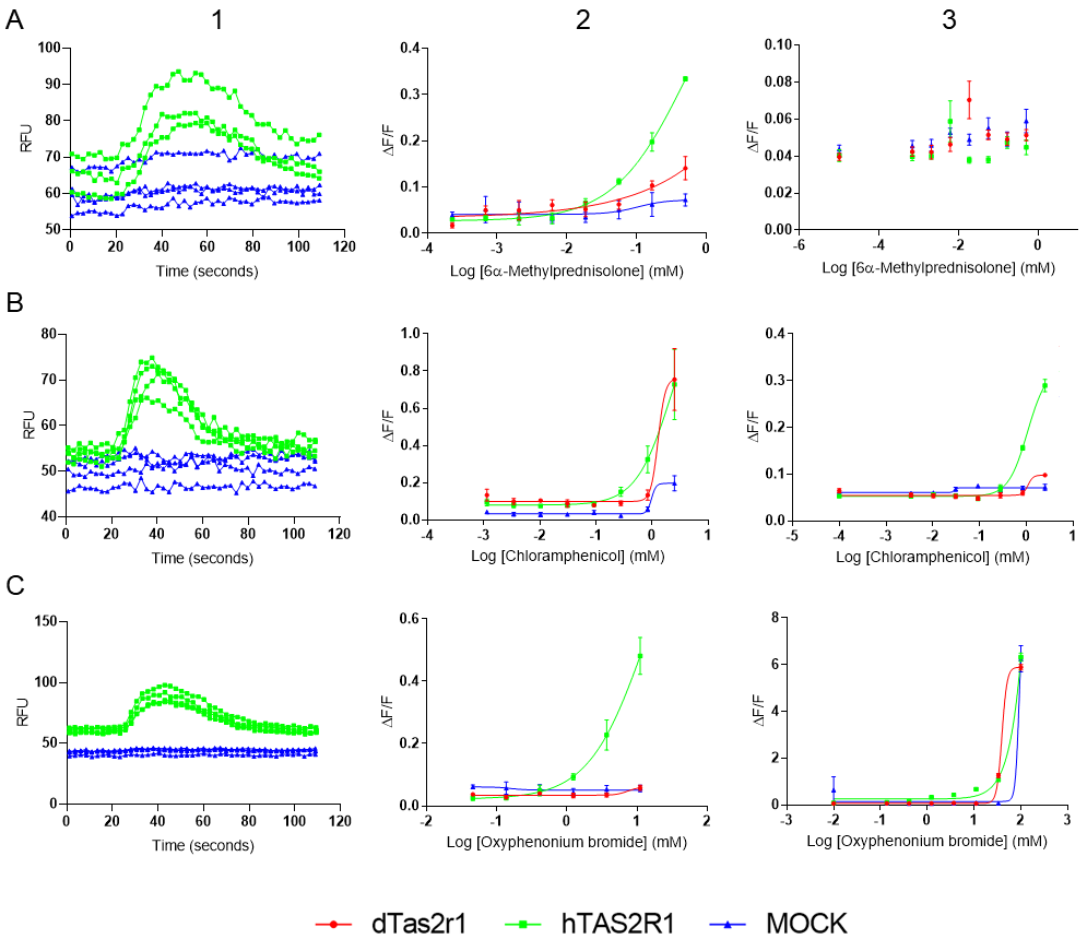

Figure 2.17: A. Compounds showing specific activity for hTAS2R1, but not dTas2r1 Rows A-C each show data from one compound. A) 6α-Methylprednisolone, B) Chloramphenicol, C) Oxyphenonium bromide. Column 1 shows raw data for the highest concentration where a specific response was seen with hTAS2R1. Column 2 shows full concentration-response data for the initial phase testing. Column 3 shows concentration-response data from the repeat phase. The initial phase includes FlexStation data produced at the Waltham laboratory (n=1, error bars=SD). The repeat phase includes data produced at the IMAX Discovery laboratory with the Hamamatsu FDSS/µCELL system (n=3, error bars=SEM).

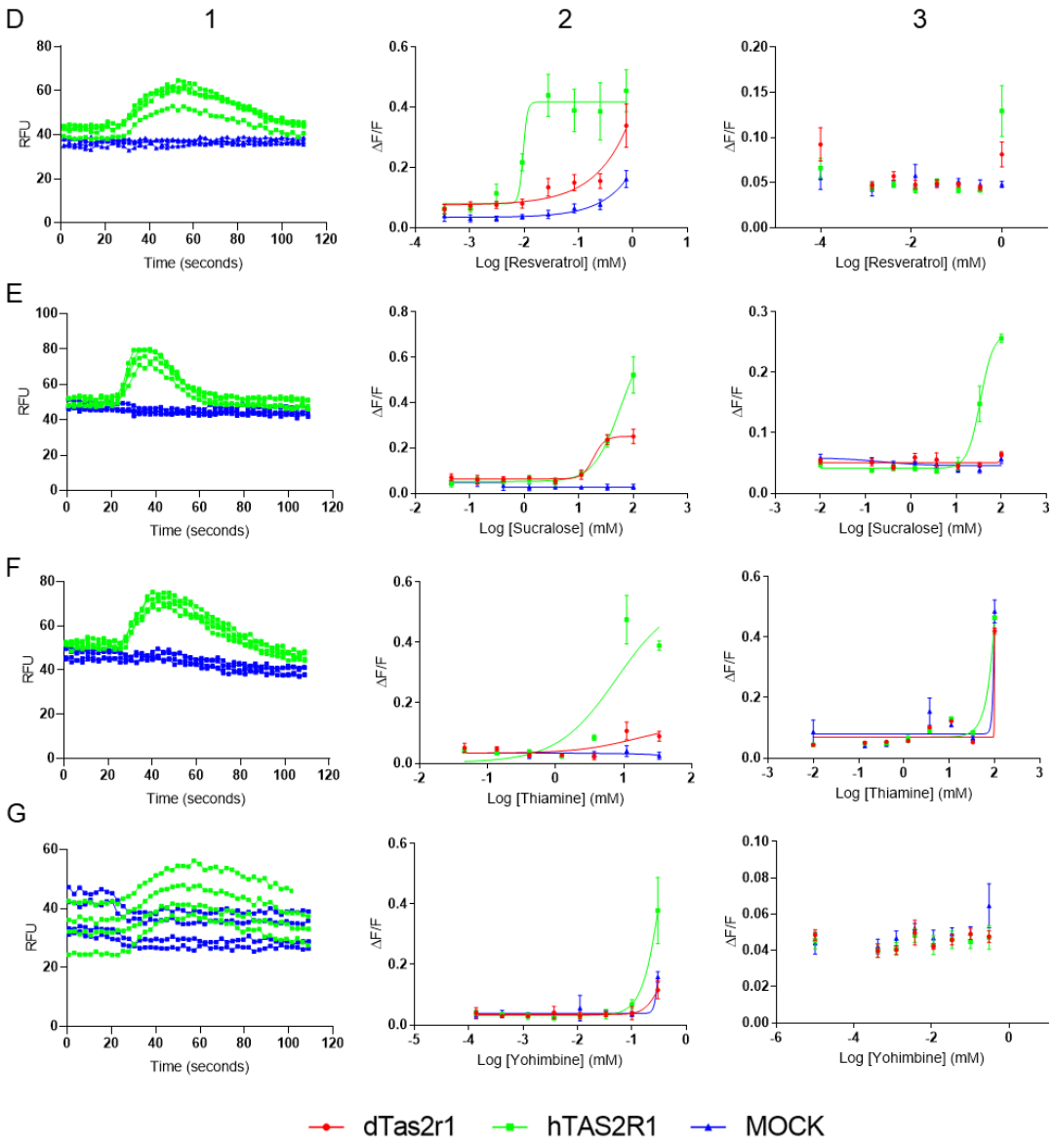

Figure 2.17: B. Compounds showing specific activity for hTAS2R1, but not dTas2r1
Rows D-G each show data from one D) Resveratrol, E) Sucralose, F) Thiamine, G) Yohimbine. Column 1 shows raw data for the highest concentration where a specific response was seen with hTAS2R1. Column 2 shows full concentration-response data for the initial phase testing. Column 3 shows concentration-response data from the repeat phase. The initial phase includes FlexStation data produced at the Waltham laboratory (n=1, error bars=SD). The repeat phase includes data produced at the IMAX Discovery laboratory with the Hamamatsu FDSS/µCELL system (n=3, error bars=SEM).

2.4.2.1.3. Common responses of dog and humanTas2r1 in concentration-response tests

In the case of 6-nitrosaccharin both the dog and the human version of the Tas2r1 receptor gave similar responses. In the initial phase data the responses are generally higher with a ΔF/F value of ~1 for the second point in the dilution series (3.3mM) compared to a ΔF/F value of ~0.22 for the data generated in the repeat phase. The data from the FlexStation also shows slightly higher sensitivity, with a threshold concentration of 0.37mM for hTAS2R1 and 0.12mM for dTas2r1. The data from the FDSS/µCELL system is indistinguishable from baseline at this point (Figure 2.18). 6-Nitrosaccharin is a known ligand of hTAS2R1, being identified in the Senomyx patent at a test concentration of 0.3mM (Li *et al.*, 2008). The response to 10mM 6-nitrosaccharin was reduced in the replicate experiments conducted with the FDSS/µCELL system (although not in the FlexStation experiment). Further experiments with 6-nitrosaccharin (Chapter 4) also showed this effect, and similar data has been published for other human receptors (Pronin *et al.*, 2004).

The monoterpene (-)-α-thujone is an example of compound that activated both dog and human Tas2r1, but with very different potency (Figure 2.18). In all experiments the dog version of the receptor was more sensitive to the compound, with a threshold of 25µM compared to 690µM for the human receptor. Again the magnitude of the responses seen differed between the two sets of experiments, with the initial phase data giving higher ΔF/F values. This compound has been tested previously with hTAS2R1, but was not found to give a response (Meyerhof *et al.*, 2010). In the published, data the maximum test concentration used was 0.3mM, with higher concentrations causing responses in the mock-transfected cells. Here, the lowest concentration giving a specific response with hTAS2R1 was 0.69mM, with no response in the mock-transfected cells, and so the data is compatible with that already published, the key difference being seen in the sensitivity of the mock-transfects.

The terpenoid (-)-camphor was tested in this study. The opposite enantiomer (+)-camphor was previously tested and was found to activate several human TAS2Rs,

but not hTAS2R1 at concentrations up to a maximum of 1mM (Meyerhof *et al.*, 2010). In this study, higher concentrations were testable without responses being evident in the mock-transfected cells. The highest test concentration of 12.5mM was slightly above the limit of solubility for this compound, which means the subsequent concentrations are somewhat approximate. A concentration of ~1.39mM was found to specifically activate both dog and human Tas2r1 equally (Figure 2.18). However, as concentrations increased above 3mM the mock-transfected cells did respond.

The naturally occurring (-)-menthol has not been previously published as a hTAS2R1 ligand. In this study it proved to be similarly active for both dog and human Tas2r1, with threshold activation at around 58µM for dog and 19µM for human in the initial phase experiments. Specific activation in both receptors was also seen in the repeat phase experiments conducted on the FDSS/µCELL system, but again the threshold was elevated (Figure 2.18).

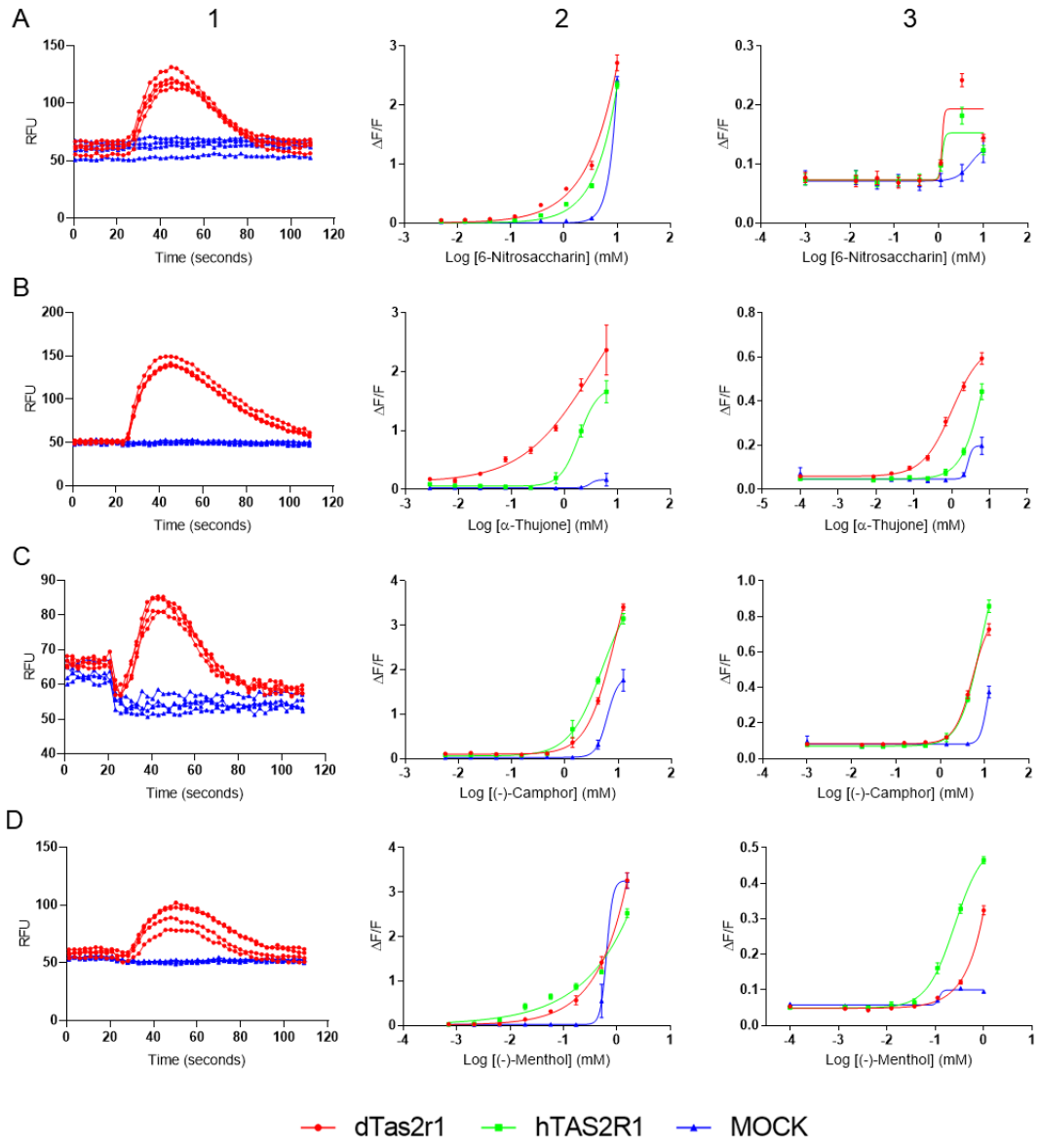

Figure 2.18: Compounds showing specific activity for hTAS2R1 and dTas2r1
Rows A-D each show data from one of the four compounds A) 6-Nitrosaccharin, B) (-)-α-Thujone, C) (-)-Camphor, D) (-)-Menthol. Column 1 shows raw data for the highest concentration where a specific response was seen with dTas2r1. Column 2 shows full concentration-response data for the initial phase testing. Column 3 shows concentration-response data from the repeat phase. The initial phase includes FlexStation data produced at the Waltham laboratory (n=1, error bars=SD). The repeat phase includes data produced at the IMAX Discovery laboratory with the Hamamatsu FDSS/µCELL system (n=3, error bars=SEM).

Similar to hTAS2R1 the dTas2r1 receptor displayed sensitivity to a variety of compounds. Positive compounds fell reasonably evenly into the three categories of dTas2r1 active (5 compounds), hTAS2R1 active (7 compounds), or active against both versions of the receptor (4 compounds). As one of the more active dog receptors in

this study, dTas2r1 was a good candidate for assessing the impact of variations in the receptor sequence, a subject which was explored in more detail in Chapter 4.

2.4.2.2. Tas2r2 concentration-response testing

Tas2r2 is a pseudogene in humans. As such no prediction for breadth of tuning could be made before testing. Concentration-response testing was carried out with six compounds for dTas2r2. Of these, only four were retested in the repeat phase screening conducted at the IMAX Discovery laboratory. The two compounds not tested in the repeat testing were denatonium benzoate and diphenidol. Denatonium benzoate gave a small response in the initial phase data, but only at the highest concentration tested with no evidence of dose-dependency. Diphenidol did not give a specific response in the initial phase.

In the initial phase testing 1, 10-phenanthroline gave a specific response with dTas2r2, with a threshold concentration of 1.1mM. At higher concentrations, strong responses were seen in the mock-transfected cells. This result was not replicated in the data produced at IMAX Discovery, but evidence of a specific response was seen at the next highest concentration of 3.33mM. This was obscured in the peak data due to an initial drop in baseline signal upon compound injection, but can be seen in the raw data (Figure 2.19). A further repeat test was subsequently performed at Waltham and was in agreement with the initial phase testing.

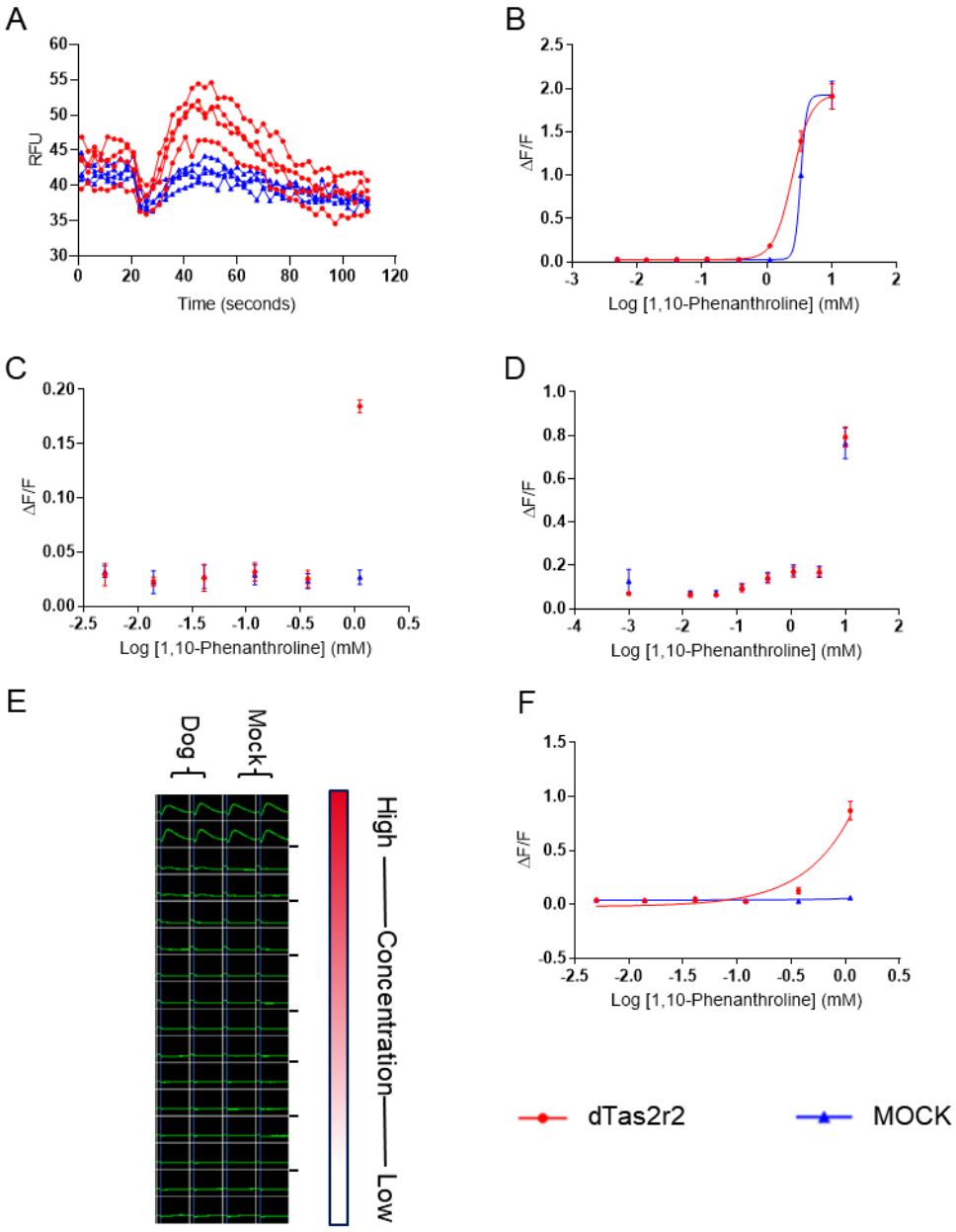

Figure 2.19: Concentration-response data for Tas2r2 and 1, 10-phenanthroline
A) Raw data for the highest concentration where a specific response was seen with dTas2r2. B) Full concentration-response data produced in an initial phase of testing. C) Concentration-response data from the initial phase testing limited to the highest concentration where a specific response was seen (no activation in the mock cell line). D) Full concentration-response data produced in a repeat phase of testing. E) Raw data traces from one run of the repeat phase testing, concentrations are as for panel D. F) Repeat testing on the FlexStation to confirm the result from the initial phase. The initial phase includes FlexStation data produced at the Waltham laboratory (n=1, error bars=SD). The repeat phase includes data produced at the IMAX Discovery laboratory with the Hamamatsu FDSS/µCELL system (n=3, error bars=SEM). In this case another repeat was performed on the FlexStation to confirm the result.

For colchicine, a specific response was seen for dTas2r2 in the initial phase data. However, this response was not replicated in the repeated experiments at IMAX Discovery (Figure 2.20). This compound precipitated at higher concentrations. A subsequent repeat test at Waltham with a lower maximum concentration confirmed the result from the initial phase, suggesting the lack of response in the repeat phase testing was related to the lower sensitivity that was observed in this phase.

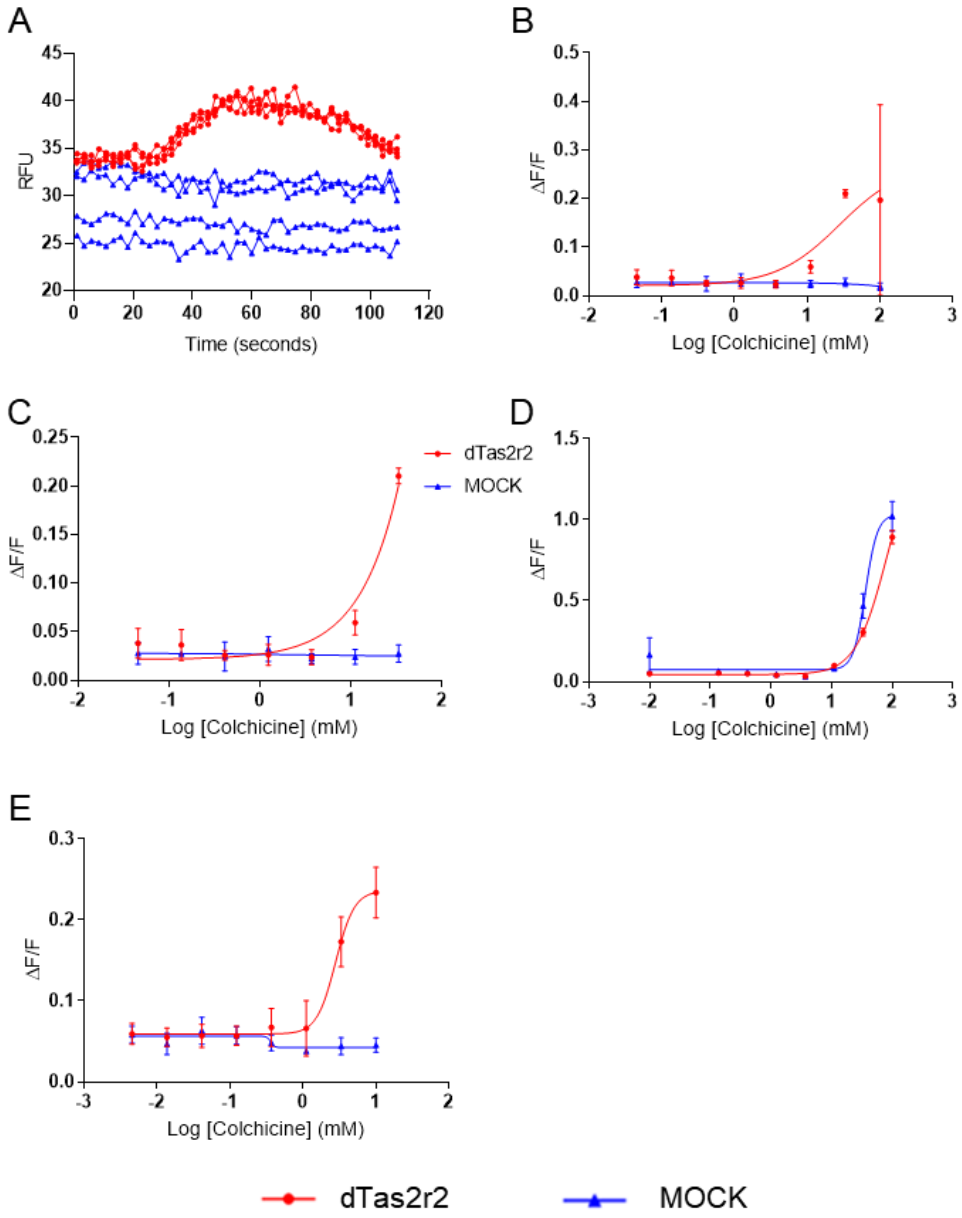

Figure 2.20: Concentration-response data for Tas2r2 and colchicine
A) Raw data for the highest concentration where a specific response was seen with dTas2r2. B) Full concentration-response data produced in an initial phase of testing. C) Concentration-response data from the initial phase testing limited to the highest concentration where a specific response was seen (no activation in the mock cell line). D) Full concentration-response data produced in a repeat phase of testing. E) Repeat testing on the FlexStation with a reduced maximum concentration to confirm the result from the initial phase. The initial phase includes FlexStation data produced at the Waltham laboratory (n=1, error bars=SD). The repeat phase includes data produced at the IMAX Discovery laboratory with the Hamamatsu FDSS/µCELL system (n=3, error bars=SEM).

Aurintricarboxylic acid proved to be an extremely potent activator of dTas2r2. The concentration used in the initial phase proved to be far too high and was adjusted for the repeat phase testing at IMAX Discovery. The threshold concentration was 3µM in the repeat testing, but this would possibly be lower in a repeat of the initial phase testing due to the issues seen in the repeat phase testing with assay sensitivity (Figure 2.21). The EC_{50} was 6.9µM with 95% confidence intervals of 4.76 to 10.82µM in the repeat phase testing.

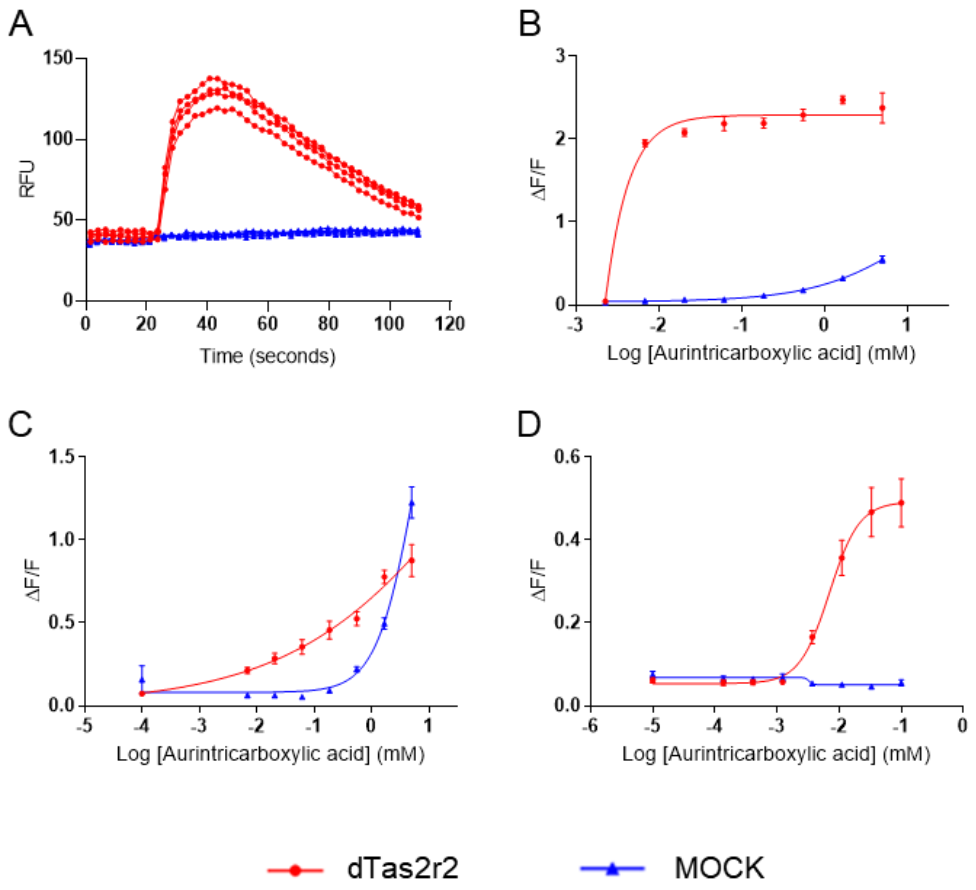

Figure 2.21: Concentration-response data for Tas2r2 and aurintricarboxylic acid
A) Raw data for the highest concentration where a specific response was seen with dTas2r2. B) Full concentration-response data produced in an initial phase of testing. C) Full concentration-response data produced in a repeat phase of testing. D) Full concentration-response data produced in a repeat phase of testing with a reduced maximum concentration. The initial phase includes FlexStation data produced at the Waltham laboratory (n=1, error bars=SD). The repeat phase includes data produced at the IMAX Discovery laboratory with the Hamamatsu FDSS/µCELL system (n=3, error bars=SEM).

Ofloxacin gave a specific response in the initial phase with a threshold of 0.69mM. However, this was not as strong in the repeat testing. A positive response was apparent in the data, but an initial drop in baseline fluorescence on compound injection masked the response when peak data was extracted. Inspection of the raw response traces from the repeat phase testing clearly shows the difference between the receptor and mock-transfected cells, but at the highest concentration only (Figure 2.22).

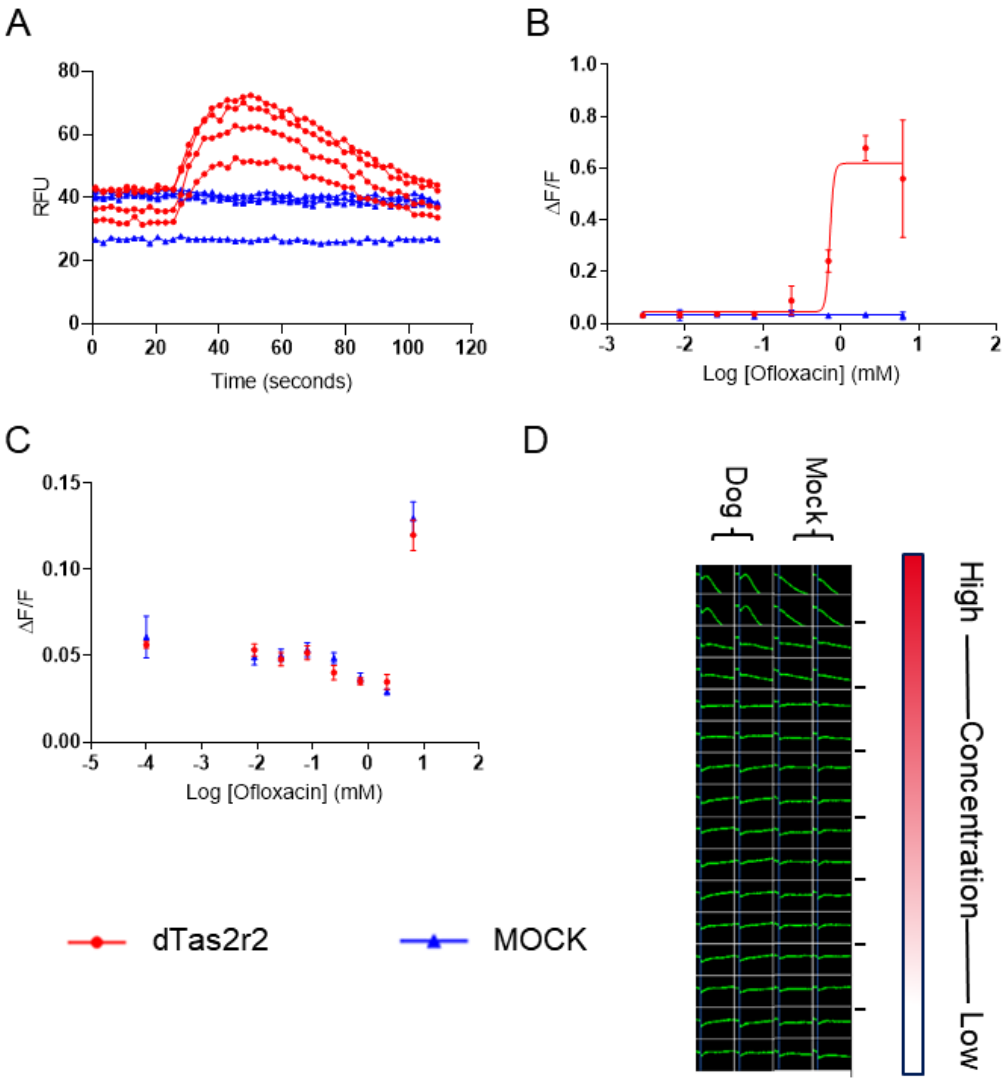

Figure 2.22: Concentration-response data for Tas2r2 and ofloxacin
A) Raw data for the highest concentration where a specific response was seen with dTas2r2. B) Full concentration-response data produced in an initial phase of testing. C) Full concentration-response data produced in a repeat phase of testing. D) Raw data traces from one run of the repeat phase testing. Concentrations are as for panel C. The initial phase includes FlexStation data produced at the Waltham laboratory (n=1, error bars=SD). The repeat phase includes data produced at the IMAX Discovery laboratory with the Hamamatsu FDSS/µCELL system (n=3, error bars=SEM).

Although it was not broadly tuned here dTas2r2 was certainly an active receptor, with 4 ligands identified. In particular, aurintricarboxylic acid was a potent agonist. Data for dog receptors with no human orthologue are particularly interesting, as without these receptors an overall assessment of the dog's perception of bitter taste cannot be made.

2.4.2.3. Tas2r3 concentration-response testing

In total 16 compounds were selected from the test library for concentration-response testing with Tas2r3 based on the pre-screen data. However, in the initial testing phase only three of these showed evidence of specific responses and these were retested with the FDSS/µCELL system.

Chloroquine is the only published ligand for hTAS2R3, with an activating concentration reported as 10mM (Li *et al.*, 2008; Meyerhof *et al.*, 2010). In the work presented here the application of chloroquine resulted in some cell responses that were unique among the tested library of compounds. Chloroquine proved highly-soluble and was tested at a maximum concentration of 200mM. Responses in the mock-transfected cells were observed at this, and the next highest concentration of 66.7mM. The following concentrations of 22.2mM and 7.4mM did not show these non-specific responses, and with hTAS2R7 (for which chloroquine is also a known ligand) clear specific activation of the receptor-transfected cells could be seen (see section 2.4.2.6). At concentrations lower than this a different non-specific response could be seen in both receptor and mock-transfected cells. With hTAS2R3, no specific response was observed at either the 7.4mM or the 22.2mM concentrations. Some elevation in the response of h*TAS2R3*-transfected cells at 66.6mM was observed, but given the high concentration and lack of any dose-dependency the test was not repeated during the retesting phase.

In previous, unpublished work done at Waltham, a different assay format was used with this receptor-compound combination. The same assay with the utilisation of a stably-expressed photosensitive protein, natClytin, was used with this receptor-compound combination and a luminescent assay readout (Figure 2.23). In this case clear activation of dTas2r3 by chloroquine was observed, indicating the unusual results seen here with chloroquine are related to how this receptor-compound combination performs in the fluorescent version of the assay.

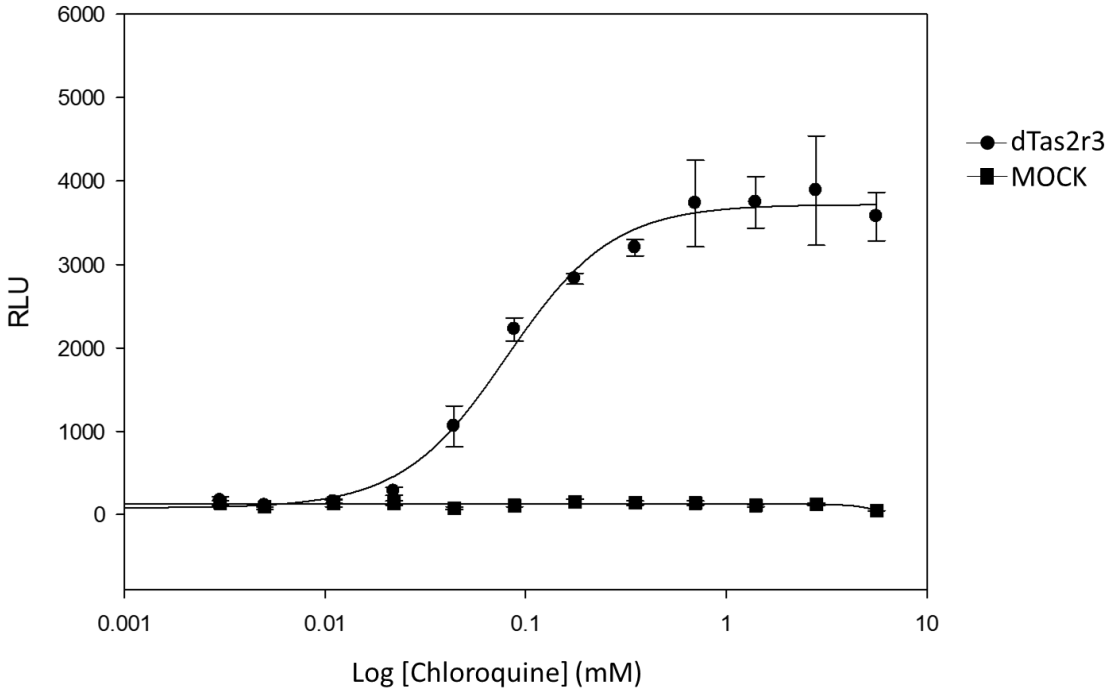

Figure 2.23: Previously generated data for dTas2r3 with chloroquine in a luminescent assay format
Luminescent output is given in Relative Luminescent Units (RLU). This data was produced on the FlexStation (n=1, error bars=SD). EC_{50} was calculated as 0.081mM.

For the three compounds that were retested in the repeat phase, namely 6-nitrosaccharin, chlorhexidine and cucurbitacin B, none showed evidence of specific responses in the data generated in this phase of testing, meaning dTas2r3 was not deorphanised as part of this study, but does show activation by chloroquine in a luminescence-based assay.

2.4.2.4. Tas2r4 concentration-response testing

A total of 21 compounds were selected from the pre-screen for concentration-response testing with dTas2r4. The selection included the previously published hTAS2R4 ligands denatonium benzoate, diphenidol, parthenolide, quinine and sucralose (Li *et al.*, 2008; Meyerhof *et al.*, 2010; Lossow *et al.*, 2016).

Of these 21 compounds, 11 showed evidence of specific activity in the initial phase and were selected for the repeat phase of testing. Diphenidol and parthenolide were not selected due to a lack of specific responses in the initial testing phase.

Aristolochic acid was initially tested at a maximum concentration of 3.13mM. While appearing to initially dissolve, the compound quickly precipitated. These high concentrations also caused activation in the mock-transfected cells. This was revised for the repeat phase testing with a maximum concentration of 0.5mM being used which did not activate the mock cells. Aristolochic acid is not a published ligand for hTAS2R4, despite being tested before (Meyerhof *et al.*, 2010). It is a ligand for hTAS2R43 and hTAS2R44, with sub-micromolar concentrations stimulating these receptors. Here dTas2r4 proved to be sensitive to the compound, while hTAS2R4 was completely insensitive. A threshold concentration of 38.5µM was found to stimulate the dog receptor (Figure 2.24). In the initial phase data the EC_{50} was 0.039mM while in the repeat phase it was 0.041 with 95% confidence intervals of 0.034 to 0.049.

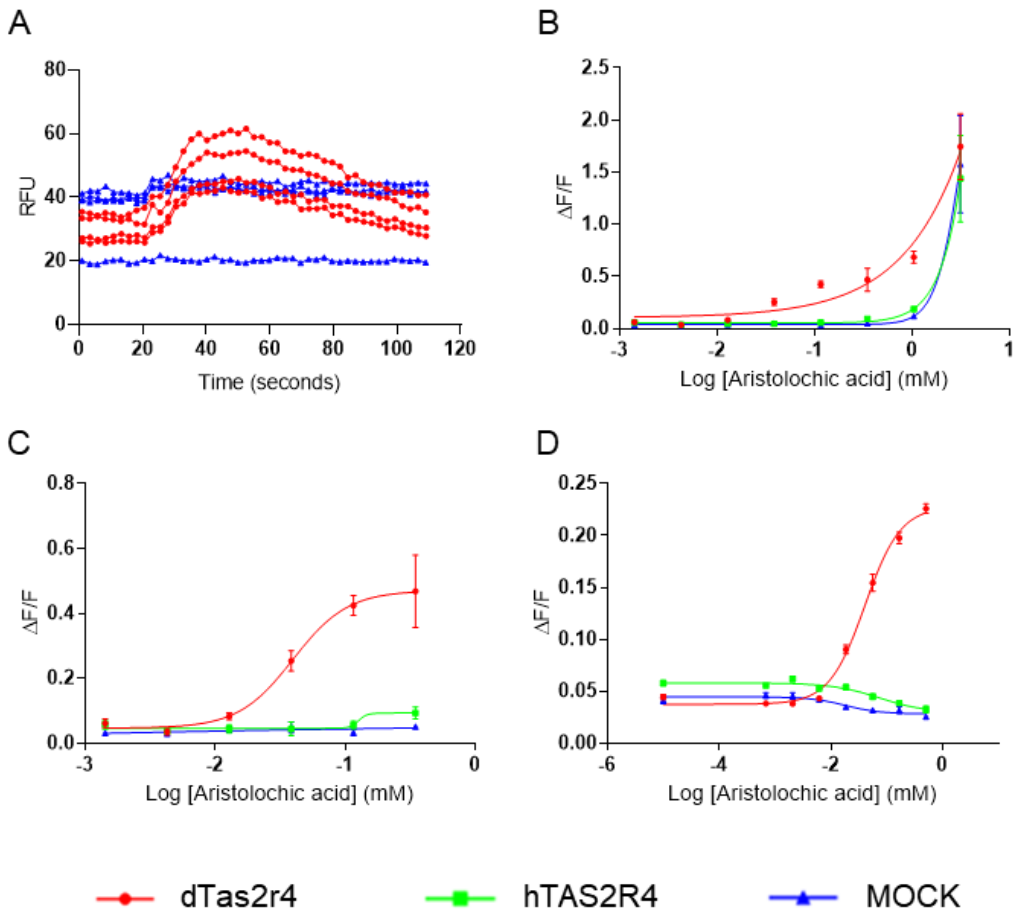

Figure 2.24: Concentration-response data for Tas2r4 and aristolochic acid
A) Raw data for the highest concentration where a specific response was seen with dTas2r4. B) Full concentration-response data produced in an initial phase of testing. C) Concentration-response data from the initial phase testing limited to the highest concentration where a specific response was seen (no activation in the mock cell line). D) Full concentration-response data produced in a repeat phase of testing. The initial phase includes FlexStation data produced at the Waltham laboratory (n=1, error bars=SD). The repeat phase includes data produced at the IMAX Discovery laboratory with the Hamamatsu FDSS/µCELL system (n=3, error bars=SEM).

(+)-Camphor was previously shown to be a ligand for hTAS2R4 with a threshold concentration of 300µM (Meyerhof *et al.*, 2010). In this study (-)-camphor was used, but a distinct response was seen with hTAS2R4 at elevated concentrations of 1.4mM in the initial testing and 4.2mM in the repeat phase testing. A specific response could not be confirmed for dTas2r4 (Figure 2.25).

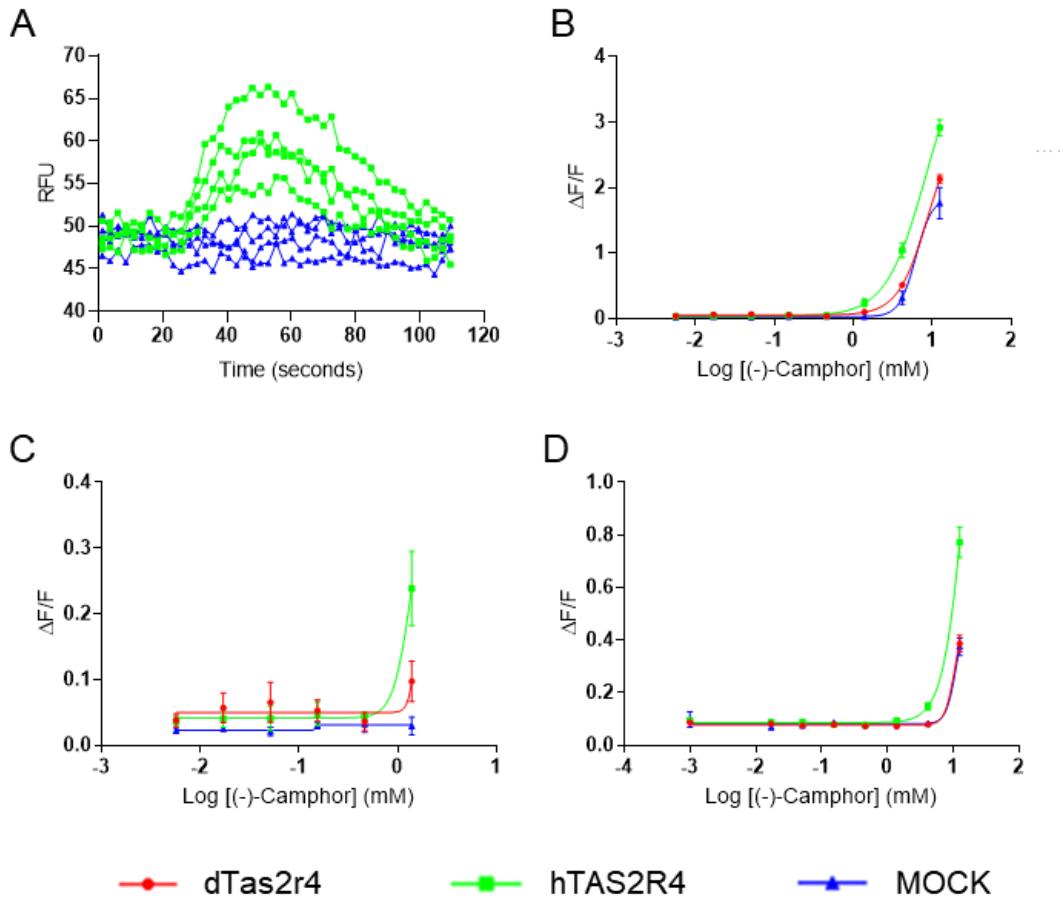

Figure 2.25: Concentration-response data for Tas2r4 and (-)-camphor
A) Raw data for the highest concentration where a specific response was seen with hTAS2R4. B) Full concentration-response data produced in an initial phase of testing. C) Concentration-response data from the initial phase testing limited to the highest concentration where a specific response was seen (no activation in the mock cell line). D) Full concentration-response data produced in a repeat phase of testing. The initial phase includes FlexStation data produced at the Waltham laboratory (n=1, error bars=SD). The repeat phase includes data produced at the IMAX Discovery laboratory with the Hamamatsu FDSS/µCELL system (n=3, error bars=SEM).

Chloramphenicol is not a known ligand of hTAS2R4 and did not give any convincing indication that it may act as such in this study. There was a very small response in dTas2r4 with the second highest concentration of 0.83mM in the initial phase test but this was not replicated in the repeat phase of testing. Also there was no indication of dose-dependency (Figure 2.26). This was not considered to be a hit for dTas2r4.

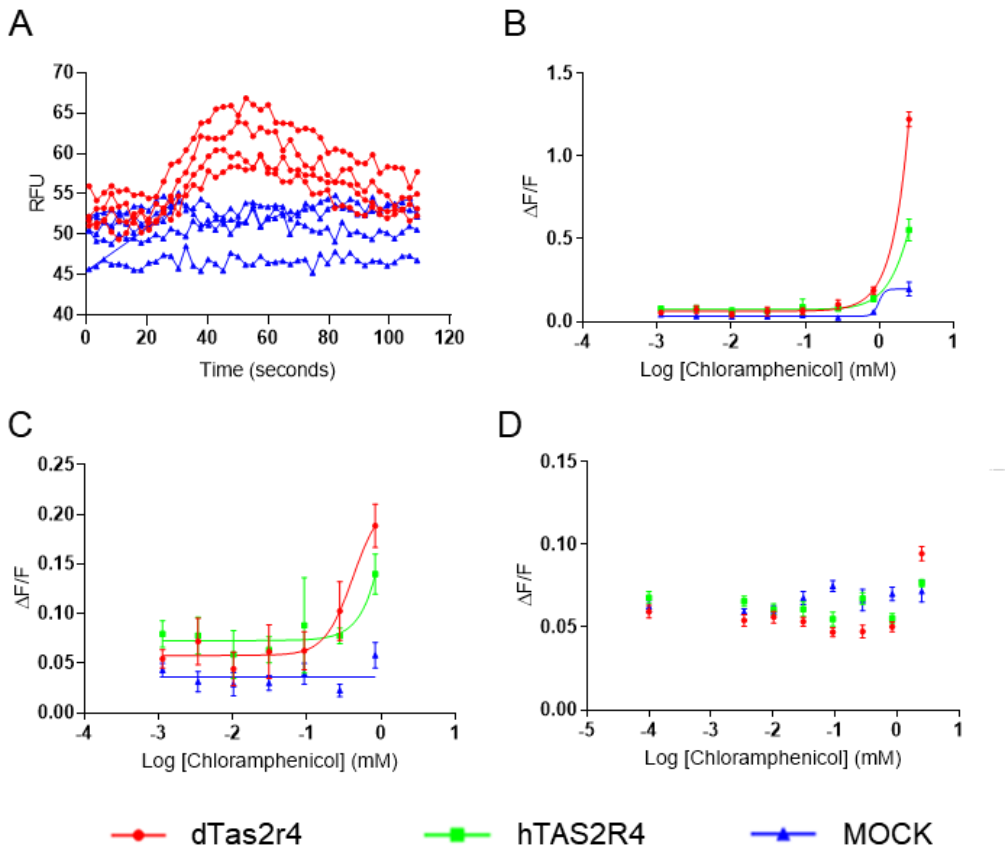

Figure 2.26: Concentration-response data for Tas2r4 and chloramphenicol
A) Raw data for the highest concentration where a specific response was seen with dTas2r4. B) Full concentration-response data produced in an initial phase of testing. C) Concentration-response data from the initial phase testing limited to the highest concentration where a specific response was seen (no activation in the mock cell line). D) Full concentration-response data produced in a repeat phase of testing. The initial phase includes FlexStation data produced at the Waltham laboratory (n=1, error bars=SD). The repeat phase includes data produced at the IMAX Discovery laboratory with the Hamamatsu FDSS/µCELL system (n=3, error bars=SEM).

Chlorhexidine was previously tested, but a maximum concentration of only 1µM was used (Meyerhof *et al.*, 2010). Only hTAS2R14 was found to respond, with a threshold concentration of 0.1µM. Here a higher maximum concentration of 0.1mM was used and initial testing showed evidence of specific responses with both human and dog Tas2r4, with a threshold concentration of 33µM. These were confirmed in the repeat testing phase with a threshold of 11µM (Figure 2.27). This is two orders of magnitude higher that that published for hTAS2R14. However, they were specific to Tas2r4 as other receptors tested here with chlorhexidine, Tas2r3 for example, showed only responses identical to the mock-transfected cells.

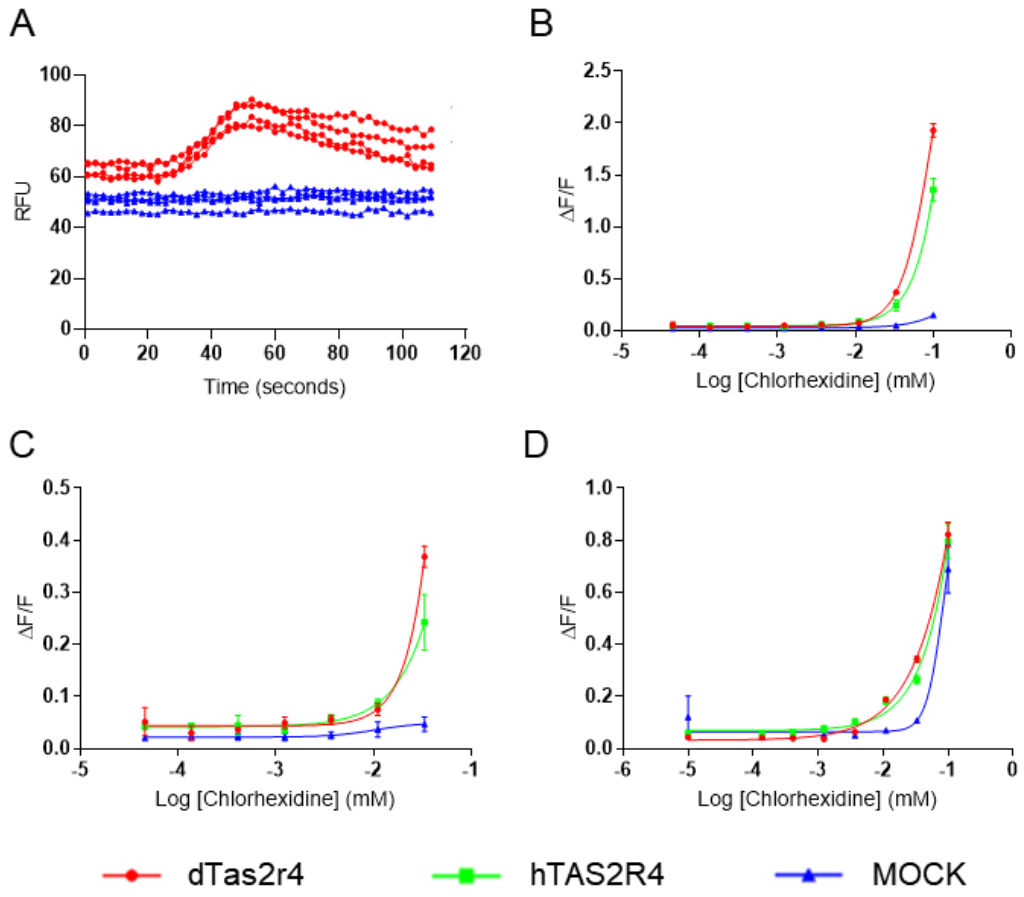

Figure 2.27: Concentration-response data for Tas2r4 and chlorhexidine
A) Raw data for the highest concentration where a specific response was seen with dTas2r4. B) Full concentration-response data produced in an initial phase of testing. C) Concentration-response data from the initial phase testing limited to the highest concentration where a specific response was seen (no activation in the mock cell line). D) Full concentration-response data produced in a repeat phase of testing. The initial phase includes FlexStation data produced at the Waltham laboratory (n=1, error bars=SD). The repeat phase includes data produced at the IMAX Discovery laboratory with the Hamamatsu FDSS/µCELL system (n=3, error bars=SEM).

Colchicine was previously reported as a hTAS2R4 ligand at a threshold concentration of 100µM (Meyerhof *et al.*, 2010). However, in this study hTAS2R4 did not give any specific responses to this compound. The dog version of the receptor did give some specific responses, but only at elevated concentrations with a threshold of 11.1mM (Figure 2.28).

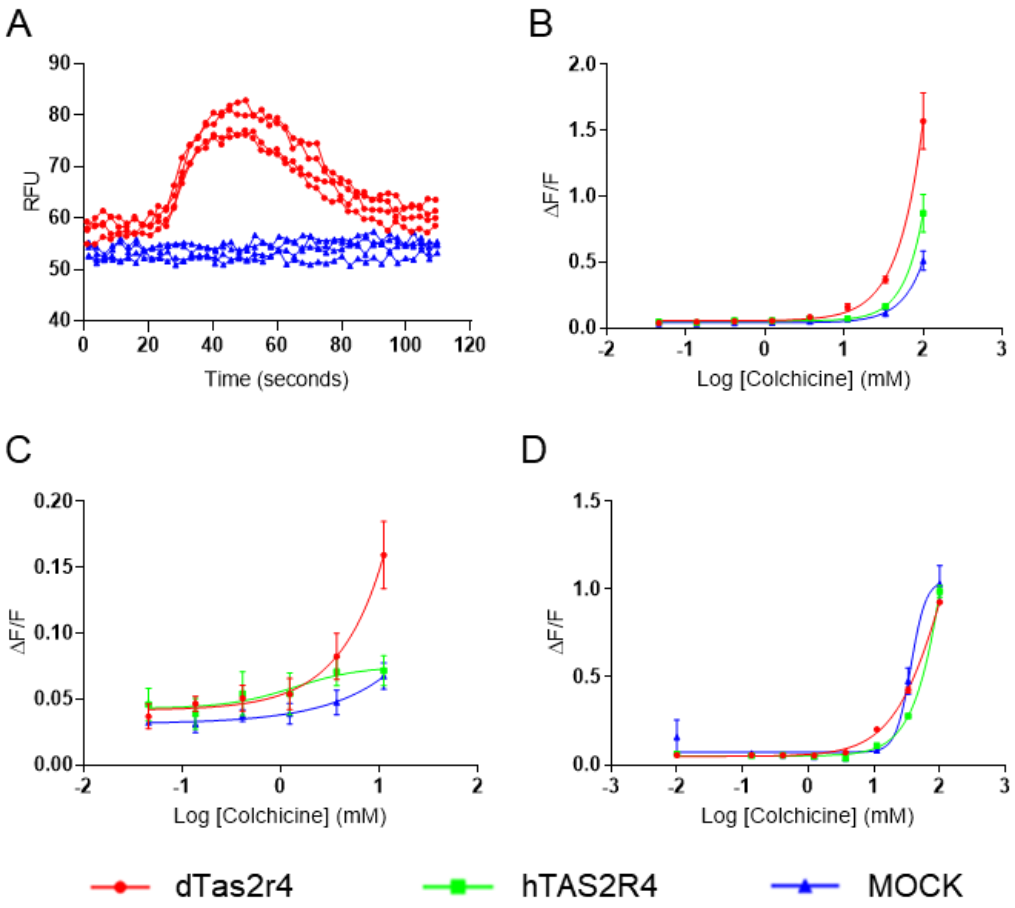

Figure 2.28: Concentration-response data for Tas2r4 and colchicine
A) Raw data for the highest concentration where a specific response was seen with dTas2r4. B) Full concentration-response data produced in an initial phase of testing. C) Concentration-response data from the initial phase testing limited to the highest concentration where a specific response was seen (no activation in the mock cell line). D) Full concentration-response data produced in a repeat phase of testing. The initial phase includes FlexStation data produced at the Waltham laboratory (n=1, error bars=SD). The repeat phase includes data produced at the IMAX Discovery laboratory with the Hamamatsu FDSS/µCELL system (n=3, error bars=SEM).

Cucurbitacin B is not a published ligand for hTAS2R4, but did give a specific response here with both hTAS2R4 and dog Tas2r4 at concentrations of 0.5mM and 0.17mM in the initial testing. However, these responses were not seen in the repeated testing phase (Figure 2.29). This test was also repeated at IMAX Discovery independently (data not shown) and no activation was seen, hence this is not considered a hit compound. It is not clear why such a response was seen in the initial phase of testing, but this does illustrate the need for repeated independent testing to identify any irregular results.

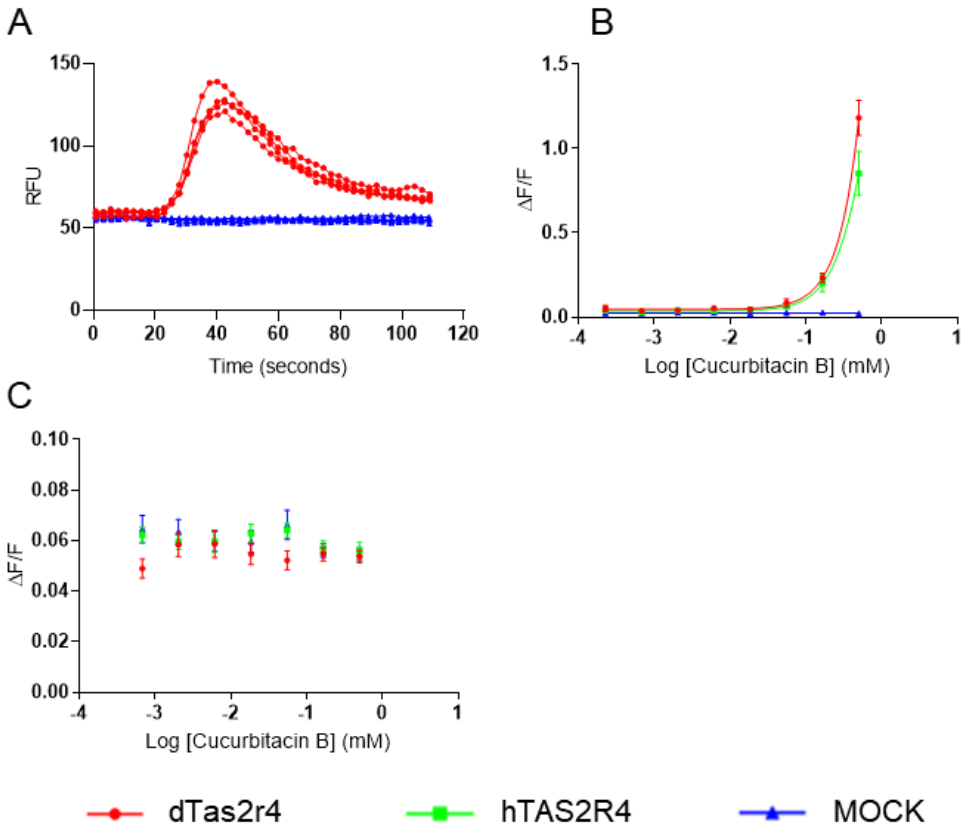

Figure 2.29: Concentration-response data for Tas2r4 and cucurbitacin B
A) Raw data for the highest concentration where a specific response was seen with dTas2r4. B) Full concentration-response data produced in an initial phase of testing. C) Full concentration-response data produced in a repeat phase of testing. The initial phase includes FlexStation data produced at the Waltham laboratory (n=1, error bars=SD). The repeat phase includes data produced at the IMAX Discovery laboratory with the Hamamatsu FDSS/µCELL system (n=3, error bars=SEM).

Denatonium benzoate was reported as an agonist of hTAS2R4 with a threshold concentration of 0.3mM in one study (Meyerhof *et al.*, 2010), but not in another (Li *et al.*, 2008). In the initial testing phase a maximum concentration of 100mM was used but this proved too high, giving strong responses in the mock-transfected cells. The maximum concentration was reduced to 10mM for the repeat phase testing. In both the initial phase and the repeat phase testing a specific response was seen for dTas2r4, but not hTAS2R4. In the case of the repeat phase testing the response was masked in the concentration-response curve, due to a drop in baseline signal at the point of compound injection. However, the response was clearly visible if the raw data were examined directly. The threshold concentration for dTas2r4 was 0.4mM (Figure 2.30), while the EC_{50} was 3.78mM in the initial phase experiments.

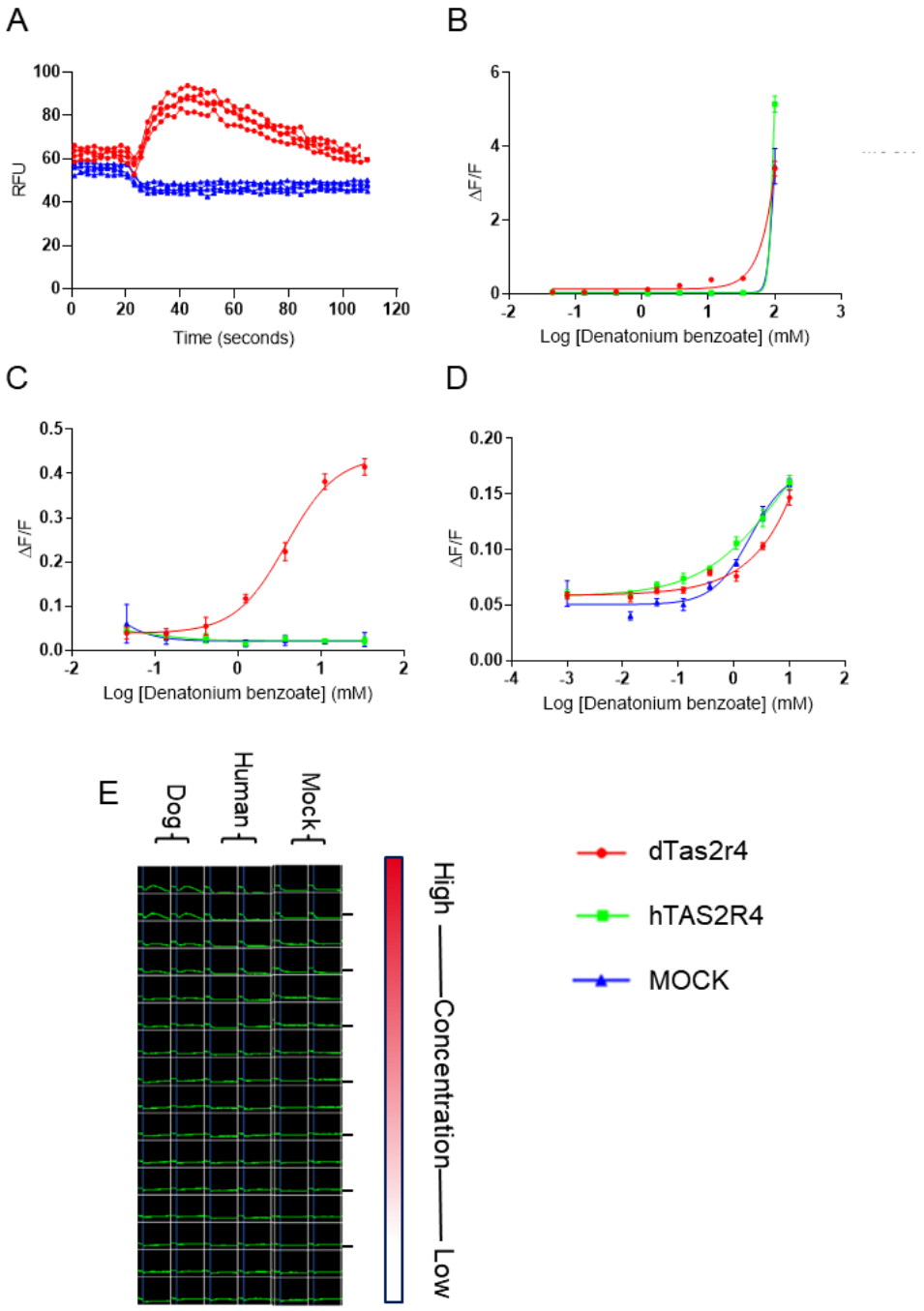

Figure 2.30: Concentration-response data for Tas2r4 and denatonium benzoate
A) Raw data for the highest concentration where a specific response was seen with dTas2r4. B) Full concentration-response data produced in an initial phase of testing. C) Concentration-response data from the initial phase testing limited to the highest concentration where a specific response was seen (no activation in the mock cell line). D) Full concentration-response data produced in a repeat phase of testing. E) Raw data traces from one run of the repeat phase testing. The initial phase includes FlexStation data produced at the Waltham laboratory (n=1, error bars=SD). The repeat phase includes data produced at the IMAX Discovery laboratory with the Hamamatsu FDSS/µCELL system (n=3, error bars=SEM).

Aurintricarboxylic acid is not a previously published test compound with Tas2rs but has been identified as an agonist of hT2R7 previously (IMAX Discovery, unpublished data). In the initial testing, a distinct response for dTas2r4 was seen compared to either hTAS2R4 or the mock-transfected cells, with a threshold of 7µM. The response of dTas2r4 was confirmed in the repeat phase (Figure 2.31).

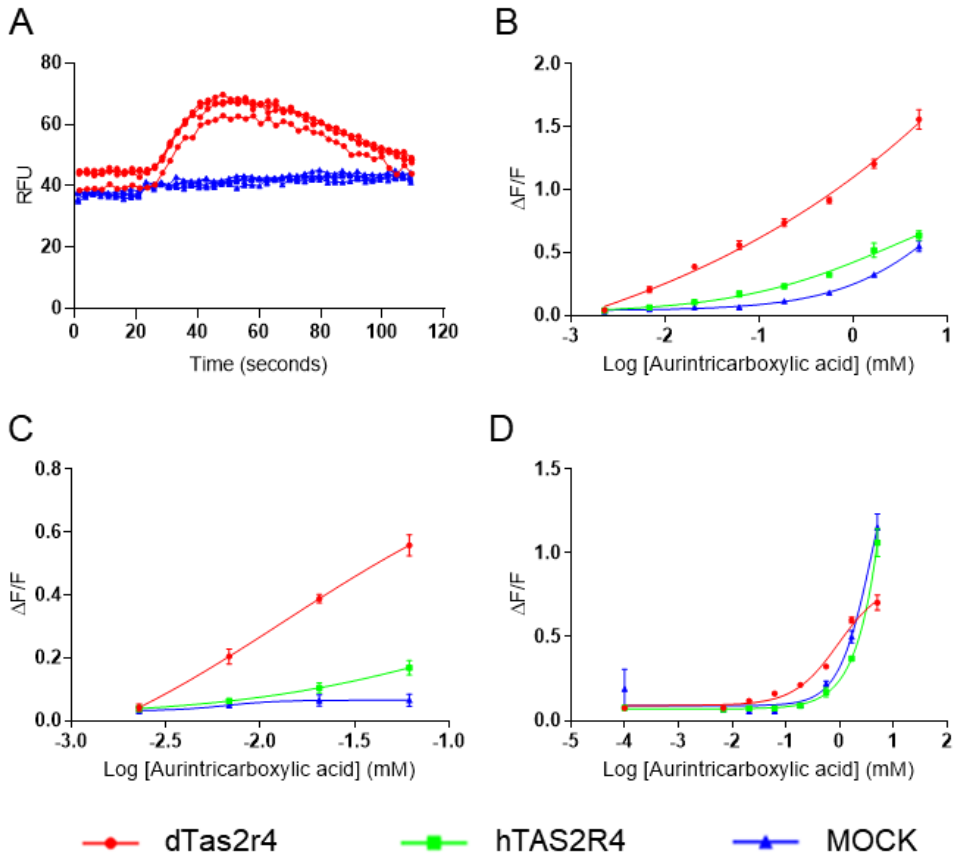

Figure 2.31: Concentration-response data for Tas2r4 and aurintricarboxylic acid
A) Raw data for the highest concentration where a specific response was seen with dTas2r4. B) Full concentration-response data produced in an initial phase of testing. C) Concentration-response data from the initial phase testing limited to the highest concentration where a specific response was seen (no activation in the mock cell line). D) Full concentration-response data produced in a repeat phase of testing. The initial phase includes FlexStation data produced at the Waltham laboratory (n=1, error bars=SD). The repeat phase includes data produced at the IMAX Discovery laboratory with the Hamamatsu FDSS/µCELL system (n=3, error bars=SEM).

Quinine was a previously reported ligand for hTAS2R4 with concentrations of 10µM (Meyerhof *et al.*, 2010) or 75µM (Li *et al.*, 2008). In the initial phase of testing, a significant response for hTAS2R4 was seen at a concentration of 26µM. However,

the response was not completely specific, with some activation of the mock and d*Tas2r4*-transfected cells. Higher concentrations caused strong activation in the mock-transfected cells. In the repeat testing phase, the maximum concentration was reduced to 200µM in an attempt to see a specific response without a response in the mock cells. The data were somewhat hard to interpret. Both receptor and mock cells responded at 200µM. At the second highest concentration of 66.6µM a specific response in the h*TAS2R4*-transfected cells could be seen, but activation was quite low. No specific response was seen from d*Tas2r4*-transfected cells (Figure 2.32).

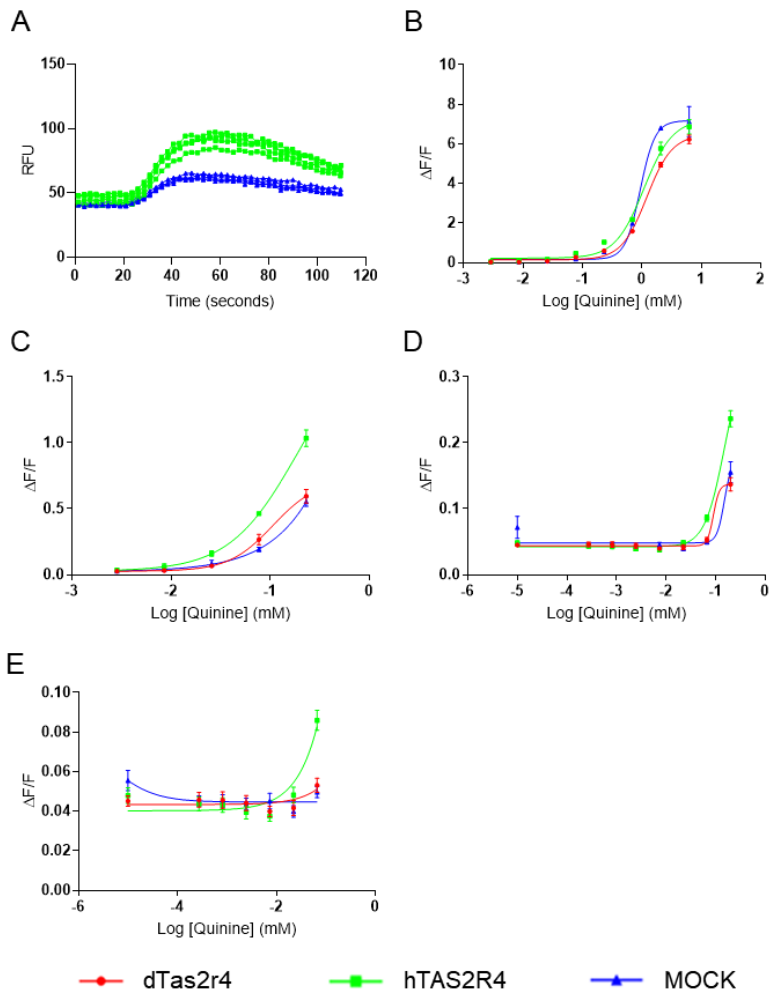

Figure 2.32: Concentration-response data for Tas2r4 and quinine
A) Raw data for hTAS2R4 where a marginally non-specific response was seen. B) Full concentration-response data produced in an initial phase of testing. C) Concentration-response data from the initial phase testing with the highest concentrations omitted. D) Full concentration-response data produced in a repeat phase of testing. E) Concentration-response data from the repeat phase testing with the highest concentration omitted. The initial phase includes FlexStation data produced at the Waltham laboratory (n=1, error bars=SD). The repeat phase includes data produced at the IMAX Discovery laboratory with the Hamamatsu FDSS/µCELL system (n=3, error bars=SEM).

Resveratrol is not a known ligand of hTAS2R4. In the initial testing, a small response was seen with both hTAS2R4 and dTas2r4, but it was not specific. In the repeat testing a small elevation in signal was seen for dTas2r4, but only for the highest concentration (Figure 2.32). This was not considered a hit for dTas2r4.

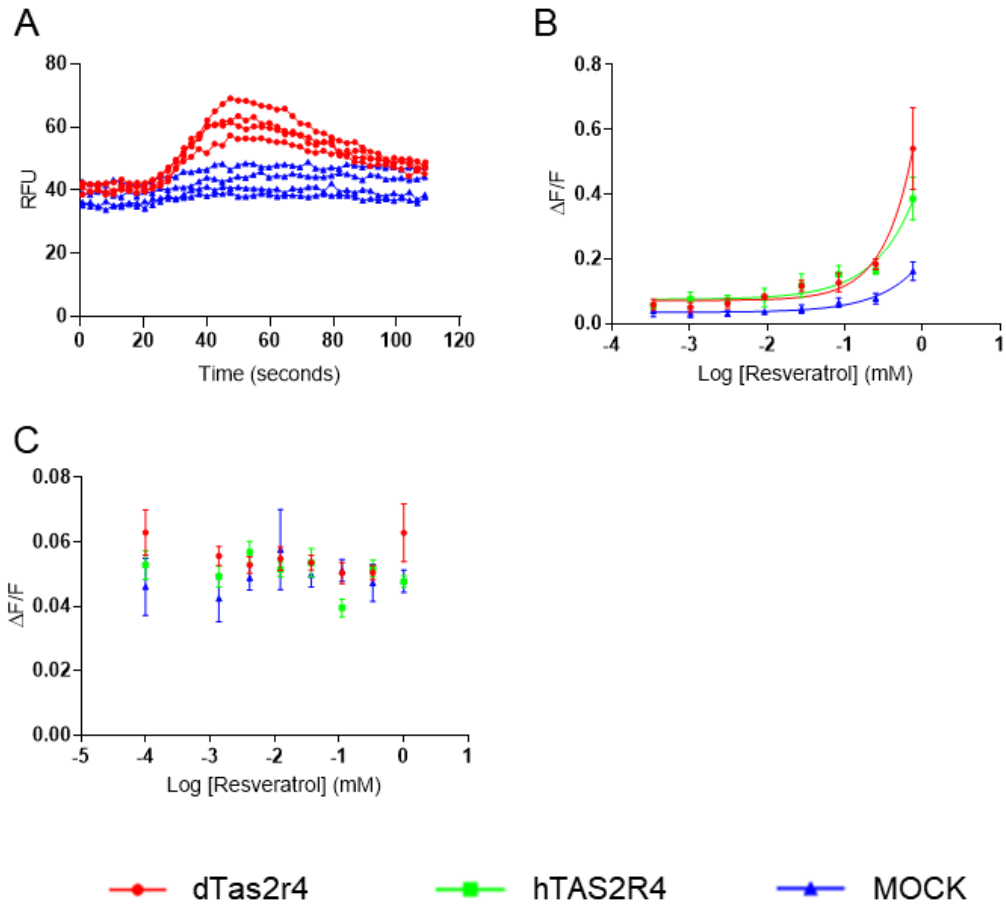

Figure 2.33: Concentration-response data for Tas2r4 and resveratrol
A) Raw data for the highest concentration where a specific response was seen with dTas2r4. B) Full concentration-response data produced in an initial phase of testing. C) Full concentration-response data produced in a repeat phase of testing. The initial phase includes FlexStation data produced at the Waltham laboratory (n=1, error bars=SD). The repeat phase includes data produced at the IMAX Discovery laboratory with the Hamamatsu FDSS/µCELL system (n=3, error bars=SEM).

Sucralose has been reported previously as an agonist of hTAS2R4 (Lossow *et al.*, 2016). In this study specific activation for hTAS2R4 was seen only in the initial phase, while dTas2r4 showed specific activation in both the initial and the repeat testing phase. The threshold concentrations from the initial phase data were 3.7mM for both dTas2r4 and hTAS2R4. While these concentrations were high, no activation was seen in the mock-transfected cells (Figure 2.34).

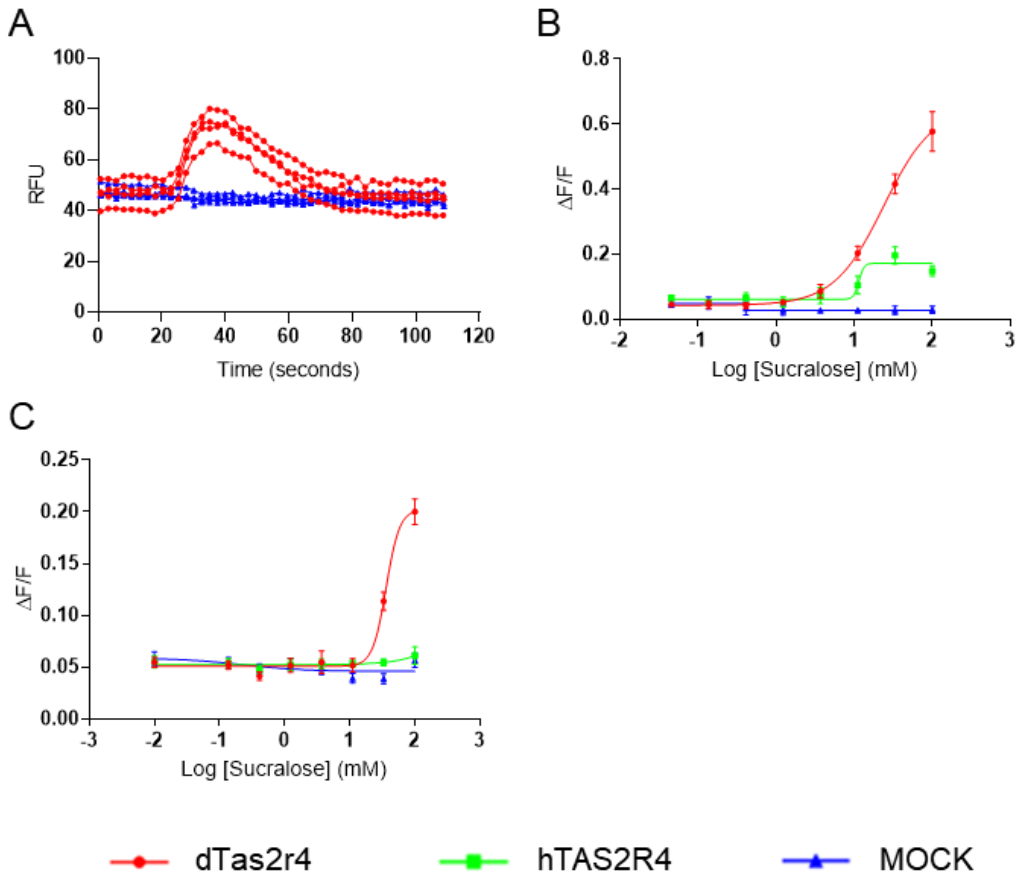

Figure 2.34: Concentration-response data for Tas2r4 and sucralose
A) Raw data for the highest concentration where a specific response was seen with dTas2r4. B) Full concentration-response data produced in an initial phase of testing. C) Full concentration-response data produced in a repeat phase of testing. The initial phase includes FlexStation data produced at the Waltham laboratory (n=1, error bars=SD). The repeat phase includes data produced at the IMAX Discovery laboratory with the Hamamatsu FDSS/µCELL system (n=3, error bars=SEM).

Overall dTas2r4 appeared to be intermediate in its tuning breadth. Most interestingly dTas2r4 was the only dog receptor to respond robustly to denatonium benzoate in this study. It was much less sensitive than the most sensitive human receptor, but this is in line with data generated *in vivo* for dogs (see section 2.5.1, Figure 2.60).

2.4.2.5. Tas2r5 concentration-response testing

A total of 8 compounds were selected from the pre-screen testing for follow-up testing with Tas2r5. In the initial testing, 5 compounds showed positive responses and were tested again in the repeat phase.

One compound, 1, 10-phenanthroline, was mistakenly omitted from the repeat phase testing. The initial phase testing showed a specific response for dTas2r5, with a threshold concentration of 370µM. However, the human receptor did not respond. This is not in agreement with published data which does show the compound as active for hTAS2R5 at a threshold concentration of 100µM (Meyerhof *et al.*, 2010) (Figure 2.35).

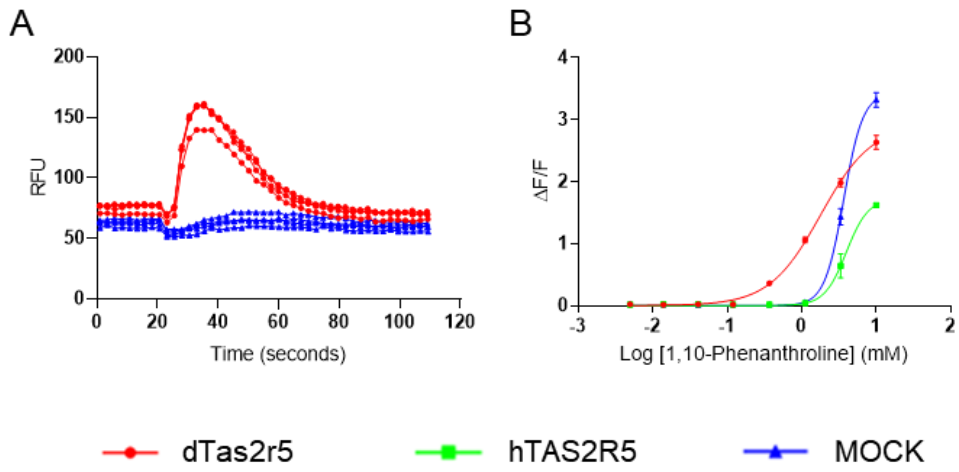

Figure 2.35: Concentration-response data for Tas2r5 and 1, 10-phenanthroline
A) Raw data for the highest concentration where a specific response was seen with dTas2r5. B) Full concentration-response data produced in an initial phase of testing. The initial phase includes FlexStation data produced at the Waltham laboratory (n=1, error bars=SD).

Neither (+)-camphor or (-)-camphor are known to be ligands for hTAS2R5 (Meyerhof *et al.*, 2010). In this study, a slight response was seen in both dog and human Tas2r5, but it was not specific in the repeat testing, with a smaller response in the mock-transfected cells. This was only present at very high concentrations of 5mM and above and there was no evidence of a dose dependant relationship below this, making the data rather unconvincing in this case. Based on these data, (-)-camphor is not considered a hit for Tas2r5 (Figure 2.36).

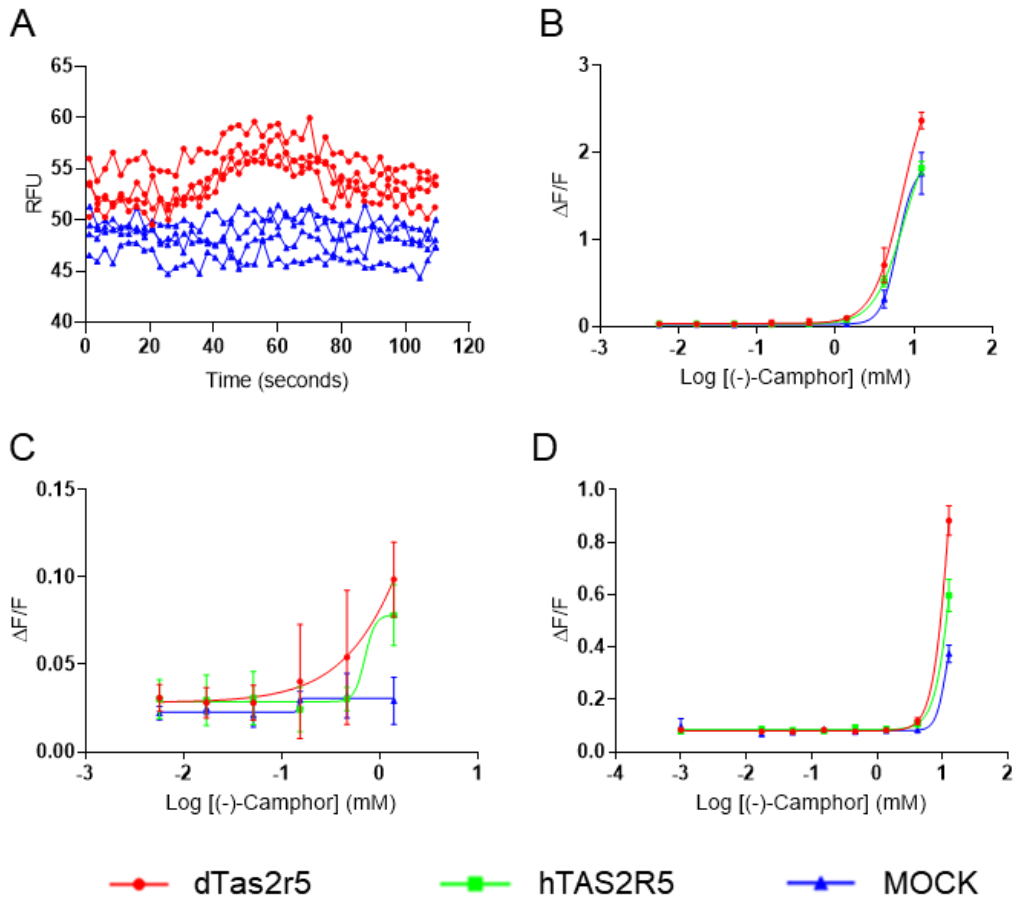

Figure 2.36: Concentration-response data for Tas2r5 and (-)-camphor
A) Raw data for the highest concentration where a specific response was seen with dTas2r5. B) Full concentration-response data produced in an initial phase of testing. C) Concentration-response data from the initial phase testing limited to the highest concentration where a specific response was seen (no activation in the mock cell line). D) Full concentration-response data produced in a repeat phase of testing. The initial phase includes FlexStation data produced at the Waltham laboratory (n=1, error bars=SD). The repeat phase includes data produced at the IMAX Discovery laboratory with the Hamamatsu FDSS/µCELL system (n=3, error bars=SEM).

Cucurbitacin B has not been previously identified as a Tas2r5 agonist (Meyerhof *et al.*, 2010). In the initial testing phase it gave some specific responses at high concentrations, but these were not reproduced in the repeat phase (Figure 2.37). This test was also repeated at IMAX Discovery (data not shown) but no responses were seen, hence it is not considered to be a hit for dTas2r5. It is not clear why responses were seen in the initial phase, but does emphasise the importance of repeated testing.

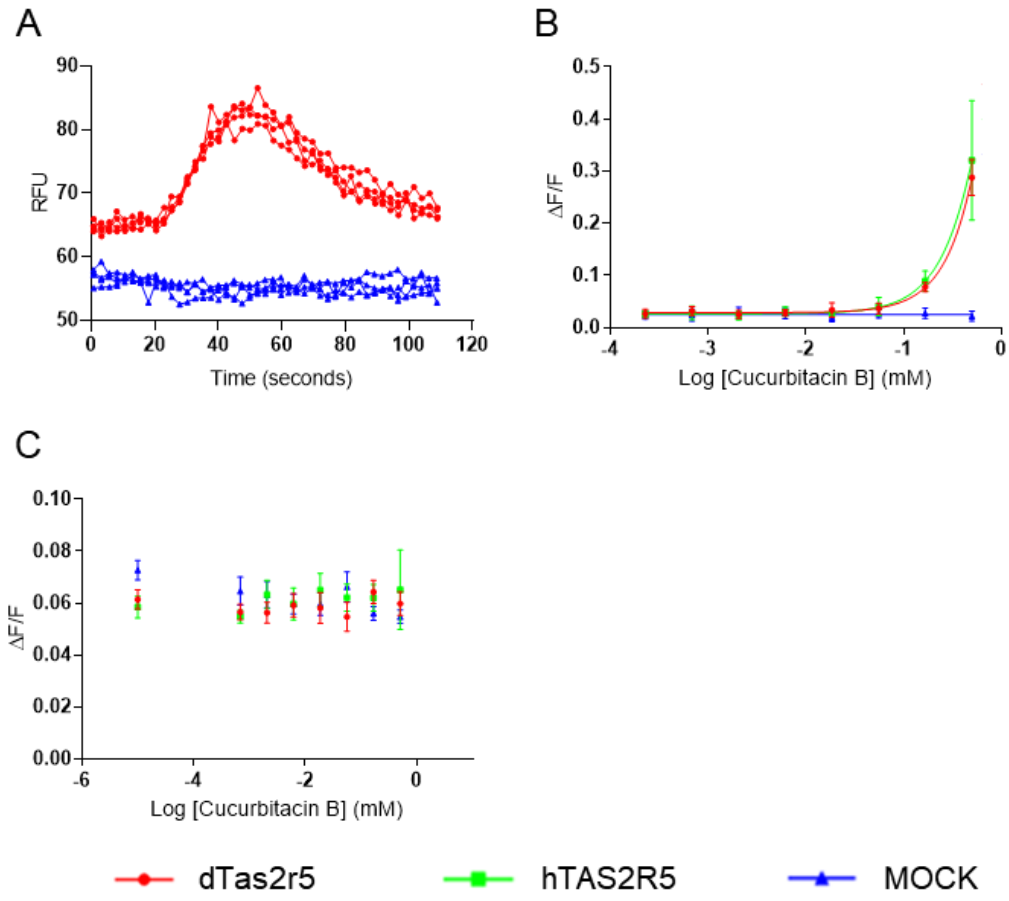

Figure 2.37: Concentration-response data for Tas2r5 and cucurbitacin B
A) Raw data for the highest concentration where a specific response was seen with dTas2r5. B) Full concentration-response data produced in an initial phase of testing. C) Full concentration-response data produced in a repeat phase of testing. The initial phase includes FlexStation data produced at the Waltham laboratory (n=1, error bars=SD). The repeat phase includes data produced at the IMAX Discovery laboratory with the Hamamatsu FDSS/µCELL system (n=3, error bars=SEM).

Aurintricarboxylic acid gave specific activation of dTas2r5, but not hTAS2R5. Responses in the initial phase were more easily interpreted than those in the repeat phase, but a specific, dose-dependent response was still seen, with a threshold of 21µM in the initial phase (Figure 2.38).

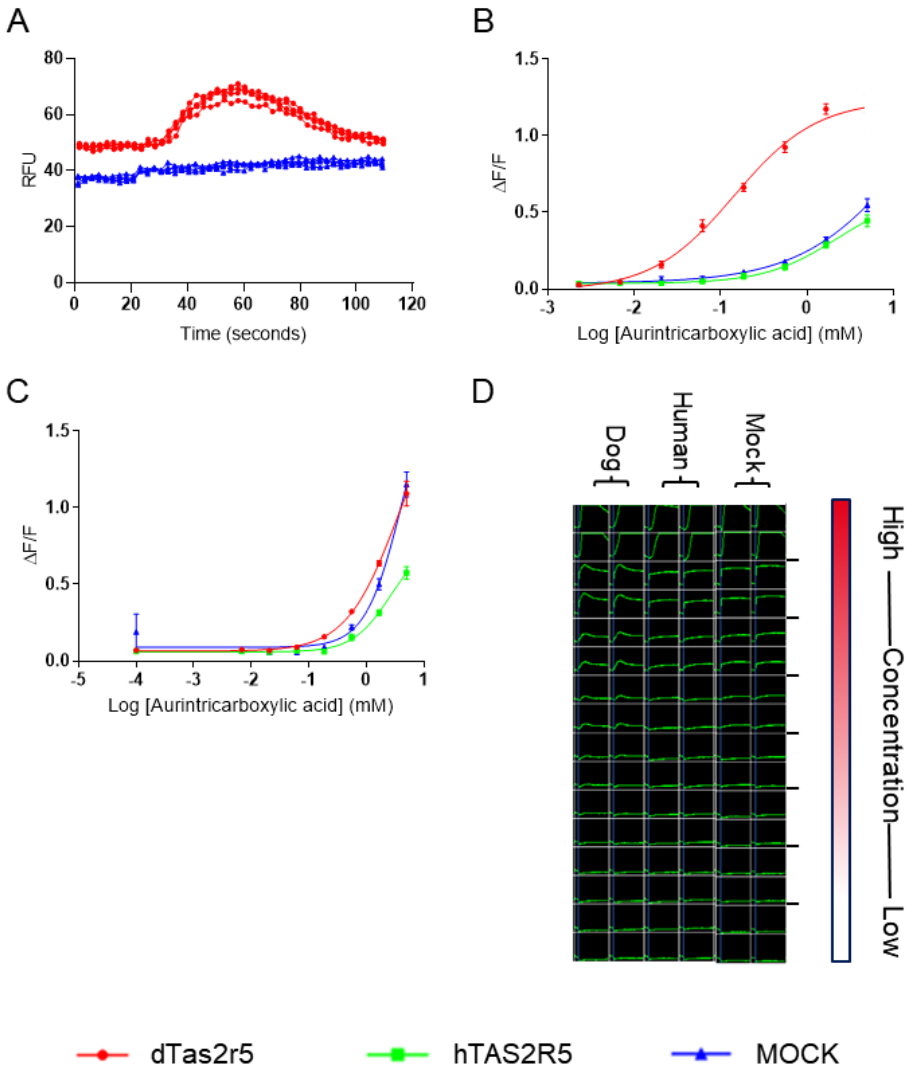

Figure 2.38: Concentration-response data for Tas2r5 and aurintricarboxylic acid
A) Raw data for the highest concentration where a specific response was seen with dTas2r5. B) Full concentration-response data produced in an initial phase of testing. C) Full concentration-response data produced in a repeat phase of testing. D) Raw data traces from one run of the repeat phase testing. Concentrations are as for panel C. The initial phase includes FlexStation data produced at the Waltham laboratory (n=1, error bars=SD). The repeat phase includes data produced at the IMAX Discovery laboratory with the Hamamatsu FDSS/µCELL system (n=3, error bars=SEM).

Oxyphenonium bromide is not a known ligand of hTAS2R5 (Li et al., 2008) and no response with hT2R5 was seen in this study. However, dT2R5 did give a specific response, with a threshold of 3.7mM. Although the concentrations giving activation were quite high, the response was specific and dose-dependent (Figure 2.39).

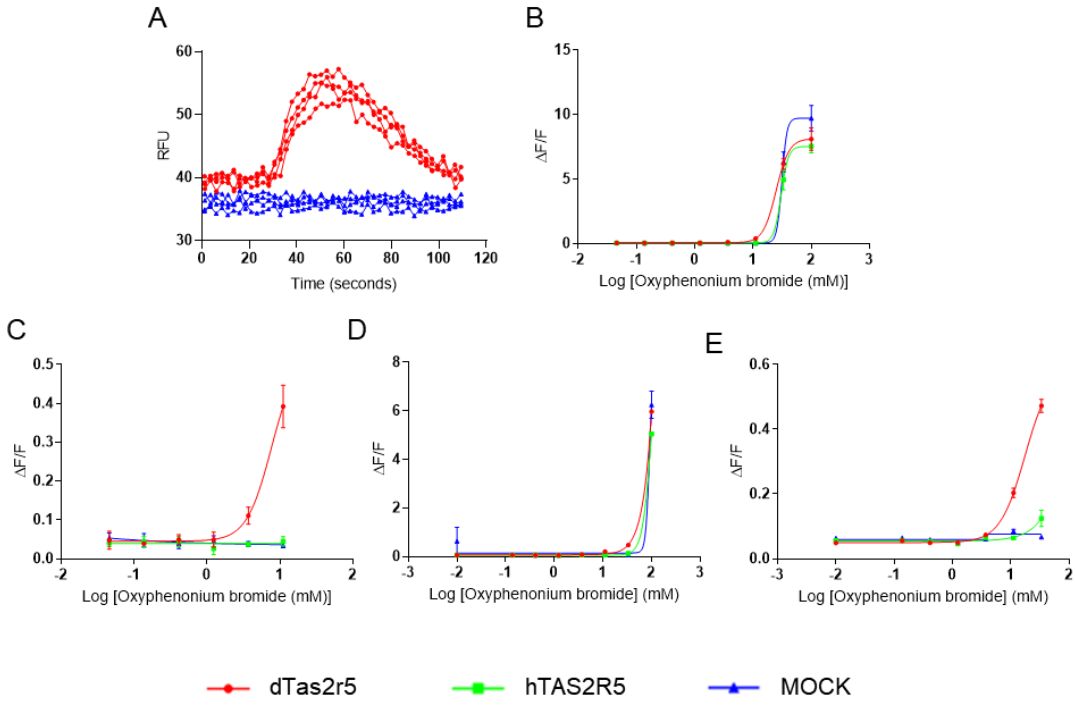

Figure 2.39: Concentration-response data for Tas2r5 and oxyphenonium bromide A) Raw data for the highest concentration where a specific response was seen with dTas2r5. B) Full concentration-response data produced in an initial phase of testing. C) Concentration-response data from the initial phase testing limited to the highest concentration where a specific response was seen (no activation in the mock cell line). D) Full concentration-response data produced in a repeat phase of testing. E) Concentration-response data from the repeat phase testing limited to the highest concentration where a specific response was seen (no activation in the mock cell line). The initial phase includes FlexStation data produced at the Waltham laboratory (n=1, error bars=SD). The repeat phase includes data produced at the IMAX Discovery laboratory with the Hamamatsu FDSS/µCELL system (n=3, error bars=SEM).

Sucralose was recorded previously as activating hTAS2R5 (Lossow *et al.*, 2016). In this study hTAS2R5 did not respond, but dTas2r5 did give a specific response at very high concentrations of 33mM in the initial phase and 100mM in the repeat phase. A reduction in sensitivity was a feature in much of the repeat phase testing (Figure 2.40).

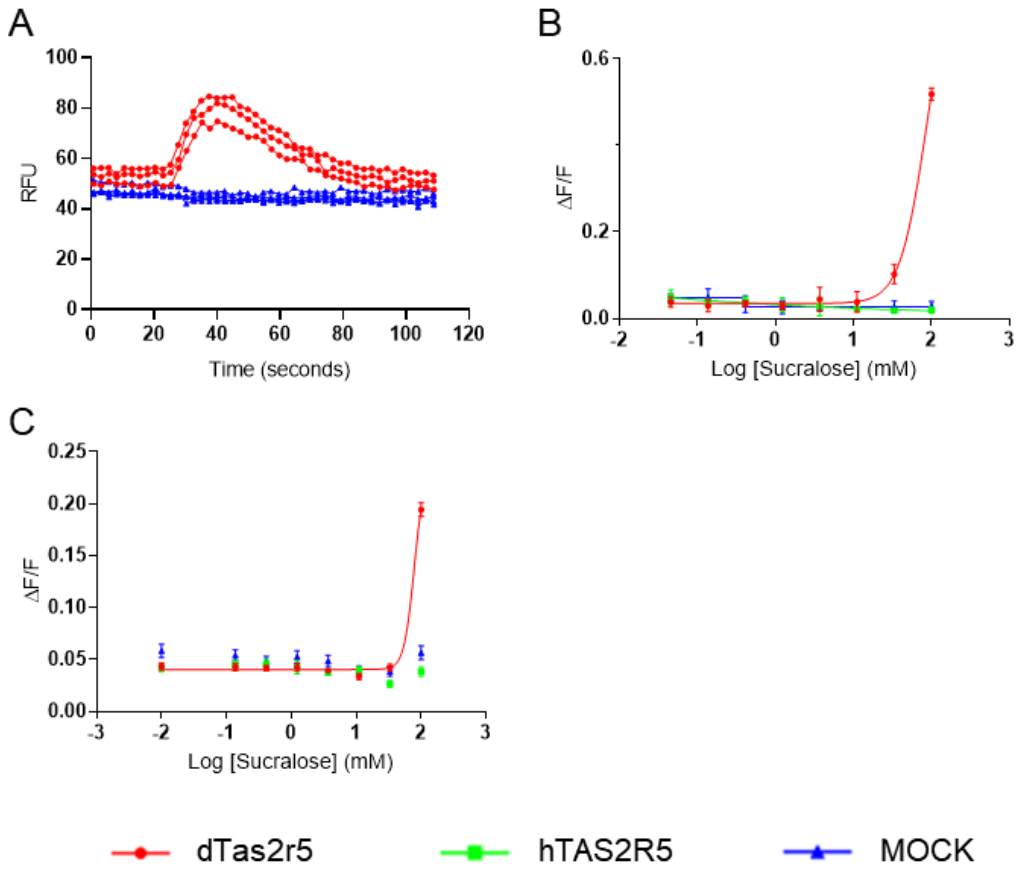

Figure 2.40: Concentration-response data for Tas2r5 and sucralose
A) Raw data for the highest concentration where a specific response was seen with dTas2r5. B) Full concentration-response data produced in an initial phase of testing. C) Full concentration-response data produced in a repeat phase of testing. The initial phase includes FlexStation data produced at the Waltham laboratory (n=1, error bars=SD). The repeat phase includes data produced at the IMAX Discovery laboratory with the Hamamatsu FDSS/µCELL system (n=3, error bars=SEM).

This study identified four ligands for dTas2r5. This is a relatively high hit rate given that only 6 ligands have been identified for hTAS2R5, despite far more extensive testing than that performed here. Two ligands, 1, 10-phenanthroline and sucralose, were shared based on data published for hTAS2R5 elsewhere, although hTAS2R5 did not respond here.

2.4.2.6. Tas2r7 concentration-response testing

A total of 19 compounds from the pre-screen phase were selected for concentration-response testing with Tas2r7 in the initial test phase. Of these, 6 showed some evidence of specific responses and were taken forward to the repeat testing phase. 6α-Methylprednisolone was not previously noted as an agonist of hTAS2R7 when tested at a concentration of 0.1mM (Li *et al.*, 2008). However, a small response was seen in the initial testing phase at concentrations of 55µM and above. This was confirmed in the repeat phase with a small, but specific response at a concentration of 0.16mM. No response was observed with dTas2r7 (Figure 2.41).

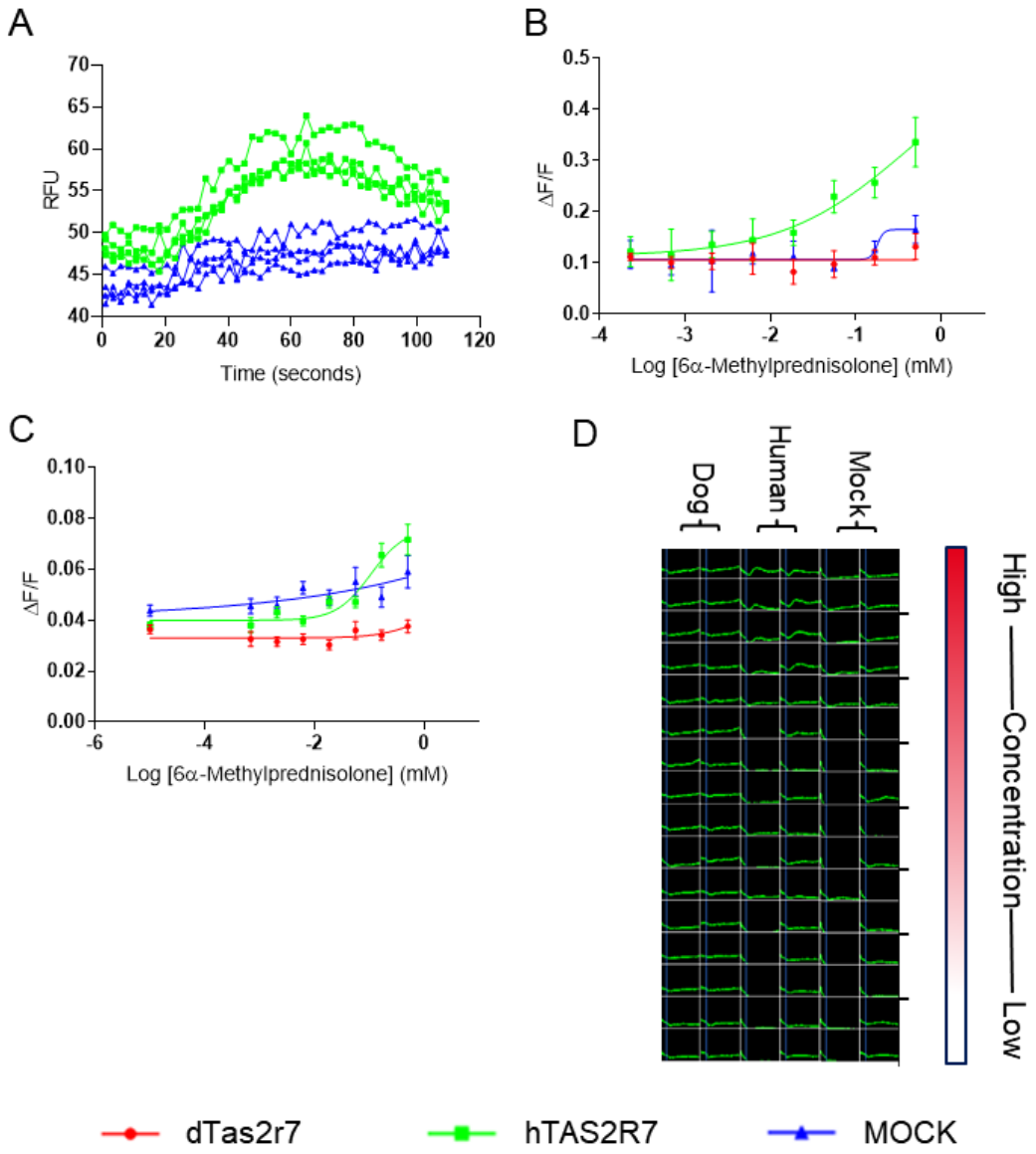

Figure 2.41: Concentration-response data for Tas2r7 and 6α-methylprednisolone
A) Raw data for the highest concentration where a specific response was seen with hTAS2R5. B) Full concentration-response data produced in an initial phase of testing. C) Concentration-response data from the initial phase testing limited to the highest concentration where a specific response was seen (no activation in the mock cell line). D) Full concentration-response data produced in a repeat phase of testing. E) Raw data traces from one run of the repeat phase testing. Concentrations are as for panel C. The initial phase includes FlexStation data produced at the Waltham laboratory (n=1, error bars=SD). The repeat phase includes data produced at the IMAX Discovery laboratory with the Hamamatsu FDSS/µCELL system (n=3, error bars=SEM).

(+)-Camphor did not stimulate hTAS2R7 in a previous study (Meyerhof *et al.*, 2010). In this study (-)-camphor showed some evidence of activation in the initial phase, but the response was neither specific nor concentration-dependent in the repeat testing phase. It was not considered as active based on these data (Figure 2.42).

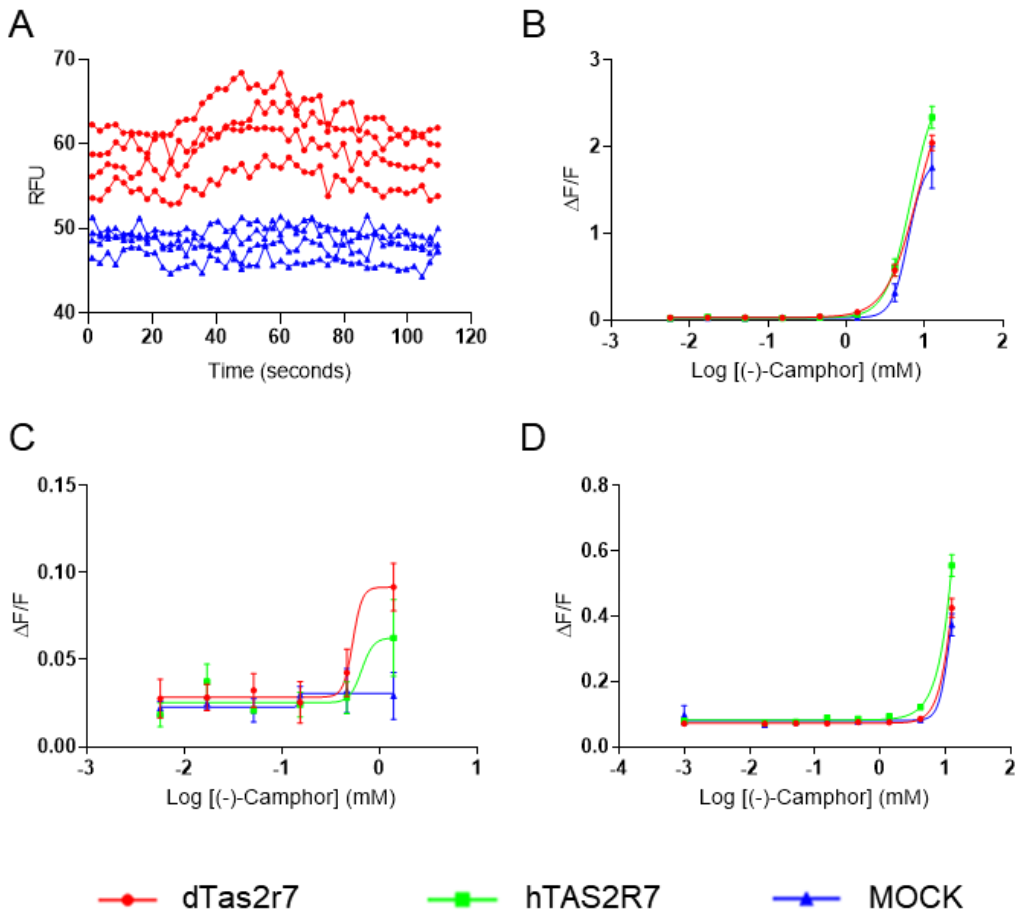

Figure 2.42: Concentration-response data for Tas2r7 and (-)-camphor
A) Raw data for the highest concentration where a specific response was seen with dTas2r7. B) Full concentration-response data produced in an initial phase of testing. C) Concentration-response data from the initial phase testing limited to the highest concentration where a specific response was seen (no activation in the mock cell line). D) Full concentration-response data produced in a repeat phase of testing. The initial phase includes FlexStation data produced at the Waltham laboratory (n=1, error bars=SD). The repeat phase includes data produced at the IMAX Discovery laboratory with the Hamamatsu FDSS/µCELL system (n=3, error bars=SEM).

Chloroquine was recorded as an agonist of hTAS2R7 at a concentration of 10mM in one study (Li *et al.*, 2008), but did not show activity in another study when used at the same concentration (Meyerhof *et al.*, 2010). Here specific activation of hTAS2R7

occurred at concentrations of 7.4mM and above while no activation of dTas2r7 was observed. At lower concentrations, a non-specific artefact was present in all tested cells, including the mock-transfected cells. This phenomenon was unique to chloroquine and is clearly visible in the concentration-response data presented in Figure 2.43.

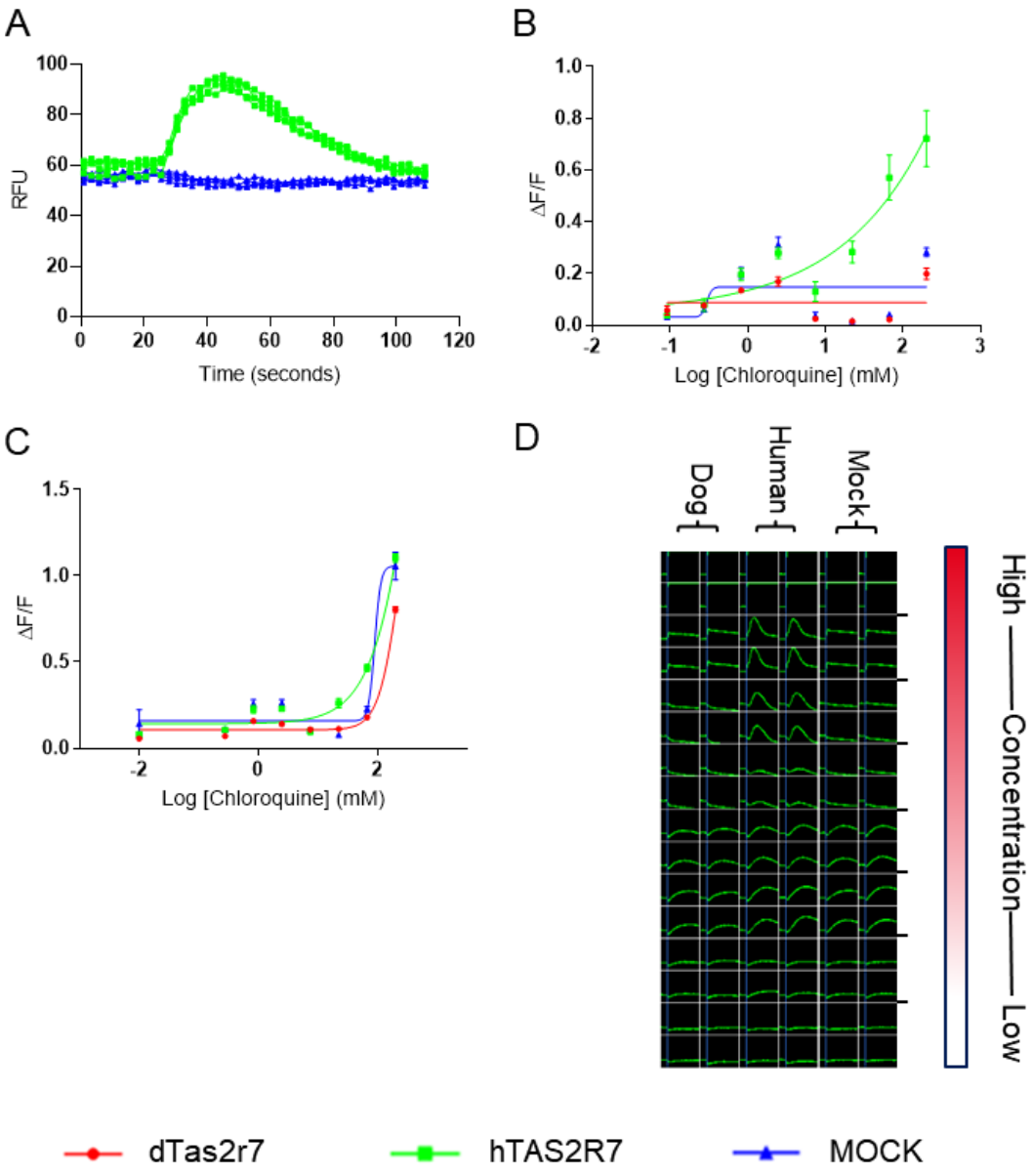

Figure 2.43: Concentration-response data for Tas2r7 and chloroquine
A) Raw data for the highest concentration where a specific response was seen with hTAS2R7. B) Full concentration-response data produced in an initial phase of testing. C) Full concentration-response data produced in a repeat phase of testing. D) Raw data traces from one run of the repeat phase testing. The initial phase includes FlexStation data produced at the Waltham laboratory (n=1, error bars=SD). The repeat phase includes data produced at the IMAX Discovery laboratory with the Hamamatsu FDSS/µCELL system (n=3, error bars=SEM).

The previously untested compound aurintricarboxylic acid proved to be a potent stimulator of hTAS2R7, but not of dTas2r7. In the initial testing phase a maximum concentration of 5mM was used, but this proved to be far too high. In the repeat

phase the maximum concentration was reduced to 0.1mM. Activation was seen at a threshold concentration of 3.7µM (Figure 2.43), although this may be lower given the issues encountered with sensitivity in the repeat phase.

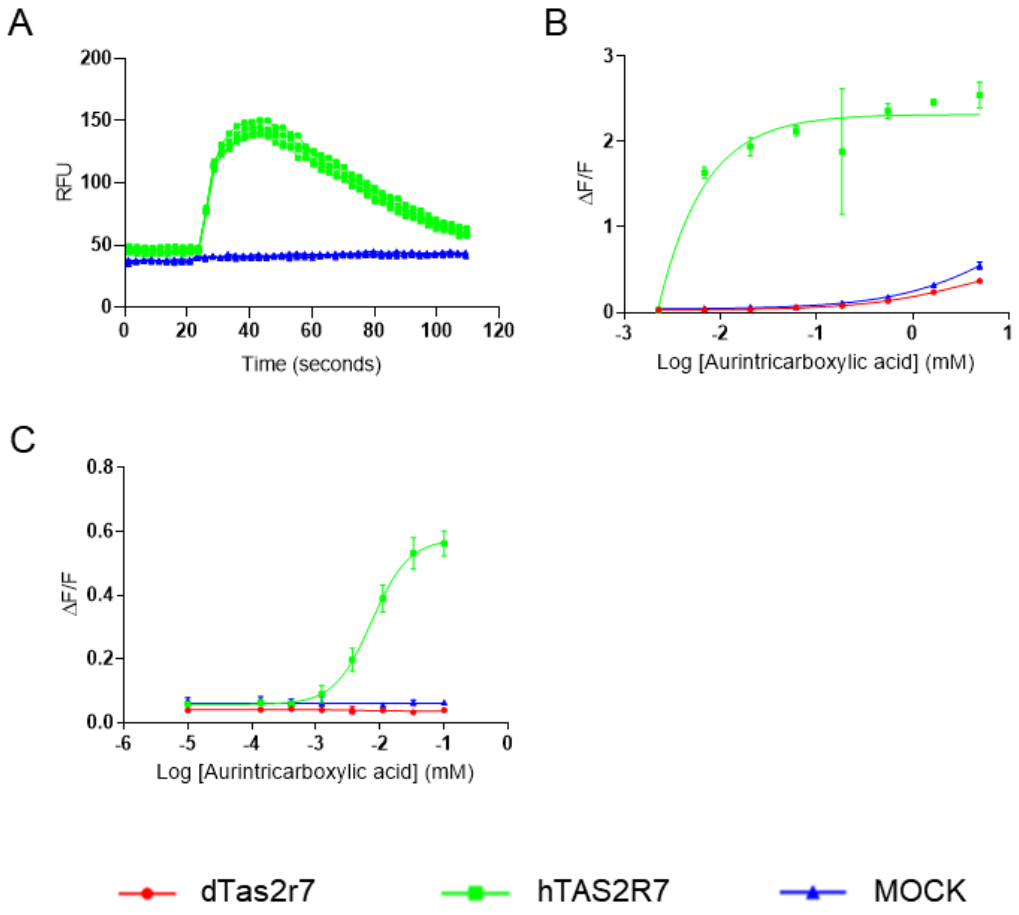

Figure 2.44: Concentration-response data for Tas2r7 and aurintricarboxylic acid
A) Raw data for the highest concentration where a specific response was seen with hTAS2R7. B) Full concentration-response data produced in an initial phase of testing. C) Full concentration-response data produced in a repeat phase of testing. The initial phase includes FlexStation data produced at the Waltham laboratory (n=1, error bars=SD). The repeat phase includes data produced at the IMAX Discovery laboratory with the Hamamatsu FDSS/µCELL system (n=3, error bars=SEM).

Oxyphenonium bromide was previously shown to stimulate hTAS2R7 at a concentration of 2.5mM (Li *et al.*, 2008). Here stimulation of hTAS2R7 was also seen in both the initial testing and the repeat phase. A threshold concentration of 3.7mM was observed in the repeat phase testing, which was a rare example of the repeat phase data showing greater sensitivity than the initial phase data, where a threshold

of 11.1mM was observed. No specific activation of dTas2r7 was apparent with the exception of the highest test concentration. However this was rather unconvincing, with no evidence of a concentration dependent response (Figure 2.45).

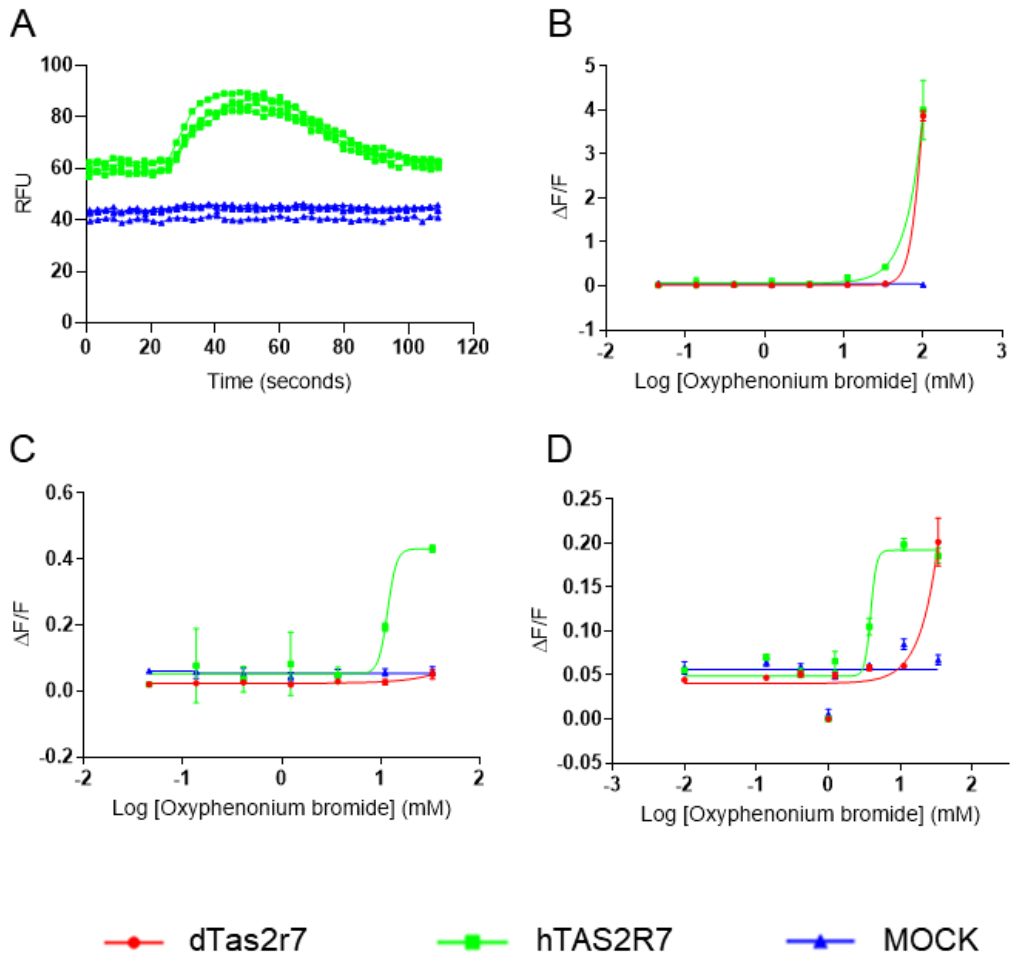

Figure 2.45: Concentration-response data for Tas2r7 and oxyphenonium bromide
A) Raw data for the highest concentration where a specific response was seen with hTAS2R7. B) Full concentration-response data produced in an initial phase of testing. C) Concentration-response data from the initial phase testing limited to the highest concentration where a specific response was seen (removal of large artefact at top concentration). D) Full concentration-response data produced in a repeat phase of testing (top concentration not shown due to large artefact). The initial phase includes FlexStation data produced at the Waltham laboratory (n=1, error bars=SD). The repeat phase includes data produced at the IMAX Discovery laboratory with the Hamamatsu FDSS/µCELL system (n=3, error bars=SEM).

Sucralose was previously noted as an agonist of hTAS2R7, but concentrations were not detailed (Lossow *et al.*, 2016). It was also active here, with small responses at concentrations of 11mM and above. The dog orthologue of the receptor was unresponsive (Figure 2.46).

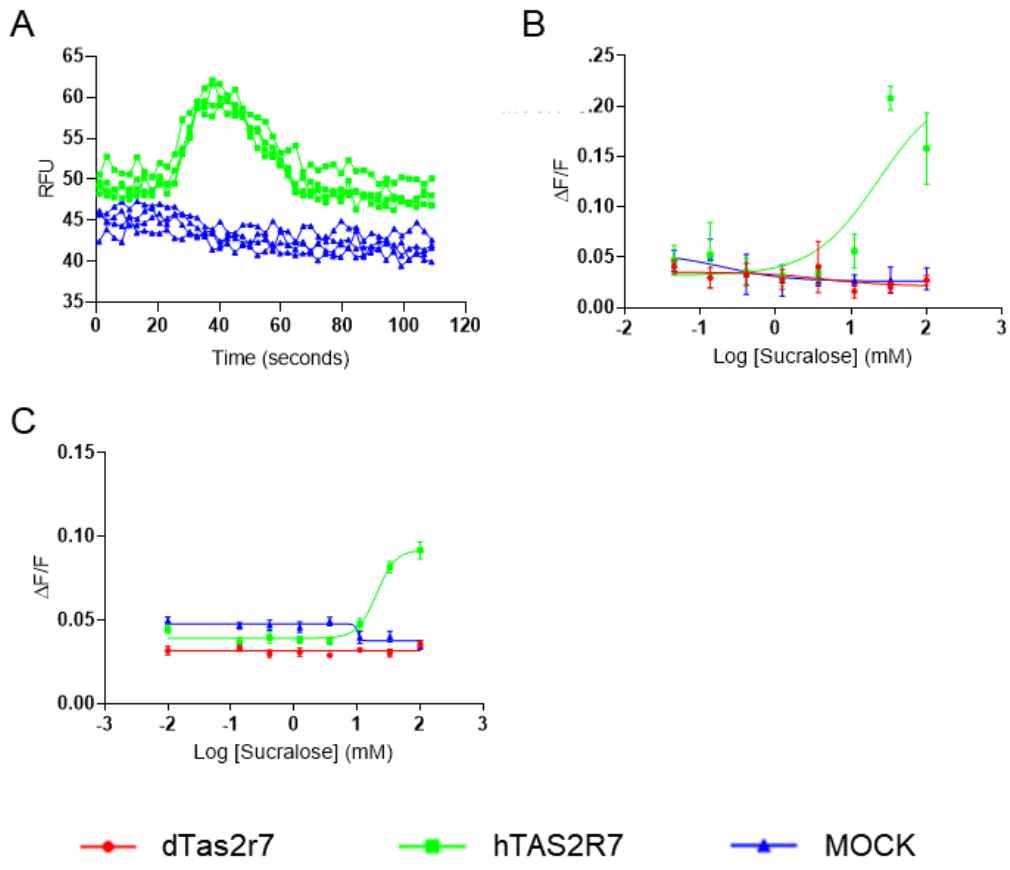

Figure 2.46: Concentration-response data for Tas2r7 and sucralose
A) Raw data for the highest concentration where a specific response was seen with hTAS2R7. B) Full concentration-response data produced in an initial phase of testing. C) Full concentration-response data produced in a repeat phase of testing. The initial phase includes FlexStation data produced at the Waltham laboratory (n=1, error bars=SD). The repeat phase includes data produced at the IMAX Discovery laboratory with the Hamamatsu FDSS/µCELL system (n=3, error bars=SEM).

A ligand for dTas2r7 was not discovered as part of this study. It appears that the receptive range of dTas2r7 differs from that of its human orthologue.

2.4.2.7. Tas2r10 concentration-response testing

Of the 48 compounds tested in the pre-screening phase 21 were tested in the initial concentration-response testing phase with Tas2r10. Of these 12 were tested again in the retest phase.

2.4.2.7.1. Selective responses of hTAS2R10 in concentration-response tests

Chloramphenicol was previously recognised as an agonist of hTAS2R10 at concentrations of 100µM (Meyerhof *et al.*, 2010) or 200µM (Li *et al.*, 2008). In the initial testing phase a specific response was seen with hTAS2R10, with no response from the dog orthologue. A threshold concentration of 0.27mM was observed (Figure 2.47A). However, this was not replicated in the repeat phase of the testing, where no response was seen. As the data from the initial testing seemed to fit well with published data, the test was repeated under the same conditions as for the initial test at the Waltham laboratory. A similar result was seen compared to the first test (data not shown). The lack of observed response in the repeat phase of the testing may be related to the overall reduced sensitivity observed in this phase.

Chloroquine was previously identified as an agonist of hTAS2R10 at a concentration of 10mM (Li *et al.*, 2008; Meyerhof *et al.*, 2010). However, despite a response in the initial testing with hTAS2R10, no responses were seen in the repeat phase testing with either hTAS2R10 or dTas2r10. The data warrant repeat testing under the same conditions as the initial testing, but this was not performed as no responses were apparent in the dog orthologue, which was the focus of this study (Figure 2.47A).

Denatonium benzoate is a well-known bitter-tasting substance for humans and is a ligand for eight hTAS2Rs (Meyerhof *et al.*, 2010). Of these, hTAS2R47 has the lowest threshold concentration at 0.03µM, while the next most sensitive receptor is hTAS2R10 with a 3µM threshold. Dogs lack an orthologue for hTAS2R47 and in the testing done in this study dTas2r10 was unresponsive to denatonium benzoate. The threshold for hTAS2R10 was less than 45µM (the lowest concentration tested in the data from Waltham), but was elevated in the data from the FDSS/µCELL system, again indicating some loss of sensitivity in this phase of the testing. At very high concentrations non-specific activation of the mock-transfected cells was seen, and the maximum concentration was reduced in the repeat testing phase. With a concentration of 10mM a near complete reduction in signal was observed compared

to lower concentrations. This is similar to the effect seen with 6-Nitrosaccharin and Tas2r1 (Figure 2.47A).

Ethylpyrazine was identified as a hTAS2R10 ligand at a concentration of 20mM in one previous study (Li *et al.*, 2008), but not in another (Meyerhof *et al.*, 2010). Here a threshold concentration of 11.1mM was found in the initial testing, with higher concentrations stimulating the mock-transfected cells. In the repeat phase of testing no response was observed. No specific activation was seen with dog Tas2r10 at any of the concentrations tested (Figure 2.47A).

Oxybutynin chloride stimulated hTAS2R10 at a concentration of 100µM in a previous study (Li *et al.*, 2008). Here specific stimulation was observed at concentrations as low as 3.7µM, but only the human receptor was responsive (Figure 2.47A).

Oxyphenonium bromide was previously identified as a ligand of hTAS2R10 at a concentration of 2.5mM (Li *et al.*, 2008). Here a threshold of 137µM was seen in the initial testing phase, but the repeat phase data suggested this may be even lower. A maximum concentration of 100mM resulted in large non-specific artefacts, so that only a maximum of 11.1mM and 33.33mM could be plotted on a concentration-response curve in the initial and repeat phases, respectively. Only activation of the human receptor was seen (Figure 2.47B).

Parthenolide is a known ligand of hTAS2R10 with a threshold concentration of 30µM (Meyerhof *et al.*, 2010). In the initial phase of testing similar data was seen with a threshold of 27µM for hTAS2R10. In the repeat phase hTAS2R10 also showed specific responses, but the threshold was again higher at 66µM (Figure 2.47B). No activation of dTas2r10 was observed.

Pirenzepine was previously noted to activate hTAS2R10 at a concentration of 2.5mM (Li *et al.*, 2008). In this study some evidence of a specific response with hTAS2R10, but not dTas2r10, was seen in the initial testing at concentrations of 2.7 and 8.3mM,

while higher concentrations of 25mM resulted in no specific response. However, this was not confirmed in the repeat phase of testing (Figure 2.47B).

Strychnine was found to activate hTAS2R10 at a concentration of 2.5mM (Li *et al.*, 2008) or 3µM (Meyerhof *et al.*, 2010). In this study hT2R10 was also activated by strychnine at a threshold concentration of 37µM for the initial testing. The dog orthologue was unresponsive. Sensitivity was reduced in the repeat phase testing (Figure2.47B).

Sucralose was previously identified as an agonist of hTAS2R10, although test concentrations were not published (Lossow *et al.*, 2016). Here only hTAS2R10 was responsive with a threshold concentration of 3.7mM based on the initial phase of testing (Figure 2.47B).

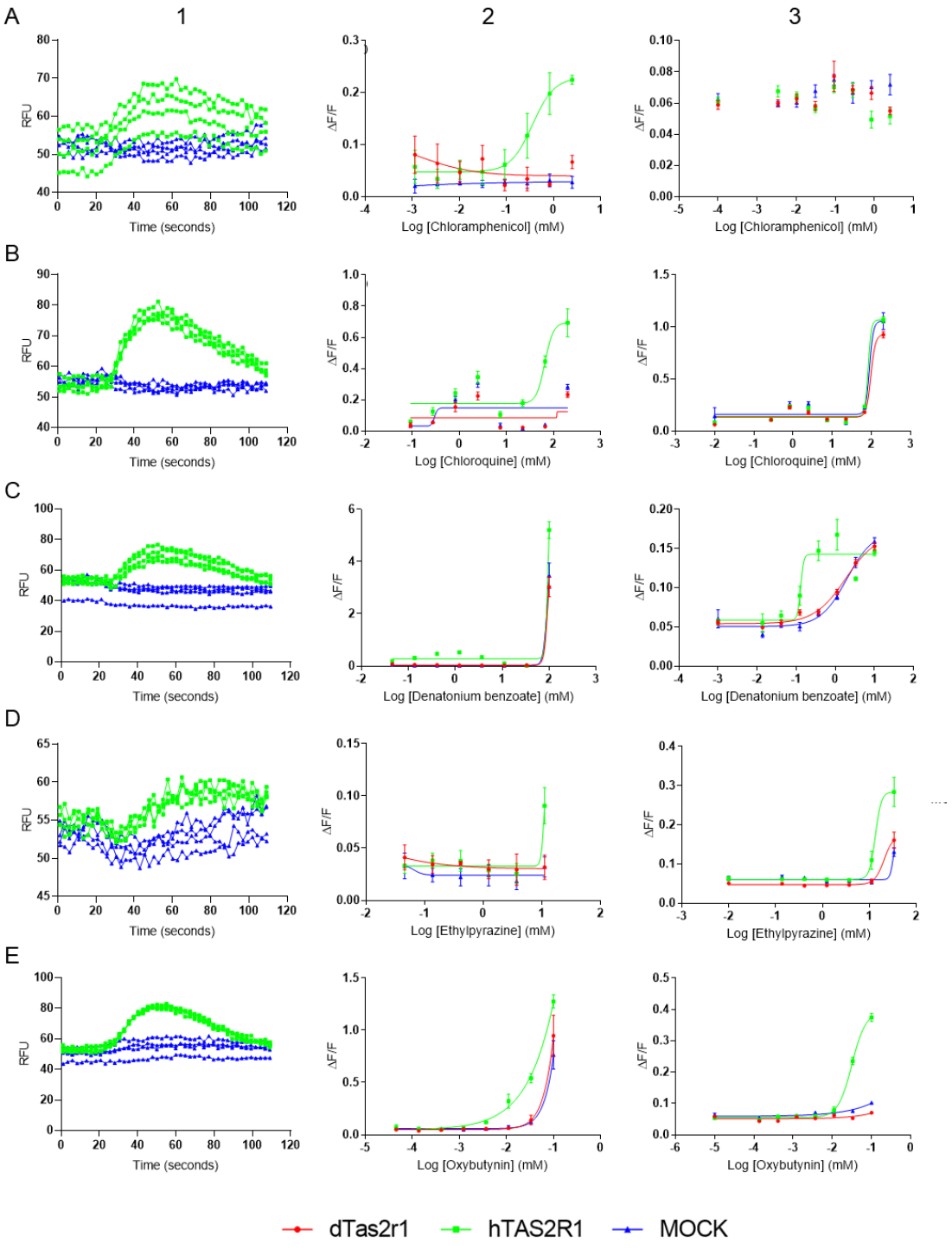

Figure 2.47: A. Compounds showing specific activity for hTAS2R10 but not dTas2r10

A) Raw data for the highest concentration where a specific response was seen with hTAS2R10. B) Full concentration-response data produced in an initial phase of testing. C) Full concentration-response data produced in a repeat phase of testing. D) Repeat testing on the FlexStation to confirm the result from the initial phase. The initial phase includes FlexStation data produced at the Waltham laboratory (n=1, error bars=SD). The repeat phase includes data produced at the IMAX Discovery laboratory with the Hamamatsu FDSS/µCELL system (n=3, error bars=SEM).

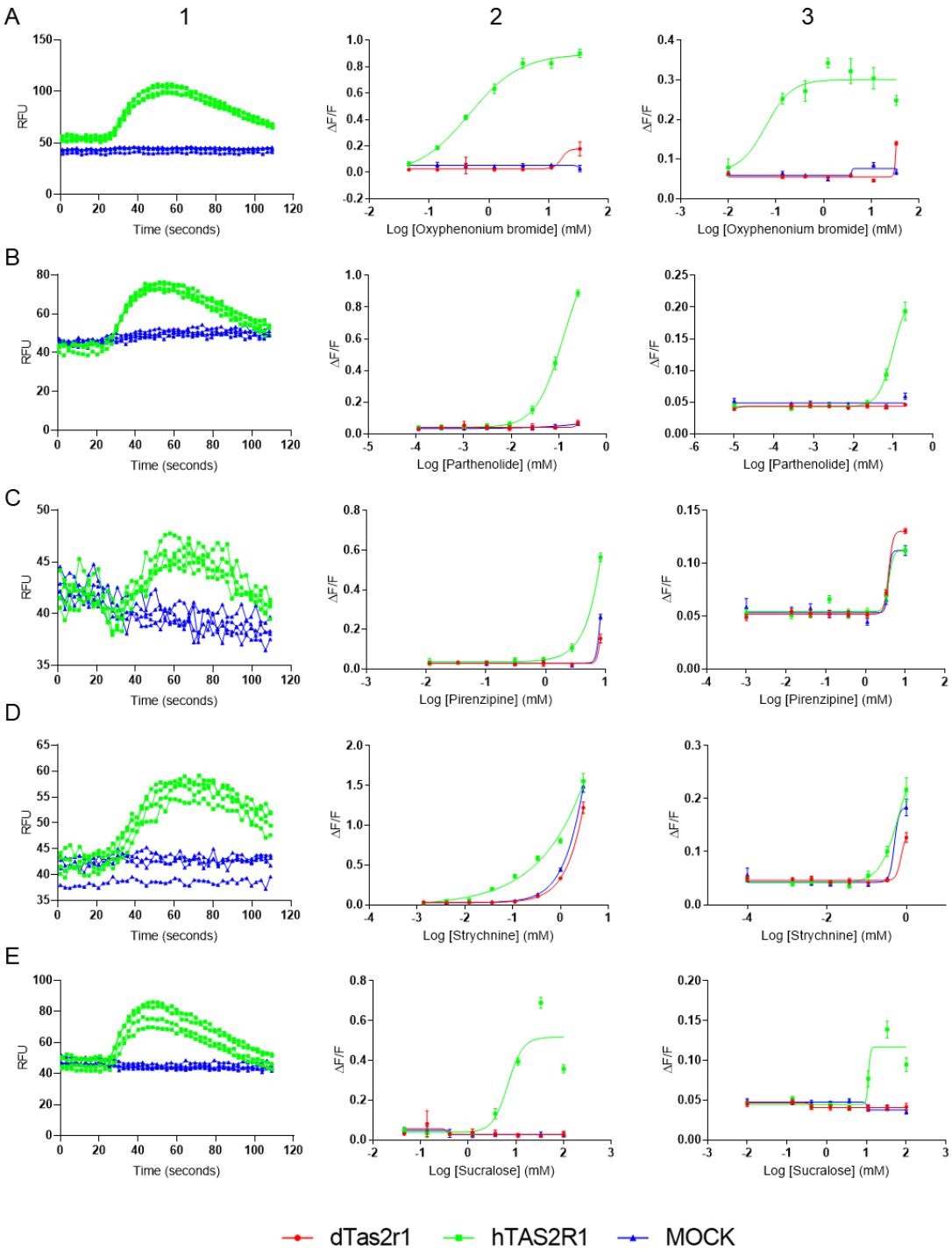

Figure 2.47: B. Compounds showing specific activity for hTAS2R10 but not dTas2r10 A) Raw data for the highest concentration where a specific response was seen with hTAS2R10. B) Full concentration-response data produced in an initial phase of testing. C) Full concentration-response data produced in a repeat phase of testing. The initial phase includes FlexStation data produced at the Waltham laboratory (n=1, error bars=SD). The repeat phase includes data produced at the IMAX Discovery laboratory with the Hamamatsu FDSS/µCELL system (n=3, error bars=SEM).

2.4.2.7.2. Common responses of dog and human Tas2r10 in concentration-response tests

Cucurbitacin B was identified as a potent ligand of hTAS2R10 previously, at a concentration of 0.01µM (Meyerhof et al., 2010). This also proved to be the case for dTas2r10, with both versions of the receptor having threshold concentrations of 0.68µM here. Cucurbitacin B proved to be an ideal ligand from a testing perspective, being highly soluble and causing no response in the mock-transfected cells, even at the highest tested concentration of 0.5mM (Figure 2.47). The EC_{50} for dTas2r10 in the initial phase was 1.46µM while in the repeat phase it was 13.18µM with 95% confidence intervals of 10.69 to 16.09µM. The hTAS2R10 receptor had similar EC_{50} values of 3.37µM in the initial phase and 36.37µM (95% CI 27.46 to 48.10) in the repeat phase.

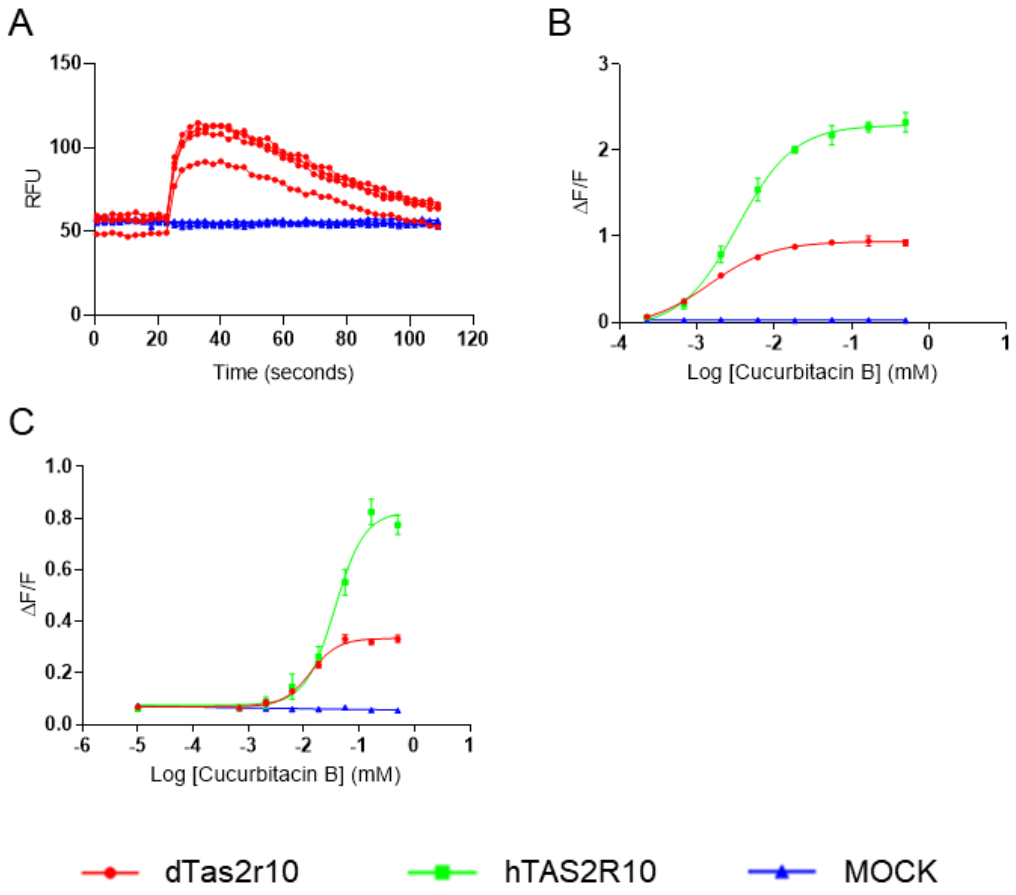

Figure 2.48: Concentration-response data for Tas2r10 and cucurbitacin B
A) Raw data for the highest concentration where a specific response was seen with dTas2r10. B) Full concentration-response data produced in an initial phase of testing. C) Full concentration-response data produced in a repeat phase of testing. The initial phase includes FlexStation data produced at the Waltham laboratory (n=1, error bars=SD). The repeat phase includes data produced at the IMAX Discovery laboratory with the Hamamatsu FDSS/µCELL system (n=3, error bars=SEM).

The monoterpene (-)-α-thujone was previously identified as an agonist of hTAS2R10 with a threshold concentration of 100µM (Meyerhof *et al.*, 2010). In this study hTAS2R10 and dTas2r10 were activated by this compound, with a threshold concentration of 77µM and 2mM, respectively, based on the initial testing phase (Figure 2.49). Activation of dTas2r10 was very weak and did not show evidence of dose dependency. The specific activation of dT2R10 was not replicated in the repeat phase and it was not considered a hit compound here.

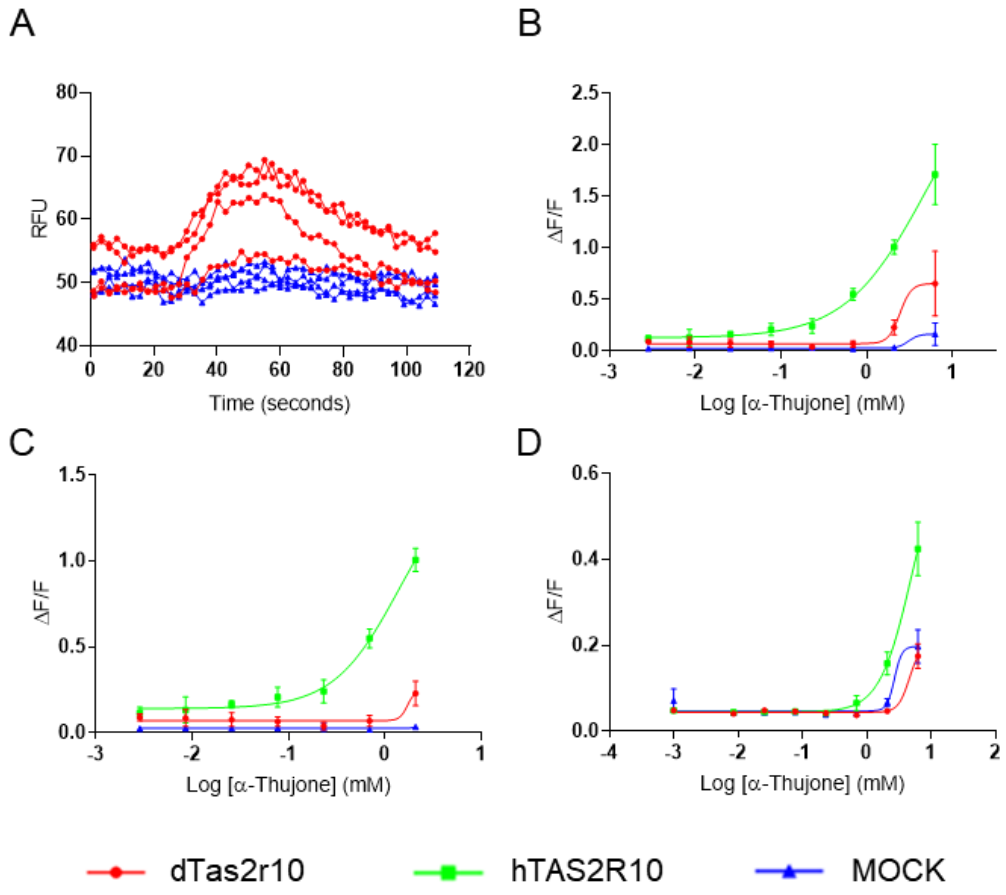

Figure 2.49: Concentration-response data for Tas2r10 and (-)-α-thujone
A) Raw data for the highest concentration where a specific response was seen with dTas2r10. B) Full concentration-response data produced in an initial phase of testing. C) Concentration-response data from the initial phase testing limited to the highest concentration where a specific response was seen (no activation in the mock cell line). D) Full concentration-response data produced in a repeat phase of testing. The initial phase includes FlexStation data produced at the Waltham laboratory (n=1, error bars=SD). The repeat phase includes data produced at the IMAX Discovery laboratory with the Hamamatsu FDSS/µCELL system (n=3, error bars=SEM).

Tuning of dTas2r10 appears to be much narrower than that of hTAS2R10. Numerous published responses of hTAS2R10 were replicated in this study but dTas2r10 responded robustly to only one compound, cucurbitacin B. While the EC_{50} for cucurbitacin B was similar for both receptors the maximal stimulation level with dTas2r10 was approximately half that of hTAS2R10. This may indicate that cucurbitacin B acts only as a partial agonist of dTas2r10, but without another common agonist for both receptors to show that maximal stimulation was equal in both cases this observation is speculative.

2.4.2.8. Tas2r12 concentration-response testing

TAS2R12 is a pseudogene in humans, but appeared to be a full length functional gene in dogs. Only four compounds were selected from the pre-screen for concentration-response testing in the initial phase and of these only one was carried forward to the retesting phase.

Flavone gave a seemingly robust response in the initial testing phase, but this was not replicated in the repeat phase (Figure 2.50). Repeating this test under the same conditions as the initial testing showed a response similar to that previously obtained. It is not clear why this was not seen during the repeat phase testing.

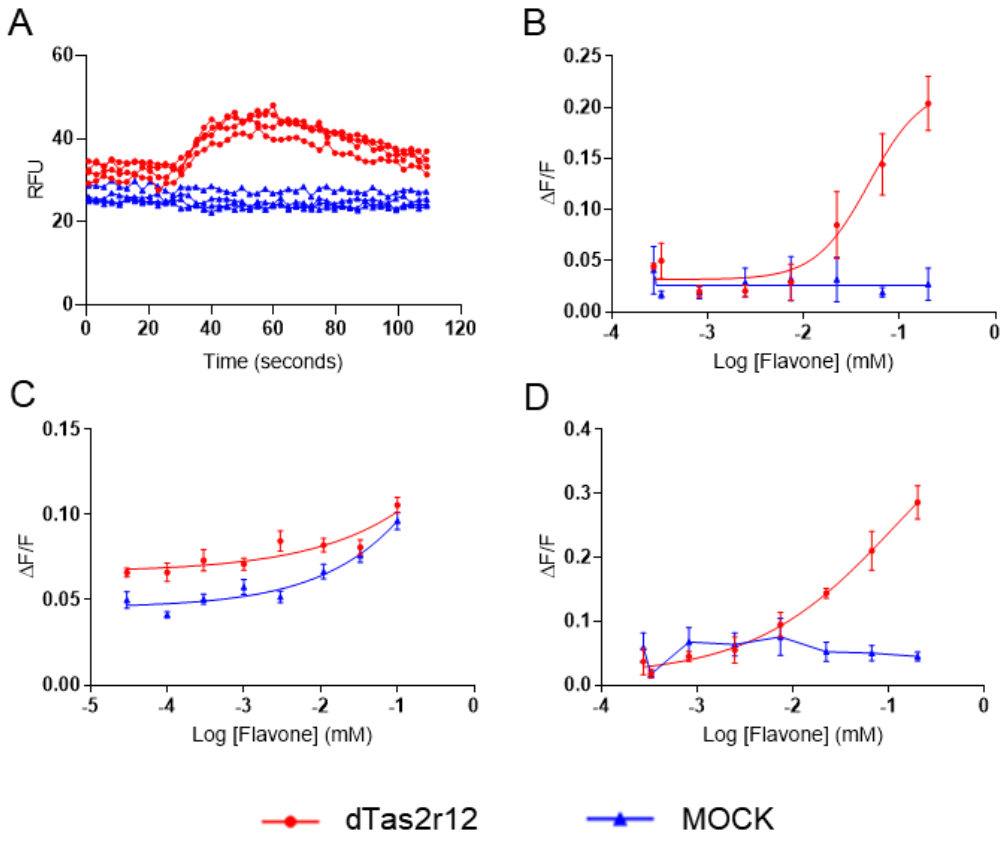

Figure 2.50: Concentration-response data for Tas2r12 and flavone
A) Raw data for the highest concentration where a specific response was seen with dTas2r12. B) Full concentration-response data produced in an initial phase of testing. C) Full concentration-response data produced in a repeat phase of testing. D) Full concentration-response data produced in a repeat of the initial phase of testing. The initial phase includes FlexStation data produced at the Waltham laboratory (n=1, error bars=SD). The repeat phase includes data produced at the IMAX Discovery laboratory with the Hamamatsu FDSS/µCELL system (n=3, error bars=SEM).

Without a comparable human orthologue the tuning breadth of dTas2r12 can only be evaluated based on the data generated here. With only one active compound tuning would appear to be narrow. However, flavone is the simplest member of a large group of compounds collectively known as the flavones. All share the basic structure of flavone, but have additional chemical features. It would be interesting to test a wider array of these compounds, particularly as two human receptors, TAS2R14 and TAS2R39, are broadly responsive to this compound class.

2.4.2.9. Tas2r38 concentration-response testing

A total of 18 compounds were taken through to the initial concentration-response phase of testing for Tas2r38. Only four were taken forward to the repeat testing phase.

Sinigrin is a known ligand of hTAS2R38(PAV) with a threshold concentration of 100µM (Meyerhof *et al.*, 2010). In the initial testing a threshold of 617µM was observed for hTAS2R38(PAV), while dTas2r38 was unresponsive. This was not confirmed in the repeat testing phase however, where no specific responses were seen (Figure 2.51).

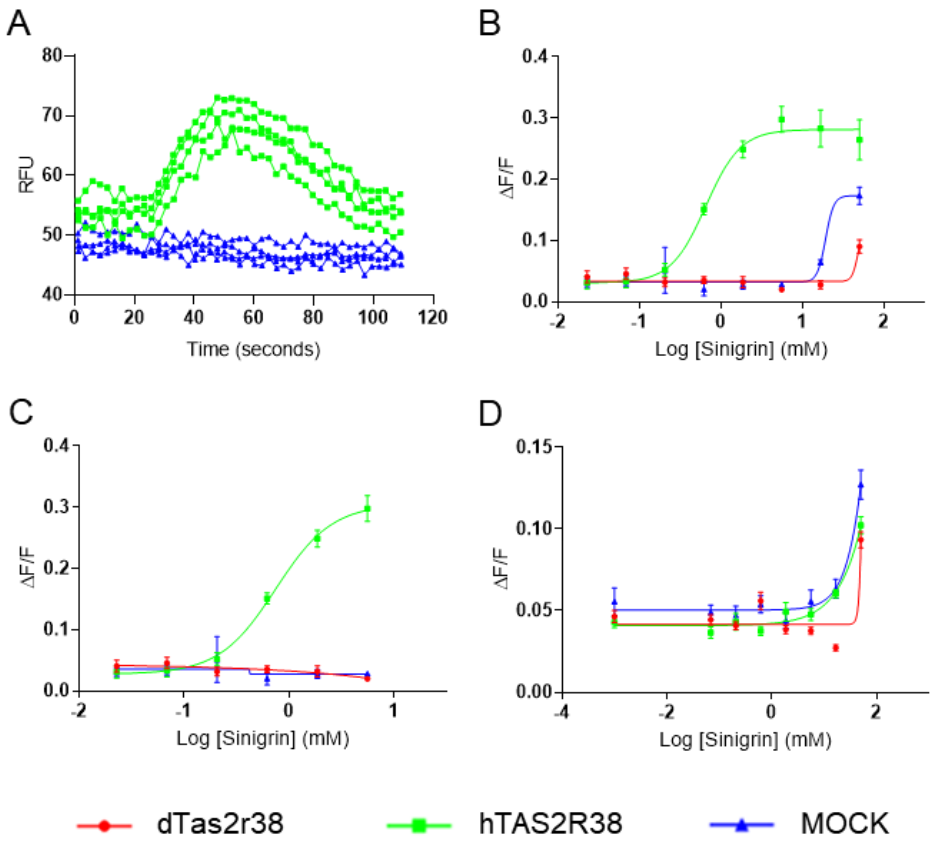

Figure 2.51: Concentration-response data for Tas2r38PAV and sinigrin
A) Raw data for the highest concentration where a specific response was seen with hTAS2R38. B) Full concentration-response data produced in an initial phase of testing. C) Concentration-response data from the initial phase testing limited to the highest concentration where a specific response was seen (no activation in the mock cell line). D) Full concentration-response data produced in a repeat phase of testing. The initial phase includes FlexStation data produced at the Waltham laboratory (n=1, error bars=SD). The repeat phase includes data produced at the IMAX Discovery laboratory with the Hamamatsu FDSS/µCELL system (n=3, error bars=SEM).

(-)-α-Thujone was not previously shown to be active with hTAS2R38(PAV) (Meyerhof *et al.*, 2010). No activity with hTAS2R38(PAV) was seen in this study either, but in the initial testing phase dTas2r38 did show some specific activity with a threshold concentration of 231µM. However, this was not confirmed in the repeat phase of the testing (Figure 2.52). A further test was carried out under the same conditions as the initial phase testing but the original response was not replicated. Given the lack of reproducibility of this result (-)-α-thujone is not considered to be a dTas2r38 agonist at this time.

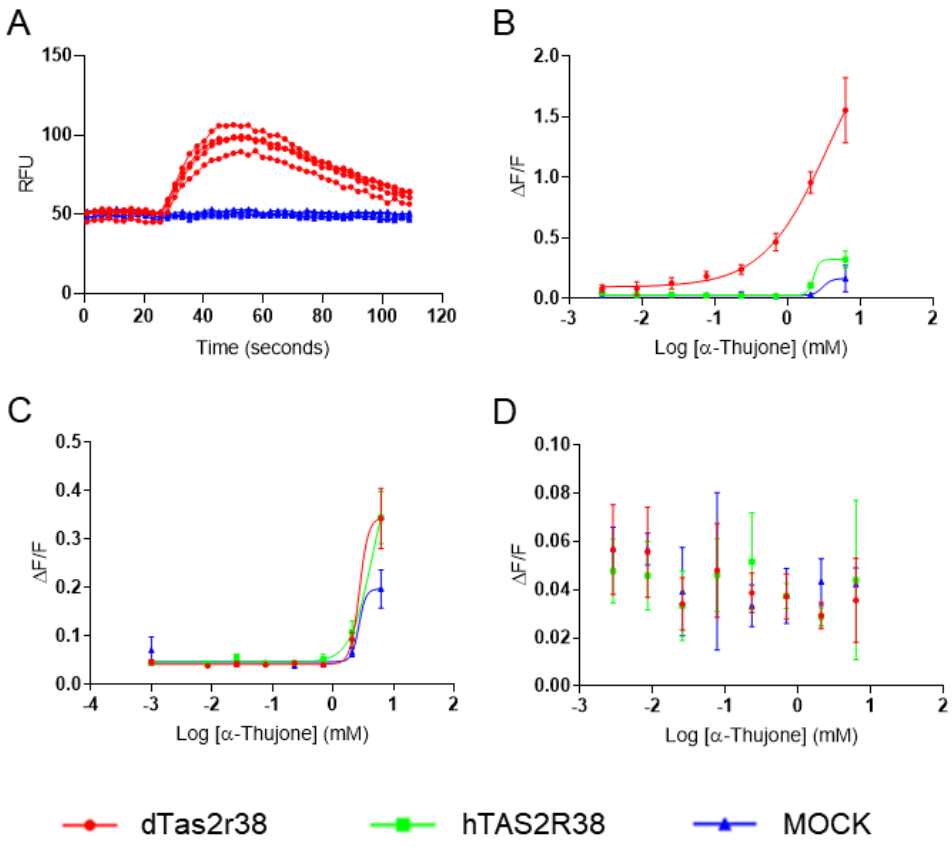

Figure 2.52: Concentration-response data for Tas2r38PAV and (-)-α-thujone
A) Raw data for the highest concentration where a specific response was seen with dTas2R38. B) Full concentration-response data produced in an initial phase of testing. C) Full concentration-response data produced in a repeat phase of testing. D) Repeat testing on the FlexStation to confirm the result from the initial phase. The initial phase includes FlexStation data produced at the Waltham laboratory (n=1, error bars=SD). The repeat phase includes data produced at the IMAX Discovery laboratory with the Hamamatsu FDSS/µCELL system (n=3, error bars=SEM).

The known hTAS2R38 ligand PROP was also tested in the repeat phase. With hTAS2R38(PAV), PROP has been shown to have a threshold concentration of 0.06µM (Meyerhof *et al.*, 2010). This high sensitivity to PROP was not replicated in this study, although some specific activity to PROP was detected with hTAS2R38(PAV) in the initial testing phase, with a threshold concentration of 35µM. However, this was not confirmed in the repeat testing phase. Activity for dTas2r38 was observed, but only with very high concentrations that also activated the mock-transfected cells (Figure 2.53). This was not considered a hit for dTas2r38.

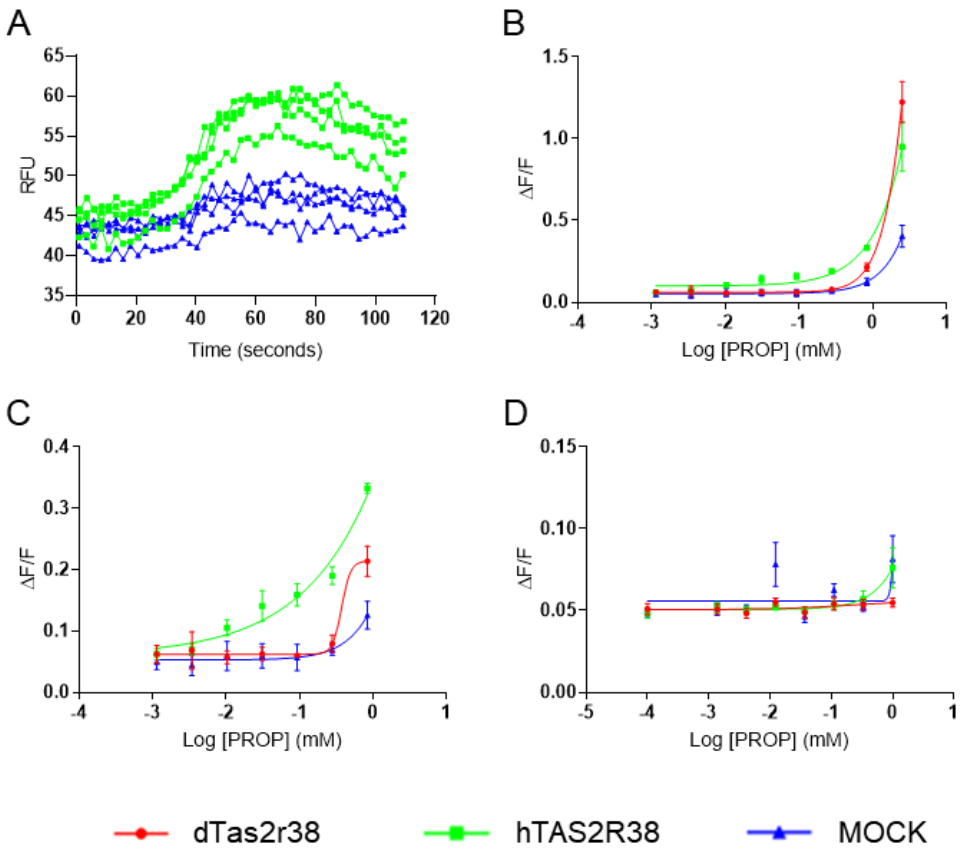

Figure 2.53: Concentration-response data for Tas2r38PAV and PROP
A) Raw data for the highest concentration where a near-specific response was seen with hTAS2R38. B) Full concentration-response data produced in an initial phase of testing. C) Concentration-response data from the initial phase testing limited to the highest concentration where a specific response was seen (no activation in the mock cell line). D) Full concentration-response data produced in a repeat phase of testing. The initial phase includes FlexStation data produced at the Waltham laboratory (n=1, error bars=SD). The repeat phase includes data produced at the IMAX Discovery laboratory with the Hamamatsu FDSS/µCELL system (n=3, error bars=SEM).

The related compound PTC is also a known ligand for hTAS2R38(PAV) with a threshold concentration of 0.02µM. In this study a much higher threshold of 277µM was observed for hTAS2R38(PAV). Responses for dTas2r38 were only seen at concentrations that also activated the mock-transfected cells, but this was not confirmed in the repeat testing phase (Figure 2.54). This was not considered a hit for dTas2r38.

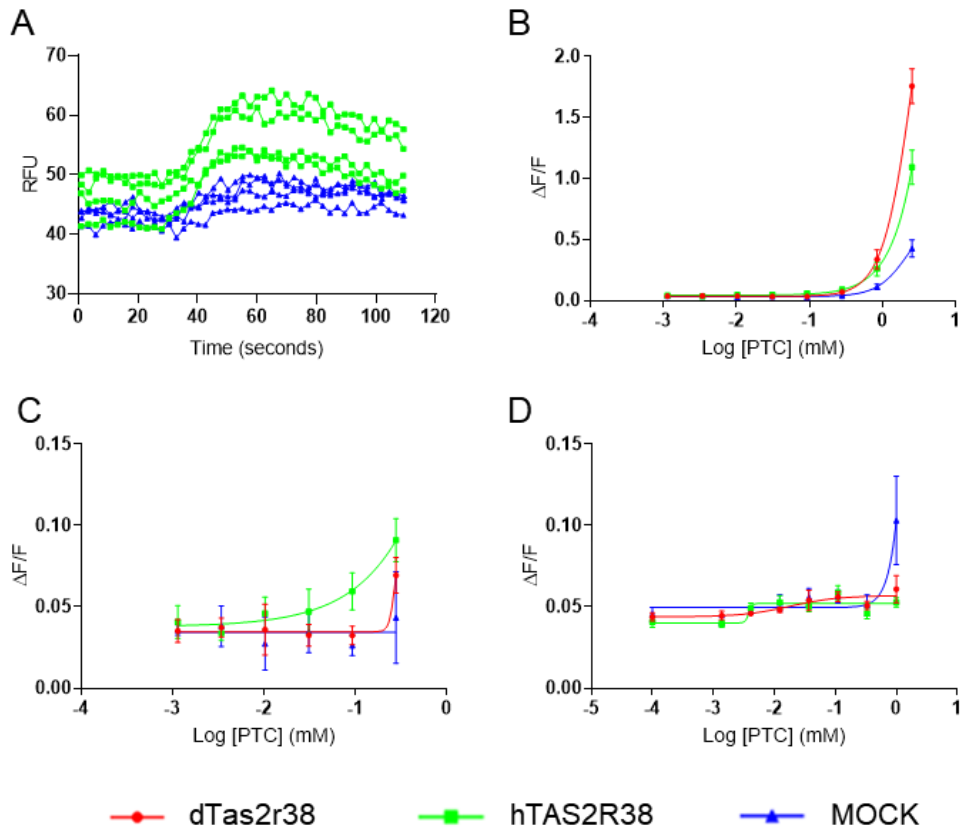

Figure 2.54: Concentration-response data for Tas2r38PAV and PTC
A) Raw data for the highest concentration where a near-specific response was seen with hTAS2R38. B) Full concentration-response data produced in an initial phase of testing. C) Concentration-response data from the initial phase testing limited to the highest concentration where a specific response was seen (no activation in the mock cell line). D) Full concentration-response data produced in a repeat phase of testing. The initial phase includes FlexStation data produced at the Waltham laboratory (n=1, error bars=SD). The repeat phase includes data produced at the IMAX Discovery laboratory with the Hamamatsu FDSS/µCELL system (n=3, error bars=SEM).

2.4.2.10. Tas2r39 concentration-response testing

A total of 14 compounds were selected for the initial phase of concentration-response testing with Tas2r39. Of these only three showed evidence of specific activity and were taken to the retesting phase.

Acetaminophen was previously noted as a hTAS2R39 agonist at concentrations of 10mM (Li *et al.*, 2008) or 3mM (Meyerhof *et al.*, 2010). In the initial testing phase a threshold concentration of 1.85mM was observed for hTAS2R39, while dTas2r39 was unresponsive. The repeat phase testing showed a large drop in baseline signal at the point of compound injection. This masked the response of hTAS2R39 in the response

curves, but inspection of the raw data did show evidence of a specific response in hTAS2R39 only (Figure 2.55).

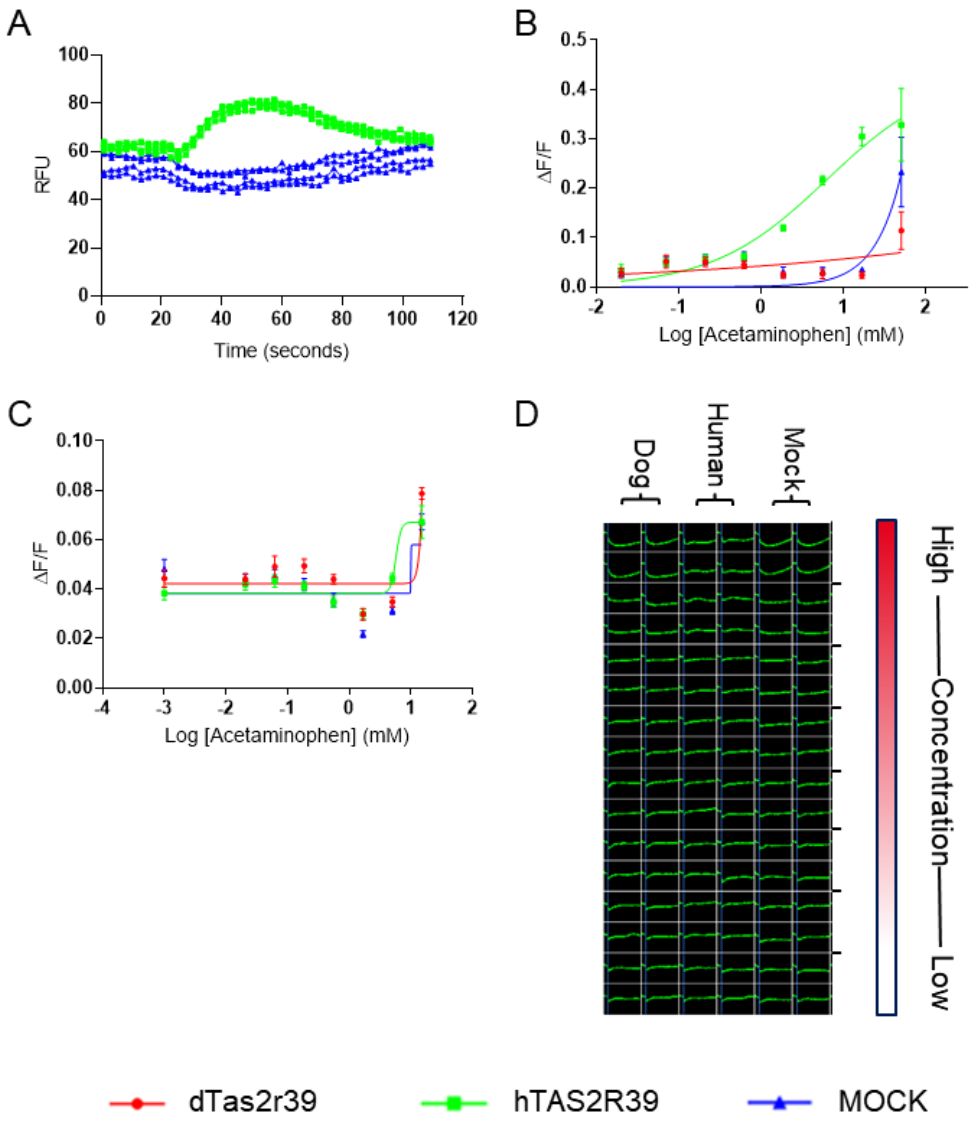

Figure 2.55: Concentration-response data for Tas2r39 and acetaminophen
A) Raw data for the highest concentration where a specific response was seen with hTAS2R39. B) Full concentration-response data produced in an initial phase of testing. C) Full concentration-response data produced in a repeat phase of testing. D) Raw data traces from one run of the repeat phase testing. Concentrations are the same as for panel C. The initial phase includes FlexStation data produced at the Waltham laboratory (n=1, error bars=SD). The repeat phase includes data produced at the IMAX Discovery laboratory with the Hamamatsu FDSS/µCELL system (n=3, error bars=SEM).

Sucralose is also a known ligand of hTAS2R39 (Lossow *et al.*, 2016). In the initial testing phase a threshold concentration of 11.1mM was observed. This was confirmed in the repeat phase testing. The dog orthologue was unresponsive (Figure 2.56).

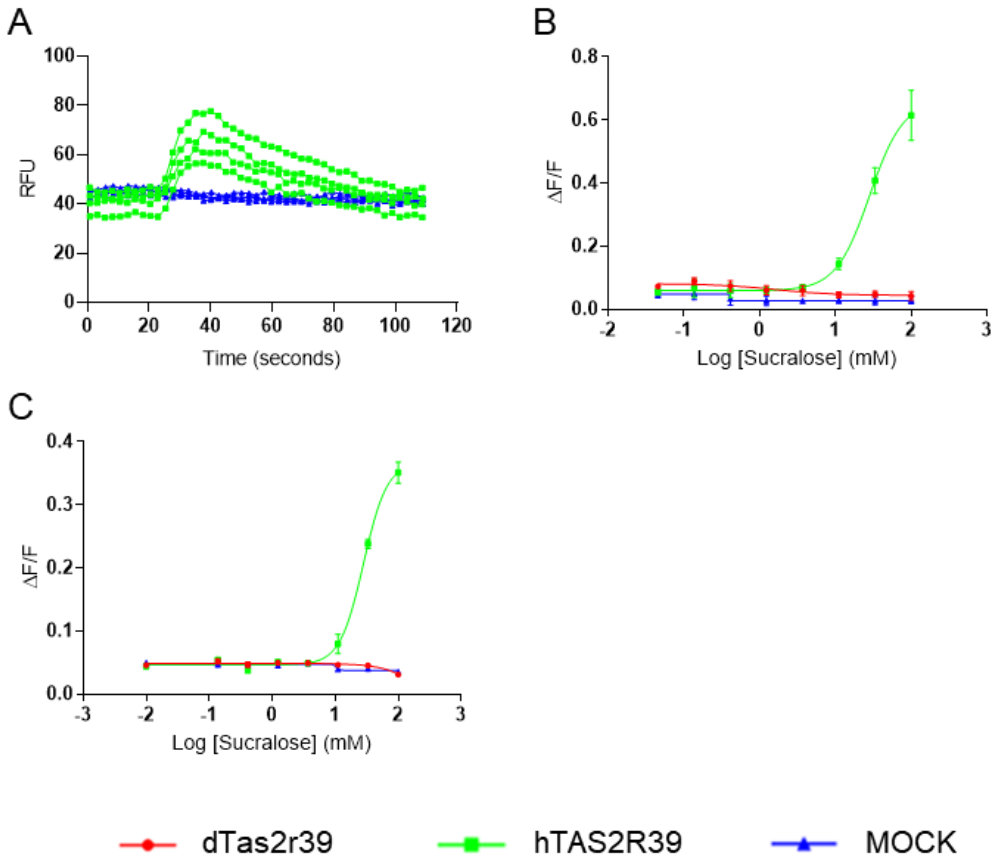

Figure 2.56: Concentration-response data for Tas2r39 and sucralose
A) Raw data for the highest concentration where a specific response was seen with hTAS2R39. B) Full concentration-response data produced in an initial phase of testing. C) Full concentration-response data produced in a repeat phase of testing. The initial phase includes FlexStation data produced at the Waltham laboratory (n=1, error bars=SD). The repeat phase includes data produced at the IMAX Discovery laboratory with the Hamamatsu FDSS/µCELL system (n=3, error bars=SEM).

Thiamine was previously reported to be a ligand of hTAS2R39 with a threshold concentration of 1mM (Meyerhof *et al.*, 2010). In the initial testing phase some specific activity of Thiamine was observed, with a threshold of 11.1mM. The repeat testing showed some issues with large drops in baseline signal at the point of compound injection. Inspection of the raw data showed indications of a specific

response for hTAS2R39 at 33mM and 11mM. The data was not convincing for dog Tas2r39 and it was not considered to be a hit, despite some differences in the raw data when compared to the mock-transfected cells in the repeat phase data at the 11mM concentration point (Figure 2.57).

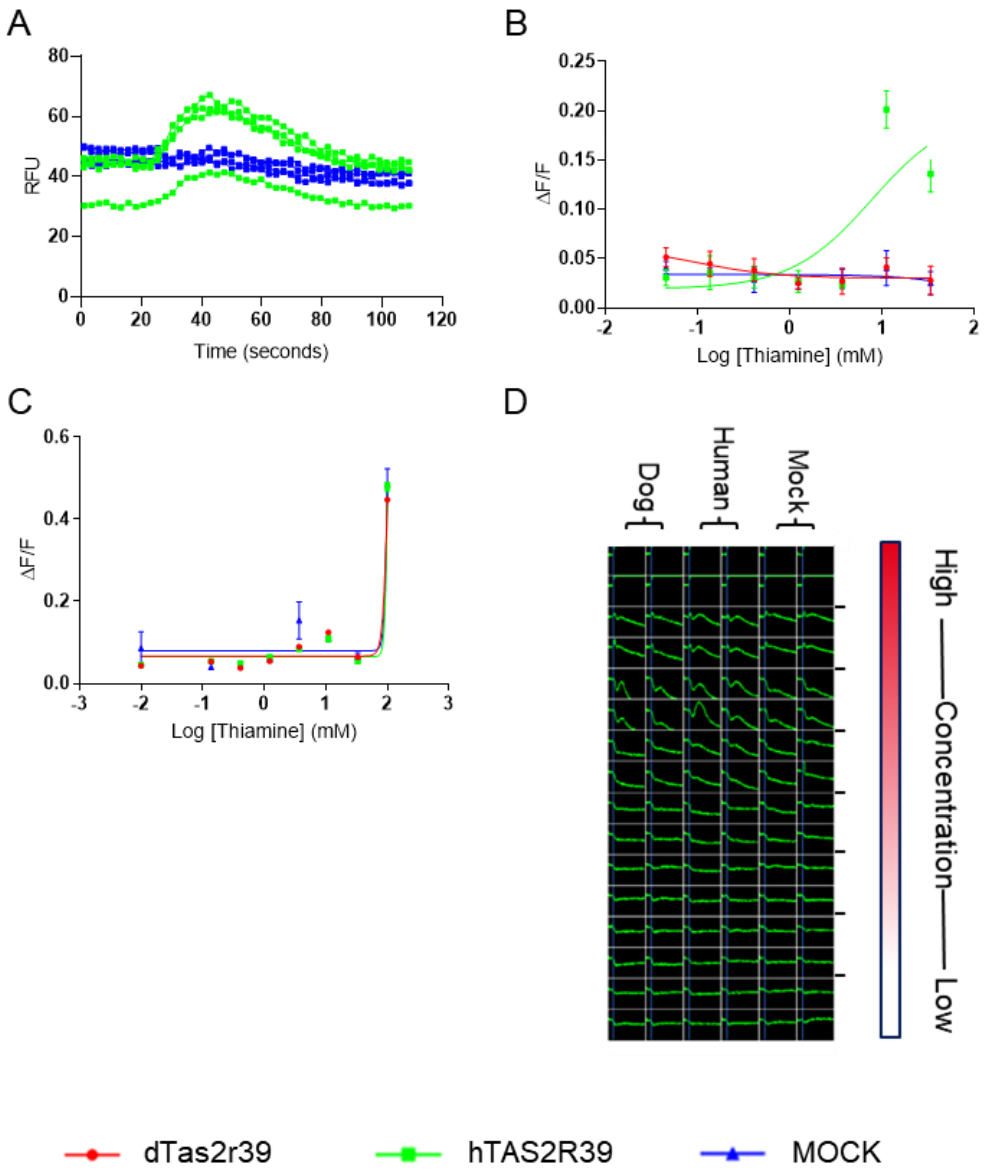

Figure 2.57: Concentration-response data for Tas2r39 and thiamine
A) Raw data for the highest concentration where a specific response was seen with hTAS2R39. B) Full concentration-response data produced in an initial phase of testing. C) Full concentration-response data produced in a repeat phase of testing. D) Raw data traces from one run of the repeat phase testing. Concentrations are as for panel C. The initial phase includes FlexStation data produced at the Waltham laboratory (n=1, error bars=SD). The repeat phase includes data produced at the IMAX Discovery laboratory with the Hamamatsu FDSS/µCELL system (n=3, error bars=SEM).

The human TAS2R39 receptor is one of the most broadly tuned of all human TAS2Rs. It was therefore somewhat surprising that the dog orthologue tested here was not deorphanised. This finding warrants further investigation, and a broader screening of

known hTAS2R39 ligands may confirm that dTas2r39 is functional in this cell model, but much more narrowly tuned than its human orthologue.

2.4.2.11. Tas2r40 concentration-response testing

Only 5 compounds were selected from the pre-screening phase for concentration-response testing with dTas2r40. Of these only diphenidol was a previously identified ligand for hTAS2R40, with a threshold concentration of 30µM (Meyerhof *et al.*, 2010). However, no compounds showed evidence of specific activity in the initial test phase and none were taken through to the repeat testing phase. In the case of diphenidol, responses were not seen below concentrations of 93µM, at which point the mock-transfected cells showed similar responses to the receptor-transfected cells.

2.4.2.12. Tas2r41 concentration-response testing

A selection of 12 compounds from the pre-screening work were tested in the initial concentration-response phase with Tas2r41. There are only 2 known agonists of hTAS2R41, chloramphenicol and sucralose (Thalmann et al., 2013b; Lossow et al., 2016). These were tested in the initial phase, but responses from human and dog Tas2r41 were not apparent.

Oxyphenonium bromide showed evidence of specific activation with dTas2r41, while hTAS2R41 was unresponsive. The maximum test concentration of 100mM caused large non-specific artefacts in all tests, while the second concentration of 33mM also caused this issue in the initial test phase. The threshold concentration for dTas2r41 was 1.24mM in the initial test phase (Figure 2.58).

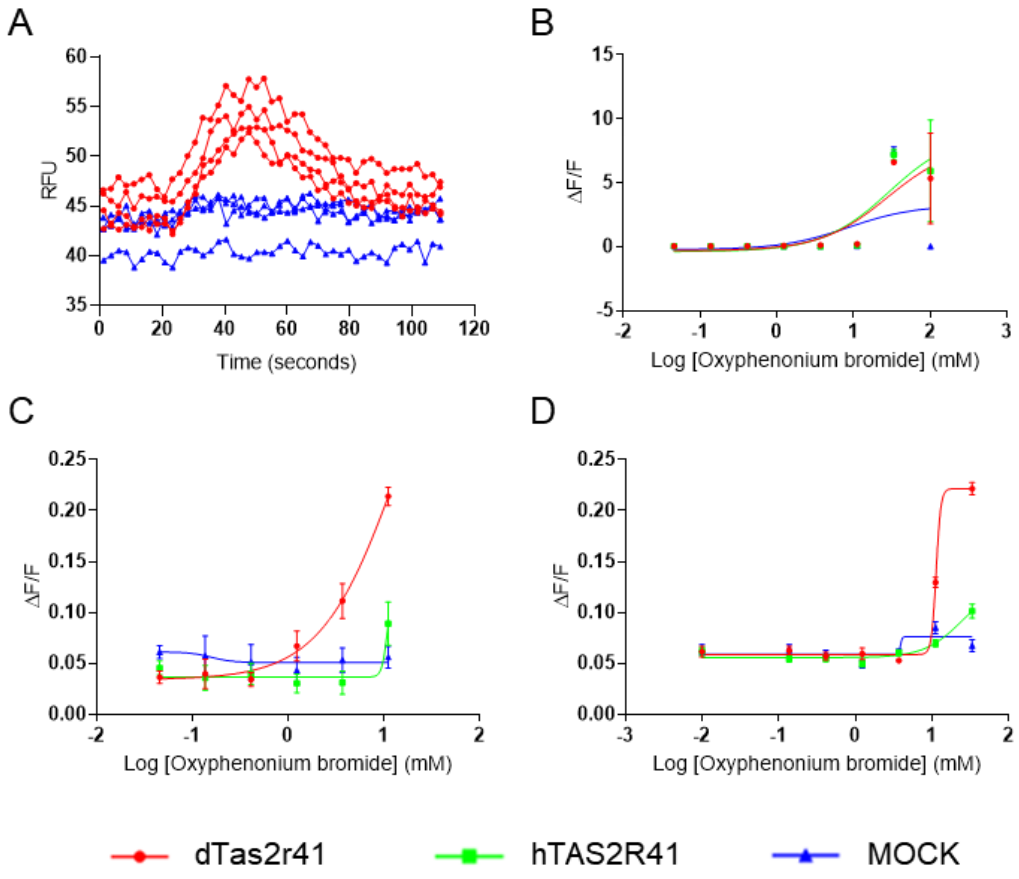

Figure 2.58: Concentration-response data for Tas2r41 and oxyphenonium bromide A) Raw data for the highest concentration where a specific response was seen with dTas2r41. B) Full concentration-response data produced in an initial phase of testing. C) Concentration-response data from the initial phase testing limited to the highest concentration where a specific response was seen (no activation in the mock cell line). D) Concentration-response data from a repeat phase of testing limited to the highest concentration where a specific response was seen (no activation in the mock cell line). The initial phase includes FlexStation data produced at the Waltham laboratory (n=1, error bars=SD). The repeat phase includes data produced at the IMAX Discovery laboratory with the Hamamatsu FDSS/µCELL system (n=3, error bars=SEM).

2.4.2.13. Tas2r42 concentration-response testing

Four compounds from the pre-screen phase were selected for further testing with Tas2r42, but no specific responses were identified for either dog or human versions of the receptor. This receptor currently has no published ligand identified for any species.

2.4.2.14. Tas2r43 concentration-response testing

Seven compounds from the pre-screen phase were tested in the initial concentration-response phase with Tas2r43. Of these only aristolochic acid gave specific responses with hTAS2R43, while dTas2r43 was unresponsive. In the initial phase the maximum test concentration of 3.12mM was too high and gave large non-specific responses in all cells (Figure 2.59). The maximum concentration was reduced to 10µM in the repeat testing phase, where a threshold concentration of 0.12µM was observed. This is higher than that published at 0.0013µM (Meyerhof et al., 2010), but this is most likely related to the low sensitivity observed throughout most of the repeat phase data.

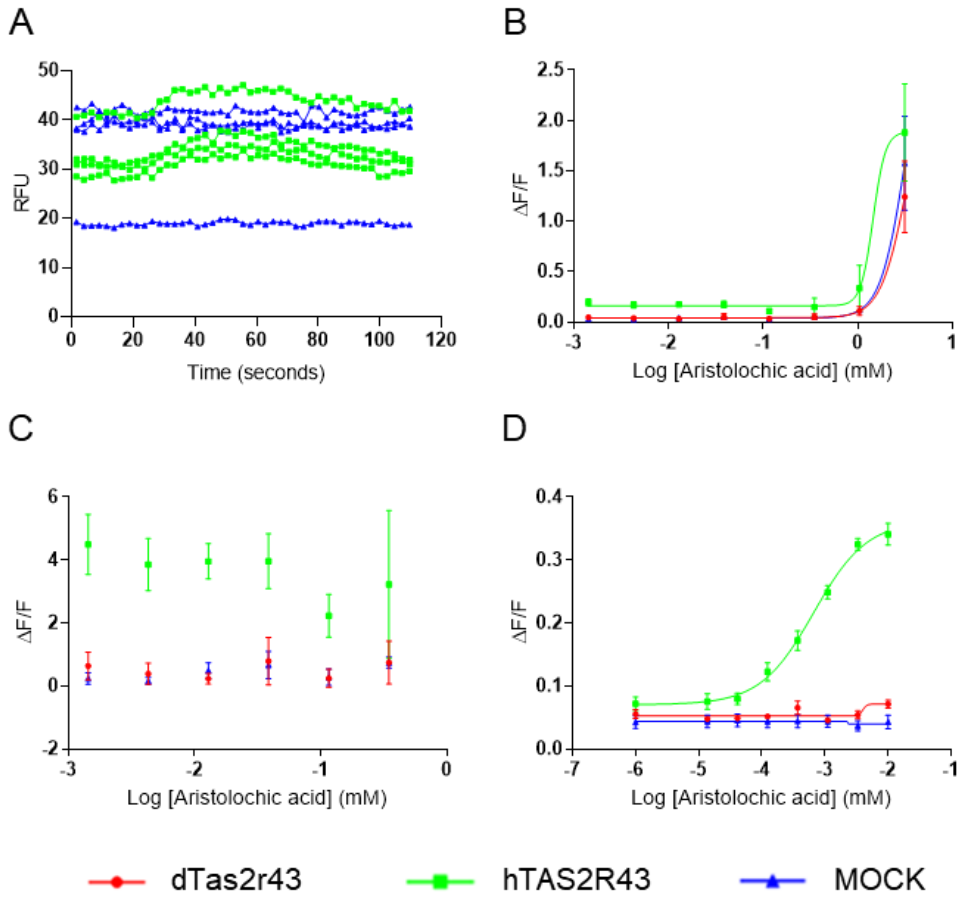

Figure 2.59: Concentration-response data for Tas2r43 and aristolochic acid
A) Raw data for the highest concentration where a specific response was seen with hTAS2R41. B) Full concentration-response data produced in an initial phase of testing. C) Concentration-response data from the initial phase testing limited to the highest concentration where a specific response was seen (no activation in the mock cell line). D) Concentration-response data from a repeat phase of testing limited to the highest concentration where a specific response was seen (no activation in the mock cell line). The initial phase includes FlexStation data produced at the Waltham laboratory (n=1, error bars=SD). The repeat phase includes data produced at the IMAX Discovery laboratory with the Hamamatsu FDSS/µCELL system (n=3, error bars=SEM).

2.4.2.15. Tas2r62 concentration-response testing

A total of 11 compounds were tested in the initial concentration-response testing phase for dTas2r62. However, no evidence of specific responses was observed and no compounds were tested in the repeat phase testing.

2.4.2.16. Tas2r67 concentration-response testing

Three compounds were tested in the initial concentration-response testing phase for dTas2r67. However, no evidence of specific responses was observed and no compounds were tested in the repeat phase testing.

2.4.3. Other responses

In some cases responses were observed in the initial phase of testing, but not followed-up in the repeat phase. This was the case for several responses observed with diphenidol. The human receptors hTAS2R7, hTAS2R10 and hTAS2R39 all gave small, but statistically significant responses with diphenidol at 31µM, 11µM and 31µM, respectively. These responses were not completely specific, but in each case the response of the receptor-expressing cells was above the response of the mock-transfected cells. At higher concentrations the response of the mock-transfected cells increased and the difference was less marked. These responses were considered as partial evidence of receptor activation, however they are similar to other published data for cat Tas2rs (Lei *et al.*, 2015). The data was not as clear as for other combinations and no dog receptor showed such responses, hence these combinations were not taken to the retesting phase.

2.4.4. Comparison with the $G_{\alpha16/gust44}$ chimera based assay

During the course of the concentration-response testing it became clear that the heterologous expression assay used here was only partially successful in replicating previously published data for human TAS2Rs. Some receptor-compound

combinations gave data similar to that reported elsewhere, while others showed either higher threshold concentrations or no activity at all.

The most obvious difference when comparing the assay system used here and that which is most widely used in the literature is the G protein chimera. The $G_{\alpha16/gust44}$ chimera has been used in many publications, some of which related *in vitro* data closely to *in vivo* taste perception thresholds (Bufe *et al.*, 2002). In order to try to resolve some of these differences, permission to use the $G_{\alpha16/gust44}$-expressing cell line was sought from the patent holder, Givaudan. Permission was granted for the scope of this project only, and the cell line was obtained via the laboratory of Loic Briand at the Centre for Taste and Feeding Behaviour in Dijon, France.

To evaluate any differences in response profiles between the $G_{\alpha16/gust/o}$ and $G_{\alpha16/gust44}$ cell lines, all 48 compounds in the test library were retested with both cell lines in a full concentration-response experiment with dog and human Tas2r1. In general, the responses of the two cell lines were similar, although in some cases $G_{\alpha16/gust44}$ was slightly less sensitive than the $G_{\alpha16/gust/o}$ cell line in these experiments.Figure 2.60 shows data for Tas2r1 and (-)-α-thujone. In this interesting case data for the $G_{\alpha16/gust/o}$ was similar to that generated previously (Figure 2.18). With the $G_{\alpha16/gust44}$-expressing cell line responses with *dTas2r1* transfected cells are reduced, while responses in the mock transfected cells are elevated, rendering the identification of a specific response impossible. This result matches published data for (-)-α-thujone when tested using the $G_{\alpha16/gust44}$ chimera (Meyerhof *et al.*, 2010), where no response was identified.

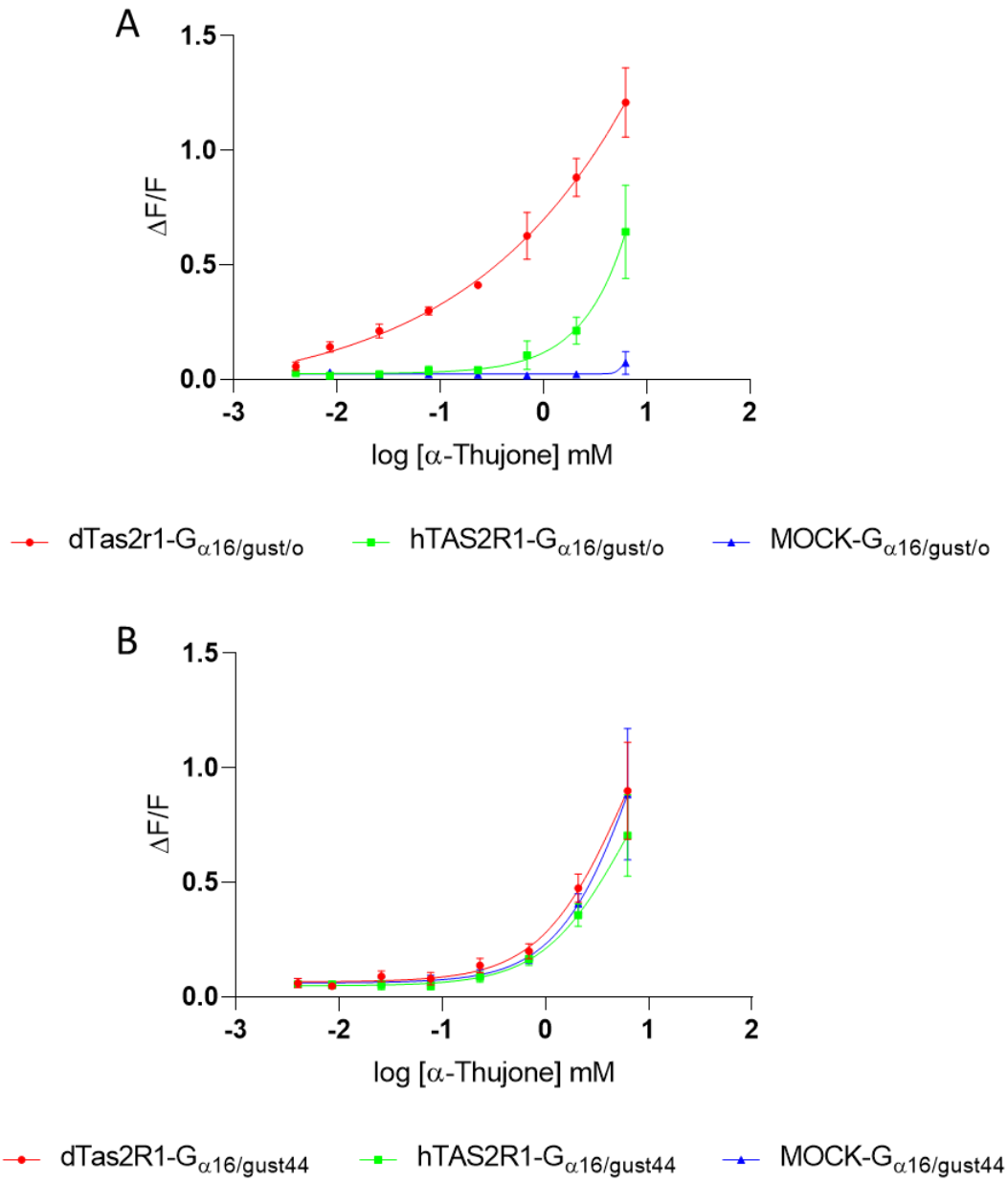

Figure 2.60: Concentration-response curves for Tas2r1 and (-)-α-thujone from comparative testing with the A) $G_{\alpha16/gust/o}$ and B) $G_{\alpha16/gust44}$ expressing cell lines (n=1, error bars=SD).

Interestingly, no new responses were observed with $G_{\alpha16/gust44}$. Compounds such as diphenidol and parthenolide, previously published as hTAS2R1 agonists, but not active with hTAS2R1 and the $G_{\alpha16/gust/o}$ cell line, were also not active with the $G_{\alpha16/gust44}$ cell line when tested here. These data indicate that assay sensitivity may be more of a concern than pharmacological differences mediated by the different G-protein chimeras. Some other aspect of the assay, perhaps handling of the cells or

transfection protocol, must be playing a role in the poorer performance of the $G_{\alpha16/gust44}$ cell line here. This may also be behind the lack of responses seen for the $G_{\alpha16/gust/o}$ cell line and some of the previously published active compound-receptor combinations, and also for the elevated threshold levels seen for some of the active combinations.

The impact of experimental protocol on assay sensitivity was clearly demonstrated in the repeat phase work conducted at IMAX Discovery. Despite using the same cell line and reagents, sensitivity between the two sets of experiments was quite different, and in some cases previous hit receptor-compound combinations were not replicated. A different instrument was used for the assay at IMAX Discovery, which may relate to some of the differences seen. Some experiments where a hit was clear in the initial phase, but not confirmed in the repeat phase, were repeated again under the same conditions as for the initial phase at the Waltham laboratory. In these cases the initial phase data was replicated, with the exception of (-)-α-thujone with Tas2r38. Here the initial response was not replicated and so this was not considered a hit combination. Where data were successfully replicated they have been included in the summary (Table 2.6).

Despite these issues a total of 25 dog Tas2r-compound combinations were identified, with 16 compounds stimulating 7 dog Tas2rs (Table 2.6). Interpretation of tests where no response was seen is complicated by the assay sensitivity issues, and a lack of response has not been classed as a negative result because of this. However, 32 compounds did not give a convincing, dose dependent, repeatable response with any of the dog Tas2rs tested here.

Table 2.6: Summarised data for all dog Tas2rs deorphanised as part of this study
Threshold values are given as mM concentrations with EC_{50} values or not determined (n.d.) in parentheses.

Compound	dTas2r1	dTas2r2	dTas2r4	dTas2r5	dTas2r10	dTas2r12	dTas2r41
1, 10-Phenanthroline	0.37(n.d.)	1.10(n.d.)		0.37(n.d.)			
6-Nitrosaccharin	0.12(n.d.)						
(-)-α-Thujone	0.025(n.d.)						
Aristolochic acid I			0.039 (0.041)				
(-)-Camphor	~1.39(n.d.)						
Chlorhexidine			0.033(n.d.)				
Colchicine	1.24(n.d.)	11.10(n.d.)	3.70(n.d.)				
Cucurbitacin B hydrate					0.00069 (0.0132)		
Denatonium benzoate			0.41 (3.78)				
Ethylpyrazine	3.70(n.d.)						
Flavone	0.002(n.d.)					0.002(n.d.)	
Aurintricarboxylic acid	0.062(n.d.)	0.004 (0.007)	0.007(n.d.)	0.021(n.d.)			
L-Menthol	0.058(n.d.)						
Ofloxacin		0.69(n.d.)					
Oxyphenonium bromide				3.70(n.d.)			1.24(n.d.)
Sucralose			3.70(n.d.)				

2.5. Discussion

In this chapter the receptive ranges of dog Tas2rs were explored using a recombinant cell line and a calcium mobilisation assay. A panel of 48 compounds were screened against dog Tas2rs and their human orthologues. In total 25 agonists for dog Tas2rs were discovered, with 7 of the 16 identified dog Tas2rs being deorphanised. Both similarities and differences between dog and human Tas2r activity were seen in breadth of tuning and sensitivity, indicating that bitter taste perception may not be assumed to be the same between these species.

2.5.1. Comparison of Tas2r responses with dog *in vivo* data

When dealing with human TAS2Rs there is a large amount of information on the actual *in vivo* taste of the test compounds used here. They are known to taste bitter *in vivo* and hence false negatives are easy to identify if all known hTAS2Rs are tested. In dogs there is very little data on the taste or rejection of these compounds *in vivo*, making false negative results more difficult to identify.

One of the few examples of a compound where dog *in vivo* data is available is denatonium benzoate. This compound is often described as the most bitter-tasting compound to humans, as it tastes bitter even at very low concentrations. Threshold data for humans of different ages shows a threshold of between 10-35nM for the compound (Schiffman *et al.*, 1994). Data previously produced by Waltham (not as part of this study) does show that dogs are also sensitive to the bitter taste of denatonium benzoate, preferring plain water in a two-bottle choice test (unpublished data). A study with 10 dogs at Waltham did not show rejection with 10µM denatonium benzoate, while a later study with 90 dogs and a test concentration of 100µM did show clear, but not complete, rejection of the denatonium containing solution (Figure 2.60), suggesting the threshold for rejection in dogs is between 10 and 100µM. This data is in agreement with previously published data for pigs (Nelson *et al.*, 1997), which showed pigs reject denatonium benzoate robustly at 100µM, but rejection becomes weaker at lower concentrations

of 20 and 5µM. Similar data has been published for mice (Lossow *et al.*, 2016). In extensive *in vitro* testing, no mouse Tas2r was shown to have an activation threshold lower than 100µM for denatonium, while lick ratio data indicated no changes between concentrations of 0.03 and 0.3mM concentrations. Higher concentrations of 3mM and above showed obvious reductions in licking. This would suggest lick ratios were not affected until concentrations exceeded the minimum threshold for any Tas2r.

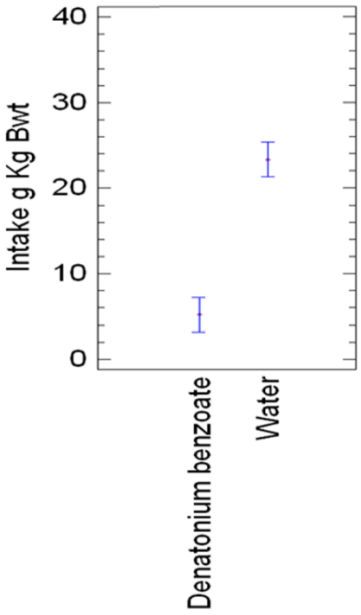

Figure 2.61: Responses of dogs to denatonium benzoate at a concentration of 100µM vs plain water
Dogs (n=90) were offered denatonium benzoate or plain water in a two-bottle, free choice paradigm (previously unpublished data). Multifactor ANOVA analysis of the variance between intakes (normalised for grams per kilogram bodyweight). A significantly higher intake of water over denatonium benzoate was observed (p = 0.0000).

A higher threshold of detection for denatonium benzoate in dogs also fits with the *in vitro* data generated here. The two most sensitive receptors for denatonium benzoate in human TAS2R *in vitro* testing are hTAS2R30(47) and hTAS2R10 (Meyerhof *et al.*, 2010). Dogs lack an orthologue for hTAS2R30(47). The dog orthologue of hTAS2R10 was found to be unresponsive to denatonium (Figure

2.47A). In fact only one dog receptor was found to respond to this compound, dTas2r4. The human orthologue of this receptor has also been seen to respond to denatonium (although it did not in this study) with a threshold concentration of 0.3mM (Meyerhof *et al.*, 2010). The threshold of activation for dTas2r4 in the assay used here was found to be 0.4mM, which did not match with that determined *in vivo*. This may be due to lower sensitivity in the assay, or to another receptor with a lower threshold that was not identified here.

Humans routinely respond to denatonium benzoate at concentrations of 22.3 µM (10ppm). Levels of 67-111.5µM (30-50ppm) have been proposed as required deterrents to ingestion of toxic household substances such as ethylene glycol-based antifreeze in the US (ABA_Act, 2005). These concentrations should be well-above threshold detection for humans, but may be close to threshold detection for pet animals such as dogs. Given the potential for individual variation in taste thresholds for denatonium, a higher upper limit might be considered if deterring ingestion by pet animals was a primary concern.

2.5.2. Dog Tas2r-responsive ranges and breadth of tuning

In some cases sufficient data was collected to give some insight into the breadth of tuning of dog Tas2rs. In the case of dTas2r10, a positive hit was identified with two compounds, (-)-α-thujone and cucurbitacin B. Cucurbitacin B had a very similar activation threshold and EC_{50} to the orthologous human receptor. However, the human receptor also responded to 8 other compounds in the initial phase of concentration-response testing. This data would suggest a difference in tuning breadth for the two orthologues, with dog being noticeably more narrowly tuned.

For Tas2r1 although the array of compounds found to activate the dog and human orthologues was slightly different, the total number of compounds activating each receptor was similar. This would indicate a similar breadth of tuning for these receptors. However, the 48 compounds tested in this study are only a small sample of those available, and those tested in the concentration-response phases were

already pre-screened for activity with dog Tas2rs, which might bias the selection in favour of active compounds for dog.

The dTas2r2 receptor appeared to be putatively functional based on the gene sequence identified in Chapter 1. This was proven to be the case here, with 4 compounds showing activation of the receptor. This would appear to indicate an intermediate breadth of tuning for this receptor. Another example of a Tas2r that appeared to be functional in dog while being a pseudogene in humans was dTas2r12. Only one activating compound for dTas2r12 was identified, the compound flavone, also known as 2-phenylchromone, which is a flavonoid found in dill, pomegranate and rosemary. Flavone is part of a large group of related compounds, and further testing of this family with dTas2r12 may reveal more active compounds for this receptor. Other putative dog Tas2rs without a functional orthologue in human, namely dTas2r62 and dTas2r67, were not deorphanised in this study.

At the initiation of this study, dTas2r4 was annotated as a pseudogene in the reference genome sequence (Shang *et al.*, 2017). Based on the analysis done as part of this project (Chapter 1) this was identified as incorrect, and the receptor proved to be the second most broadly tuned dog receptor in the compound screening stage, with six ligands identified. In humans TAS2R4 is regarded as having intermediate tuning breadth, with 33 identified ligands in the BitterDB (Wiener *et al.*, 2012; Dagan-Wiener *et al.*, 2018).

2.5.3. Pre-screening of dTas2rs with 48 compounds

At the initiation of this study the option of using a high-throughput screening platform such as the FLIPR or FDSS/µCELL system was not available. The study plan involved screening with the FlexStation only, and running all 48 compounds against all 16 dog Tas2rs in a full concentration-response experiment was prohibitively time consuming. In order to try to retain the library size of 48 compounds, but to reduce the amount of time spent screening, a pre-screen phase was designed to highlight compounds most likely to be a positive hit, for full concentration-response testing.

Three compound concentrations were used in the pre-screen phase, the maximum soluble concentration, followed by 1/10 and 1/100 dilutions. The main drawback of such a pre-screen is that some compounds may result in specific responses without any activation of the mock transfected cells only at concentrations falling between any two of these points. In order to mitigate this risk some compounds were taken through to the concentration-response testing phase based on their known activity with orthologous human receptors, rather than their performance in the pre-screen phase of testing. Most compounds tested showed a potential hit against at least one dog Tas2r in the pre-screen phase.

This approach was partially successful and over 200 receptor-compound combinations passed the selection criteria or were selected based on their previously shown activity with human TAS2Rs. Of those that were selected based on their activity in the pre-screen phase, responses showed typical receptor-mediated response characteristics and were specific for dTas2r-expressing cells when statistically compared to mock-transfected cells at one or more of the three tested concentrations.

Only potential agonists were identified here. It is quite possible that in some cases an agonist for the orthologous human receptor might act as an antagonist with the equivalent dog receptor. Screening for antagonists is perfectly feasible with the same assay components used for agonist screening, only the assay protocol needs to change to include stimulation of the cells with a constant concentration of an agonist while varying concentrations of the test compound are applied.

2.5.4. Concentration-response screening of dog and human Tas2rs

During the concentration-response testing phase it became clear that some variation between independent experiments was inevitable, and at least three replicate experiments would be required to add confidence to the data. This was not achievable with the FlexStation due to time constraints, and so access to a high-throughput system was investigated further. Arrangements were made to perform

the repeat phase of the testing at the IMAX Discovery laboratories in Milan, Italy, using the Hamamatsu FDSS/µCELL system. This data added to the data generated on the FlexStation, and ensured that results were reproducible in a different lab with a different instrument.

Some differences in the data were observed. In the majority of cases the data generated at the IMAX Discovery laboratory showed lower sensitivity than that generated at the Waltham laboratory. This was reflected in higher threshold values and/or lower ΔF/F values. The reasons for this are not completely clear, but may be related to the change in instrumentation. Many other different factors can impact on assay performance. Treatment of the cell line during growth, and transfection and cell density on the microplate can influence the performance of the system. Also, having no prior experience with the FDSS/µCELL system, its performance relative to the FlexStation was not well controlled with, for example, repeated tests with ATP or other stimulators of endogenously expressed receptors in the HEK cell line. However, the majority (73%) of positive hits identified in the Waltham-based screening were also positive at the IMAX Discovery laboratories, indicating that these hits were robust and repeatable.

In some cases where a hit on the FlexStation was not replicated on the FDSS/µCELL system a repeat experiment was subsequently run at Waltham. Five of these experiments were performed, with 4 replicating the original results. In most cases results exclusive to a human TAS2R were not repeated, as human TAS2R responses were not the focus of this study. However one example was repeated, hTAS2R10 with chloramphenicol, which was confirmed. The response of dTas2r38 to (-)-α-thujone was not confirmed in either the repeat phase or a subsequent repeat test at Waltham. The original result was quite clear and the reasons for the lack of reproducibility in this test are not known. These data would suggest that generally the differences in sensitivity between the initial and repeat phases of the study were the cause here, and that the positive responses observed in the FlexStation data are reproducible.

2.5.5. Comparison of Tas2r responses with published data

In some cases, no responses to compounds previously shown to stimulate human receptors were observed for either dog or human tests. Diphenidol and quinine are two examples where specific responses were not identified, with responses in the mock transfected cells being present.

Where discrepancies exist, the most obvious difference between the system used here and that used in other work is the choice of G protein chimera. The cell line used here stably expresses a $G_{\alpha16/gust/o}$ chimeric G-protein, not the $G_{\alpha16/gust44}$ chimera used in many published studies. At the time of starting this study the $G_{\alpha16/gust44}$ chimera was not available as it is patent-protected. Therefore, the $G_{\alpha16/gust/o}$ chimera was used and many robust hits have been generated with this cell line. However, without direct comparison with the $G_{\alpha16/gust44}$-expressing cell line under the same conditions it was not possible to determine the impact of the different chimera. Therefore, access to the $G_{\alpha16/gust44}$ cell line was obtained later in the project and a screen of all compounds against dog and human Tas2r1 was performed.

The data from this screen showed that the influence of the G-protein chimera was not easy to identify. The $G_{\alpha16/gust44}$ cell was, in most cases, no more sensitive than the $G_{\alpha16/gust/o}$ cell line. Therefore some aspect of the system other than the G protein chimera must be involved. For example (-)-α-thujone was identified as a Tas2r1 hit for both human and dog with the $G_{\alpha16/gust/o}$ cell line. Previously, this was not found to be the case for hTAS2R1 with the $G_{\alpha16/gust44}$ cell line (Meyerhof *et al.*, 2010). In the published data a maximum concentration of 0.3mM was used for this compound, as higher concentrations gave activation on the mock-transfected cells. This was also the case here with the $G_{\alpha16/gust44}$ cell line, but the $G_{\alpha16/gust/o}$ cell line only showed non-specific responses in the mock-transfected cells at higher concentrations, meaning a specific response at 0.69mM could be observed. Such differences in the sensitivity of the mock cells to certain compounds may be related to the clonal selection of the G protein expressing cell lines. If such responses are mediated by other cell-surface receptors endogenously expressed by the HEK cell line, the level of these could vary

between clonal cell populations and result in differences in cell sensitivity to some compounds. This could dictate the maximum concentration of a compound that may be tested successfully and so allow some cell lines to show specific responses to higher compound concentrations.

Some other results point more towards a specific difference in the behaviour of the different cell lines, possibly related to the differences in the G-protein chimera. For example a lack of response of hTAS2R5 with its ligand 1, 10-phenanthroline was observed, along with several other instances of human TAS2Rs not giving responses to compounds previously identified as ligands. These data may represent issues with the performance of the $G_{\alpha16/gust/o}$ cell line, or they may be related to assay sensitivity.

Another example of differences between the data presented here and previously published data can be seen with the performance of the assay with diphenidol. Diphenidol is the most prolific stimulator of TAS2Rs yet found, activating 15 of the 25 human TAS2Rs (Meyerhof *et al.*, 2010). Activating concentrations range from 3-100µM for the different active receptors. No activity was seen in any of the dTas2rs with this compound, and only a few instances of activation with hTAS2R7, 10 and 39 were recorded in the concentration-response initial phase testing, with a threshold concentration of 93µM. However, even these responses had weak activation of the mock-transfected cells, albeit less than for the receptor-transfected cells. Without any evidence of activation of dTas2rs, diphenidol was not taken to the repeat phase of concentration-response testing, however small changes like a slightly less-sensitive mock cell line or slightly better sensitivity in the receptor-transfected cells might have produced several more positive receptor-compound combinations. While the responses with the hTAS2Rs were not strong, such data has been published as evidence of positive responses before. In a publication focussing on cat Tas2rs (Lei *et al.*, 2015), the data in Figure 2.62 was cited as evidence for activation of cat Tas2r46 and Tas2r67 by diphenidol. In both cases the response in the receptor-transfected cells was accompanied by a smaller response in the mock-transfected cells, matching the data generated here for hTAS2R7, 10 and 39.

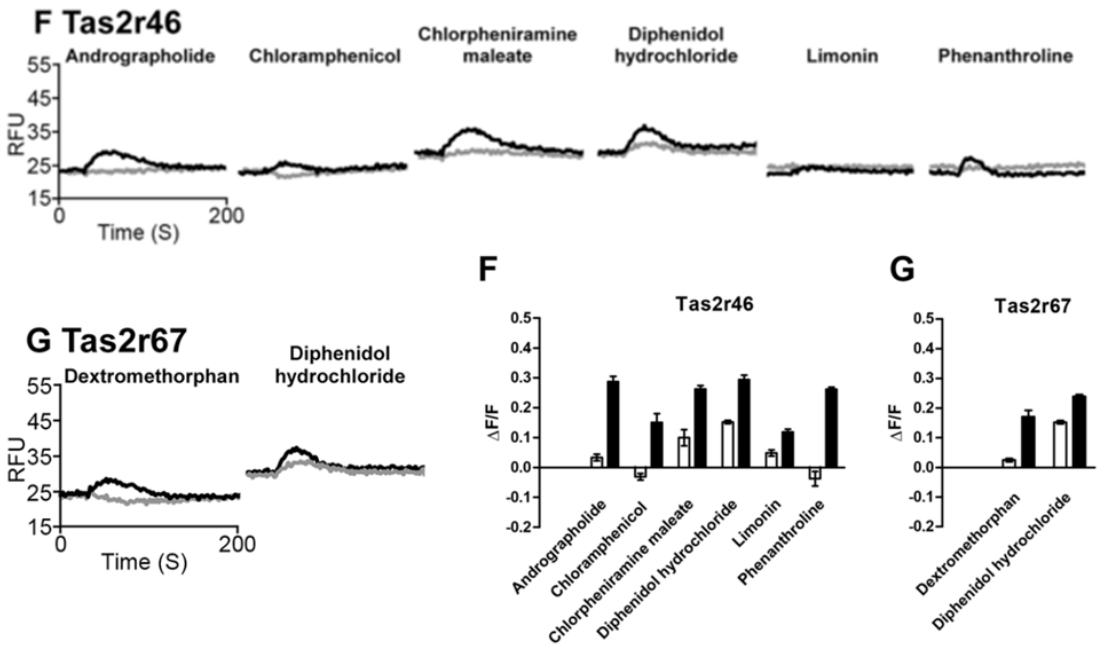

Figure 2.62: Cat Tas2r calcium response data reproduced from Lei *et al.* (2015) Published data to support the identification of diphenidol as a ligand of cat Tas2r46 (F labelled panels) and Tas2r67 (G labelled panels). In the response trace data black traces represent receptor-transfected cells and grey traces represent mock-transfected cells. Bar charts show black columns for the receptor-transfected cells. Data was calculated from three technical repeats from one experiment (n=1). Two-tailed Student's t-tests were performed to determine when responses from Tas2r-transfected cells were significantly different from that of mock-transfected cells.

Small responses like those observed for diphenidol may warrant further confirmation. The generation of cell lines stably-expressing the Tas2rs of interest should result in a greater signal output, with all cells expressing the receptor rather than only the percentage of cells successfully transfected. This should improve both assay sensitivity, and experimental reproducibility, as any variability associated with the transfection step is removed. The development of stable cell lines may be particularly attractive where only one, or a small number of Tas2rs are required for study.

There are other factors that might cause the data generated here to not agree entirely with some of the published human data. Two of the largest published deorphanisation studies (Meyerhof *et al.*, 2010; Lossow *et al.*, 2016) on human and mouse Tas2rs were performed on the Fluorescence Imaging Plate Reader (FLIPR)

instrument (Molecular Devices, San Jose, USA). The pre-screen and initial phase of the concentration-response testing for this study were performed on the FlexStation 3 (Molecular Devices, San Jose, USA), and the repeat phase of the concentration response testing on the FDSS/µCELL instrument (Hamamatsu, Japan). While all instruments can run the same assays their signal detection technology is different. The FLIPR uses a Charge Coupled Device (CCD) camera while the FlexStation uses a photomultiplier (PMT), and the Hamamatsu a different CCD camera. Excitation sources also differ between instruments. Differences between the data generated here with the FlexStation and the Hammamatsu FDSS/µCELL system were apparent, and a similar situation might be seen if a FLIPR system was used.

In the pre-screen phase, test compounds were plated out and stored at -20^{o}C until the day of testing. It is possible that this might affect the data, but it was not possible to prepare all compounds on the day of testing due to the time restrictions of running the assay. However, compounds for the subsequent concentration-response testing were prepared on the day of testing without any freezing, as less compounds were required each day.

Transfection of plasmid DNA without a Tas2r in the multiple cloning site (MCS) was used as a mock control in all experiments. This was considered to be the best option, showing that the transfection process itself and the expression vector caused no fundamental issue with the response of the cells. It is also the most widely-used method in the literature. An additional control could be the testing of un-transfected cells. This might highlight any effect of the transfection process on factors like the non-specific response of cells to compounds at higher concentrations.

However, all of these points must be must be viewed in the overall context of experiments using recombinant cell lines. While assays employing chimeric G proteins offer several advantages in relation to their ability to provide rapid and reproducible test systems, which are amenable to high throughput screening, they also have some disadvantages. Fundamentally the use of native $G_{\alpha gust}$ and the measurement of its direct downstream effects would be preferable to the use of any

chimera. Calcium may still be useful as a readout in a native system due to the action of both the $G_{\alpha gust}$ subunit and the $G_{\beta\gamma}$ complex. In work on the isolation and propagation of primary taste cells, measurable calcium responses have been recorded when cultured native cells are stimulated with bitter tasting compounds (Ozdener *et al.*, 2013). Such work could complement studies using recombinant systems.

2.5.6. Summary

In this study all putative dog *Tas2r* genes were transfected into a cell line constitutively expressing a $G_{\alpha 16/gust/o}$ chimeric G-protein, and were screened against a library of 48 chemicals known to taste bitter to humans. A pre-screen phase was used to highlight compounds acting as potential ligands for dog Tas2rs before two phases of concentration-response testing were performed with both dog Tas2rs and their human orthologues.

In total 7 of 16 putative dog Tas2rs were deorphanised, with differences in both compound binding profile and breadth of tuning being demonstrated when compared to orthologous human TAS2Rs. Threshold and EC_{50} concentrations were determined where possible, although most compounds showed low affinity, meaning high µM or low mM concentrations were required for receptor activation. This often caused the mock-transfected cells to respond, limiting the possible testing range and the ability to determine EC_{50} concentrations.

In many cases data generated here were similar to those published elsewhere, although there was a tendency for threshold concentrations to be higher here. In some cases previously published active receptor-compound combinations did not show specific activity here, which may be related to assay sensitivity or to differences between the G protein chimera used here and that used in the majority of published work. Both G protein chimeras were tested here with Tas2r1, but differences in assay specificity were not apparent, indicating that assay sensitivity here was not primarily related to the sequence of the G protein chimera. Due to the

lower sensitivity of the assay observed here caution should be exercised in interpreting lack of activity as a truly negative result.

A pre-screening strategy was used to highlight active compounds and reduce the amount of concentration-response testing required. However, in some cases compounds may only stimulate receptors specifically within a very narrow concentration range. This may mean some receptor-compound combinations were missed as the pre-screen was conducted with only three concentration points. Full concentration-response testing of any compound-receptor combinations that were not so tested here may yield further active compounds.

Assay sensitivity varied between the two phases of concentration-response testing. This could be due to several factors such as variation in cell handling, transfection efficiency, dye loading and the performance of the instrument used for the calcium mobilisation assay. One way to reduce these sources of variation would be to develop cell lines stably expressing the Tas2rs. This should also increase assay sensitivity, as all cells should respond to an activating compound, rather than just those successfully transfected. Another strategy which may be beneficial is the use of a luminescent based readout in the assay. Several compounds showed evidence of some level of autofluorescence here, and an assay that is insensitive to this may give clearer results in these cases.

The data generated here show that both receptor binding profile and breadth of tuning can vary between orthologous receptors in different species. This is in agreement with work done by Lossow *et al.* (2016), which showed that mouse Tas2rs can differ from their human one-to-one orthologues in both their ligand binding profile and their breadth of tuning.

Chapter 3. Tas2r expression in dog fungiform taste papillae

3.1. Introduction

3.1.1. Taste papillae

Taste papillae are specialised structures on the surface of the tongue. Certain kinds of taste papillae house taste buds and are referred to as gustatory papillae. Other papillae have no taste buds associated with them and are referred to as non-gustatory papillae. Taste buds are small collections of specialised cells that detect taste-active molecules in the oral cavity, the activation of which is interpreted as the sense of taste.

The first description of taste papillae came from Marcello Malpighi in 1686 (Witt *et al.*, 2015). Non-gustatory filiform papillae cover the surface of the tongue while gustatory papillae are distributed unevenly with certain types being more or less prevalent in certain areas, a pattern which is largely conserved in mammals. There are three types of mammalian gustatory papillae, fungiform (mushroom-like), foliate (leaf-like) and circumvallate (surrounded as if by a rampart) (Figure 3.1).

Fungiform papillae are small pink elevations mostly occurring on the anterior portion (the portion extending from the line of circumvallate papillae to the tongue tip) of the tongue surface. The morphology can be quite variable with papillae being more or less pronounced in different areas. In humans there is a greater concentration of fungiform papillae towards the tip of the tongue (Miller, 1986). In the dog the arrangement of the taste papillae is similar to that for human. Fungiform papillae are evenly distributed over the dorsum (Tuckerman, 1890) or slightly concentrated towards the tip (Holland *et al.*, 1989). They have variable numbers of taste buds but on average there are 3.5 per papilla in humans (Miller *et al.*, 1990a; Miller *et al.*, 1990b). This was found to be similar in dogs with an average of 3 and no more than 6 taste buds per fungiform papilla reported by Holliday (1940), and an average of 4-5 and no more than 9 reported by Holland *et al.* (1989), which in both cases appeared only on the dorsal surface of the papillae. Humans have fungiform papillae that have

no taste buds present (Arvidson *et al.*, 1980; Miller *et al.*, 1990b; Cheng *et al.*, 1991) but this does not appear to be the case for rats (Mistretta, 1984) where 98-99% of all fungiform papillae contain a taste bud.

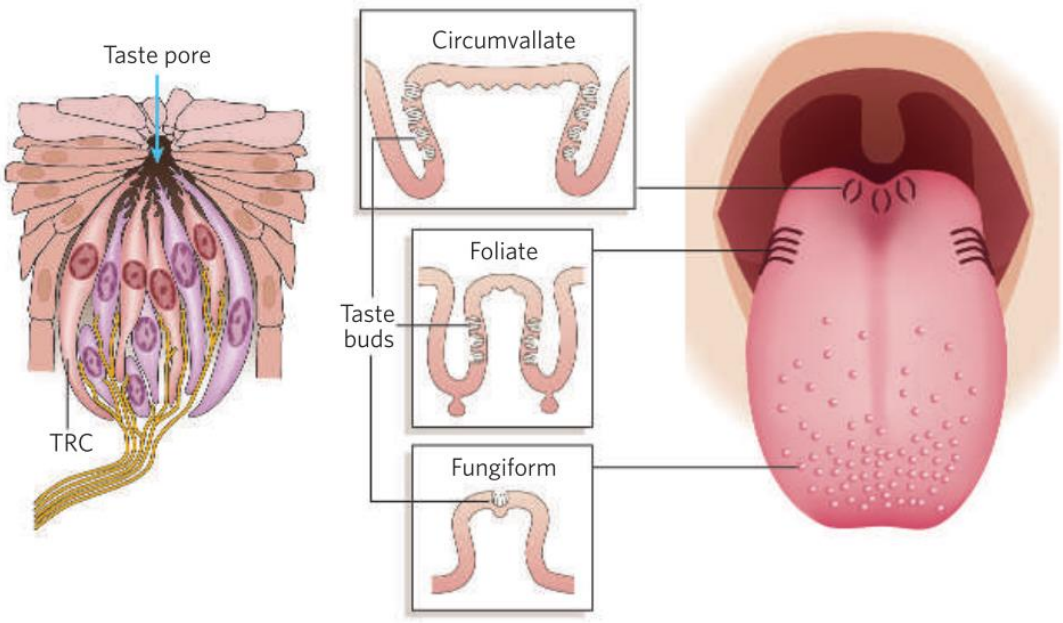

Figure 3.1: Gustatory papillae and taste buds in humans
Circumvallate papillae house the greatest number of taste buds while fungiform papillae have the least (reproduced from Chandrashekar et al. (2006)). TRC = Taste Receptor Cells.

Circumvallate papillae form a "V" shaped line across tongue in humans and this appears to be conserved in the dog (Holliday, 1940). Humans have between 4 and 18 circumvallate papillae with an average of around 9 (Munch, 1896). Dogs have between 4 and 6 circumvallate papillae (Holliday, 1940). The circumvallate papillae have numerous taste buds with average values per papillae of around 250 for humans (Witt *et al.*, 2015), the majority of which occur in the sidewall of the papillae.

Foliate papillae are located on the sides of the tongue at the mid region in parallel rows of ridges and are perhaps the least studied type generally. Dogs do have linearly arranged finger-like protrusions but they do not contain any lingual taste buds (Haddad *et al.*, 2019). This is also the case in cats, but the significance of this

difference in these two species of carnivora when compared to humans, primates and other mammals is not clear.

Taste papillae density has in some cases been linked to so-called supertasting in humans. The concept of supertasting is not particularly well-defined, being used to describe a specific taste sensitivity to the chemicals PTC and PROP in some cases and also being used to describe general taste sensitivity in others. Evidence that fungiform papillae density is linked to taste sensitivity is somewhat inconsistent. Sucrose taste threshold was shown to be correlated with fungiform taste papillae density on the anterior portion of the tongue (Miller *et al.*, 1990b; Zhang *et al.*, 2009), whereas citric acid shows inconsistent results between two studies (Miller *et al.*, 1990b; Zuniga *et al.*, 1993). PROP also showed inconsistent results between different studies (Miller *et al.*, 1990b; Garneau *et al.*, 2014). It is also the case that variation in taste papillae density may not always be comparable between species due to different average numbers of taste buds on individual fungiform papillae.

3.1.2. Taste buds

Taste buds have been described as goblet-shaped organs, taste goblets, taste buds or taste onions. Taste buds are located in the gustatory papillae, but can be present in other regions of the oral cavity including the larynx, upper oesophagus, oropharynx and epithelium of the palate (Witt *et al.*, 2015). Humans may have more taste buds than dogs on average but numbers vary between individuals, and are most marked in the circumvallate papillae. In humans, the largest proportion of taste buds occur in the circumvallate papillae (48%) while foliate (28%) and fungiform papillae (24%) have less. The total number of taste buds in the fungiform papillae are not thought to be hugely different from those observed in puppies, at around 1000 (Miller *et al.*, 1990b; Miller *et al.*, 1990a). More taste buds are present in the circumvallate papillae (~240) (Miller and Bartoshuk 1991) and there are on average more circumvallate papillae (4-18 mean 9.2 ± 1.8) (Munch, 1896) giving a total of around 2000 taste buds located in the circumvallate papillae. In addition to taste buds on the dorsal side of the tongue there are extra-lingual taste buds located in

the walls of the oral, pharyngeal and laryngeal cavities in both dogs (Kitchell, 1978) and humans (Lalonde et al., 1961). The total number of taste buds in humans can vary widely between individuals (Table 3.1) but an average is 4600 (Witt et al., 2015). For other animals, the number of taste buds can also vary.

Table 3.1: Number of taste buds in different animals adapted from Kare (1971)

Animal	**Number of taste buds**	**Ref.**
Snake	0	Payne, 1945
Chicken	24	Linden Maier and Kare, 1959
Pidgeon	37	Moore and Elliott, 1946
Bullfinch	46	Duncan, 1960
Starling	200	Bath, 1906
Duck	200	Bath, 1906
Parrot	350	Bath, 1906
Kitten	473	Elliott, 1937
Bat	800	Moncrieff, 1951
Puppy	1706	Holliday, 1940
Human	9000	Cole, 1941
Pig and Goat	15000	Moncrieff, 1951
Rabbit	17000	Moncrieff, 1951
Calf	25000	Webber, Davies and Kare, 1961
Catfish	100000	Hyman, 1942

An average number of taste buds of 1706 was determined in three tongues from dog pups distributed as shown in Figure 3.2 (Holliday, 1940). Of these 262 were in the circumvallate papillae (determined for 1 tongue) and 1444 were found in the fungiform papillae (average from three tongues).

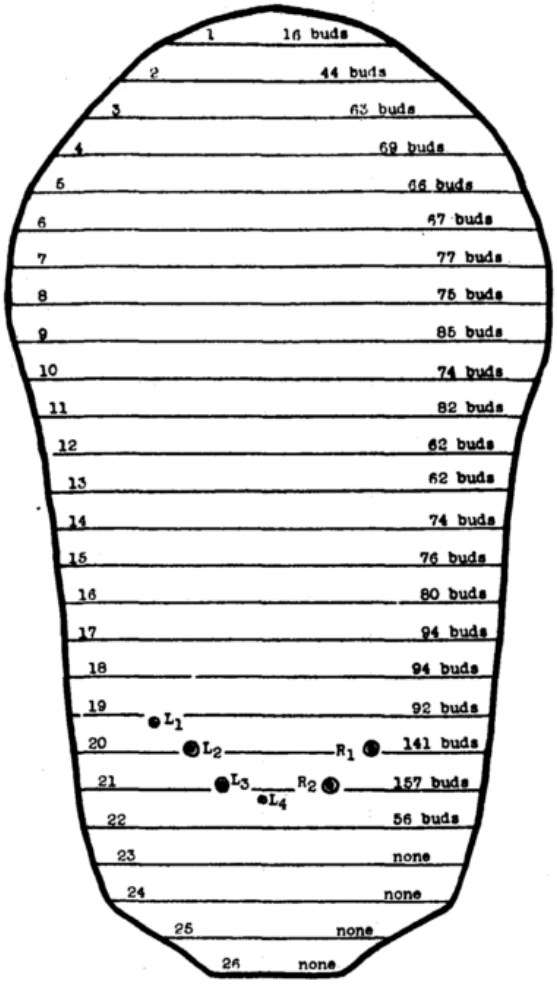

Figure 3.2: Graphic representation of the average total regional distribution of taste buds over the entire dorsum of three puppy tongues
Fungiform papillae were studied for all three tongues while circumvallate papillae were studied only for tongue number 2. Each area represents 73 sections of a 20 micron thickness. The positions of the circumvallate papillae in tongue number 2 are plotted. Reproduced from Holliday (1940).

The structure of mammalian taste buds has been studied extensively. Taste buds typically consist of up to 100 cells in humans (Chaudhari *et al.*, 2010). They are composed of a mixture of cell types, termed Type I (glial-like) cells, Type II (receptor) cells, Type III (pre-synaptic) cells, Type IV (basal) cells, and Type V (peripheral) cells. In the dog a detailed study by electron microscopy revealed a similar structure with 20-40 cells in each taste bud and identification of all the same cell types (Kanazawa, 1993).

Type I cells are also referred to as glial-like cells due to the similarity in the roles they play when compared to glial cells in the central nervous system. They express enzymes that degrade ATP (Bartel *et al.*, 2006) and they contain the GLAST glutamate transporter (Lawton *et al.*, 2000), which functions to terminate transmission and stop the spread of transmitters. Some Type I cells also express the K^+ channel ROMK which may play a role in excretion of excess K^+ through the apical pore, so that Type II and Type III cells remain excitable with a hyperpolarised resting potential. Type I cells have thin lamellae that wrap around the other cells of the taste bud (Chaudhari *et al.*, 2010).

Type II cells are known as receptor cells because these cells have been shown to be the only cells in the taste bud that express the G-protein coupled receptors associated with sweet, umami and bitter taste (Matsunami *et al.*, 2000; Tomchik *et al.*, 2007). Cells only express the receptors for one of these three taste modalities, but cells expressing bitter receptors can express multiple Tas2rs simultaneously (Adler *et al.*, 2000; Behrens *et al.*, 2007). Type II cells do not have synapses, but signal to sensory afferents or Type III cells within the taste bud by ATP release through the CALHM1 channel (Kinnamon, 2016).

Type III cells form synaptic junctions with nerve terminals using ATP (Finger *et al.*, 2005) and are therefore known as pre-synaptic cells (DeFazio *et al.*, 2006). They also respond to sour stimuli (Huang *et al.*, 2008) through the action of the proton-selective ion channel Otop1 (Teng *et al.*, 2019; Zhang *et al.*, 2019) and to carbonation in drinks (Chandrashekar *et al.*, 2009).

Type IV cells are also known as basal cells and are undifferentiated or immature taste cells (Chaudhari *et al.*, 2010). These lie at the base of the taste bud and do not extend to the apical pore.

Also known as “marginal cells” or “perigemmal cells” Type V cells may also be taste bud stem cells (Farbman, 1980).

3.1.3. *Tas2r* expression in taste bud cells

Tas2r expression has been detected in circumvallate, foliate and to a lesser extent fungiform papillae (Adler *et al.*, 2000; Matsunami *et al.*, 2000; Lipchock *et al.*, 2013). Expression occurs in cells that are distinct from those expressing the receptors for sweet and umami taste, supporting the "labelled line" model of taste coding (Figure 3.3) (Chandrashekar *et al.*, 2006). Indeed, Mueller *et al.* (2005) showed that expression of a Tas2r bitter receptor in sweet-sensing cells in transgenic mice caused the mice to develop a preference for an agonist of the receptor.

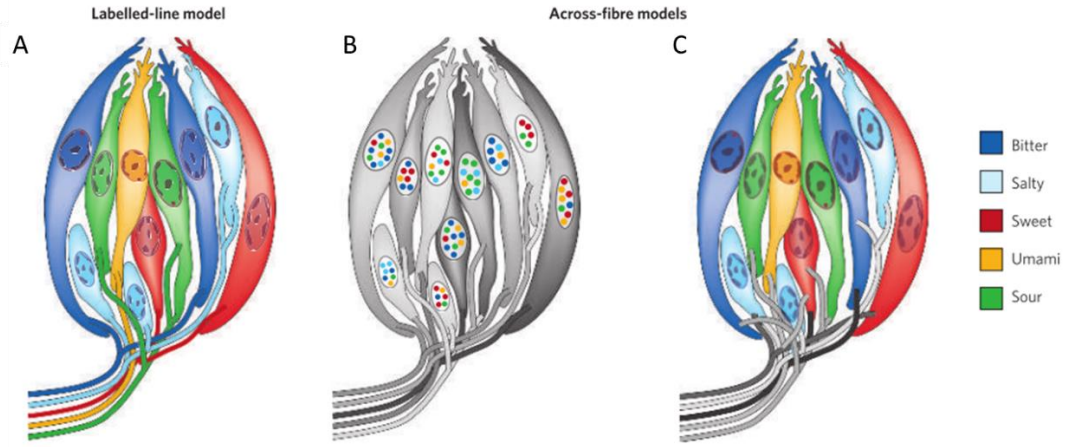

Figure 3.3: Models of taste coding at the periphery reproduced from Chandrashekar et al. (2006)
A) The labelled line model of taste coding where taste cells respond to one of the five basic taste modalities and are innervated by an individual nerve fibre. B) and C) Alternative "across-fibre" models where taste cells respond to multiple different taste modalities and innervating nerve fibres carry information for multiple taste modalities (B) or where taste cells respond to one taste modality but nerve fibres innervate multiple taste cells sensing more than one taste modality (C).

Whether bitter-sensing cells express all *Tas2rs* or only some has been studied in depth. Multiple expression of *Tas2rs* was demonstrated in early work in rats and mice, where RNA *in-situ* hybridisation with up to 17 probes showed that most cells expressed most *Tas2rs* (Adler *et al.*, 2000). More recently, the number of *TAS2Rs* to be expressed in any one cell has been refined to 4-11 in human bitter cells (Behrens *et al.*, 2007). This allows for the possibility that bitter tastes can be discriminated. It

was also shown that all *TAS2Rs* were expressed in taste buds, indicating that despite the roles of these receptors in other areas of the body (Finger *et al.*, 2011; Lee *et al.*, 2012; An *et al.*, 2018; Kok *et al.*, 2018) they likely all play a role in taste too.

3.2. Aims of this chapter

This chapter aims to show the repertoire of *Tas2r* genes that are expressed at the RNA level in dog fungiform taste papillae. Expression of *Tas2rs* in fungiform papillae has been shown to be much lower and less frequent when compared to foliate or circumvallate papillae (Adler *et al.*, 2000). However, fungiform papillae are more easily sampled than circumvallate papillae, and the fact that dogs appear to have no taste buds in foliate papillae (Haddad *et al.*, 2019) meant this was the best available option for this study. This also presented an opportunity to study *Tas2r* expression in fungiform papillae from different areas on the tongue. While the idea of a clearly-defined taste map on the surface of the tongue has been acknowledged as incorrect, it is still thought to be the case that sensitivity to different tastes can vary in different areas (Higgins *et al.*, 2019). This is presumably related to receptor expression, but may be due to some other factor(s).

3.3. Materials and methods

3.3.1. Animals used in this study

Five adult dogs were used in this study, which was reviewed and approved by the Waltham Animal Welfare Ethical Review Board. Papillae sampling was conducted under Project Licence approval in accordance with Animals (Scientific Procedures) Act 1986. Dogs were selected if they were due to undergo a scheduled veterinary dental procedure involving general anaesthesia such as a dental scale and polish or a tooth extraction. All dogs were given Acepromazine at 0.02mg/kg via intramuscular injection, and Synthadon at 0.3mg/kg via intramuscular injection as their premed. Propofol plus was given intravenously as the anaesthetic induction agent and

isoflurane as the anaesthetic maintenance drug. Dogs were not anaesthetised specifically for this study. The dogs used in the study are detailed in Table 3.2.

Table 3.2: Dogs used in this study.

Animal ID	Name	Age (yrs)	Weight (kg)	Gender	Breed
LR05834	Womble	4.1	24.8	M	Labrador Retriever
LR05309	Keisha	6.3	18.4	F	Labrador Retriever
LR05199	Elliott	7.4	24.1	M	Labrador Retriever
BE06022	Dora	3.4	11.6	F	Beagle
BE06014	Dodger	3.4	18.3	M	Beagle

Dogs were maintained on standard diets of commercially-available pet food prior to the study. Dogs were fasted before undergoing general anaesthesia according to standard veterinary procedures.

3.3.2. Taste papillae biopsy procedure

Before fungiform papillae were sampled, the surface of the tongue was photographed then stained using brilliant blue food colouring (Sensient, UK) at a concentration of 1.5mg/mL in water. Plastic hole reinforcers were used as measuring circles with an inner area of 0.8cm^2 and were placed onto the tongue in six positions bi-laterally on the anterior portion of the tongue (Figure 3.4). Fungiform papillae were counted within the inner area of the plastic circle and recorded. The procedure for sampling the papillae was adapted from a previously-published protocol for human papillae sampling (Spielman *et al.*, 2010). Before sampling, the tongue was stabilised by wrapping sterile gauze around it without obscuring the area to be sampled. One finger was placed under the tongue to push the tongue from underneath and make papillae sampling easier. Sprung micro-scissors were then used to remove the papillae. One single fungiform papillae was removed from each counted area and placed immediately into a 1.5mL DNA Lo-Bind tube (Eppendorf,

UK) containing 1mL RNALater (Thermo Fisher Scientific, UK). The tubes were immediately placed on ice and transported to the laboratory where they were stored at 4°C overnight, then transferred to a -20°C freezer for storage.

Dogs were monitored for 24hrs post-procedure for any signs of discomfort or any changes to expected behaviour such as eating and drinking. No adverse observations were made with any of the dogs sampled. Sampling and observation were carried out by trained staff at Waltham.

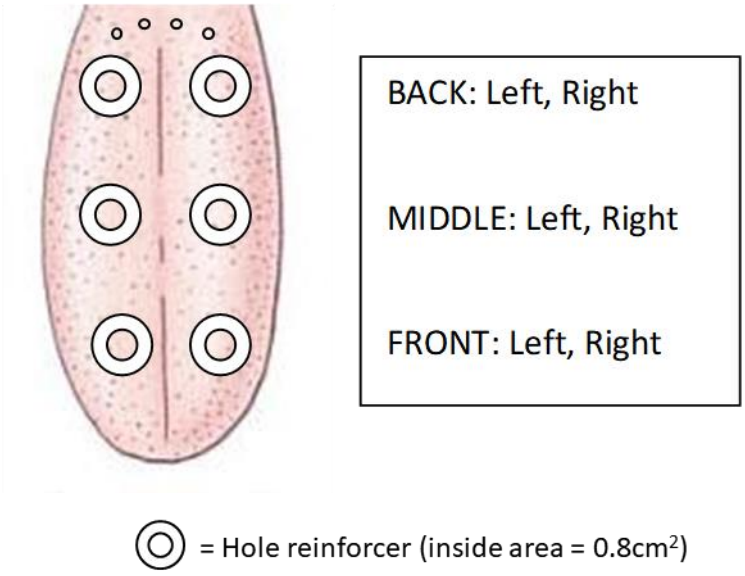

Figure 3.4: Papillae sampling sites on the tongue
Fungiform papillae were sampled from six different areas of the anterior portion of the tongue. Hole reinforcers were used to define sampling areas and papillae were counted within the centre area to estimate papillae density across the tongue.

3.3.3. RNA extraction

Fungiform papillae frozen in RNALater were thawed at room temperature. Papillae were removed from the tube and RNA was extracted using the RNeasy Plus Micro Kit (Qiagen, Germany) according to the manufacturer's protocol for total RNA extraction from animal and human tissues. Briefly, each papilla was placed into a separate 2mL SafeLock DNA-LoBind tube (Eppendorf, UK) containing 350µL Buffer RLT and one 5mm stainless steel ball bearing. Buffer RLT contains the chaotropic and denaturing

agent guanidine isothiocycanate, which serves to prepare the RNA for binding to the purification column. The tubes were shaken using a TissueLyser II (Qiagen, Germany) for 2 min at 20Hz. This step was repeated with the tubes rearranged so the innermost tubes were now on the outer side to ensure that all samples received equal treatment. Tubes were then spun in a centrifuge and the supernatant pipetted-off and used for the rest of the procedure. As part of the procedure, DNA removal was performed using the genomic DNA eliminator columns provided with the kit. This method has previously been found to be superior to on-column DNA digestion with DNase (unpublished observation). At the end of the procedure, samples were eluted using 14µL of nuclease-free water. RNA quality assessment and quantification was carried out using a Bioanalyser (Agilent, UK) with the RNA 6000 Pico Kit (Agilent, UK).

3.3.4. RNA sequencing

The primary method selected for expression detection and quantification was RNA-sequencing (RNA-seq). RNA-seq is a technique that became possible with the development of massively parallel sequencing, also known as next generation sequencing (NGS). Essentially, the technique involves poly-A selection or ribosomal RNA depletion followed by reverse transcription of an RNA sample to produce a cDNA library. This is then sequenced via NGS and the reads produced are aligned to a reference genome or transcriptome. The number of reads mapping to a particular gene or transcript give an indication of the expression level of that gene. Previously unknown transcripts and isoforms can be identified depending on how the data is analysed. Overall the data can provide a view of the transcriptional activity of the sample at the time of collection (Stark *et al.*, 2019). As the samples were likely to contain only a very small number of taste receptor cells (TRC) relative to the surrounding epithelial cells, sequencing with high-depth coverage was chosen, targeting ~40 million 150bp paired-end reads per sample.

All RNA extraction, cDNA synthesis and amplification was performed at Waltham as was all data analysis. The specialist task of library preparation and sequencing was performed by the DeepSeq core facility at the University of Nottingham.

3.3.5. RNA amplification, library generation and sequencing

For RNA-Seq, the recommended amount of total RNA for input with the Illumina TruSeq RNA Library Prep Kit v2 is 0.1-1µg of total RNA. This much total RNA was not recovered from most of the samples and so an RNA-amplification technique was used that is often applied with very small samples or for single cell RNA-seq. The SMART-Seq v4 Ultra Low Input RNA Kit for Sequencing (Takara Bio, USA) was used. Input RNA for this kit is recommended as 10pg-10ng of RNA. The samples varied in concentration, but some were as low as 0.5ng/µl. In order to use the same amount of RNA for all library preps, 5ng were added for each sample to the reaction which in some cases was the full RNA sample.

The SMART-Seq v4 Ultra Low Input RNA Kit for Sequencing incorporates a proprietary SMART® (Switching Mechanism at 5' End of RNA Template) technology. This technology relies on the template switching activity of reverse transcriptases to enrich for full-length cDNAs and to add defined PCR adapters directly to both ends of the first-strand cDNA (Zhu *et al*., 2001). This ensures the final cDNA libraries contain the 5' end of the mRNA and maintain a true representation of the original mRNA transcripts (Figure 3.5).

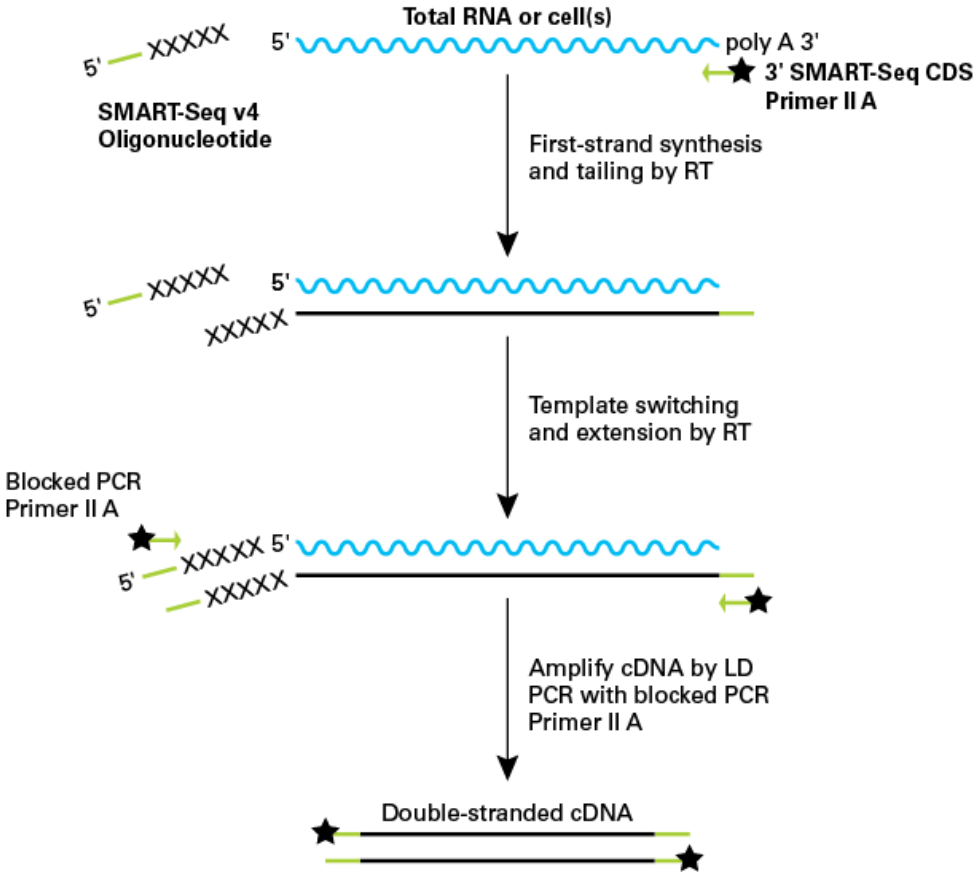

Figure 3.5: Flowchart of SMART cDNA synthesis
The SMART-Seq v4 Oligonucleotide, 3' SMART-Seq CDS Primer II A, and PCR Primer II A all contain a stretch of identical sequence. The black star indicates a chemical block on the 5' end of the oligonucleotide (reproduced from the SMART-Seq® v4 Ultra® Low Input RNA Kit for Sequencing User Manual).

For sequencing library generation, the Illumina Nextera XT kit was used. This step in the sample preparation takes the cDNA library, fragments it to the appropriate size and adds the required adapters for sequencing. Fragmentation is achieved by transposomes in a process known as tagmentation (Figure 3.6).

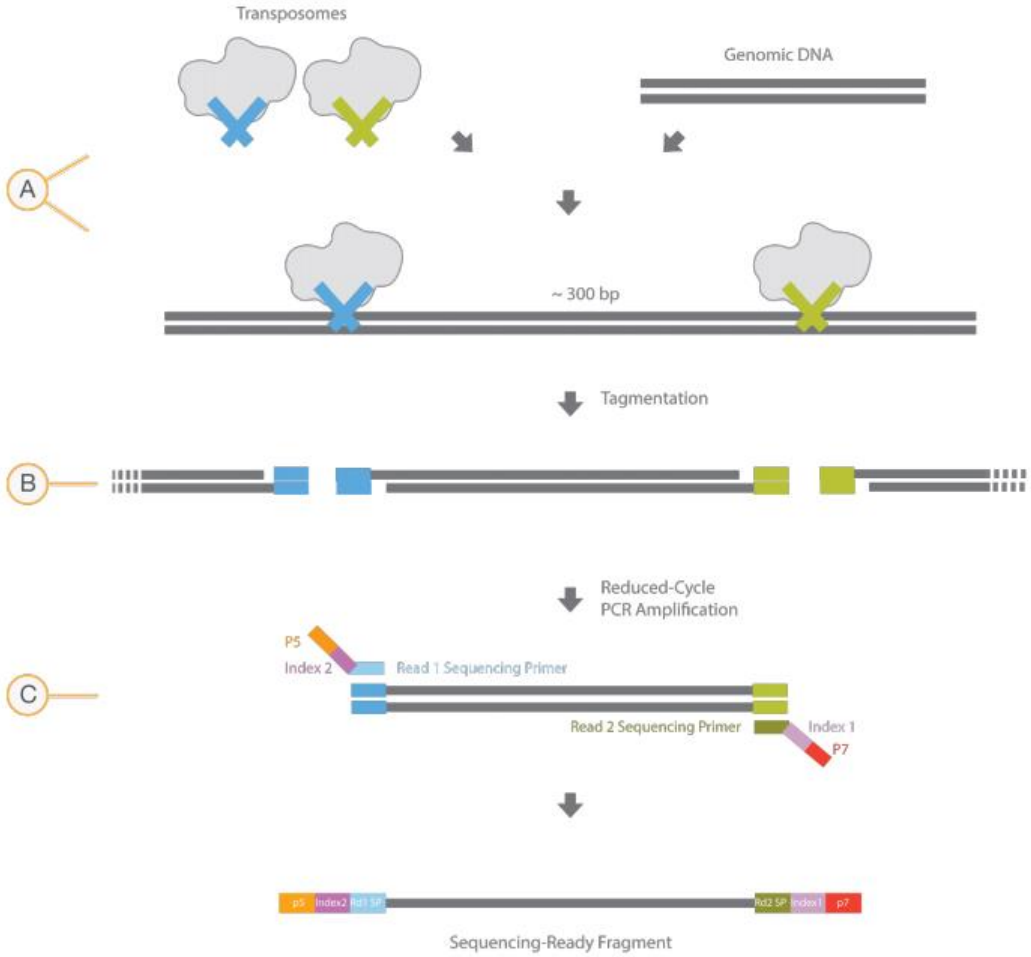

Figure 3.6: Illumina Nextera XT library preparation
Transposomes fragment and tag the DNA in a process called tagmentation. Reduced-cycle PCR with primers matching the incorporated tag sequences is then used to add index sequences and the Illumina P5 and P7 sequences which bind to the flowcell (reproduced from the Nextera XT DNA Library Prep Reference Guide).

During the initial sample preparation, both the Nextera XT and the Nextera DNA Flex library preparation kits were tried. The Nextera DNA Flex kit allows increased input DNA which reduces the number of PCR cycles required in library preparation. This can increase library complexity by reducing the number of PCR duplicates. However, the Nextera DNA Flex kit did not appear to be resulting in complete tagmentation while the Nextera XT kit did. All samples were processed with the Nextera XT kit using the recommended 150pg of input cDNA by the DeepSeq core sequencing facility at the University of Nottingham.

For sequencing, the libraries were pooled at equimolar amounts and run together over 3.6 high output 300 cycle NextSeq flow cells to deliver about 40 million 150bp paired-end reads per sample, although there was some variability in the number of reads generated for each sample.

3.3.6. RNA-seq data analysis

There are numerous strategies for RNA-seq data processing and analysis depending on the situation (Conesa *et al.*, 2016). One important factor is the availability and the quality of a reference genome for the organism being studied. In the case of the dog, the reference genome (Lindblad-Toh *et al.*, 2005) is relatively good compared to other non-model mammals. The reference transcriptome is also available. Two analysis pipelines, one based on alignment to the transcriptome and one on alignment to the genome were used here. This allowed comparison of the results between the two approaches and increased confidence in the results where agreement was seen. Prior to alignment, data was subjected to a QC process which involved the trimming of sequencing adapters and the removal of poor quality reads.

For alignment to the transcriptome kallisto was chosen (Bray *et al.*, 2016), which is based on a technique known as pseudoalignment. Kallisto uses several techniques that effectively reduce the time taken to align reads to a reference transcriptome by two orders of magnitude compared to other approaches. The program makes use of a concept called the transcriptome de Bruijn Graph (T-DBG), where reads are broken down into *k*-mers (all possible sequences of length *k* using the four nucleotide bases A, G C and T), and a read is assigned a *k*-compatibility class based on the possible places in the transcript where the *k*-mer can align.

For alignment to the genome STAR (Spliced Transcripts Alignment to a Reference) was used, which uses sequential maximum mappable seed search in uncompressed suffix arrays followed by seed clustering and stitching procedure (Dobin *et al.*, 2013). STAR is notable for its speed and accuracy when compared to older alignment

software. The STAR alignment was followed by read counting with the featureCounts program (Liao *et al.*, 2014).

Principle Component Analysis (PCA) was used to initially examine the relationships between the samples. PCA is a multivariate technique useful for dimensionality reduction while preserving variation in the data. It is quite well suited to visualisation of RNA-seq data and can make differences in gene expression patterns easier to identify when comparing groups of similar and different samples.

To test the hypothesis on the expression of *Tas2rs* in fungiform papillae from different regions of the tongue, differential expression (DE) analysis was conducted on the RNA-seq data. In this study edgeR (empirical analysis of differential gene expression in R) (Robinson *et al.*, 2010a) was used, as it is one of the more widely used packages with good documentation. edgeR uses a range of statistical techniques based on negative binomial distributions. Empirical Bayes estimation, exact tests, generalized linear models and quasi-likelihood tests are all included in the edgeR workflow.

3.3.7. Polymerase chain reaction

For a few selected samples, remaining cDNA libraries were tested for *Tas2r* expression by PCR. This was done retrospectively after counts from the RNA-seq data for *Tas2rs* were seen to be very low. JumpStart Taq ReadyMix (Sigma-Aldrich, UK) was used in a 25µL reaction with 0.25µL of each target primer at a concentration of 10µM, 2.0µL of the cDNA library and 10µL of nuclease free water (Qiagen, Germany). PCR was performed as previously described (Chapter 2). Primers for PCR were designed using Primer-BLAST (Ye *et al.*, 2012). Default parameters were used except for minimum product length, which was set to 500, and species, which was set to *Canis familiaris*. For each receptor sequence, the top-ranked primer set was chosen for synthesis by Eurofins Genomics (Ebersberg, Germany). Nucleotide sequences used for primer design are detailed in Appendix 1.1. Primer sequences are detailed in Table 3.3.

Table 3.3: dTas2r primer sequences and expected product length
All primer sets designed for PCR of Tas2rs from cDNA libraries generated by SMART-Seq amplification on dog taste papillae RNA.

Gene	Forward Primer	Reverse Primer	Tm (°C) f/r	Product length (bp)
d*Tas2r1*	ACTACTGTGCCAAGATCGCC	CGTGGAGGAGGAGCTTCTTT	59.3/59.3	573
d*Tas2r2*	CAACACCAGTGCAACTCCTT	ATTTGCCATGAAGGCAGCAA	57.3/55.3	632
d*Tas2r3*	TGGGTGCACTGCTCTTATCG	ACAGCACAGCATCTCCGTAA	59.3/57.3	500
d*Tas2r4*	GCTCAATGCCTTGTACTGCG	CCTGGAGGGTAAAAGCTGGA	59.3/59.3	519
d*Tas2r5*	GTTTGCCACTTTCCTCAGCG	TGGGATTCCCCAGGATCAGA	59.3/59.3	548
d*Tas2r7*	TTAATGCTCGTAGCAGCTGGA	GACAGCTTTCATGGCTCCCA	57.9/59.3	687
d*Tas2r10*	ACTGGAAGGCCTCCTCATTTT	GCTTCTGTACTGGGGTCTCG	57.9/61.4	657
d*Tas2r12*	GGCAGGCACAATGAAGAATGT	AGCCAGAGACACTGCAAAGG	57.9/59.3	589
d*Tas2r38*	TGTTGGCTCTGACTCCTGTT	TGCCCTTACCTTAAGGCTGC	57.3/59.3	965
d*Tas2r39*	CACCATTTGGCATCCTCTCG	GCTCTGATGGCCCCTATGTG	59.3/61.4	700
d*Tas2r40*	GAGCACAGATGCCACGGATA	ACTGAGTGGCTAGCTGGGTA	59.3/59.3	870
d*Tas2r41*	CTCCACTGGGACTTCCTGAAC	CAACAGAAGTAGCTGCCTGC	61.8/59.3	645
d*Tas2r42*	CAGAATCGCTCAGCTGTTGG	GTCTCAGCTTGCTGTTTCCC	59.3/59.3	713
d*Tas2r43*	TTGTGATGCTGTTGGGGTCT	AAGACACATGATGCTCCTCTTAT	57.3/57.1	548
d*Tas2r62*	TGGGCTCCCTGGTCTTAGTT	GAGCTTTCCAAAGCCTGGTC	59.3/59.3	504
d*Tas2r67*	GTGCTTCCACTGGGGTCTTT	TGCCACAGTAGACCTAACGC	59.3/59.3	503

The PCR conditions were optimised for each primer set using dog genomic DNA as template. Initially, all primer sets were tested with a standard 60°C annealing temperature. Any primer sets showing weak or no amplification were run as a gradient PCR with a range of annealing temperatures (50-60^{o}C). Annealing temperatures of 60°C were used, except with primers for d*Tas2r10* (50°C) and d*Tas2r42* (52°C). If any primer sets still failed to yield satisfactory results, the second primer set from the Primer-BLAST analysis was selected and tested in the same way.

PCR products were analysed using gel electrophoresis with one gel used for each sample. Gels were run as described in Chapter 2.

3.4. Results

3.4.1. Fungiform papillae biopsy

Fungiform papillae were easily identified on the anterior surface of the tongue in all dogs examined (Figure 3.7).

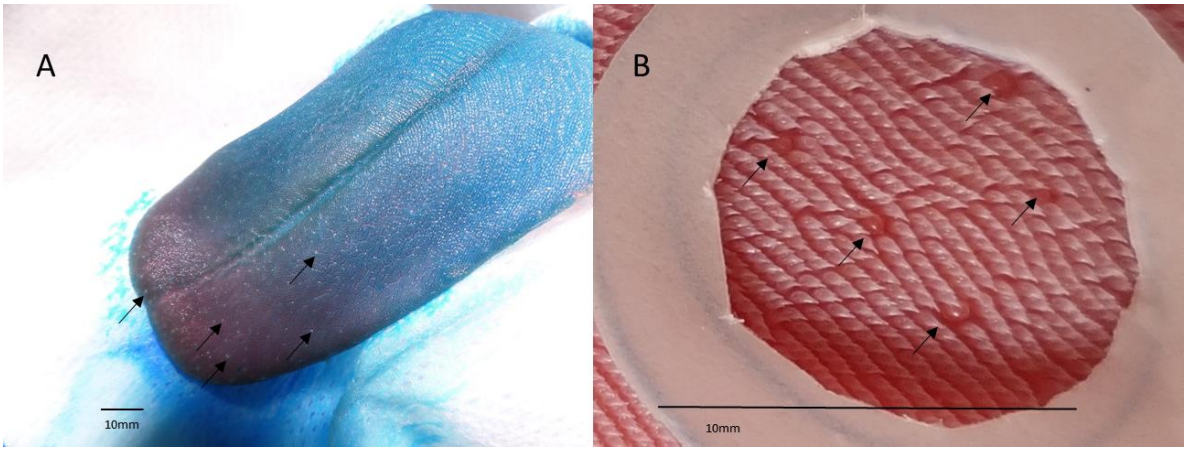

Figure 3.7: Fungiform papillae on the anterior portion of a dog tongue
A) The dogs tongue stained blue to highlight the papillae. Fungiform papillae are distributed evenly over the tongue dorsum with the exception of the tongue tip where the papillae are denser. Some individual papillae are indicated by arrows. B) Close-up of fungiform papillae on a dog's tongue. Fungiform papillae are indicated by arrows and are surrounded by non-gustatory filiform papillae.

Fungiform papillae were evenly distributed across the tongue with the exception of a higher concentration occurring at the tip. Papillae counts in the sampled areas are detailed in Table 3.4. The front location was not at the tip where the papillae were denser, but slightly back from the tip (Figure 3.3). The papillae at the tip were smaller and hard to sample. For dog LR05199, 2 papillae were collected from the back right location and were pooled into one sample tube. These were treated as one sample for further processing. For dog BE06022, a sample was not collected from the front left location, but two samples were collected from the middle left location. These samples were treated separately.

Table 3.4: Taste papillae counts and densities from dogs
Papillae were sampled from the rear, middle and front area of the anterior portion of the tongue.

Animal ID	Name	Position on tongue according to Figure 3.3	Papillae in 0.8cm^2 counting area (density /cm^2)	Papillae collected
LR05834	Womble	Back Left	6 (7.5)	1
		Back Right	5 (6.25)	1
		Middle Left	6 (7.5)	1
		Middle Right	5 (6.35)	1
		Front Left	2 (2.5)	1
		Front Right	6 (7.5)	1
LR05309	Keisha	Back Left	6 (7.5)	1
		Back Right	3 (3.75)	1
		Middle Left	3 (3.75)	1
		Middle Right	2 (2.5)	1
		Front Left	1 (1.25)	1
		Front Right	3 (3.75)	1
LR05199	Elliott	Back Left	4 (5)	1
		Back Right	5 (6.35)	2
		Middle Left	3 (3.75)	1
		Middle Right	4 (5)	1
		Front Left	4 (5)	1
		Front Right	3 (3.75)	1
BE06022	Dora	Back Left	10 (12.5)	1
		Back Right	2 (2.5)	1
		Middle Left	6 (7.5)	2
		Middle Right	3 (3.75)	1
		Front Left	4 (5)	0
		Front Right	2 (2.5)	1

BE06014	Dodger	Back Left	13 (16.25)	1
		Back Right	5 (6.35)	1
		Middle Left	6 (7.5)	1
		Middle Right	6 (7.5)	1
		Front Left	5 (6.35)	1
		Front Right	5 (6.35)	1

3.4.2. RNA extraction

Extracted RNA from each sampled papillae showed some variation across the 30 samples. Quantification and quality assessment of the RNA is summarised in Table 3.5. An RNA Integrity Number (RIN) is given by the bioanalyser. The RIN relates to the level of degradation the RNA has undergone, with 10 representing intact RNA and 1 being completely degraded RNA (Schroeder *et al.*, 2006). The impact of RNA integrity on downstream performance in various applications has been investigated. In qRT-PCR a RIN of >5 was found to be required (Fleige *et al.*, 2006) while for RNA-seq Shen (Shen *et al.*, 2018) found that samples with RIN values of >5.3 gave almost entirely equivalent results. At this point, two replicate sample IDs were created so that one sample might be used as a technical replicate. Sample BE06022_6 was used and 3 independent cDNA libraries were prepared from this sample. The sample IDs BE06022_7 and BE06022_8 appear in Table 4.5 for reference only, the RNA sample was not tested 3 times on the bioanalyser.

Table 3.5: Quality and quantity of RNA extracted from dog fungiform papillae
Assessment using a Bioanalyzer and the RNA 6000 Pico Kit (Agilent, UK).

Sample ID	Animal ID	Name	Position on tongue according to Figure 4.3	Concentration (pg/μL)	RNA Integrity Number (RIN)	Total RNA (ng)
BE06014_1	BE06014	Dodger	L-Front	3946.71	7.4	39.47
BE06014_2			R-Front	1129.99	7.9	11.30
BE06014_3			L-Middle	7180.51	7.1	71.81
BE06014_4			R-Middle	2222.86	7.6	22.23
BE06014_5			L-Back	11968.64	5.9	119.69
BE06014_6			R-Back	1512.12	6.6	15.12
BE06022_1	BE06022	Dora	R-Front	41034.28	6.7	410.34
BE06022_2			L-Middle	654.49	8.5	6.54
BE06022_3			L-Middle	4433.50	8.2	44.34
BE06022_4			R-Middle	5060.85	8.2	50.61
BE06022_5			L-Back	3385.77	7.9	33.86
BE06022_6			R-Back	5356.78	8.2	53.57
BE06022_7			R-Back	5356.78	8.2	53.57
BE06022_8			R-Back	5356.78	8.2	53.57
LR05199_1	LR05199	Elliott	L-Front	6646.35	4.8	66.46
LR05199_2			R-Front	2234.28	7.3	22.34
LR05199_3			L-Middle	3390.72	7.0	33.91
LR05199_4			R-Middle	36372.18	5.3	363.72
LR05199_5			L-Back	16806.83	7.3	168.07
LR05199_6			R-Back	2246.31	7.0	22.46
LR05309_1	LR05309	Keisha	L-Front	1287.58	7.9	12.88
LR05309_2			R-Front	433.98	7.8	4.34
LR05309_3			L-Middle	543.16	8.3	5.43
LR05309_4			R-Middle	8588.27	7.2	85.88
LR05309_5			L-Back	1480.12	8.3	14.80
LR05309_6			R-Back	2974.08	8.3	29.74
LR05834_1	LR05834	Womble	L-Front	8006.17	7.0	80.06
LR05834_2			R-Front	12925.84	7.2	129.26
LR05834_3			L-Middle	92.45	1.0	0.92

LR05834_4			R-Middle	2083.39	7.3	20.83
LR05834_5			L-Back	6847.27	7.1	68.47
LR05834_6			R-Back	935.81	7.4	9.36
LR1534_1	LR1534	Spike	Kidney	2413.00	6.9	>1000
DIEC_1	DIEC	-	DIEC RNA	2632.23	7.5	26.32

The amount of RNA recovered varied from 4.34 to ~410ng. The Middle Left sample for LR05834 could not be recovered from the RNALater as it could not be seen and so this sample is essentially a blank, meaning the observed concentration of 92.45pg/µl is no more than a background reading for the quantification technique. The RIN for this sample was very low at 1 showing the absence of any significant amount of intact RNA. Generally RIN values were above 7 for most other samples, indicating high levels of RNA integrity. However, given that samples were submerged in RNALater immediately after collection and that the samples are small and therefore the RNALater solution should saturate the tissue quickly, a higher RIN might have been expected. All but two of the samples still exceeded the RIN value of 5.3 determined to give equivalent results (Shen *et al.*, 2018) and all samples still warranted testing despite the slightly lower than expected RINs.

In addition to the papillae samples, two other RNA samples were included as controls. The purpose of these samples was to allow some perspective to be seen when comparing samples with techniques such as PCA. One RNA sample from an immortalised Dog Intestinal Epithelial Cell line (DIEC) and one sample from dog kidney were included in the analysis. The dog kidney sample was collected from a dog at Waltham which was euthanised due to unrelated health reasons in accordance with the Mars policy on the ethical treatment of animals.

3.4.3. RNA amplification

The performance of the SMART-Seq protocol was assessed by testing the samples with the Agilent High Sensitivity DNA kit (Agilent, UK). Guidelines for the expected results are given as part of the SMART-Seq manufacturer's protocol. Successful cDNA

synthesis should yield no product in the negative control and a peak centred at around ~2500bp for the RNA samples (Figure 3.8).

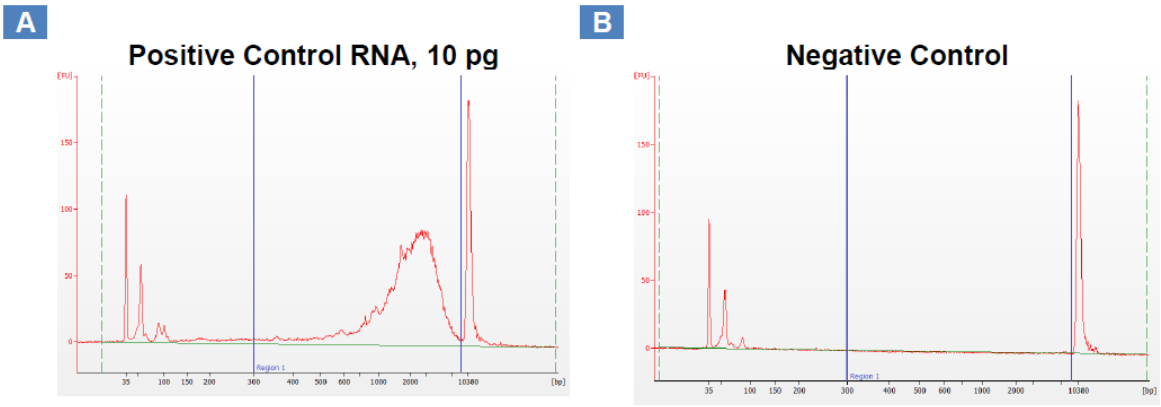

Figure 3.8: Expected results for A) positive and B) negative control samples following cDNA synthesis and amplification with the SMART-Seq® v4 Ultra® Low Input RNA Kit for Sequencing
(reproduced from the SMART-Seq® v4 Ultra® Low Input RNA Kit for Sequencing User Manual).

Results for the samples are collated in Figure 3.9. Sample LR05834_3 was the sample where no taste papillae were recovered from the RNALater solution, and so was effectively a negative control. Other negative controls were run for every run of the SMART-Seq protocol and in all cases there was no visible cDNA peak in the electropherogram (data not shown). All samples gave a peak within the expected range. Samples with lower RIN numbers tended to give poorer results, with a peak covering a larger range of smaller fragments.

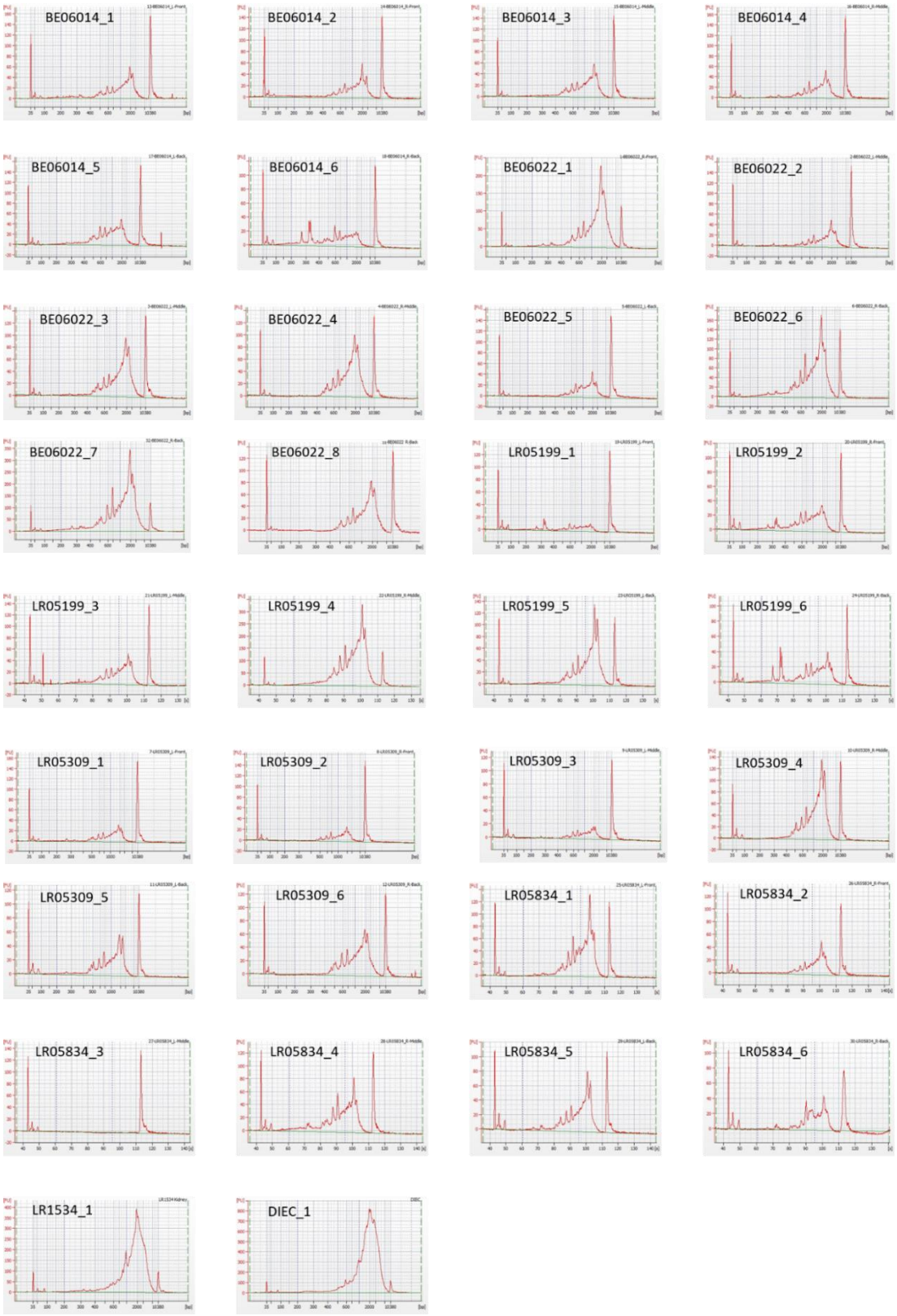

Figure 3.9: Electropherograms for all cDNA samples prepared with the SMART-Seq® v4 Ultra® Low Input RNA Kit for Sequencing
(see Table 3.5 for sample annotation).

Samples BE06022_6, BE06022_7 and BE06022_8 represent technical replicates and were all prepared from the same starting RNA sample. These were intended to detect any variation introduced as part of the SMART-Seq amplification and the RNA-seq library preparation and sequencing.

3.4.4. RNA sequencing

3.4.4.1. Sequencing library preparation

Sequencing libraries were prepared using the Illumina Nextera XT kit (Illumina, UK) by the DeepSeq sequencing facility at the University of Nottingham. The recommended 150pg of input cDNA was used with 12 PCR cycles. Superior tagmentation was observed with the Nextera XT kit as opposed to the Nextera Flex kit in a preliminary test, therefore the Nextera XT kit was used for all samples.

3.4.4.2. Sequencing

QC steps to remove sequencing adapters and poor quality reads, sequence alignment and read counting were performed before some basic sequence quality measures were calculated using the MultiQC package (Ewels *et al.*, 2016). The mean quality values for each base position in the read for each sample were plotted (Figure 3.10).

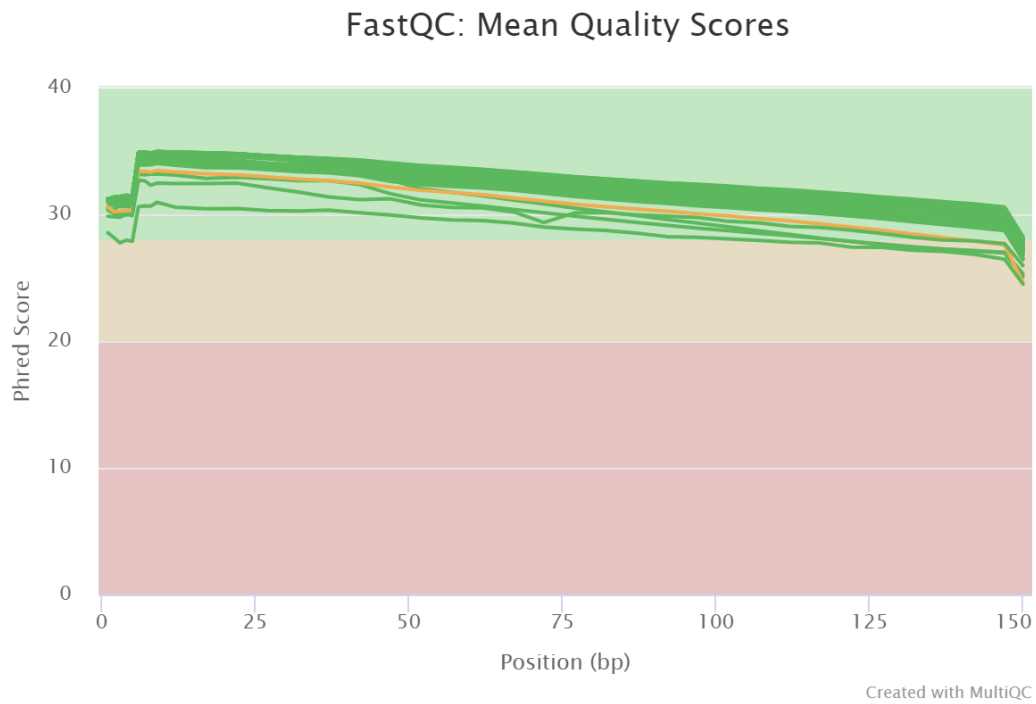

Figure 3.10: Sequencing quality (Phred score) for each base position in the read for each of the 34 samples tested
The y-axis on the graph shows the quality scores. The higher the score, the better the base call. The background of the graph divides the y axis into very good quality calls (green), calls of reasonable quality (orange), and calls of poor quality (red).

All the sequencing was of good or reasonable quality. One sample (LR05834_4_S21 reverse read) highlighted in orange was flagged with a warning as the quality degraded over the run slightly more than the others, but generally all data was good.

The STAR-based pipeline produced summary count information for all samples. A summary of the alignment output is shown in Table 3.6. A suffix was added to the sample IDs to aid with data processing.

Table 3.6: Summary of alignment output after alignment with STAR

Sample Name	% Proper Pairs	% Aligned	Aligned (Millions)	Seqs (Millions)
BE06014-1_S5	63.90%	72.20%	33.2	46.3
BE06014-2_S6	67.00%	75.80%	36.5	48.3
BE06014-3_S7	66.20%	74.80%	37.7	50.6
BE06014-4_S8	61.90%	70.90%	38.8	55
BE06014-5_S9	61.10%	72.40%	37.6	52.2
BE06014-6_S10	38.60%	53.60%	25	46.9
BE06022-1_S1	69.10%	76.90%	35.3	46.1
BE06022-2_S12	70.30%	73.80%	41.4	56.4
BE06022-3_S23	69.50%	75.90%	38	50.3
BE06022-4_S29	71.40%	77.80%	38.4	49.6
BE06022-5_S30	63.00%	72.80%	37.5	51.7
BE06022-6_S31	69.40%	74.40%	37.9	51.2
BE06022-7_S26	71.60%	73.00%	41	56.7
BE06022-8_S27	72.40%	77.50%	38.4	49.8
LR05199-1_S11	43.50%	58.20%	25.2	43.7
LR05199-2_S13	53.90%	68.50%	30.8	45.2
LR05199-3_S14	60.70%	72.80%	36.4	50.2
LR05199-4_S15	67.70%	75.80%	38.5	51.1
LR05199-5_S16	69.60%	76.80%	37.8	49.4
LR05199-6_S17	48.20%	61.10%	26.9	44.3
LR05309-1_S32	64.40%	73.60%	33	45
LR05309-2_S33	67.10%	68.80%	39	57
LR05309-3_S34	63.00%	66.50%	32.7	49.4
LR05309-4_S2	68.90%	75.50%	41.7	55.4
LR05309-5_S3	63.60%	72.90%	36.8	50.6
LR05309-6_S4	71.40%	75.80%	39.3	52.1
LR05834-1_S18	67.70%	74.40%	29.9	40.5
LR05834-2_S19	72.50%	77.60%	29.8	38.7
LR05834-3_S20	36.20%	0.90%	0.1	6.4
LR05834-4_S21	66.10%	72.70%	20.7	28.6
LR05834-5_S22	66.40%	75.30%	34.9	46.4
LR05834-6_S24	64.40%	73.00%	34.6	47.6

LR1534-1_S28	88.50%	87.30%	35.9	41.4
DIEC-1_S25	88.20%	87.80%	36.3	41.5

The target level of 40 million reads per sample was exceeded in all but one case, LR05834_4 where only 28.6 million reads were generated. Sample LR05834_3 did generate some reads despite being a negative sample, however few of them mapped to the genome. There is some relationship with samples that performed less-well here and the quality of the cDNA assessed on the electropherogram shown in Figure 4.9. The two worst-performing samples in terms of % Reads mapped in proper pairs were BE06014_6 and LR05199_1. These also had some of the worst cDNA electropherogram traces in terms of smaller fragments and lower RIN values of 6.6 and 4.8, respectively. However, RIN value did not seem to be a reliable indicator of performance as two other samples, BE06014_5 and LR05199_4 with RINs of 5.9 and 5.3, respectively, gave typical-looking electropherogram traces with no obvious signs of increased presence of smaller fragments. Samples which had lower amounts of cDNA, but no evidence of smaller fragments in the electropherogram like LR05309_1, LR05309_2 and LR05309_3 gave good sequencing results, indicating that QC of the samples and normalisation of the amount of cDNA added to the sequencing library preparation was successful.

Read counting with featureCounts also produced summary information as shown in Figure 3.11. Approximately 50% of the reads were assigned to a feature. This figure is lower than the % Uniquely mapped reads figure from STAR alignment to the genome and this represents the difference between reads mapping to the whole genome and reads mapping to a genetic feature annotated in the gene transfer format (.gtf) file.

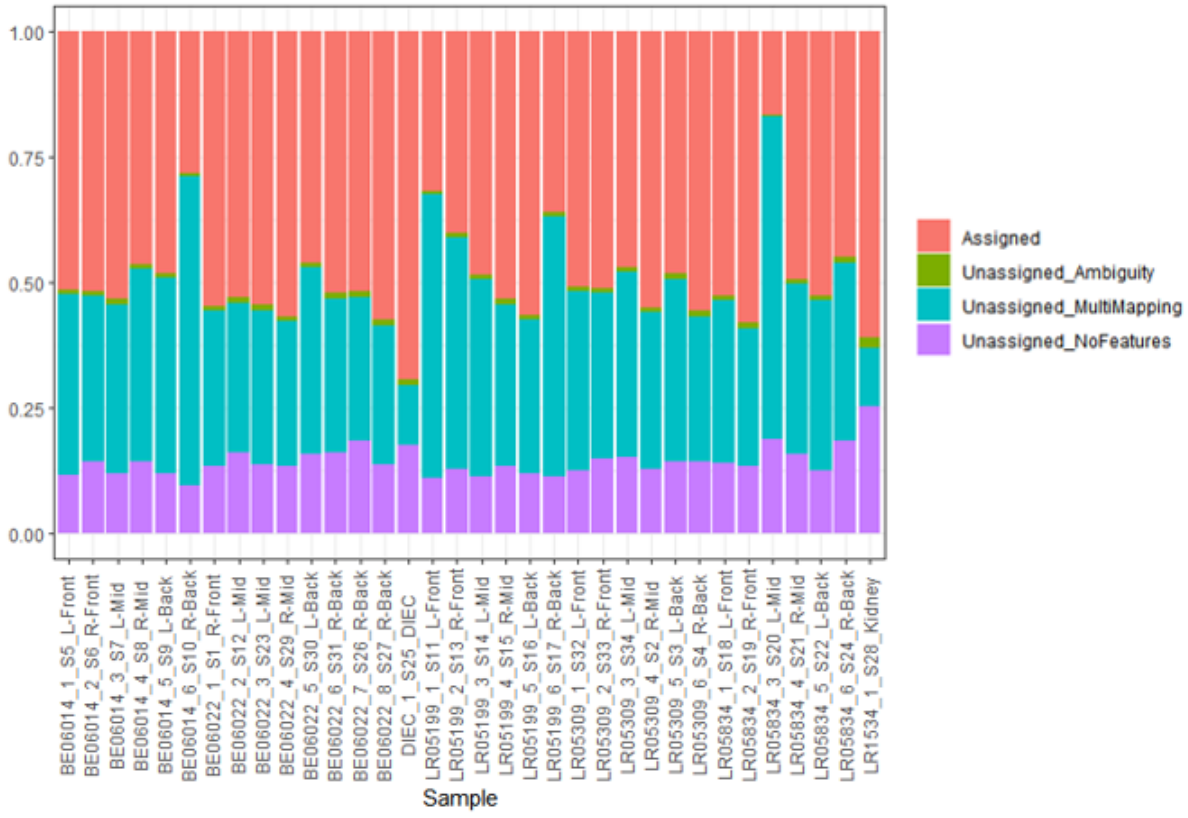

Figure 3.11: Summary counting information for RNA-seq data from dog fungiform papillae generated by featureCounts
Assigned reads were generally over 50%. Multi-mapping reads were the largest source of unassigned reads. Reads having no features to map to constituted approximately 20%.

3.4.4.3. Analysis with edgeR

Raw read counts from featureCounts were used as input for expression analysis with edgeR. In order to examine the relationship between samples taken from different areas on the tongue, a PCA was performed on the data. PCA reduces the dimensionality of the data to a number of Principal Components (PCs). PC1 represents the direction that maximises the variance of the data, while subsequent PCs represent the direction with the next highest variance, orthogonal to the previous PC. Counts were log transformed and 1 was added to all values to avoid log transforming zeros. Also genes that had the same expression in every sample were removed. To label the PCA points, the suffix identifier for each sample was used. The PCA including the DIEC, kidney and negative samples is shown in Figure 3.12. A scree

plot is included in the Figure to show the contributions of the different principle components. In this case, PC1 explained a large proportion of the variance due to the inclusion of the negative sample.

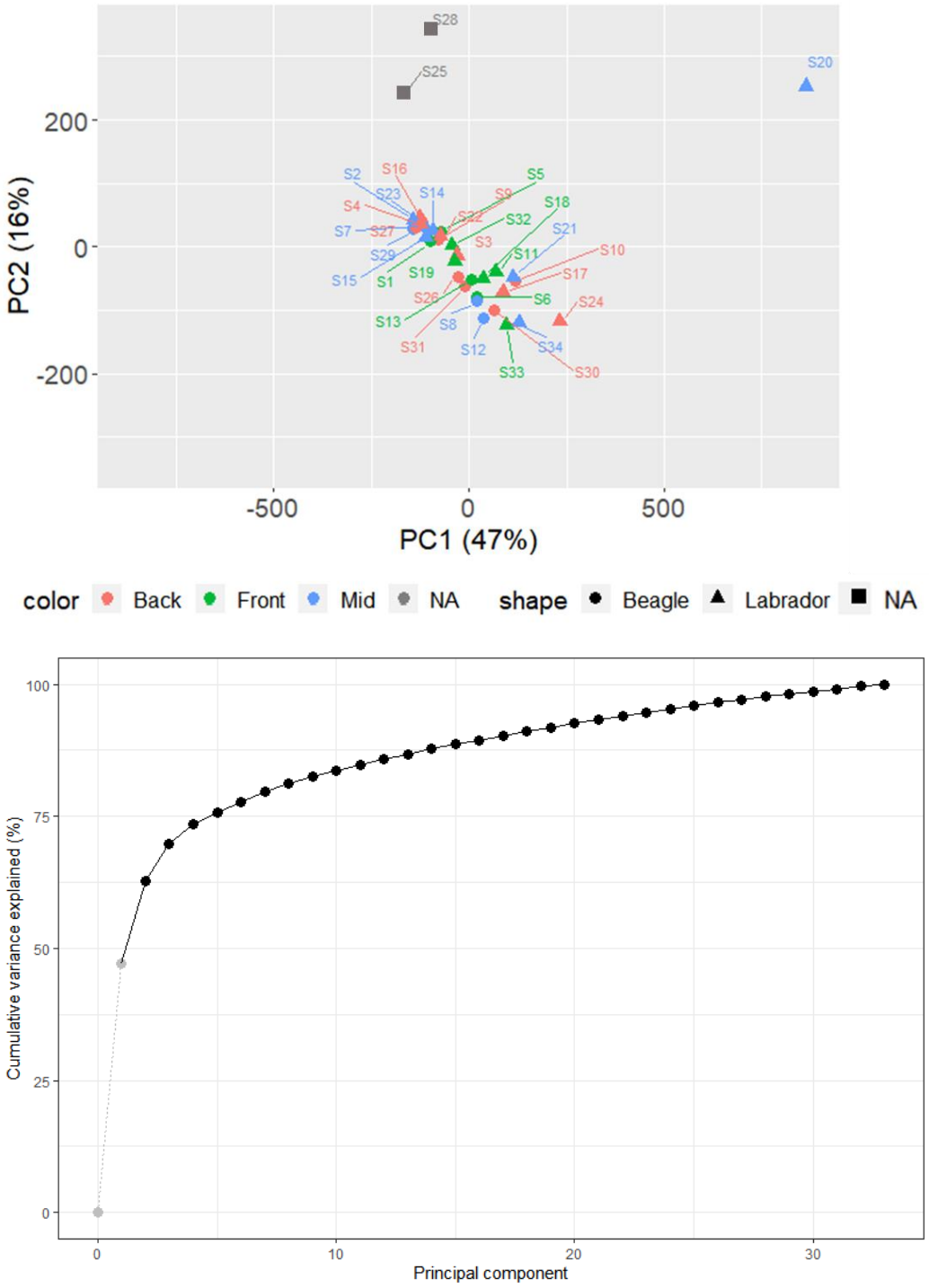

Figure 3.12: PCA analysis of gene expression in the fungiform papillae samples
Outlying samples S20=Negative sample, S28=Kidney tissue, S25=DIEC sample. Most variation was described by PC1.

To make the analysis clearer, the three outlying samples for DIEC, kidney and the negative sample were excluded. The re-run analysis is shown in Figure 3.13.

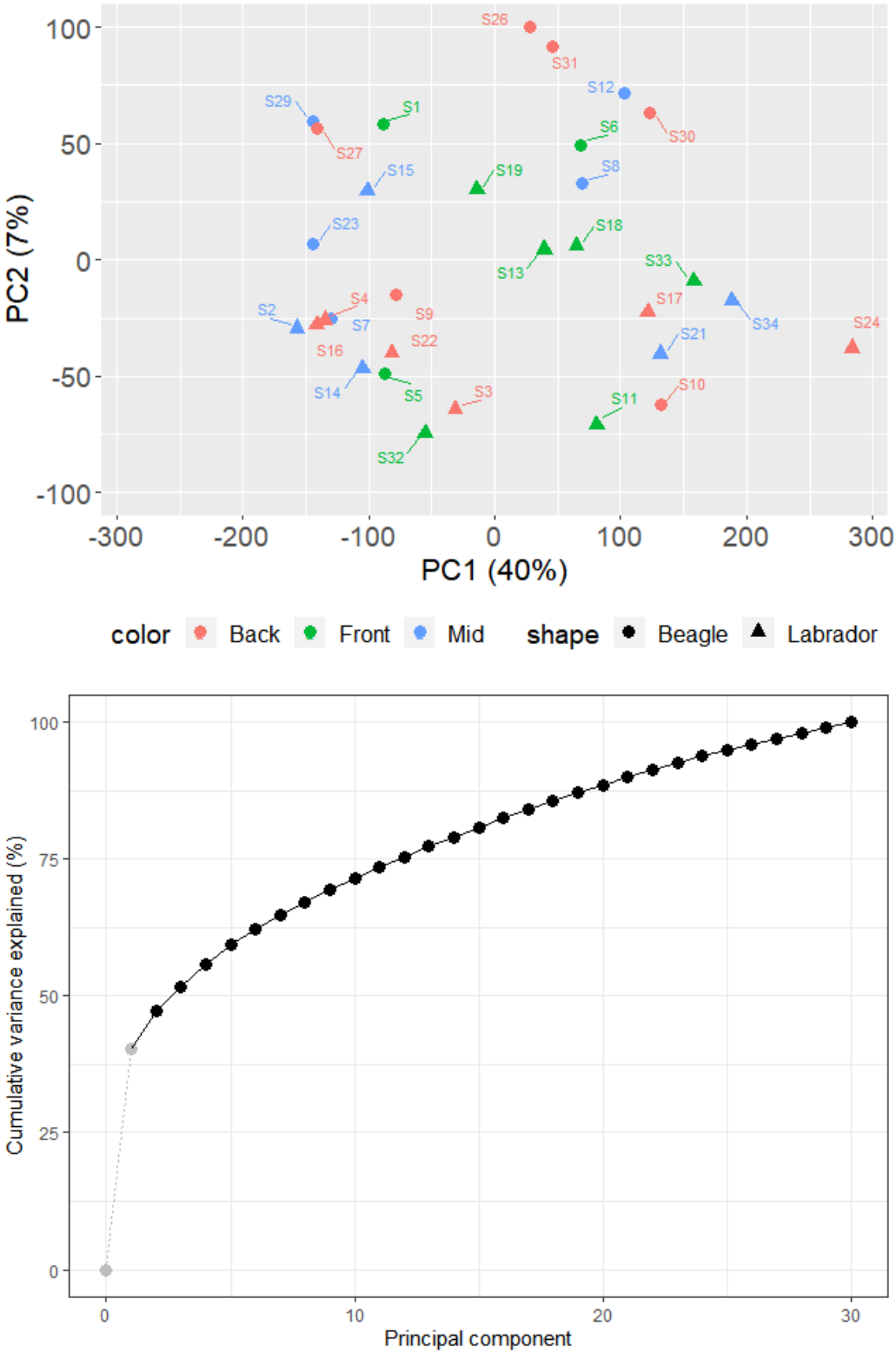

Figure 3.13: PCA analysis of gene expression in the fungiform papillae samples with DIEC, kidney and negative samples excluded
No particular pattern can be observed either by breed or location. Technical replicate samples S26, S27 and S31 were not identical.

There appeared to be no particular pattern in the data based on either location of the sample or on dog breed. PC1 and PC2 explained just under 50% of the variance in the data with subsequent PCs only accounting for small increases, meaning examination of further PCs was not necessary. Of the three technical replicate samples, two were grouped closely together (BE06022_6_S31 and BE06022_7_S26) while the third (BE06022_8_S27) was separated mostly along the PC1 axis. Given this discrepancy for the technical replicates we decided not to pool the three replicate samples for downstream analysis. This is recommended if the replicate samples can be verified to have near identical gene expression values, as the low variance between these samples can bias downstream analysis.

The next step in edgeR analysis was to filter the data and estimate the dispersion in the data. Estimates of dispersion are an important factor in RNA-seq analysis, as they are equivalent to estimating the variance relative to the mean. An underestimation of dispersion might give false positive results, indicating a gene is differentially expressed when in fact it is not. Overestimating dispersion can give the opposite effect and result in false negatives (Landau *et al.*, 2013). Data were filtered using a cpm threshold of >0.1. A gene was required to be expressed in at least 7 samples from a group which, given that the smallest group size was 9, allowed for a couple of samples in each group to be negative for expression and still retain that gene in the analysis. Normal variance or "dispersion" in the data was estimated for each gene (tagwise dispersion) and also estimated based on the assumption that dispersion is proportional to the mean, so that the biological coefficient of variation is constant (common dispersion). Also the relationship of the dispersion to the mean, assuming that the dispersion is the same for all genes with a certain mean expression (trended dispersion) was empirically estimated. The results of this analysis are shown in Figure 3.14.

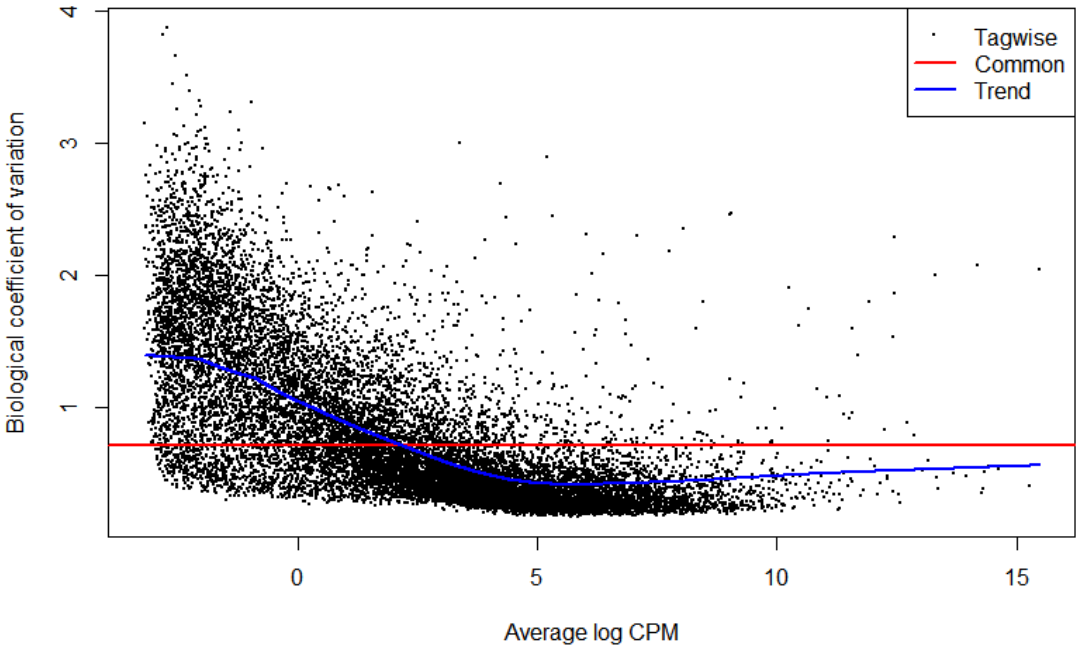

Figure 3.14: Dispersion estimates for the filtered RNA-seq data
Tagwise, Trend and Common dispersion are shown. Common dispersion was higher than expected, possibly due to the heterogeneous nature of the bulk tissue samples used.

The common dispersion estimate was relatively high when compared to the example value of 0.4 for human data given in the edgeR user's manual. This may be because of the nature of the samples, which are composed of a mixture of cell types. Each papillae may contain Tas2r-expressing cells or may not and some might contain cells expressing different repertoires of Tas2rs. There may be other cell-types in the samples that are also more or less represented in different samples. The high common dispersion may be related to these differences and is unavoidable in samples of mixed cell types.

For differential gene expression analysis the contrast for the data was set as "locationBack – locationFront". The models used in edgeR are generalised linear models, and to account for uncertainty in gene-wise estimates of dispersion, a Quasi-likelihood approach was used. The resulting gene expression differences are presented in the heatmap in Figure 3.15. The genes listed here are the top 20 genes for differential expression between the back and front sample groups. Expression

differences were log transformed before plotting and scaled by row to allow patterns for particular genes to be compared.

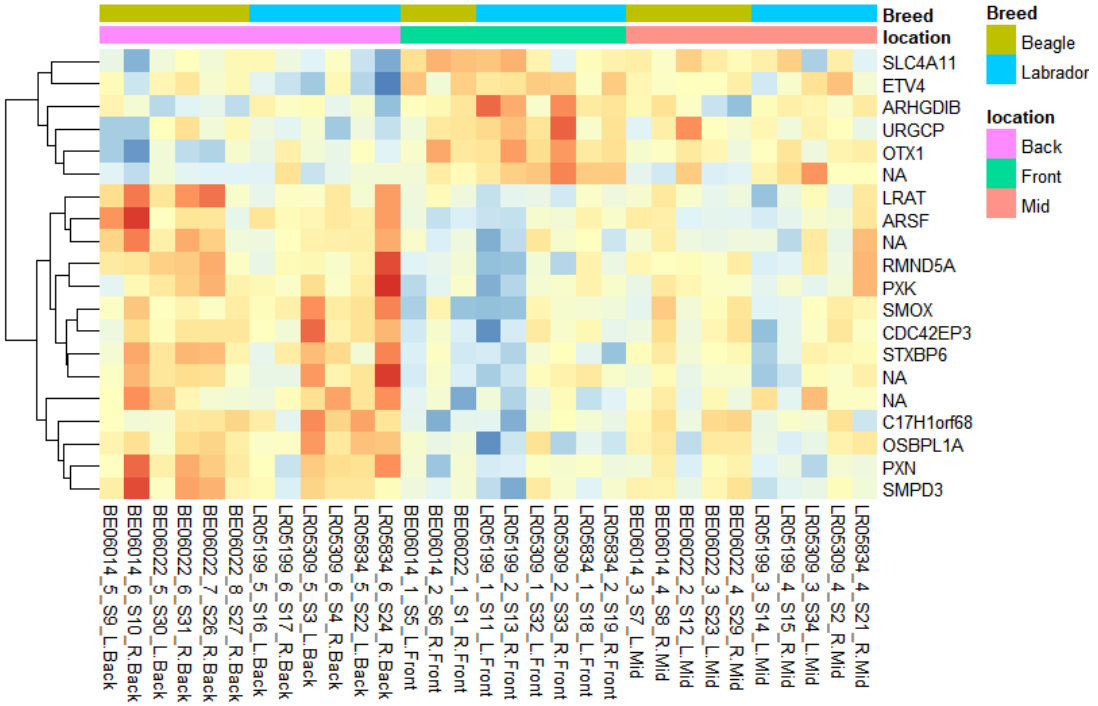

Figure 3.15: Heatmap of differential expression for the top 20 genes based on *p*-values and False Discovery Rate (FDR)
Ensembl gene names are shown on the right where NA refers to an unannotated feature. Data is log transformed and scaled by row.

Next the results were filtered based on the FDR and the fold change (FC). The FDR threshold was set at 0.05 and the FC threshold set at 2. It is important to note that genes meeting these targets should be considered targets for further validation, rather than definitive results. Differential expression data meeting these criteria were visualised using a smear plot (Figure 3.16). Differentially expressed genes are highlighted in red based on their FDR. The fold change is highlighted by the dashed lines that represent a logFC of 1 (or a FC of 2).

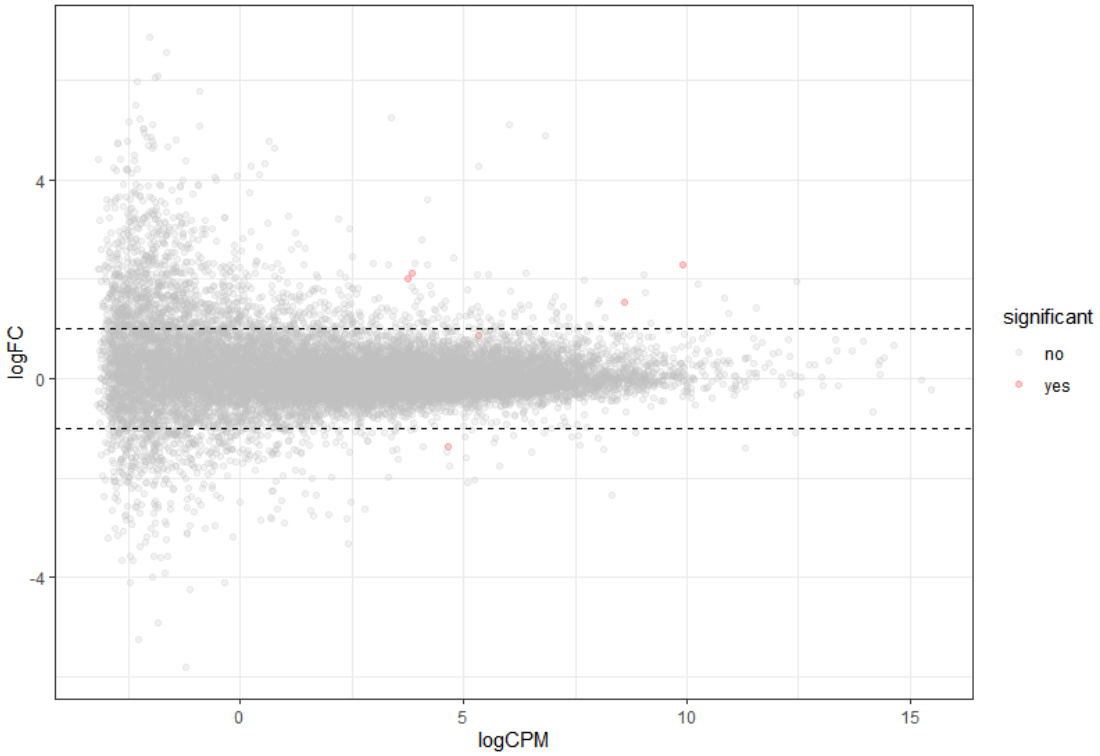

Figure 3.16: Smear plot to show differentially expressed genes
Genes in relation to expression level with an FDR of at least 0.05 (highlighted in red) and a fold change of at least 2 (points falling outside the dashed lines).

While there were many genes exceeding the 2 fold change threshold only a few also met the FDR threshold. In total, only 5 genes met both criteria. Another way in which the data were visualised was with a volcano plot. The volcano plot uses only FC and FDR and can make it easier to see all the significant genes (Figure 3.17).

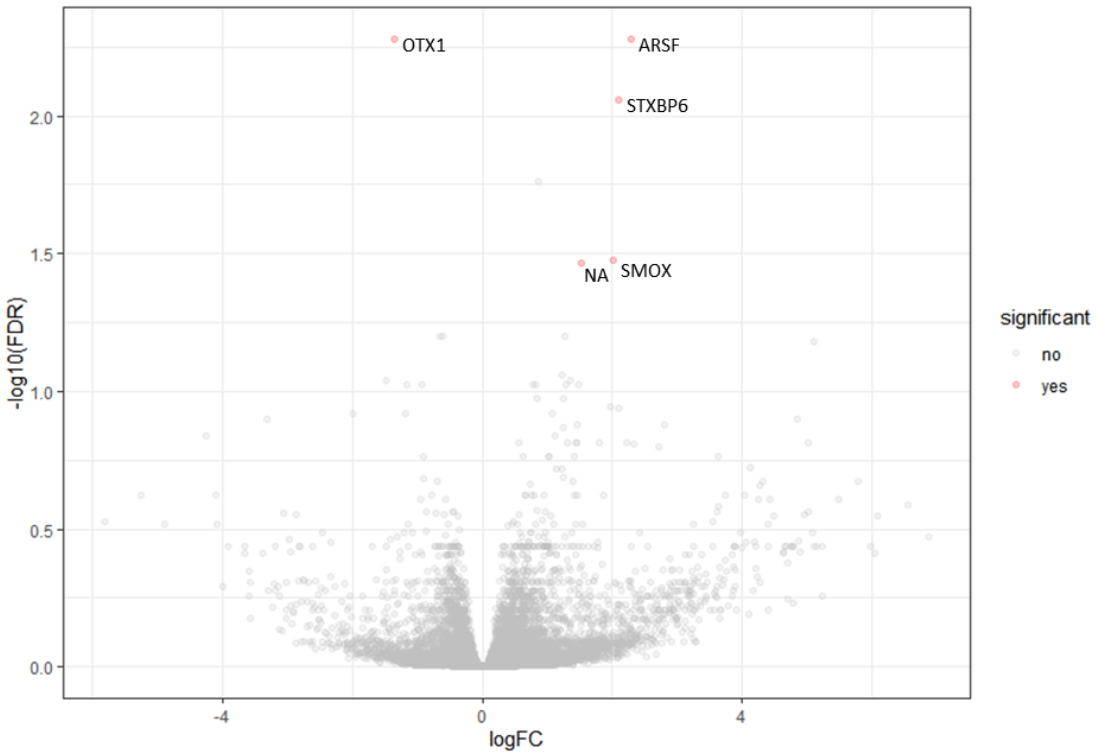

Figure 3.17: Volcano plot of log fold change (logFC) plotted on a log scale against – log10 false discovery rate (-log10(FDR))
Genes meeting the threshold criteria of 2 for fold change and 0.05 for FDR are highlighted as significant.

Only 4 genes (*Otx1, Arsf, Stxbp6* and *Smox*) and one unannotated sequence met the criteria for significance in both FC and FDR. *Otx1* was downregulated in the samples from the back locations compared to the front samples while the other 4 sequences were upregulated in the back samples. The code used to run the edgeR analysis is shown in Appendix 3.1.

It should be noted that 5 differentially expressed sequences in this case is a very small number, indicating that in many ways our samples were similar in their expression profiles. This is not surprising given the very low occurrence of taste receptor cells in the samples, however, further analysis specifically focussed on the Tas2rs was attempted.

3.4.5. Analysis of *Tas2r* gene expression

The original hypothesis for this experiment was that *Tas2r* genes would be differentially expressed in the samples from the different locations on the tongue. The data can therefore be examined in this instance without correcting for multiple testing, as is usually done as part of the edgeR workflow.

Firstly the read counts from both the STAR/featureCounts and kallisto alignments were compared using the standard *Tas2r* annotation from the canine reference genome (CanFam 3.1). Only 10 *Tas2rs* are annotated in the reference genome sequence. The read counts obtained from the two methods were almost identical, differing by at most 1-2 reads, or in one case 4 reads for a sample with 60 or 64 reads for d*Tas2r40*. Reads from kallisto are referred to as read estimates due to the nature of the pseudoalignment method used. In some cases, a read count of 1 was shown with one method while the other method showed 0 reads. This was evident 4 times overall, twice where kallisto showed a read, but STAR/featureCounts did not, and twice with the difference in the other direction. These minor differences showed that in the vast majority of cases both workflows were aligning the same reads to the same loci and that neither workflow was introducing any significant bias in the analysis.

Of the 10 annotated d*Tas2rs*, 9 were detected in at least one sample. Only d*Tas2r1* had 0 read counts in all samples. Counts ranged between 1 and 64 indicating that in all cases the *Tas2r* transcript was present only at very low levels. This was expected given the nature of the samples used. Some samples had counts recorded for only one *Tas2r*, while the sample with the most *Tas2rs* detected was LR05199_5_S16 with 6 *Tas2rs* showing at least 1 count.

The kallisto and edgeR analysis was then repeated using reference files containing the coordinates of all 16 identified dog *Tas2rs*. Results for this analysis showed counts for some of the unannotated *Tas2rs* and again, differences between the two workflows were minimal. Counts ranged between 1 and 68 and the sample with the

most *Tas2rs* detected was BE06022_4_S29 with 9 of the 16 *Tas2rs* detected. All *Tas2rs* were detected in at least one sample, with the exception of d*Tas2r1*. The receptor that was detected in the most papillae samples was d*Tas2r62*, being present in 18 samples. The next most prevalent receptor in the papillae samples was d*Tas2r42*, which was detected in 16 papillae, and also in the kidney and DIEC samples.

These comparisons showed that both methods were producing almost identical read counts. However, there was some small variation, usually not more than one or two counts in either direction. In addition to this, the count levels were very low and warranted confirmation with another independent method. PCR was carried out for all d*Tas2rs* on the cDNA libraries prepared with the SMART-Seq method. A PCR for β-actin was included as a control with high count levels in the RNA-seq data. This would confirm the validity of the RNA-seq counts and show what might be a reasonable minimum count cut-off to use. The sample that was used to produce three replicate cDNA libraries was chosen for this. This was because the count data for these replicates did not match entirely, which might indicate unreliable assignment of read counts or some other factor. The PCR data is shown in Figure 3.18.

BE06022_6_S31_R-Back

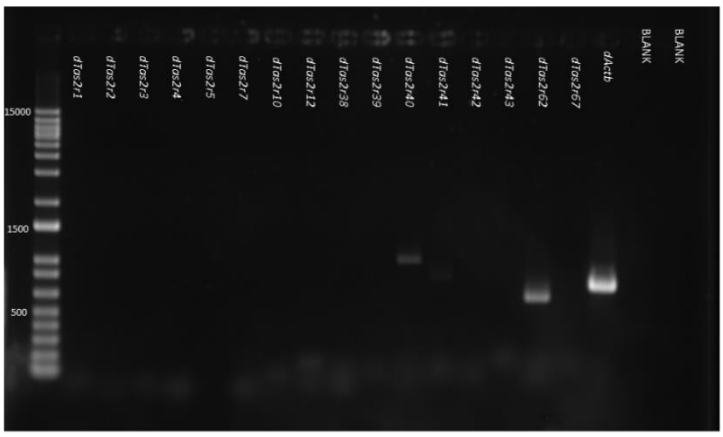

	S31 BE06022_6_S31_R-Back
target_id	est_counts
Tas2r1	0
Tas2r2	0
Tas2r3	0
Tas2r4	0
Tas2r5	0
Tas2r7	0
Tas2r10	0
Tas2r12	0
Tas2r38	0
Tas2r39	0
Tas2r40	6
Tas2r41	11
Tas2r42	2
Tas2r43	1
Tas2r62	9
Tas2r67	0
Actb	56316

BE06022_7_S26_R-Back

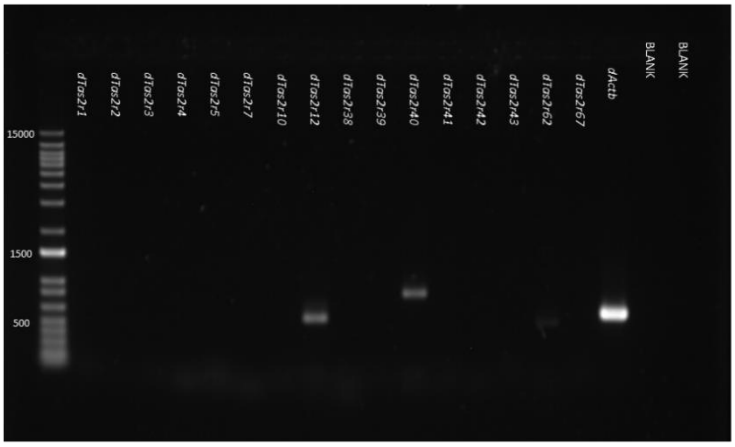

	S26 BE06022_7_S26_R-Back
target_id	est_counts
Tas2r1	0
Tas2r2	1
Tas2r3	0
Tas2r4	0
Tas2r5	0
Tas2r7	0
Tas2r10	0
Tas2r12	4
Tas2r38	0
Tas2r39	0
Tas2r40	10
Tas2r41	2
Tas2r42	2
Tas2r43	0
Tas2r62	20
Tas2r67	0
Actb	70073

BE06022_8_S27_R-Back

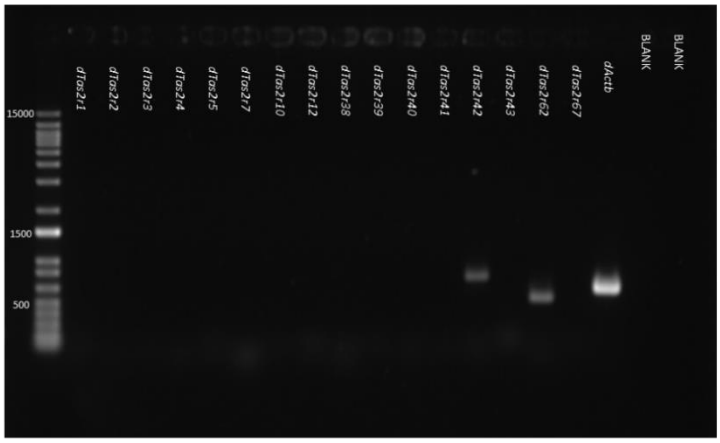

	S27 BE06022_8_S27_R-Back
target_id	est_counts
Tas2r1	0
Tas2r2	24
Tas2r3	0
Tas2r4	0
Tas2r5	0
Tas2r7	0
Tas2r10	6
Tas2r12	0
Tas2r38	0
Tas2r39	0
Tas2r40	0
Tas2r41	0
Tas2r42	13
Tas2r43	0
Tas2r62	11
Tas2r67	7
Actb	96111

Figure 3.18: PCR results for all d*Tas2rs* from the three replicate cDNA libraries made from the same RNA sample

Corresponding count data from the kallisto workflow is shown on the right. Counts that were confirmed by a visible band in the PCR are highlighted in blue.

The PCR analysis revealed some interesting aspects of the data. With one exception every read count ≥10 was matched with a visible band in the PCR. Only the count of 24 reads for d*Tas2r2* in sample BE06022_8_S27 was not confirmed by the PCR. Counts of <10 reads were more variable. Two counts of 6 reads for d*Tas2r10* and 7 reads for d*Tas2r67* in sample BE06022_8_S27 were not confirmed by the PCR. However, a count of 4 for d*Tas2r12* in sample BE06022_7_S26 and counts of 6 reads for d*Tas2r40* and 9 reads for d*Tas2r62* in sample BE06022_6_S31 were confirmed. Low counts of 1-2 reads were not supported by the PCR data in any case.

The same PCR analysis was repeated for the sample showing the highest number of *Tas2rs* expressed, sample BE06022_4_S29 with 9 of the 16 *Tas2rs* detected. Results for this sample are shown in Figure 3.19.

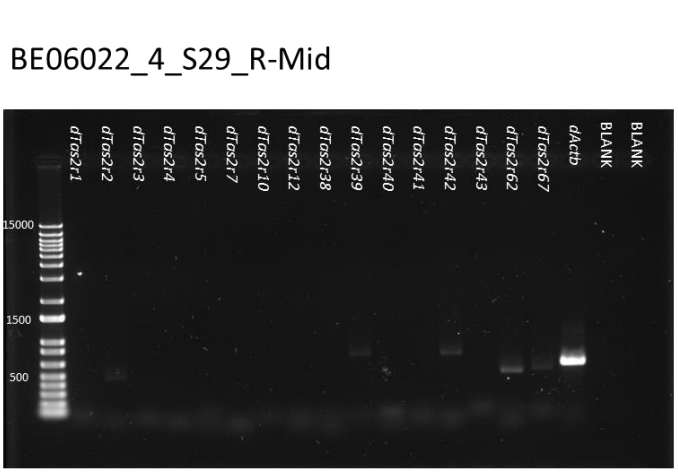

	S29
	BE06022_4_S29_R-Mid
target_id	est_counts
Tas2r1	0
Tas2r2	14
Tas2r3	0
Tas2r4	10
Tas2r5	6
Tas2r7	0
Tas2r10	0
Tas2r12	0
Tas2r38	0
Tas2r39	4
Tas2r40	1
Tas2r41	0
Tas2r42	11
Tas2r43	6
Tas2r62	9
Tas2r67	15
Actb	89535

Figure 3.19: PCR results for the papillae sample found to express the highest number of d*Tas2rs*
Higher counts were confirmed with a positive result in the PCR. Generally, counts of ≥10 were confirmed although d*Tas2r4* was an exception in this sample.

With this sample there was also one exception to the confirmation of counts ≥10. For d*Tas2r4* a read count of 10 was not confirmed by the PCR analysis, but all other counts ≥10 were, along with some counts of <10.

Combined, these data provided good evidence that a minimum cut-off value of ≥10 read counts was appropriate. Counts lower than this may still be real, but were not consistently confirmed by the PCR analysis.

The other most notable insight from the data is that the 3 cDNA libraries prepared from the same RNA sample did not give identical results in either the RNA-seq or the PCR analysis. This is likely to be due to the very low amounts of template present in the original sample. The SMART-Seq protocol uses a limited number of PCR cycles to amplify poly-A tailed mRNA molecules. This is unlikely to be biased to any particular mRNA, but when template targets are very low (<10 copies), amplification can become unreliable as the chances of template amplifying at the start of each cycle is limited by the low numbers of template molecules. This is a well-known phenomenon in PCR and is referred to as the "Monte Carlo" effect (Bustin *et al.*, 2004). This also has implications for how the data may be used. While the detection of the transcripts must represent the detection of molecules that were present in the original RNA sample, such low levels result in quantification that is unlikely to be reliable. The data was treated accordingly in the downstream analyses, favouring the comparison between presence and absence rather than quantification and setting a threshold of 10 counts for classification as present.

The two non-papillae samples that were analysed in the RNA-seq experiment both showed expression of some d*Tas2rs*. This was not entirely unexpected as it has been shown that *Tas2rs* are expressed in many different tissues in mammals, including the kidney and the small and large intestine (Finger *et al.*, 2011; Uhlen *et al.*, 2015). The counts from these samples were similar to those of the papillae samples, indicating low levels of expression in these samples also. For the DIEC cells that were tested, *Tas2r* expression must be very low indeed as this is not a mixed cell sample as is the case for the taste papillae, all cells should have the same, or similar expression profiles.

Raw read counts are normalised as part of the edgeR analysis to account for differences in library size between samples. Many different strategies for

normalisation have been used, however, performance is not always equivalent (Dillies *et al.*, 2013). In edgeR, the method used is the Trimmed Mean of M-values (TMM) (Robinson *et al.*, 2010b). It is based on the assumption that most genes are not differentially expressed. Correction factors are applied to library sizes and then re-scaled. Read counts are then adjusted by dividing by the re-scaled normalisation factors. The resulting TMM values are the transformed, normalised counts. For all d*Tas2rs*, the TMM values were compared to the original raw read counts. There were no major differences in library size within the study and so the TMM data largely reflected the raw count data. Notably, the .gtf file used for edgeR processing contained more annotation for the *Tas2rs* than either the genome or the transcriptome files used for STAR and kallisto alignments. 14 of the 16 dog *Tas2rs* were annotated with only d*Tas2r4* and d*Tas2r62* requiring addition to the file before processing.

Due to the problems with quantifying the low counts from the d*Tas2r* count data, the data were examined only from the point of presence or absence. If a receptor recorded between 0-9 counts it was classed as absent while 10 or more counts was classed as present. In the case of the TMM data, a similar cut-off of 0.25 was applied in the analysis. To test the null-hypothesis that expression of *Tas2rs* would be equal across all papillae locations (front, mid or back), each receptor was assessed individually using a generalised linear model in R, with read counts ≥10 classed as "present". In this case, none of the *TAS2Rs* showed significantly different counts at the 5% level. Analysis of the TMM values was performed with a linear model but the same was true of the TMM values using the level of >=0.25 as classification for a "present" call. However, for any one particular receptor many of the samples had zero counts. Therefore, the sum of all *Tas2rs* for each sample was compared, both as counts and as TMM values (Figure 3.20).

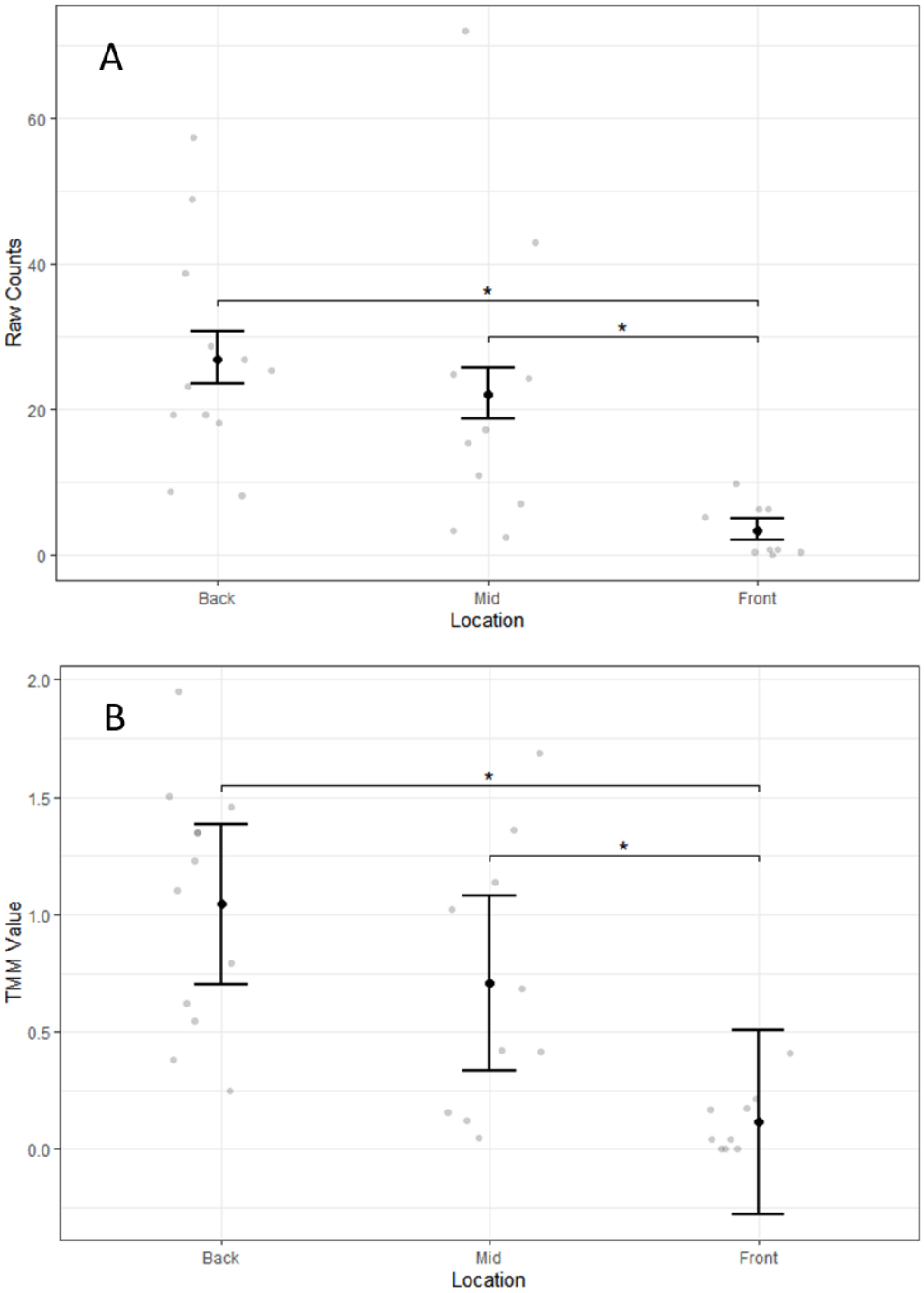

Figure 3.20: Raw read counts and TMM values summed by sample
A) The sum of all d*Tas2r* raw read counts for each sample plotted by location on the tongue with significance shown based on presence or absence (present ≥10) classification in a generalised linear model (Back –Front p=<1x10^{-8}, Mid-Front p=<1x10^{-8}). B) The sum of normalised TMM values for each *Tas2r* for each sample with significance based on presence or absence (present ≥0.25) classification in a linear model (Back-Front p=0.00029, Mid-Front p=0.02668). Error bars represent mean with 95% confidence intervals.

The same function as before, together with Pearson's Chi-squared test, were applied to the data using the same cut-off limits for classification as present or absent. In this case, the comparison between the locations showed a *p*-value of $<1x10^{-8}$ (Back-Front and Mid-Front) in the generalised linear model and of 0.002 in the Chi-squared test for the raw count data. For the TMM values the *p*-values were 0.00029 and 0.02668 for the Back-Front and Mid-Front comparisons, respectively. The chi-squared test gave a *p*-value of 0.0006 for the TMM values. These data indicate significant association of the location with the count or TMM value and suggest that overall *Tas2r* expression was significantly lower in the papillae samples from the front of the tongue.

3.5. Discussion

3.5.1. Fungiform papillae density and total taste bud number in dogs

In this chapter the expression of *Tas2rs* in the fungiform papillae of the dog from different areas of the tongue surface was investigated. The fungiform papillae were distributed fairly evenly across the surface of the tongue with an increase in density on the tongue tip. On average the papillae were found to be at a density of around 5.8/cm^2. If four taste buds on average in each papillae is assumed, which is between the estimates of Holliday (3 on average) (Holliday, 1940) and Holland (4-5 on average) (Holland *et al.*, 1989) and an average tongue surface area of 50cm^2 is estimated that would give an average number of 1160 taste buds. Given that this does not account for the taste buds present in the circumvallate papillae or the increased density of fungiform papillae on the tip of the tongue this seems to be in line with a total number of taste buds of ~1700 as previously reported (Holliday, 1940). This is less than for humans, where an average of around 4600 is seen (Witt *et al.*, 2015) but this estimate varies between human subjects widely, with some adults having as few as 500 taste buds (Linden, 1993).

3.5.2. RNA extraction and sequencing library generation

RNA was easily extracted from the papillae samples and was generally of good quality. The quantity of RNA recovered was quite low and an amplification method was used in order to create enough cDNA for sequencing library preparation. The Nextera XT kit was found to be preferable to the Nextera Flex kit for these samples, due to evidence of more complete tagmentation.

Sequencing of the libraries was largely successful with the targeted 40 million reads being achieved for all but two samples. One sample, LR05834_2_S19 was just below this target with 38.7 million reads while the other, LR05834_4_S21, was much lower with 28.6 million. Alignment results were as expected with ~70% of reads mapping uniquely to the reference genome. This reduces to ~50% when reads are assigned to annotated gene features in the transcriptome or .gtf files.

3.5.3. Data analysis method performance

Two different methods for aligning and counting reads were used. The first, kallisto, was chosen as it is a pseudo-alignment technique which gives great time and resource savings over true alignment methods. Kallisto aligned reads to the transcriptome quickly and provided estimated counts in one operation. The second method used STAR/featureCounts and is based on a true alignment to the genome. Read counts for all the d*Tas2rs* were compared between the two methods and were found to be very close, generally being identical or showing a discrepancy of 1 or 2 reads at the most. Using both a genome alignment and a separate alignment to the transcriptome proved to be a useful way of confirming the low read counts for the *Tas2rs* with relatively little extra resource required given the speed of kallisto.

Raw read counts are not suitable for differential expression analysis for several reasons. When comparing between samples sequencing library sizes will almost always be different resulting in more or less reads for a particular target between samples, even if the true expression is equal. Other aspects such as transcript length

and GC-content are an issue for within sample comparisons, but can be assumed to be equal when comparing between samples. The edgeR program and elements of the R programming language were used to process the raw read counts, normalise between samples and apply appropriate statistical correction for multiple testing to the data. The resulting analyses showed that the papillae samples were largely homogeneous in their expression, especially when compared to the DIEC and kidney samples. This was expected given that the samples were mostly made up of cell types other than taste receptor cells where gene expression is assumed to be mostly equal.

3.5.4. Differentially expressed genes discovered with edgeR

The edgeR analysis did highlight 5 sequences as differentially expressed between the back samples and the front samples. The differentially expressed gene *Otx1* (Orthodenticle homeobox 1), is a transcription factor and is implicated in the development of some sensory organs, including the olfactory bulb and epithelia of the nasal and oral cavities (Simeone *et al.*, 1993) . It is also known to be relatively highly-expressed in the brain, skin and prostate (Fagerberg *et al.*, 2014). However, currently no rationale or sound explanation for the observed downregulation in the papillae from the back of the tongue is available. Similarly, *Arsf* (an arylsulfatase associated with the formation of bone and cartilage), *StxBp6* (Syntaxin binding protein 6, binds components of the SNARE complex which is involved in intracellular vesicle trafficking) and *Smox* (Spermine oxidase, involved with the oxidation of polyamines) are not currently associated with taste papillae in the literature and there is no rationale for these differences based on what is currently known about these genes. No differentially expressed genes were found when either the back samples were compared to the middle samples, or when the middle samples were compared to the front samples.

It is possible that such a low number of identified DE genes could represent false rejection of the null hypothesis, in which all genes would be expected to have equal expression regardless of sampling location. The fold change for these genes, while

meeting the threshold criteria of 2, was not particularly high at around 4 at most. Also the FDR again, while meeting the criteria of 0.05, was not very low at around 0.0035 for three of the genes and 0.024 for the others. RNA-seq data alone is not usually considered sufficient for robust hypothesis testing. qRT-PCR is often used to confirm expression differences generated in RNA-seq, while western blots and immunohistochemical techniques are often used to confirm that RNA differences result in subsequent matching protein differences.

3.5.5. *Tas2r* expression analysis

In the case of the *Tas2rs* a separate analysis was justified, given the existing hypothesis that expression would differ depending on the location of the papillae on the tongue. Both raw read counts and normalised values from edgeR which had undergone the TMM normalisation procedure to account for differences in sequencing library size were compared. PCR analysis on the remaining cDNA prepared with the SMART-Seq kit was also conducted.

The PCR analysis revealed that generally raw read counts of ≥10 were detectable, indicating that these sequences were present in the original sample and not caused by misalignment or incorrect assignment of reads to the *Tas2r* genes. Read counts lower than this were often not confirmed by the PCR, indicating that they may be unreliable.

In all cases for the *Tas2rs*, the read counts were so low as to make any attempt at expression quantification unreliable. We therefore focused the analysis on a simple presence or absence approach. No individual *Tas2r* showed significantly greater presence in any sample location. However, when all *Tas2r* reads or TMM values for individual samples were pooled together the back and middle locations did show significantly more *Tas2r* expression than the samples from the front of the tongue.

Low expression of the *Tas2rs* in fungiform papillae is in line with previous reports. Matsunami *et al.* (2000) tested tissue samples from the tongue tip of mice with both

degenerate *Tas2r* primers and specific primers for two individual *Tas2rs* (*Tas2r140* and *Tas2r103*). Only one of the two specific reactions showed a weak positive result, the others were negative. Adler *et al.* (2000) examined hundreds of fungiform papillae from rats using *in situ* hybridisation but found that less than 10% of them were positive for *Tas2r* expression. Both Kim *et al.* (2003) and Behrens *et al.* (2007) also used in *in situ* hybridisation with fungiform papillae to look for *Tas2r* expression in mouse and human subjects respectively. In both cases no expression was detected. None of these three studies include information on the location of sampling for the papillae and therefore successful detection in the study by Adler *et al.* (2000) may have been related to selection of papillae from the middle or back section of the tongue. Lipchock *et al.* (2013) pooled 6-8 fungiform papillae from 18 human subjects and detected the expression of *TAS2R38* in 11 of them via real-time quantitative Reverse Transcription PCR (qRT-PCR). Most of the samples in this study were collected from the front or middle areas of the anterior tongue, but not the tip.

Analysis of the *Tas2r* read levels in all the samples showed that the expression of the complete *Tas2r* repertoire in these papillae was not seen. No reads were found for d*Tas2r1* in any of the samples. For d*Tas2r3, 5, 10, 12, 38, 39* and *43* some reads were found, but they did not exceed 10 reads in any case. The most abundant receptor was d*Tas2r62* which was found in 18 of the samples, 6 of which had read counts ≥10. Second most abundant was d*Tas2r42* appearing in 16 samples, but only 3 of which had counts ≥10. The d*Tas2r40* gene was actually present at or above the threshold value of 10 counts more often with 6 samples meeting the cut-off but only 11 samples in total showing counts for this receptor. A summary of the count data and the normalised TMM adjusted data is shown in Appendix 3.2.

The highest count for any d*Tas2r* in any sample was recorded in the sample of DIEC cells which showed 68 counts for d*Tas2r40*. Other d*Tas2rs* were detected in the DIEC sample (d*Tas2r39*, *42* and *67*), but the counts were <10 in all cases. This might be expected if DIECs express d*Tas2r40* at a low level as the DIEC sample is not a mixture of cell types as is the case for the papillae samples. Even with very low expression,

higher counts would be expected here. The kidney sample also showed some counts for 4 d*Tas2rs*, but only d*Tas2r40* exceeded the threshold level.

3.5.6. Alternative methods

RNA-seq was chosen primarily because the acquisition of tissue samples of this type is a very rare occurrence within the ethical constraints of animal care at Waltham. RNA-seq would provide not only information on the *Tas2r* gene family, but on other taste related genes too. The correlation of RNA-seq data to data obtained by qRT-PCR has previously been shown to be high, and superior to that of microarrays (Ibarra-Soria *et al.*, 2014). qRT-PCR would be an obvious alternative to quantify only the *Tas2r* expression in the samples and is still viewed as the gold standard for RNA quantification due to its high sensitivity and broad dynamic range.

In situ RNA hybridisation is another alternative for transcript detection and quantification. It has been used frequently for the localisation of *Tas2r* transcripts in taste papillae and has been critical to confirming cellular sites of expression and that *Tas2rs* are not expressed in surrounding tissues (Adler *et al.*, 2000; Behrens *et al.*, 2007; Lossow *et al.*, 2016).

The low counts observed for the *Tas2rs* are due to the scarcity of the type II *Tas2r*-expressing taste receptor cells in the samples. This is an unavoidable disadvantage of using a bulk tissue sample like a whole taste papillae and the problem is worse for fungiform papillae compared with circumvallate papillae due to the relatively small size and low numbers of taste buds present. During the course of this study, new research was published using a single-cell RNA-seq approach (scRNA-seq) to profile the expression of *Tas1r3*-positive type II cells and type III cells from mice (Sukumaran *et al.*, 2017). This approach would allow accurate quantification of expression levels of taste receptor genes across the tongue surface. It does, however, require the target cells to be identified in some way, either with a detectable label (transgenic mice with a green fluorescent protein (GFP) controlled by a taste-cell-type specific

promotor) or by a physiological or morphological method (measuring cell depolarisation to a specific stimulus), both of which were used in the recent study.

Another limitation of the bulk tissue approach is that there is no control over the number of taste buds or type II *Tas2r*-expressing cells in each sample. While it can be said that overall *Tas2r* expression was lower in the samples located at the front of the tongue, it is not known if this was due to lower expression within the *Tas2r* expressing cells, a reduced number of *Tas2r* expressing cells or a reduced number of taste buds per papillae overall, although earlier work (Figure 3.2) suggests the latter is unlikely.

3.5.7. Summary

This is the first study to show differences in the abundance of *Tas2r* transcripts from fungiform papillae located on different regions of the anterior portion of the tongue. As with all RNA expression-based work, further confirmation of the protein expression level is required before firm conclusions can be drawn, but the data do indicate that overall *Tas2r* expression may be lower in fungiform papillae situated near the front of the tongue. Work using an alternative detection method such as *in situ* hybridisation would be useful in confirming the differences observed here.

Chapter 4. Sequence variation in dog *Tas2rs* and its impact on receptor function.

4.1. Introduction

4.1.1. The discovery of functional polymorphisms in taste receptors

Genetic variation in both taste and olfactory receptors contributes to the individual differences that can be observed in the perception of flavour in humans (Hayes *et al.*, 2013; Mainland *et al.*, 2014). The *TAS2R* bitter receptor family contains some of the most well documented examples of variation from one person to another, which can affect sensitivity to certain bitter tastes and have been linked with food choice (Dinehart *et al.*, 2006; Feeney *et al.*, 2011). Variation in the *TAS2R*s is unusually high (Kim *et al.*, 2005), possibly driven by the role *TAS2R*s play in helping animals avoid the ingestion of toxic plants and localised specialisation within different geographical populations.

The most studied example of *TAS2R* variation leading to functional differences in taste perception is the relationship between *TAS2R38* and the chemicals PROP and PTC (Wooding, 2006; Behrens *et al.*, 2013). The fact that the ability to perceive PTC as bitter varies greatly between individuals was first discovered in 1932 by Arthur L. Fox who, while working with PTC in his laboratory, found that when some of the powder "flew around in the air" his co-worker C.R. Noller complained of the bitter taste of the powder while he found it to be tasteless. This discovery led to further work which showed that the bitterness of some other chemicals with a similar structure to that of PTC, sharing an N-C=S moiety, was correlated to that of PTC (Fox, 1932) . The distribution of the "taster" and "non-taster" traits was found to vary but had an average of ~50% each (Wooding, 2006). Work by Albert F. Blakeslee (Blakeslee, 1932) showed that the trait was inherited in a way close to, but not quite consistent with, a simple Mendelian manner. This indicated that, while more than one gene might be involved, the majority of the observed variation was likely to be caused by a single gene.

Over time the molecular basis of the PTC "taster" and "non-taster" phenotype has been revealed to be three amino acid changes within the TAS2R38 receptor. The

changes TAS2R38$_{A49P}$, TAS2R38$_{V262A}$, and TAS2R38$_{I296V}$ form two major haplotypes, PAV and AVI, and several less common ones. Expression and testing of the different haplotypes *in vitro* has helped to confirm that the PAV haplotype is the "taster" while the AVI haplotype is the "non-taster" (Bufe *et al.*, 2005). Modelling of the TAS2R38 receptor has suggested that the location of these residues is not directly relevant for ligand binding, but that they are likely to be involved in mediating G-protein interactions. The A49P variant is predicted to be in the first intracellular loop region, which is a difficult region to model (Marchiori *et al.*, 2013). The V262A$^{6.54}$ variant is located in TM6 while the I296V$^{7.52}$ variant is in TM7. These variant residues may restrict the movement of TM6 (Floriano *et al.*, 2006) which has been proposed as part of the mechanism by which changes in receptor conformation stimulate G protein signalling (Weis *et al.*, 2018).

Other functional polymorphisms in bitter taste receptors have also been confirmed by using *in vitro* cell models. A functional variation in the human *TAS2R16* gene translates to a TAS2R16$_{K172N}$ amino acid change which appears to alter the sensitivity of the receptor to an array of structurally divergent glycosides (Soranzo *et al.*, 2005). In the TAS2R43 receptor two common haplotypes have been identified involving amino acid positions 35 and 212. The TAS2R43$_{S35W,\ R212H}$ variant haplotype was shown to be much more sensitive to the bitter plant compounds aloin and aristolochic acid than TAS2R43$_{S35,\ R212}$ version. The changes in sensitivity were primarily related to the tryptophan at position 35 which is predicted to be in the first intracellular loop (Pronin *et al.*, 2007). As part of the same study, both TAS2R43 and TAS2R44 were shown to mediate the bitter off taste of the artificial sweetener saccharin, again with the tryptophan at position 35 conferring increased sensitivity both *in vitro* and *in vivo*.

While coding variations abound in the *TAS2Rs,* it is not the case that all possible haplotypes exist in nature. For example, while there are seven non-synonymous SNPs in the human *TAS2R38* gene not all of the possible 128 (2^7) haplotypes are observed. In fact, only seven haplotypes have been confirmed worldwide (Wooding *et al.*, 2004; Kim *et al.*, 2005). It is also the case that long-range haplotypes covering

more than one *TAS2R* loci can be implicated in the sensitivity of individuals to certain bitter compounds. Haplotype blocks have been identified on both chromosome 7 and 12 where multiple *TAS2R* sequences are present (Roudnitzky *et al.*, 2015). Individual sensitivity to different bitter compounds was associated with multiple *TAS2R* loci in several cases. For example grosheimin sensitivity was linked to *TAS2R43* and *TAS2R46*, both of which harbour high and low sensitivity variations. In this case variants were maintained so that the sensitive allele of *TAS2R43* was linked with the sensitive allele in *TAS2R46* and both insensitive alleles were also linked, resulting in a strong correlation between the contributions of both loci. In many cases a bitter compound may activate more than one TAS2R and one TAS2R may recognise more than one compound. This, combined with significant levels of linkage disequilibrium across *TAS2R* loci, can result in a more complex relationship between genotype and phenotype than that seen with PTC/PROP and *TAS2R38*.

4.1.2. Genetic variation in dogs

In the case of dogs little published information exists on the levels of variation within the TAS2Rs, however there are some reasons to suspect that both the levels of variation and the distribution of variants among dog populations may differ from that of humans. As discussed in Chapter 1 dog domestication has resulted in two genetic bottlenecks (Figure 4.1). These events resulted in a number of consequences including short-range linkage disequilibrium (LD) between breeds and long range LD within breeds, which has yet to be broken down by recombination (Lindblad-Toh *et al.*, 2005; Parker *et al.*, 2017). In theory this should reduce variation in a group of genes like the *Tas2rs* and result in less taste differences, particularly in dogs of the same breed. It may also have resulted in some specific differences that exist only in one, or a few closely related breeds.

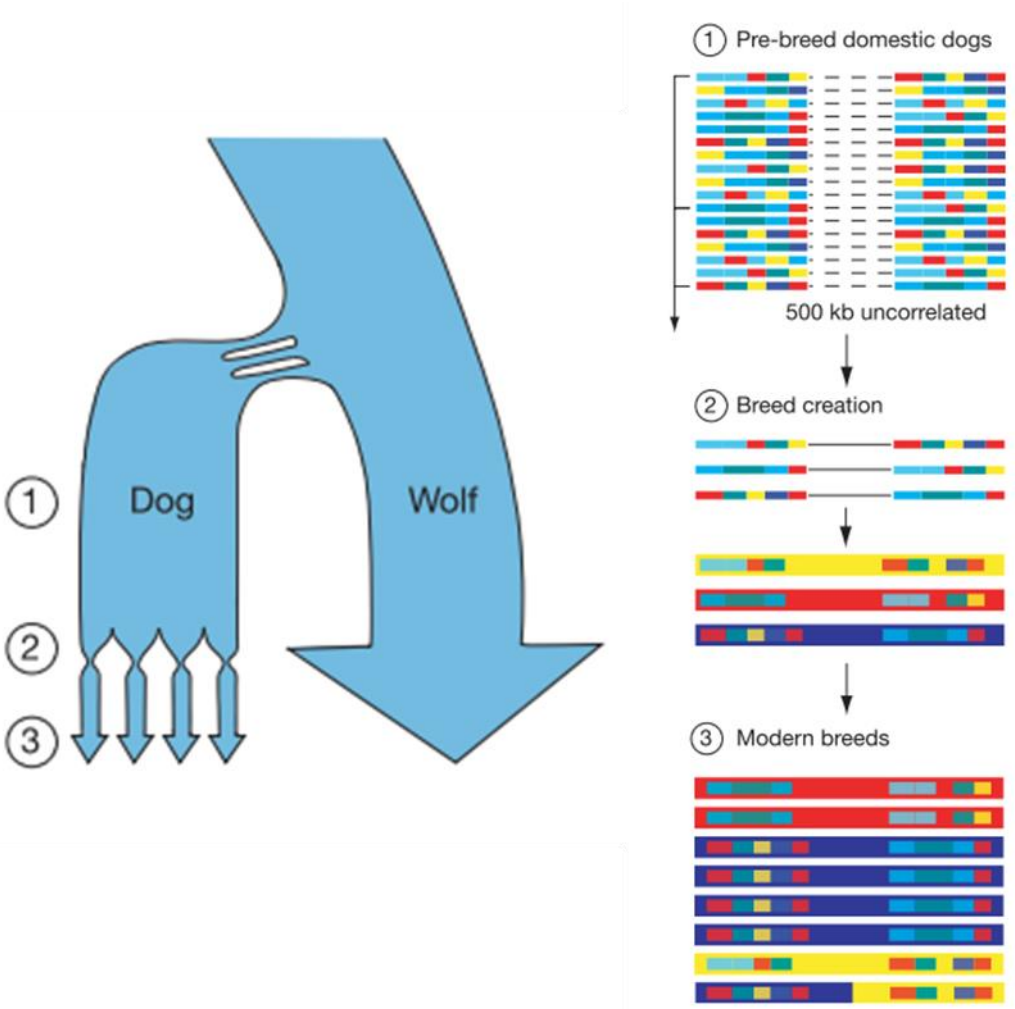

Figure 4.1: Dog domestication resulted in a two genetic bottlenecks, reducing genetic diversity in the ancestors of modern dogs
The first occurred during the domestication of wolves. A second bottleneck resulted from the creation of modern dog breeds in the 1800s. 1) The ancestral dog population displayed the short-range LD expected from the domestication event(s). 2) Creation of modern breeds resulted in long-range LD within breeds. 3) The effects of breed creation have yet to be broken down by recombination (reproduced and adapted from Lindblad-Toh et al., 2005).

Some of these effects can be seen in the prevalence of particular disease causing variants in some dog breeds. In a small minority of cases disease-associated alleles have become completely specific to a single dog breed. This is the case for the Lagotto Romagnolo breed, which carries a disease variant for juvenile epilepsy at a carrier frequency of 28.3% while the variant is absent in other dogs (Donner *et al.*, 2018). Another example is a disease variant for neonatal encephalopathy carried by

the Standard Poodle at a frequency of 16.8%. However, most disease variants are carried by both mixed breed and purebred dogs alike. Purebred dogs are more likely to be at risk of genetic disease not because they carry more disease-causing variations, but because they are more likely to be homozygous for the disease-causing allele. Mixed breed dogs actually carry more variants, but suffer less genetic disease due to being heterozygous at more loci (Donner *et al.*, 2018).

The unique niche occupied by dogs in the field of genomics has led to their use in the study of disease genetics, morphological variation and traits associated with behaviour. Such interest has led to several initiatives aimed at collating whole genome sequences from different dog breeds into central repositories to facilitate comparison and enhance research efforts throughout the scientific community. One such initiative is known as the Dog Biomedical Variant Database Consortium (DBVDC) (Jagannathan *et al.*, 2019). As Mars, Inc. was a contributor to this initiative, early access to one of the first versions of this variant database was available, which allowed investigation of SNPs and other variants in the dog *Tas2r* repertoire as part of this study.

4.2. Aims of this chapter

The aim of this chapter was to assess the levels of variation in the dog *Tas2r* repertoire and compare it with that of human. Further, it aimed to examine known functionally relevant human variations in dog *Tas2r*s and discover any potential new variants that are specific to dogs or even to individual dog breeds. Ultimately, the goal was to help answer the question of whether dogs experience individual differences in bitter taste perception, as is the case for humans.

4.3. Materials and methods

4.3.1. The Dog Biomedical Variant Database Consortium (DBVDC)

In Chapter 1 the sequences of the dog *TAS2R* genes were established based on annotated sequences and searches of the dog genome using human and mouse *Tas2r* sequences. However, all of these sequences are based on one dog, a female Boxer named Tasha whose genome sequence currently serves as the dog reference sequence (Lindblad-Toh *et al.*, 2005; Hoeppner *et al.*, 2014).

Information on variants contained within the dog genome has been somewhat scarce until recently. Two dog genome sequences were the main contributors to the dog SNPs contained within the Single Nucleotide Polymorphism Database (dbSNP) (Wheeler *et al.*, 2007). These were the aforementioned Boxer and a Standard Poodle sequence (Kirkness *et al.*, 2003). However, the dog has been a long-standing disease model for many conditions that occur in humans (Shearin *et al.*, 2010). This interest and the arrival of high throughput genome sequencing, have led to a large increase in the amount of dog genomes being sequenced through various initiatives globally. In 2015, a resource called DoGSD (Bai *et al.*, 2015) made the SNPs from a collection of 77 wolves and dogs of different breeds, combined with existing dbSNP data for dogs, available online. More recently, larger data sets have become available with a project releasing SNP details from 722 canids funded by the National Institutes of Health (Plassais *et al.*, 2019), while the DBVDC released SNP data from 582 dogs from 126 breeds and eight wolves (Jagannathan *et al.*, 2019).

Mars, Inc. has been a member of the DBVDC since 2017, contributing a large number of whole dog genomes to the project. As a contributor, Mars, Inc. had access to the database much earlier than the public release of the data in 2019. This earlier version of the data was used to assess variation in the dog Tas2rs. This version contained the genomes for a total of 465 dogs from 101 different breeds. These were not revised in later releases.

4.3.2. SNP and haplotype analysis

SNP analysis was conducted using the variant call file (.vcf) available from the DBVDC project and the Variant Effect Predictor (VEP) tool (McLaren *et al.*, 2016) available through the Ensembl genome portal (www.ensembl.org). Coordinates for the coding regions of all 16 putative dog *Tas2r*s were used to filter the .vcf file to these regions only. The VEP tool was used to classify variations occurring in the 16 putative Tas2r gene sequences. The VEP classified variants as either low, moderate or high impact based on their possible effect on the expressed protein. Low impact variants include synonymous variants or variations that code for alternative start or stop codons. Moderate impact variants include non-synonymous variants or in-frame insertions or deletions. High impact variants include lost start or stop codons, gained stop codons and frameshift variants. For the purposes of this study, only moderate or high impact variations were of interest and low impact variations were ignored.

4.3.3. Epitope tagging of d*Tas2r*s

When looking at the impact of a SNP or other variation on the function of a receptor in a cell-based model, one important consideration is whether the variation has any other effects on the receptor that might account for any differences observed. Effects on receptor expression are possible, and would not be specifically identified in a calcium mobilisation assay, as these changes alone might result in a reduced or increased agonist potency or maximal response for that particular variant. In order to check for equivalent levels of cell-surface expression, epitope tags can be employed. Several epitope tags have previously been used successfully with *Tas2r*s. In some cases improved receptor maturation and an epitope tag have been achieved with the same sequence. The first 39 amino acids of bovine rhodopsin have been used as both a tag to enhance cell-surface expression and as a target for assessment of cell-surface expression via a monocolonal anti-rhodopsin antibody (Chandrashekar *et al.*, 2000). The tag for plasma membrane targeting used in this project, the 45 amino acids from the N-terminal region of rat somatostatin type 3 receptor, does not serve a dual purpose but has been used in conjunction with a C-

terminal herpes simplex virus (HSV) glycoprotein D epitope (Ammon *et al.*, 2002) or with a N-terminal FLAG tag (Sandau *et al.*, 2015) for receptor quantification. N-terminal tags allow assessment of cell-surface expressed receptor only while C-terminal tags permit assessment of all receptor expression after permeabilisation of the cells.

The FLAG tag was used in this study. The FLAG tag is a short peptide tag having the sequence DYKDDDDK. It was first used for the purification of recombinant lymphokines (Hopp et al., 1988), but has since become one of the most versatile tags for antibody-mediated detection and purification of fusion proteins (Einhauer et al., 2001). The tag is highly hydrophilic, which aids with both antigenicity and the adoption of an exposed conformation. As the Sstr3 tag used here does not contain a cleavage site the FLAG tag was placed directly in front of it as shown in Figure 4.2.

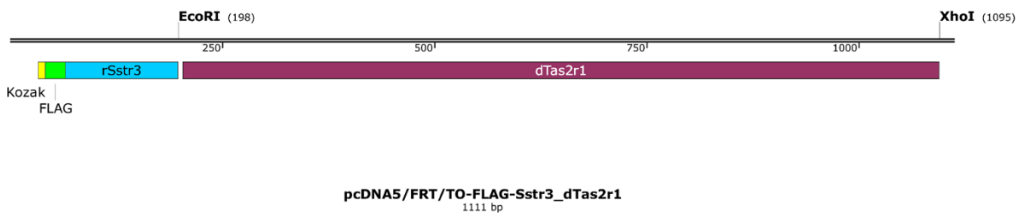

Figure 4.2: The d*Tas2r1* expression construct tagged with an N-terminal FLAG sequence for immunocytochemistry
The rest of the construct was as before with the first 44 amino acids of rat Sstr3 as a plasma membrane targeting tag in the pcDNA5/FRT/TO backbone (not shown).

Several monoclonal antibodies have been developed for FLAG (M1, M2 and M5). The mouse anti-FLAG M2 antibody (Sigma Aldrich, UK) is the most generally applicable and was chosen for this project. Secondary labelling with a goat anti-mouse AlexaFluor 488 antibody (ThermoFisher Scientific, UK) was performed.

4.3.4. Site directed mutagenesis of d*Tas2r1*

Gene sequence analysis revealed that dogs did not possess any of the *TAS2R* variations previously shown to alter receptor function in humans. Therefore, d*Tas2r1* was selected as a test receptor for further work as it had a reasonably high number of variants in dogs and also several ligands as identified in Chapter 2.
In order to assess any functional impact of the SNPs identified in d*Tas2r1*, each variation was tested in a cell-based calcium mobilisation assay as described in Chapter 2. Variations in the receptor coding sequence were introduced using site-directed mutagenesis (SDM) with the QuickChange II Site-Directed Mutagenesis Kit (Agilent, UK). This technique utilises a high fidelity *PfuUltra* DNA polymerase and variation containing oligonucleotide primers to synthesise a new plasmid from the existing plasmid template which then contains the new variant. The template plasmid DNA is then digested by the action of a *Dpn I* endonuclease. This endonuclease is specific for methylated and hemimethylated DNA and therefore digests only the parental template. The remaining variation containing plasmid is then transfected into competent *E.coli* and prepared as for standard plasmid DNA with the methods described in Chapter 2. An overview of the technique is presented in Figure 4.3.

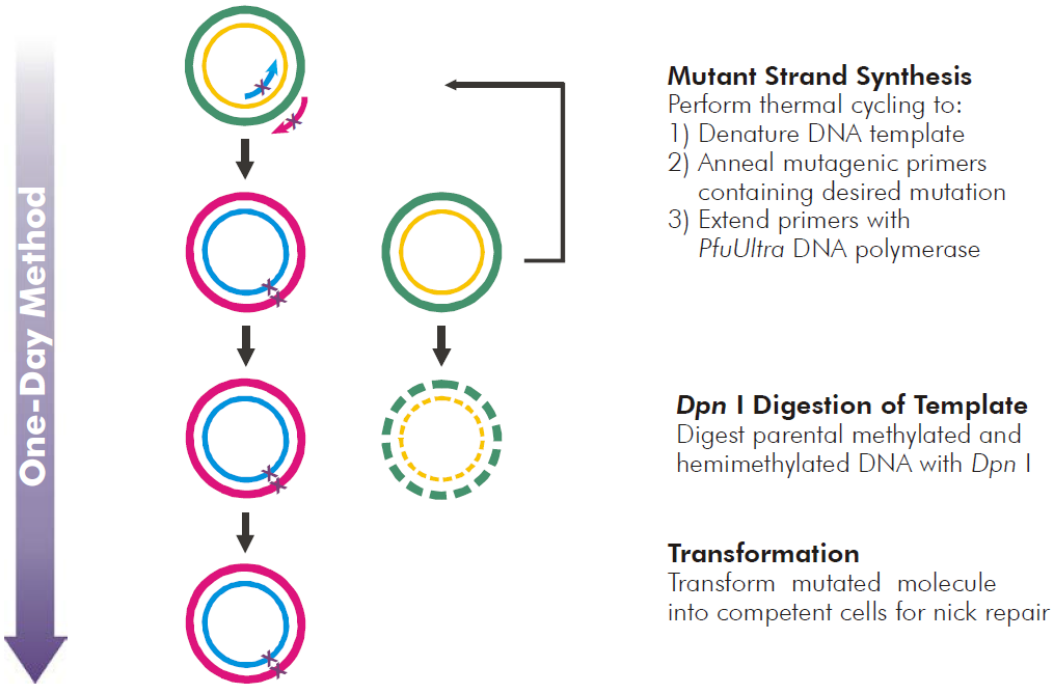

Figure 4.3: The Agilent QuickChange II SDM technique
Primers for the parental plasmid are designed so that each primer contains the variant site(s), approximately in the centre of the primer sequence. A primer design program is provided online by the manufacturer as there are several other specific requirements for their design including a length of between 25-45 bases, Tm of >= 78°C, GC content of ~40% and a terminal sequence with one or more G or C residues (reproduced from the QuickChange II user manual, 2018).

Primers were designed for SDM of the wild type expression vector for d*Tas2r1* using the parameters specified in the QuickChange II protocol (Agilent). Primers are listed in Table 4.1.

Table 4.1: Primers used for site directed mutagenesis of the *dTas2r1* containing expression vector.

Variant	Forward Primer (5'-3')	Reverse Primer (5'-3')
t41a	tatccattttcttttcacagagatgcaatttctcatcgggg	ccccgatgagaaattgcatctctgtgaaaagaaaatggata
g146t	cttggctctccttctttttctgtctggcgatttcc	ggaaatcgccagacagaaaagaaggagagccaag
g156a	ccttctttgctgtctggcaatttccaggatttgtcta	tagacaaatcctggaaattgccagacagcaaagaagg
t169g	gtctggcgatttccaggattggtctacaattgatcatctt	aagatgatcaattgtagaccaatcctggaaatcgccagac
a181g	tccaggatttgtctacaattggtcatcttcttcatgaatctgg	ccagattcatgaagaagatgaccaattgtagacaaatcctgga
g256a	ctacttgctgataattttgtaattttcatgtttgtaaatgaattg ggactttgg	ccaaagtcccaattcatttacaaacatgaaaattacaaaattatc agcaagtag
g299a	ttcgccacatggcttgaggtttactactgtgcc	ggcacagtagtaaacctcaagccatgtggcgaa
g394a	gccatggctgatcctcaggtccatgatgtatgc	gcatacatcatggacctgaggatcagccatggc
g415a	ccatgatgtatgcatccatcccttctgttttctgc	gcagaaaacagaagggatggatgcatacatcatgg
a444g	cttctgttttctgcagcaaacagatgtgggtttattcccaaa	tttgggaataaacccacatctgtttgctgcagaaaacagaag
c491t	ccagccttttttccccaaacgtaactcaaatcaaagaaacatc	gatgtttctttgatttgagttacgtttggggaaaaaaggctgg
c680t	cacgtgagcacgatcctgttcgttctatccttcc	ggaaggatagaacgaacaggatcgtgctcacgtg
g682t	gagcacgatcctgtcctttctatccttcctggt	accaggaaggatagaaaggacaggatcgtgctc
c722t	ctctcccactacatggtagctgctttgctctct	agagagcaaagcagctaccatgtagtgggagag
t730a	ccactacatggcagctgctatgctctcttttcaga	tctgaaaagagagcatagcagctgccatgtagtgg

The manufacturer's instructions were followed for the whole procedure. Reactions were prepared in 0.2mL thin-wall microtubes (Thermo Fisher Scientific, UK) with a final reaction volume of 50µL. One microliter of DNA template, in this case 25ng of the FLAG-Sstr3-d*Tas2r1* construct, was added to 5µL of 10X reaction buffer. A mixture of forward and reverse oligonucleotide primers containing 125ng of each primer in a 2.5µL volume was added. One microliter of the dNTP mix provided with the kit was added, although the concentration is not given by the manufacturer. Nuclease free water (Qiagen, Germany) was added to achieve a final volume of 50µL and then 1µL of *PfuUltra* high fidelity DNA polymerase (2.5U/µL) was added just prior to the tubes being gently mixed and transferred to the thermal cycler. Reactions were incubated at 95°C for 30 seconds, followed by 12 cycles of 95°C for 30 seconds, 55°C for one minute and 68°C for 1 minute/kb of plasmid length. Reactions were then held at 4°C. On collection 1µL of *Dpn I* (10U/µL) was added to each reaction followed by a one hour incubation at 37°C.

Transformation with XL1-Blue supercompetent cells was conducted by thawing and aliquoting cells into pre-chilled 14mL BD Falcon polypropylene round bottom tubes (Beckton Dickinson, UK). DNA from the *Dpn I* digestion was added to the cells (1µL)

and swirled gently. Tubes were incubated on ice for 30 minutes then a heat-shock at 42°C was applied for 45 seconds in a waterbath. The cells were transferred back onto ice for 2 minutes before adding 0.5mL of SOC medium (Sigma Aldrich, UK) pre-warmed to 42°C. Cells were then incubated at 37°C for 1 hour with shaking at 225rpm. Cells were then plated onto 2 agar plates containing 100µg/mL ampicillin (250µL per plate) and plates were incubated overnight at 37°C. Colonies were picked and re-streaked on a fresh agar plate with ampicillin before being grown for plasmid DNA extraction. Extraction was done with either the miniprep method or the midiprep method described in Chapter 2. All plasmids were re-sequenced to check for the presence of the correct variation and to check for unwanted sequence changes. Purified DNA was sequenced using primers targeting the CMV promoter site for the forward primer (5'-CGCAAATGGGCGGTAGGCGTG-3') and the BGH terminator site for the reverse primer (5'-TAGAAGGCACAGTCGAGG-3') to cover the full receptor cDNA. In each case the desired variation was confirmed to have been incorporated into the receptor sequence with the exception of the a444g site. Despite two attempts with this primer combination, the variation was not incorporated into the new plasmid and therefore this variation was not tested in the downstream analysis.

4.3.5. Calcium mobilisation assay for d*Tas2r1* variants

All modified plasmids were subsequently used in the calcium mobilisation assay as previously described (Chapter 2). To assess the functional impact of any of the identified sequence variants in d*Tas2r1*, a previously identified agonist for dTas2r1, 6-nitrosaccharin, was used as an agonist at a maximum concentration of 10mM with 6 half concentration dilutions and a blank final point that contained only assay buffer. The concentrations used were the same as for the previous testing, as was the overall methodology (Chapter 2). The data points were replicated in quadruplicate on each plate and the wild type receptor was included along with cells transfected with a mock plasmid which did not contain the d*Tas2r1* sequence. Experiments were repeated three times.

4.3.6. Flow cytometry analysis for d*Tas2r1* variants

The cell surface expression of d*Tas2r1* and each of the tested variants was quantified using flow cytometry. Cells were prepared as they were for the calcium mobilization assay (Chapter 2), but poly-D-lysine coated 96-well plates (Greiner Bio One 655090, UK) were used, and the seeding density was increased accordingly to 60,000 cells per well. Transfection was performed with the same ratio of cells/Lipofectamine 2000/plasmid DNA as used previously. Approximately 24hrs after transfection, the cells were treated with trypsin, transferred to a low-bind 96-well round bottom plate (Corning, UK) and washed in 100µL DMEM + 10% FBS before being collected by centrifugation at 350 x g for 2 minutes at 4°C. All of the following steps were performed on ice to minimise endocytosis of the receptor. Cells were washed once with 100µL serum-free DMEM/0.1% BSA and incubated for 10 minutes at 4°C. Another collection step was performed at 350 x g for 2 minutes at 4°C. Media was replaced with 50µL serum-free DMEM/0.1% BSA containing 2.5µg/mL M2 mouse anti-FLAG antibody (Sigma Aldrich, UK). Cells were incubated for 30 minutes at 4°C and then washed with 1X PBS for 5 minutes, then again with 1X PBS/1% BSA for 5 minutes at 4°C. The supernatant was then replaced with a solution of 1X PBS/ 1% BSA with 1µg/mL goat anti-mouse AlexaFluor488 secondary antibody (Thermo Fisher Scientific, UK) and the cells were incubated on ice for 45 minutes in the dark. Two washes were then performed with PBS/1%BSA with incubation on ice for 2 minutes. Two more washes with PBS were then performed with incubation on ice for 5 minutes. The cells were then fixed using 3% paraformaldehyde solution for 15 minutes before a final wash with PBS. After resuspension in PBS the cells were acquired on the flow cytometer (MACSQuant Analyzer 10, Miltenyi Biotec, UK).

The flow cytometer was calibrated before each use. As only one fluorophore was used, compensation was not required. The instrument was set to aspirate 80µL of the final 100µL sample volume containing the fixed cells in PBS. Excitation with the 488nm laser and the B1 525/50nm emission detector was used. Data were saved for later analysis using the FlowJo v10 software (Beckton Dickinson, UK).

4.3.7. Data analysis

In order to determine if dogs showed any evidence of reduced variation in their *Tas2r* genes when compared to wolves a Kruskal Wallis test was applied to wolves (n=3) and any dog breed which also had three representatives in the database. In the case of comparisons of the frequency of a single variant between any two particular dog breeds a chi-squared test was used. Analyses were performed in GraphPad Prism V8.2.1 (GraphPad Software, USA)

To help normalise data from different calcium mobilisation experiments, all data was normalised to the wild type responses for each respective experiment and expressed as a percentage of the maximum response (5mM of the agonist) of the wild type receptor. Data were charted in GraphPad Prism V8.2.1 (GraphPad Software, USA) with log transformation of the agonist concentrations and non-linear regression curve fitting using a four parameter model. EC_{50} values and E_{max} (calculated as Top-Bottom values from the non-linear regression analysis) values from the three experiments were compared using unpaired t-tests, with multiple t-tests being performed simultaneously. In the analysis performed with GraphPad Prism standard deviation was not assumed to be consistent between rows. Statistical significance was chosen as the test criteria with an alpha of 0.05. Correction for multiple comparisons was performed using the Holm-Sidak method.

4.4. Results

4.4.1. *Tas2r* genes and the DBVDC

The DBVDC data was supplied as a variant call file (.vcf file) and an accompanying spreadsheet containing metadata relating to the dogs in the database. The dog breed assigned to the samples in the DBVDC was checked using an algorithm previously developed by Mars, Inc. for a commercially available breed ancestry test called the WISDOM Panel 3.0 breed identification test (Mars Veterinary). The algorithms used in this test were applied to the data contained within the .vcf file by members of the Mars Veterinary research team and confirmed almost all the

assigned breed identities as correct. In a small number of cases the assigned breed was refined based on the result of the WISDOM panel test, in all cases to a closely related breed. The total number of breeds represented in the database after adjustment was 101. Some further cleaning of the metadata was necessary to correct misspellings of some breed names and to harmonise formatting to allow easier data processing.

Previously defined co-ordinates for dog Tas2r genes (Chapter 2) were used to filter the .vcf file before using the VEP tool to classify all variations for each receptor in each sample in the database. LOW impact variants were present with similar frequency to MODERATE and HIGH impact variants. On average individual dogs had 5.5 LOW impact variants each. Dog *Tas2r* genes contained an average of 3 LOW impact variants, with a range of 1-6. In all cases LOW impact variants were synonymous. Distribution of MODERATE and HIGH impact variants is shown in Figure 4.4. All breeds with more than 1 representative are included and the mean number of MODERATE and HIGH impact variants is shown, with error bars representing minimum and maximum values.

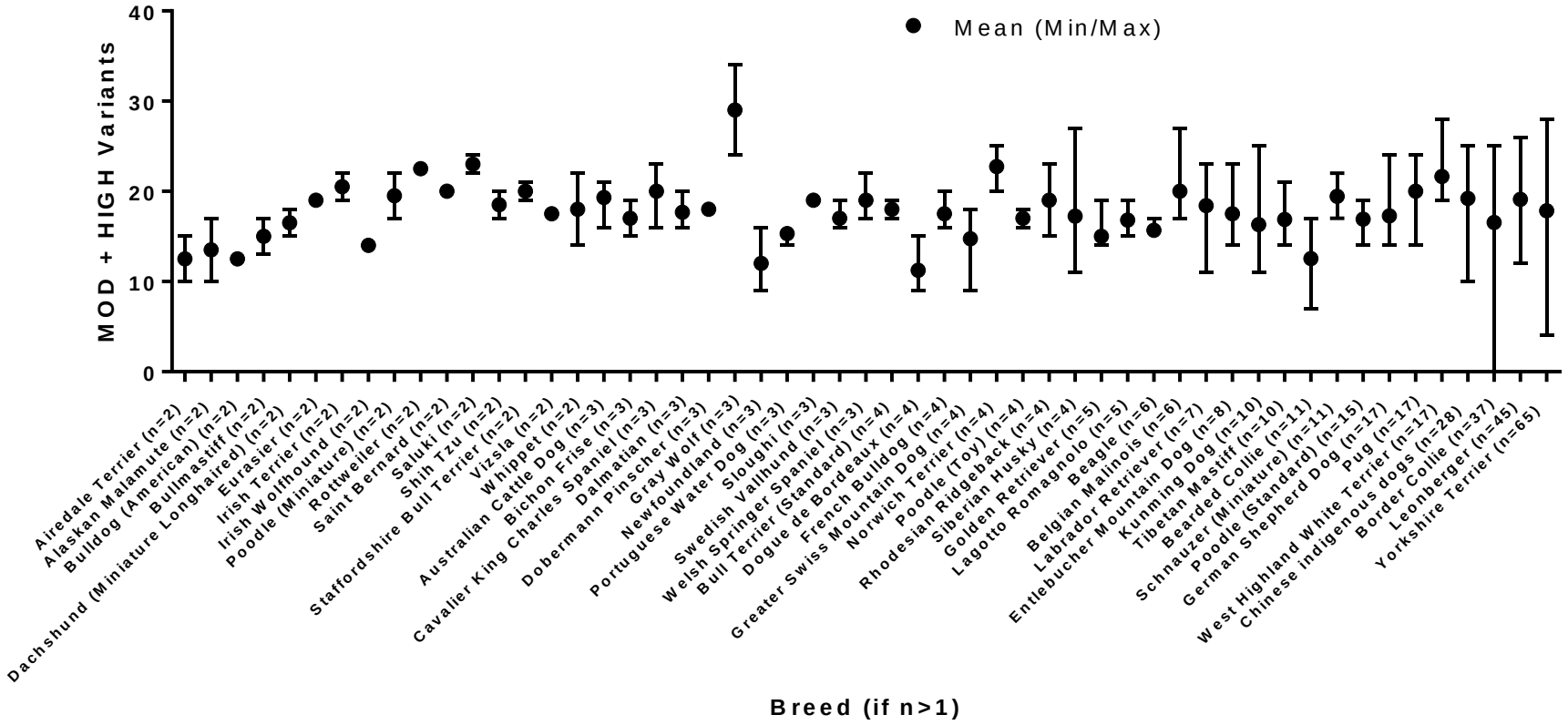

Figure 4.4: Variations in dog *Tas2r* gene sequences that have the potential to alter or eliminate receptor function
The x-axis shows categorical data for dog breeds with the number of dogs of that breed represented in the DBVDC database (if n>1). The y-axis shows the cumulative number of MODERATE and HIGH impact variations counted across all 16 putatively functional *Tas2r*s. Mean numbers of variants are plotted with error bars representing the range.

One notable observation from this analysis was the higher level of variation seen in the wolf samples. Statistical analysis of wolves and other breeds with n=3 in the database using a Kruskal Wallis test confirmed that for two of the dog breeds, namely Newfoundlands and Portuguese Water Dogs, this difference was significant (adjusted *p*-values of 0.0031 and 0.0119 respectively). This is most likely to be an example of reduced genetic diversity in domestic dog breeds caused by selective breeding and genetic bottlenecks. Domestic dog breeds all showed comparable levels of variation from the reference sequence.

Breed related variation was also visualised in terms of how many breeds a particular variant occurred in. In Figure 4.5 all 86 identified MODERATE and HIGH impact variants are shown against the number of breeds harbouring those variants.

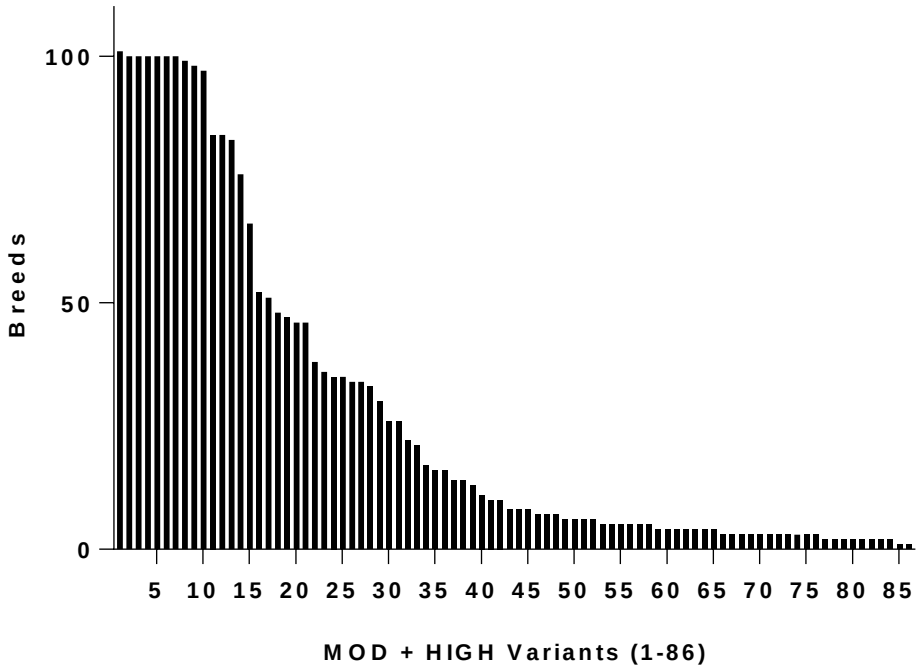

Figure 4.5: Specificity of different *Tas2r* variants to different breeds
The x-axis represents all the individual MODERATE and HIGH impact variants identified, arranged by level of breed occurrence. The y-axis represents the breed occurrence for each variant up to a maximum of 101, which was the total number of different breeds represented in the database. In some cases particular variants were present in all dog breeds studied, most likely indicating an error or rare variant in the reference sequence. In other cases variants were only observed in a small number of breeds.

The distribution of variants between the different *Tas2r* sequences was also assessed. Receptors had between 1 and 16 non-synonymous SNPs, a figure which is close to that reported for humans at 1-12 (Kim *et al.*, 2005). Average numbers of variants per gene were also similar between dogs and humans with 5.4 and 4.2 variants per gene; respectively.

4.4.2. Epitope tagging of d*Tas2r1*

For epitope tagging of the receptor, a new version of the d*Tas2r1* expression vector was synthesised (Eurofins, Germany). The FLAG tag sequence was added to the MCS directly in front of the rSstr3 plasma membrane targeting tag. The new vector was

tested in the calcium mobilisation assay along with the standard vector expressing rSstr3 only, tagged dTas2r1 and the previously identified dTas2r1 agonist 6-nitrosaccharin (Figure 4.6).

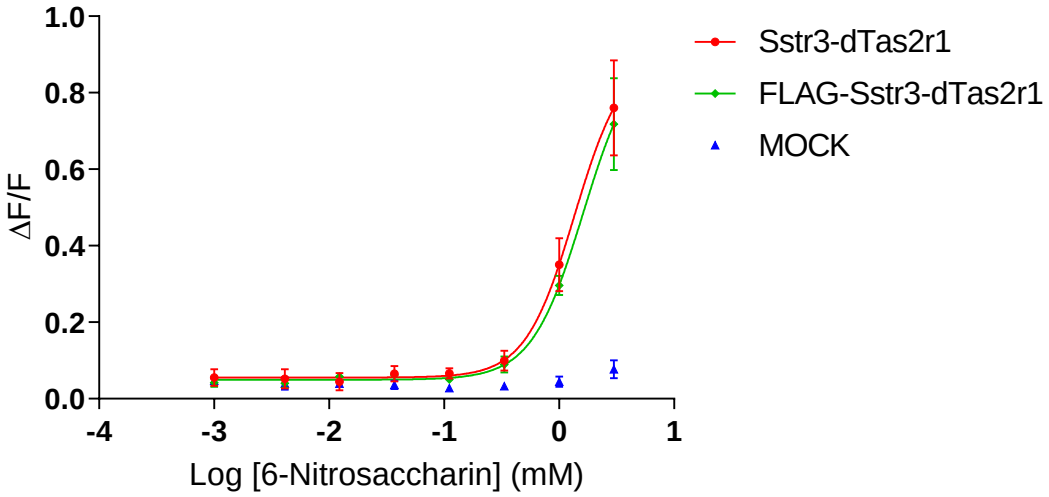

Figure 4.6: FLAG labelled and unlabelled dTas2r1 with 6-nitrosaccharin
Incorporation of an N-terminal FLAG sequence did not impact on receptor function. Error bars represent SD of 4 replicate wells (n=1).

Based on these data there was no difference in receptor response when the FLAG tag was included upstream of the rSstr3 sequence in the expression vector. The FLAG tag was included in all experiments with sequence variants of d*Tas2r1*.

4.4.3. Functional variation in d*Tas2r1*

The similarities seen in the levels of variation between dog and human *Tas2r*s suggest that variation may play a role in taste sensitivity in dogs as it does in humans. One obvious way to confirm this would be if dogs showed the same variation in the *TAS2R38* gene that accounts for differences in PROP and PTC taste perception in humans. However, analysis of the DBVDC data for *Tas2r38* sequences shows that the amino acid residues in these positions are conserved in dogs, not variable as in humans. The dog has an intermediate haplotype of PVI rather than the taster (PAV) or non-taster (AVI) haplotypes prevalent in humans. Coding variations were identified in dog *Tas2r38*, but none of the 4 variations identified were located

in the same positions as for the human coding variations related to *TAS2R38*/PTC sensitivity. The variants identified in dog were A27T, L175R, I195V and G234S.

Other variations in human *TAS2R16* or *TAS2R31(44)* could not be compared as dogs lack an orthologue for these receptors (Chapter 1). The *TAS2R43*$_{WH/SR}$ haplotype (Pronin *et al.*, 2007) was investigated, but the *TAS2R43*$_{W35S}$ variation did not appear to be present in the DBVDC data as the tryptophan residue was conserved. There was variation in the other position, but dogs showed a d*Tas2r43*$_{G212S}$ variant as opposed to the *Tas2r43*$_{H212R}$ variant seen in humans. The dog orthologue is longer than the human receptor, at 349 amino acid residues compared to 309, but the sequences align well up to residue 332, at which point the dog sequence shows two insertions.

Without these obvious examples to focus on, other criteria were selected to identify a dog receptor that might show functional variation. A receptor with a relatively high level of non-synonymous variation and a selection of positive ligands in the calcium mobilisation assay (Chapter 2) was ideal. The d*Tas2r1* receptor met these criteria and was selected for further investigation.

Use of the VEP tool in conjunction with the DBVDC .vcf file resulted in the overall identification of 21 SNPs in dTas2r1, of which 15 were non-synonymous. During the course of this project, an updated version of the DBVDC database was made available with 648 dog genomes included. Four new non-synonymous variants were found, although each occurred only once in the database (Table 4.2).

Table 4.2: All variants found in the dTas2r1 sequence using the DBVDC database
Some variants were identified in a later release of the DBVDC where more genomes were included.

Chromosome	Position	Ref Allele	Alt Allele	Ref AA	Alt AA	Status	Alt Allele Count	Alt Allele Freq
34	4537672	T	A	Val	Glu	Non-synonymous	12	0.011
34	4537777	G	T	Leu	Phe	Non-synonymous	3	3.24E-03
34	4537787	G	A	Ala	Thr	Non-synonymous	1	7.85E-04
34	4537800	T	G	Cys	Gly	Non-synonymous	3	3.25E-03
34	4537812	A	G	Ile	Val	Non-synonymous	3	3.23E-03
34	4537887	G	A	Val	Met	Non-synonymous	1	7.85E-04
34	4537930	G	A	Gly	Glu	Non-synonymous	1	1.09E-03
34	4538025	G	A	Gly	Glu	Non-synonymous	1	7.85E-04
34	4538046	G	A	Val	Ile	Non-synonymous	1	7.85E-04
34	4538075	A	G	Ile	Met	Non-synonymous	3	3.23E-03
34	4538122	C	T	Ala	Val	Non-synonymous	33	0.036
34	4538183	A	G	Pro	Pro	Synonymous	4	4.31E-03
34	4538210	A	G	Leu	Leu	Synonymous	7	7.56E-03
34	4538311	C	T	Ser	Phe	Non-synonymous	1	1.09E-03
34	4538313	G	T	Val	Phe	Non-synonymous	1	1.09E-03
34	4538321	C	T	Ser	Ser	Synonymous	2	2.18E-03
34	4538353	C	T	Ala	Val	Non-synonymous	1	1.08E-03
34	4538361	T	A	Leu	Met	Non-synonymous	98	0.106
34	4538393	C	T	Ser	Ser	Synonymous	2	2.17E-03
34	4538403	C	T	Leu	Leu	Synonymous	1	1.08E-03
34	4538447	T	C	Ser	Ser	Synonymous	3	3.24E-03

In all but one case, the variants detected were quite rare (allele frequency <0.05) when the whole database was considered. Of more interest was the allele frequency within breed. For example, the first variation at position 4537672 in the chromosome was present 10 times in the 465 version of the database having an allele frequency of 0.011. However, this was not evenly distributed between breeds. The variant appeared in 7 different breeds. The variant was found in the Dandie Dinmont Terrier (1 of 1), the Labrador Retriever (1 of 7), the Standard Poodle (4 of 15), the Shih Tzu (1 of 2), the French Bulldog (1 of 4), the Yorkshire Terrier (1 of 65) and the Miniature Schnauzer (1 of 9). In the later 648 version of the database, 1 of 2 Friesian Stabyhouns also carried this variant and this animal was the only homozygote found, with all other carriers being heterozygotes. If the allele frequency of this variant is compared between Standard Poodles and Yorkshire Terriers (the most numerous breed in the database with 65 individuals) using a chi-squared test, the chi-square value is 12.71 with 1 degree of freedom. This is

statistically significant with a *p*-value of 0.0004, indicating that this variant is more likely to occur in Standard Poodles than Yorkshire Terriers.

Another example of a variant with uneven distribution between breeds was the 4538122 variant. The occurrence of this variant was mostly seen in the Leonberger breed occurring in 23 of 45 individuals. It also occurred in the Rottweiler (1 of 2), Border Collie (1 of 37), Tibetan Mastiff (2 of 10) and one mixed breed dog which were added to the later version of the database. This variant was homozygous in 7 of the Leonbergers, but heterozygous in all other cases. If the occurrence of the variant allele in Leonbergers is compared to that of Yorkshire Terriers with a chi-squared test, a chi-square value of 51.57 with 1 degree of freedom is calculated. This is statistically significant with a *p*-value of less than 0.0001.

The third example and most prevalent SNP in the database was at position 4538361. This SNP was found in a larger selection of breeds including Border Collies, Bearded Collies, German Shepherds, Pugs, Yorkshire Terriers and Miniature Schnauzers. It was also present as a homozygote in a selection of different breeds.

The other coding SNPs identified here were more limited in number, appearing in only a few individuals and almost always only as a heterozygote. A summary of the data from the 648 version of the database for the non-synonymous variations is presented in Table 4.3.

Table 4.3: Summary of breeds carrying all identified non-synonymous SNPs in dTas2r1

Analysis based on the 648 version of the DBVDC database.

Position	Variant	Carrier Breeds (carriers/total)	Heterozygotes/Homozygotes
4537672	t41a	Dandie Dinmont Terrier (1/1)	1/0
		Labrador Retriever (1/7)	1/0
		Standard Poodle (4/15)	4/0
		Shih Tzu (1/2)	1/0
		French Bulldog (1/4)	1/0
		Border Terrier (1/1)	1/0
		Yorkshire Terrier (1/65)	1/0
		Miniature Schnauzer (1/11)	1/0
		Friesian Stabyhoun (1/2)	0/1
4537777	g146t	Grey Wolf (2/4)	1/1
4537787	g156a	Mixed Breed (1/6)	1/0
4537800	t169g	Old English Sheepdog (1/1)	1/0
		Standard Poodle (2/15)	2/0
4537812	a181g	Labrador Retriever (1/7)	1/0
		Cavalier King Charles Spaniel (1/3)	1/0
		Weimaraner (1/1)	1/0
		Welsh Springer Spaniel (1/3)	1/0
		Pomerainian (1/4)	1/0
4537887	g256a	Grey Wolf (1/4)	1/0
4537930	g299a	Yorkshire Terrier (1/65)	1/0
4538025	g394a	Grey Wolf (1/4)	1/0
4538046	g415a	Grey Wolf (1/4)	1/0
4538075	a444g	Bichon Frise (1/4)	1/0
		Pug (2/17)	2/0
4538122	c491t	Border Collie (1/36)	1/0
		Leonberger (28/45)	19/9
		Mixed Breed (1/6)	1/0
		Rottweiler (1/2)	1/0
		Tibetan Mastiff (2/10)	2/0
4538311	c680t	Cavalier King Charles Spaniel (1/3)	1/0
4538313	g682t	Cavalier King Charles Spaniel (1/3)	1/0
4538353	c722t	Chinese Indigenous Dog (1/28)	1/0
4538361	t730a	Alpine Dachsbracke (2/2)	2/0
		American Staffordshire Terrier (2/3)	1/1
		Bearded Collie (7/11)	7/0
		Border Collie (26/36)	19/7
		Bavarian Hound (1/1)	1/0
		Standard Bull Terrier (2/4)	2/0
		Bullmastiff (1/2)	1/0
		Dogue de Bordeaux (3/6)	3/0
		Cane Corso (1/1)	1/0
		Curly Coated Retriever (5/5)	5/0
		Wirehaired Dachshund (1/1)	1/0
		Chinese Indigenous Dog (5/28)	5/0
		German Shepherd (2/17)	2/0
		English Mastiff (2/2)	2/0
		Eurasier (1/2)	1/0

		Friesian Stabyhoun (1/2)	1/0
		Havanese (2/3)	2/0
		Heideterrier (1/1)	1/0
		Unknown Breed (1/1)	1/0
		Irish terrier (1/3)	1/0
		Irish Wolfhound (2/3)	1/1
		Swedish Vallhund (1/2)	1/0
		Lagotto Romagnolo (1/5)	1/0
		Pug (7/17)	6/1
		Kerry Blue Terrier (1/1)	1/0
		Rhodesian Ridgeback (2/4)	2/0
		Scottish Deerhound (2/3)	2/0
		Pembroke Welsh Corgi (1/3)	1/0
		Portuguese Podengo (1/1)	1/0
		Yorkshire Terrier (11/65)	11/0
		Basset Bleu de Gascogne (1/1)	0/1
		Central Asian Shepherd Dog (1/1)	0/1
		Saluki (1/2)	0/1
		Staffordshire Bull Terrier (1/2)	0/1

In many cases where variant allele representation was low, only a limited number of the breed(s) carrying the variant were available. This limitation of the database makes it impossible to know how widely the variant allele might be distributed within a particular breed. Because of this, testing of the variants for functionality was not limited to variants with allele frequencies of above 0.05. All non-synonymous variations were tested based on the possibility that they may be prevalent in some specific breeds. The DBVDC is a constantly growing resource with additional genomes being added all the time. Future releases may contain greater numbers for individual breeds making more meaningful analysis of breed specific variation possible.

Calcium mobilisation from the variant receptors was expressed as a percentage of the response from the WT receptor when stimulated with 5mM 6-nitrosaccharin. The 10mM concentration of 6-nitrosaccharin caused a complete loss of response in the cells, with these points showing only baseline fluorescence levels. This data was excluded from further analysis. Inhibitory effects of high concentrations of this compound have been noted previously in other assay systems (Pronin *et al.*, 2004).

Based on the logEC_{50} values, only one variant, dTas2r1$_{A241V}$, was identified as being significantly different (Table 4.5). However, this result is may be an artefact of the

curve fitting procedure. The curves for this variant are similar to the wild type, but poor definition of the E_{max} for the 5mM concentration cause a marked increase in the logEC_{50} values for these curves (Figure 4.7 and Table 4.5). As the curves do not reach a plateau, due to the loss of signal at the 10mM concentration, it was difficult to know if this indicated a true change in potency.

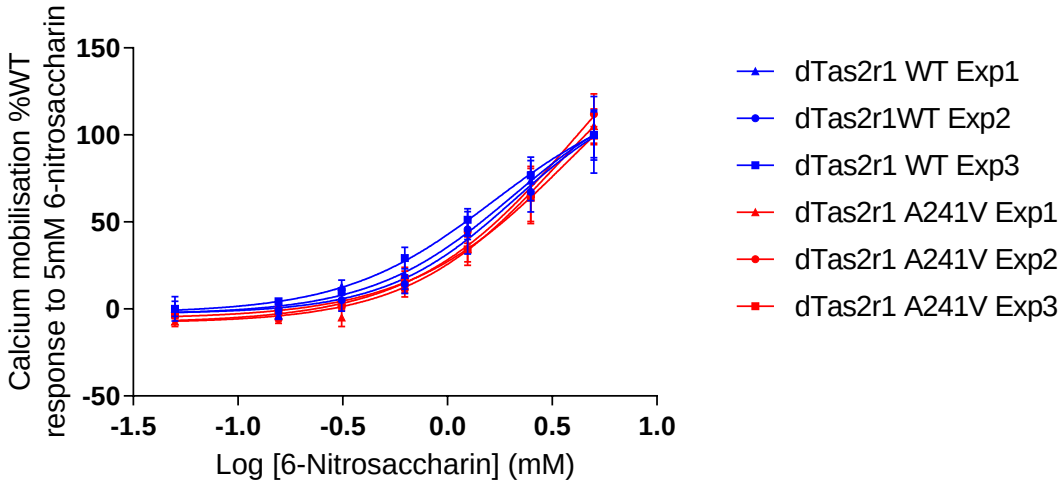

Figure 4.7: Concentration-response data for the dTas2r1$_{A241V}$ variant compared to the WT receptor with 6-nitrosaccharin
Individual experiments (error bars represent mean± SD from quadruplicate wells) are presented, expressed as a percentage of the 6-nitrosaccharin WT response at the maximal testable concentration of 5mM (n=3). Non-linear regression curves were used to calculate EC_{50} and E_{max} values, which are presented in Table 4.4.

The E_{max} analysis was more predictable, in that receptor variants showing a complete loss of response to 6-nitrosaccharin also gave a significant change in the E_{max}. Three variants exhibited this signal loss, namely dTas2r1$_{V14E}$, dTas2r1$_{G100E}$ and dTas2r1$_{G132E}$ (or t41a, g299a and g394a). In these cases baseline levels of fluorescence remained similar to the WT receptor but no response to any concentration of 6-nitrosaccharin was seen (Figure 4.8).

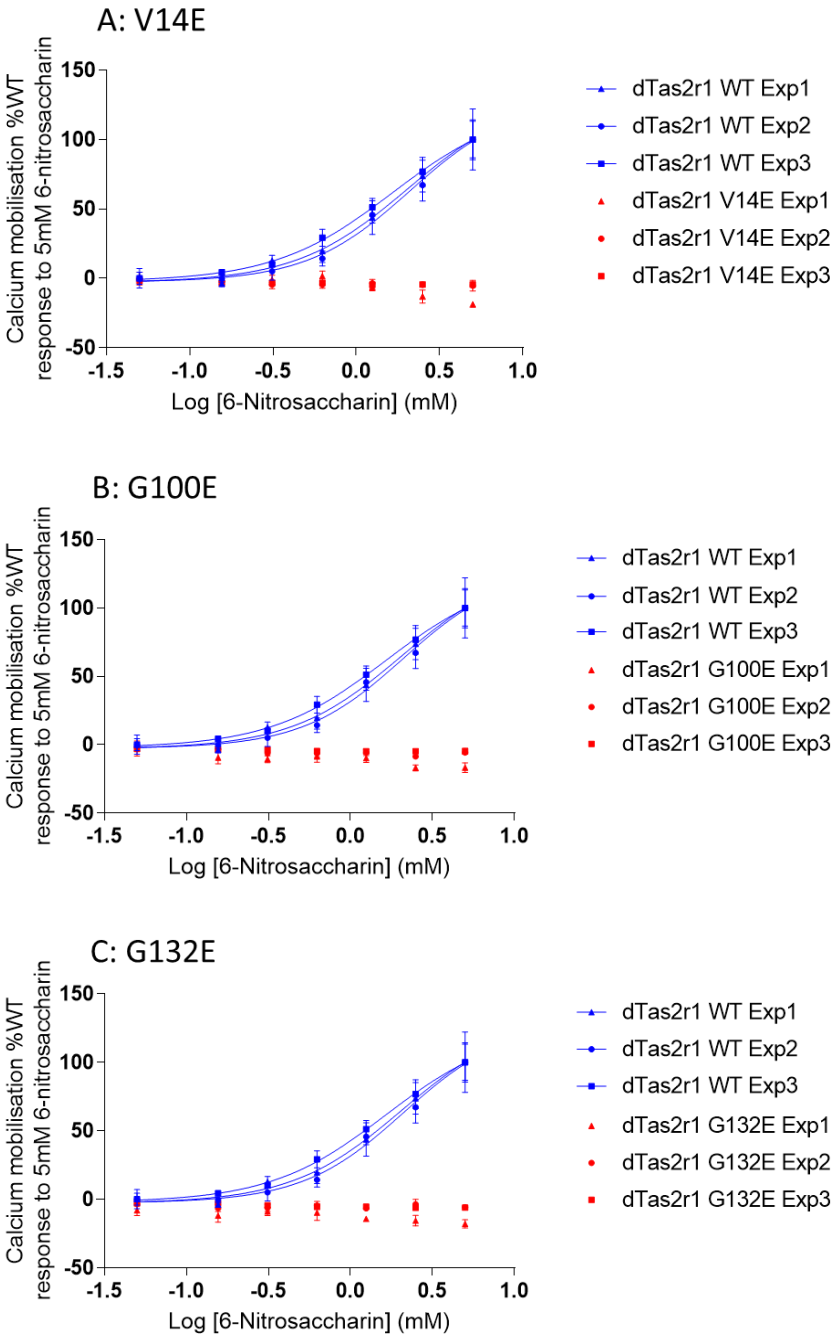

Figure 4.8: Concentration-response data for the dTas2r1$_{V14E}$, dTas2r1$_{G100E}$ and dTas2r1$_{G132E}$variants compared to the WT receptor with 6-nitrosaccharin
The V14E (A), G100E (B) and G132E (C) variants discovered in dTas2r1 lead to a loss of calcium mobilisation response to 6-Nitrosaccharin. Individual experiments (error bars represent mean± SD from quadruplicate wells) are presented, expressed as a percentage of the 6-nitrosaccharin WT response at the maximal testable concentration of 5mM (n=3). Non-linear regression curves were used to calculate EC_{50} and E_{max} values, which are presented in Table 4.4.

Two other variants altered the E_{max}, dTas2r1$_{A52T}$ (g156a) and dTas2r1$_{S227F}$ (c680t). In both cases, visual observation of the curves suggested that these differences were in agreement with the overall curve fitting (Figure 4.9). The dTas2r1$_{A52T}$ variant resulted in a slight reduction in the E_{max} while the dTas2r1$_{S227F}$ variant showed an increase in the E_{max}.

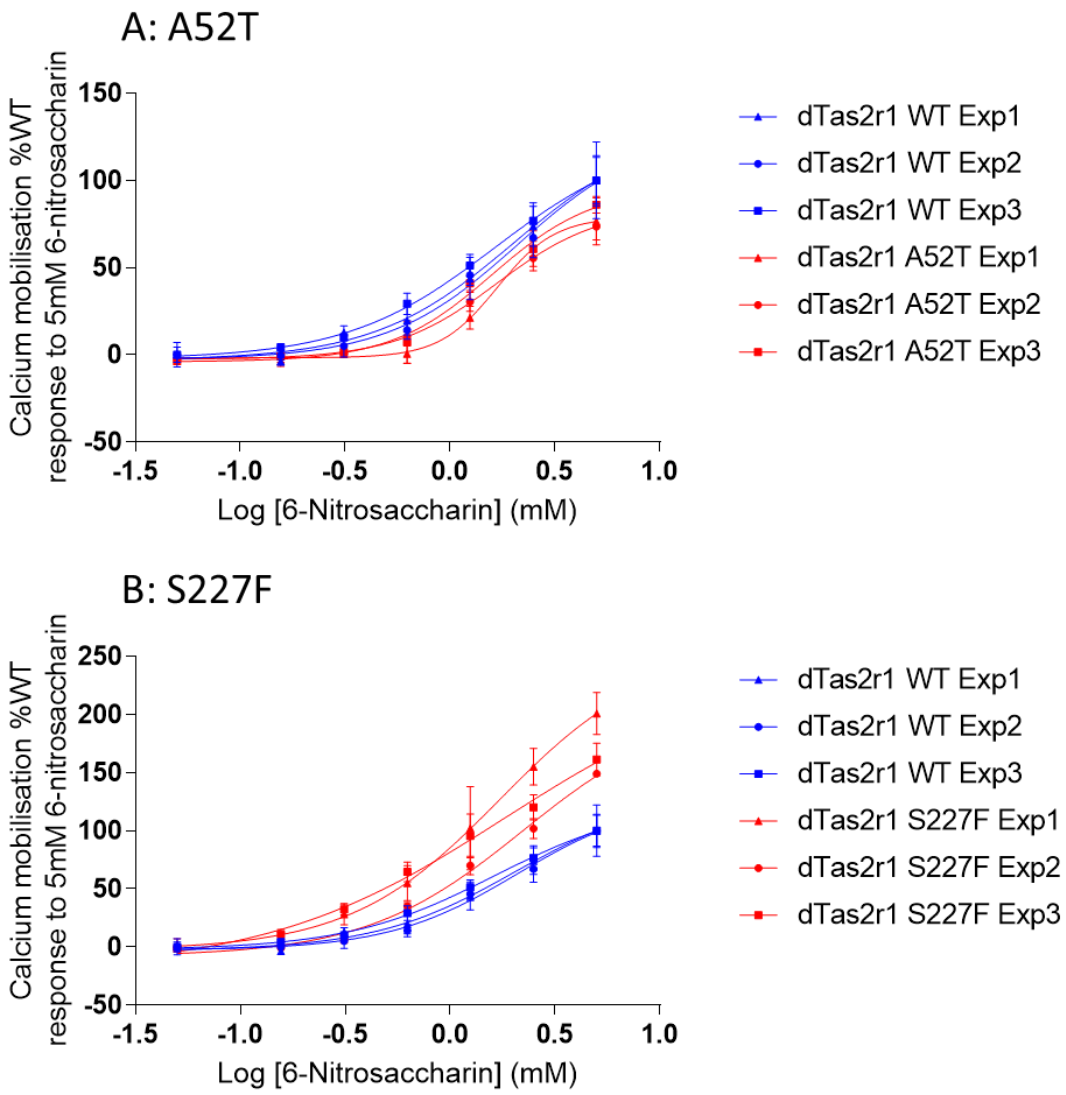

Figure 4.9: Concentration-response data for the dTas2r1$_{A52T}$ and dTas2r1$_{S227F}$ variants compared to the WT receptor with 6-nitrosaccharin
Individual experiments (error bars represent mean± SD from quadruplicate wells) are presented, expressed as a percentage of the 6-nitrosaccharin WT response at the maximal testable concentration of 5mM (n=3). Non-linear regression curves were used to calculate EC_{50} and E_{max} values, which are presented in Table 4.4.

The remaining variants investigated did not lead to significant changes in potency or maximal response compared to WT (Table 4.5). Of note however, the dTas2r1$_{V86M}$ variant lead to a reduction in 6-nitrosaccharin E_{max} that was close to significance (p=0.052) and may warrant further investigation. Another two variants gave results that may indicate a change in the E_{max} value, dT2R1$_{V86M}$ (g256a) and dT2R1$_{A241V}$ (c722t). Visual inspection of the data for dT2R1$_{V86M}$ supported the possibility of a difference in E_{max}, and this variant may also warrant further investigation alongside

those called as significant (Table 4.4). Charts showing the response curves of all the variants compared to the wild type receptor not shown here are presented in Appendix 4.1. A summary of the statistical analysis of the data presented in Table 4.4.

Table 4.4: Summary of concentration-response data in the calcium mobilisation assay for WT and variant dTas2r1

Data for all variants was compared to WT. Significant differences based on analysis by unpaired t-test for $logEC_{50}$ or E_{max} values are indicated by *p*-values ≤0.05 and are marked with "*".

Variant	$logEC_{50}$ mean (± SEM)	$logEC_{50}$ Adjusted *p*-value	E_{max} mean (±SEM) (%WT response to 5mM 6-nitrosaccharin)	E_{max} Adjusted *p*-value
WT	0.283 (0.027)	-	131.7 (1.8)	-
dTas2r1V14E	-3.677 (0.365)	0.777	11.9 (5.8)	0.005*
dTas2r1L48F	0.525 (0.077)	0.527	145.1 (13.8)	0.728
dTas2r1A52T	0.218 (0.006)	0.596	89.2 (4.6)	0.022*
dTas2r1C57G	0.299 (0.054)	0.995	146.1 (9.1)	0.618
dTas2r1I61V	0.133 (0.021)	0.235	162.0 (15.5)	0.569
dTas2r1V86M	0.210 (0.009)	0.597	71.2 (9.4)	0.052
dTas2r1G100E	-0.534 (0.131)	0.123	3.1 (1.1)	0.001*
dTas2r1G132E	-0.223 (0.194)	0.588	5.6 (1.3)	0.001*
dTas2r1V139I	0.455 (0.089)	0.688	203.9 (28.7)	0.485
dTas2r1A164V	0.273 (0.005)	0.995	118.8 (4.6)	0.485
dTas2r1S227F	0.282 (0.027)	0.995	245.6 (12.2)	0.018*
dTas2r1V228F	0.609 (0.035)	0.051	172.1 (43.5)	0.728
dTas2r1A241V	0.573 (0.051)	0.036*	192.7 (9.1)	0.051
dTas2r1L245M	0.424 (0.023)	0.596	233.6 (21.1)	0.113

4.4.4. Cell surface expression of dTas2r1 variants

In order to confirm that all variants of the d*Tas2r1* receptor were being expressed equally, flow cytometry was used to determine levels of extracellular FLAG tag expression. Cells were initially gated to cover all cells, then subsequently gated for single cells only. FITC positive cells were clearly identifiable when compared to a control without the FLAG tag (Figure 4.10).

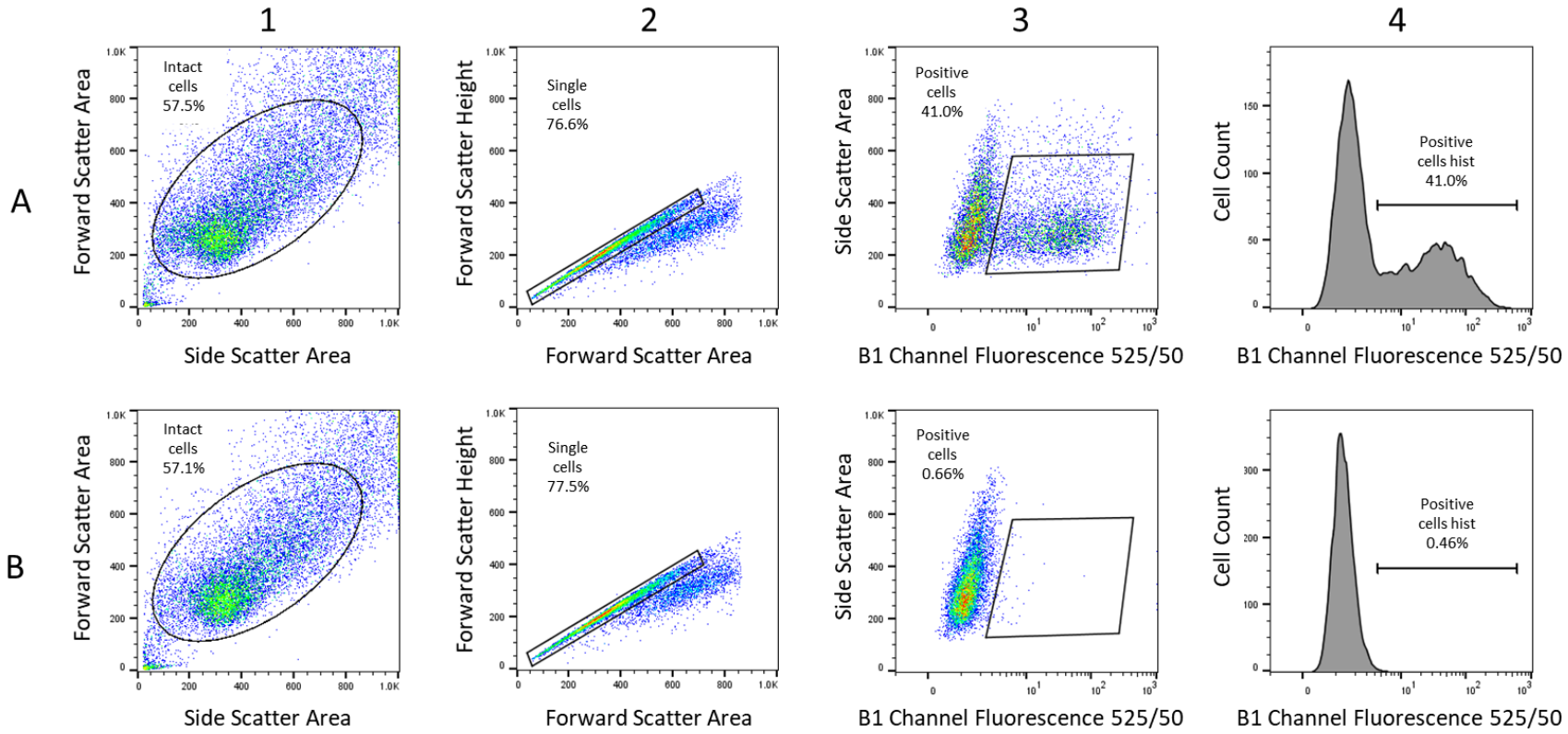

Figure 4.10: Analysis of receptor expression with flow cytometry

Gated cell populations for A) the FLAG labelled dTas2r1 WT construct and B) The WT construct without the FLAG label. 1) Intact cells were separated from debris by gating on forward and side scatter areas. 2) Single cells were separated from cell clumps by gating on forward scatter height and side scatter area. 3) Cells positive for surface expression of the FLAG label were quantified by gating all cells with elevated fluorescence on the B1 channel (525/50 filter). 4) A histogram representation of the labelled and unlabelled cell populations.

Most notably variants previously shown to result in a loss of signal to 6-nitrosaccharin in the calcium mobilisation assay also showed an almost complete lack of fluorescence, indicating that for these variants the receptor was not being expressed correctly at the cell surface (Figure 4.11). All other variants showed similar levels of fluorescence to that of the wild type receptor (Figure 4.12)

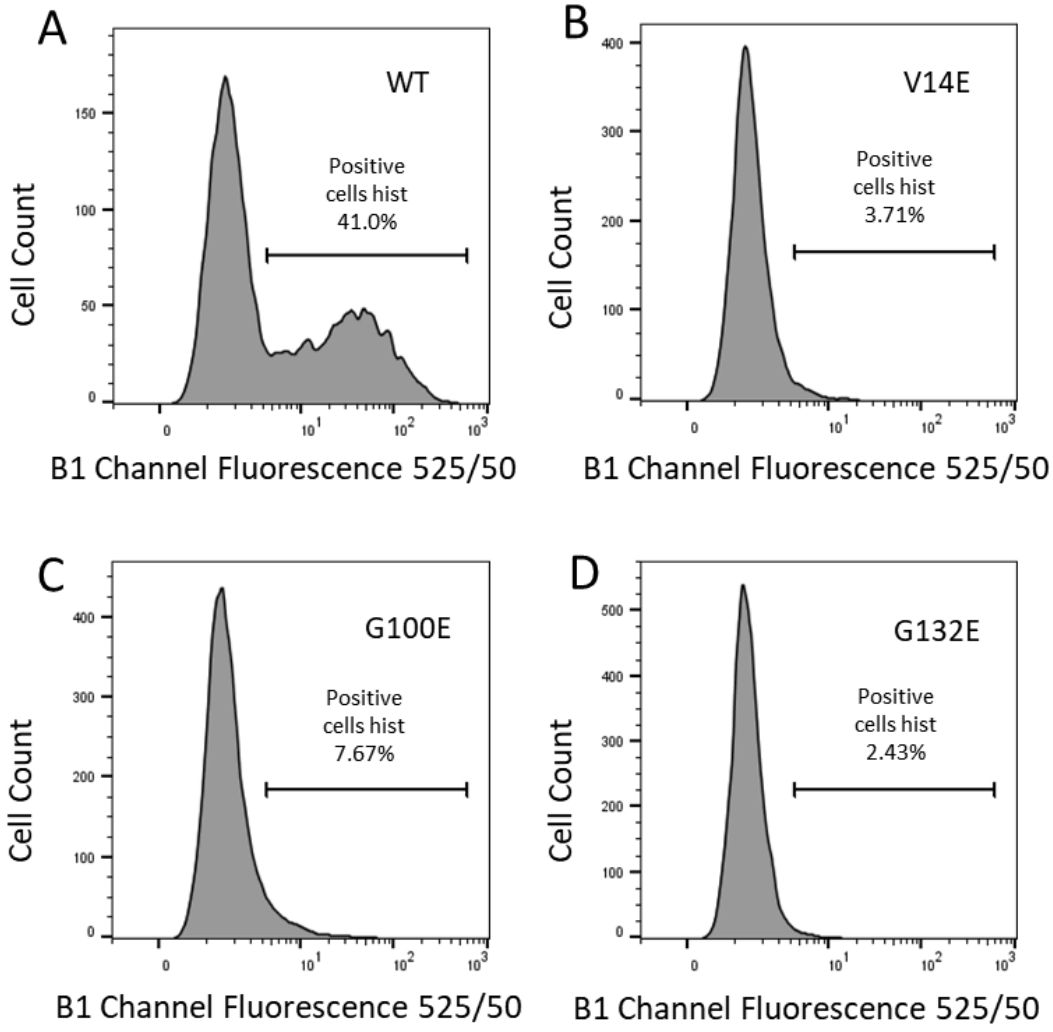

Figure 4.11: dTas2r1 variants previously shown to have almost no response to 6-nitrosaccharin also showed no FLAG labelling on the cell surface
A) Positive control with the WT receptor. B) dTas2r1$_{V14E}$ (t41a) variant. C) dTas2r1$_{G100E}$ (g299a) variant. D) dTas2r1$_{G132E}$ (g394a) variant. Elevated fluorescence in the B1 channel indicates expression of the FLAG labelled receptor at the cell surface.

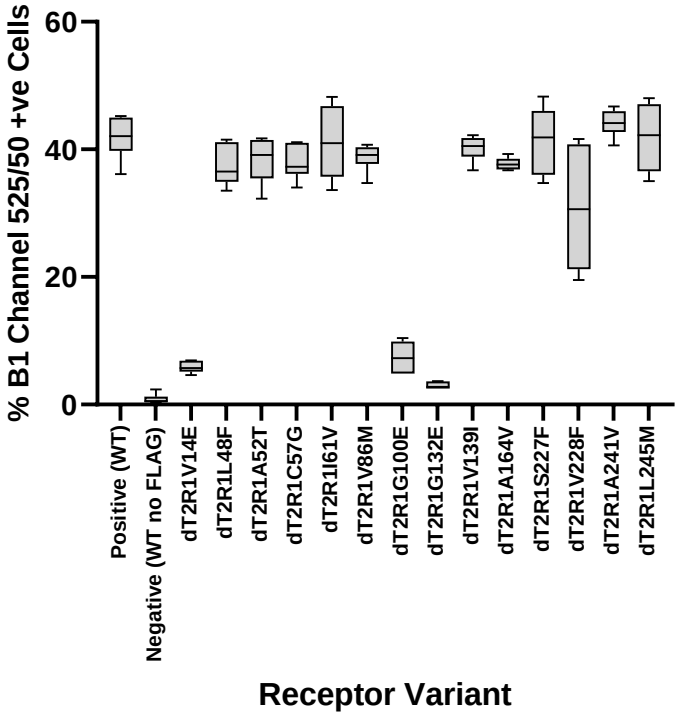

Figure 4.12: Summarised data from flow cytometry experiments with dTas2r1 variants (n=2) with three technical replicates from each
Median, interquartile range, maximum and minimum values are represented. Three variants (dTas2r1$_{V14E}$, dTas2r1$_{G100E}$ and dTas2r1$_{G132E}$) showed almost no FLAG detection indicating they were not well expressed at the cell surface.

4.5. Discussion

4.5.1. Functional variation in d*Tas2r1*

The functional impact of variation in the gene sequences of *Tas2r*s has been studied in several different species including humans (Bufe et al., 2005; Soranzo et al., 2005; Pronin et al., 2007), several other primate species (Wooding et al., 2006; Purba et al., 2017; Widayati et al., 2019), mice (Chandrashekar et al., 2000) and lemurs (Itoigawa et al., 2019). There has been a great deal of interest in the link between bitter sensitivity and diet choice in humans, with an emphasis on the impact of polymorphisms in the *TAS2R38* gene (Dinehart et al., 2006; Hayes et al., 2013). This chapter investigated the existence of functional *Tas2r* polymorphisms in dogs. It also attempted to investigate the impact of selective breeding on the distribution of such polymorphisms in different dog breeds.

Functional polymorphisms previously identified in humans did not appear to occur in dogs. The most studied PAV/AVI polymorphisms occurring in human TAS2R38 (Bufe *et al.*, 2005) were not variable in any of the dogs analysed in this study. Other polymorphisms identified in human TAS2R43 were also either not present in dogs or showed different variations.

However, dogs did show a comparable level of variation within their *Tas2r* repertoire. Humans have between 1 and 12 non-synonymous SNPs per *TAS2R* (Kim *et al.*, 2005) , with an average of 4.2 variants per gene. The same data for dogs is comparable, with 1-16 non-synonymous SNPs per gene and an average of 5.4. On an individual basis, dogs had between 0-34 coding variations with an average of 18. Notably, the three wolves in the DBVDC had a higher average of 29 coding variations per individual, which may be due to the impact selective breeding has had on levels of overall genetic variation in dogs.

Investigating all coding variations in all 16 putative dog *Tas2r*s was beyond the scope of this chapter, and without any known functional variants from orthologous human genes available, other criteria were applied to select genes to evaluate. In Chapter 2, ligands were identified for a range of dog Tas2rs. In particular dTas2r1 had a selection of positive ligands and also showed a reasonable number of coding polymorphisms in the analysis of the DBVDC data. Therefore, all coding polymorphisms for dTas2r1 were investigated for functionality with one of the discovered ligands from Chapter 2.

The 15 identified coding variations for d*Tas2r1* were spread across the length of the gene and varied widely in their prevalence. Six were present in a number of breeds, varying from 2-34. The other 9 variants were present in only one breed or the Grey Wolf. In most cases dogs were heterozygous for the variation. The exceptions to this were the dTas2r1$_{V14E}$ (t41a) variant that appeared as a homozygote in the Fresian Stabyhoun breed, the dTas2r1$_{L48F}$ (g146t) variant that was homozygous in the Grey Wolf, the dTas2r1$_{A164V}$ (c491t) variant which appeared in multiple dogs of the

Leonberger breed, and the dTas2r1$_{L245M}$ (t730a) variant which appeared as a homozygote in 8 out of the 34 different breeds in which it was present (Table 4.3).

Prior to generating d*Tas2r1* variants by site-directed mutagenesis a FLAG tag was added to the expression construct for d*Tas2r1* by gene synthesis. The FLAG tag was added to the N-terminal region of the receptor construct, in front of the plasma membrane targeting sequence from the r*Sstr3* gene. This was similar to a strategy used previously in *Tas2r* research involving human and cat receptors (Sandau *et al.*, 2015). In this study the FLAG tag was also positioned at the N-terminal. The inclusion of the FLAG tag made no difference to performance of dTas2r1 when testing with the ligand 6-nitrosaccharin.

Use of the Agilent QuickChange II system for site-directed mutagenesis resulted in successful incorporation of all the identified variants with one exception. Despite two attempts to incorporate the a444g variant, only wild type sequence was seen after DNA extraction and sequencing. It is not clear why this variant was not incorporated successfully. The process for primer design and mutagenesis was the same for all variants.

The remaining 14 variants were tested for functionality with 6-nitrosaccharin in a calcium mobilisation assay as described in Chapter 2. Three variants resulted in a complete loss of signal in the assay, namely dTas2r1$_{V14E}$ (t41a), dTas2r1$_{G100E}$ (g299a) and dTas2r1$_{G132E}$ (g394a). These changes all fall within transmembrane regions (I, III and IV) as can be seen in Figure 4.13. Analysis of receptor transfected cells by flow cytometry showed that these variants were not expressed at the cell surface and are presumably retained intracellularly, as has been reported previously for some artificially induced variations in Tas2rs (Singh *et al.*, 2011). The variations dTas2r1$_{G100E}$ and dTas2r1$_{G132E}$ were rare, but the dTas2r1$_{V14E}$ was more prevalent, appearing in 8 different breeds as a heterozygote and one as a homozygote (Table 4.3).

Naturally occurring mutations that lead to intracellular receptor retention and disease are well known in other GPCRs (Tao *et al.*, 2018). For example the majority of mutations that occur in human rhodopsin, causing the disease retinitis pigmentosa, result in misfolding, receptor retention in the ER and instability (Athanasiou *et al.*, 2018). The human luteinising hormone receptor (LHR) has also been found to harbour mutations that impact on receptor function, and can cause Leydig cell hypoplasia in males, and hypergonadotropic hypogonadism and primary amenorrhea in females (Toledo *et al.*, 1996; Latronico *et al.*, 1998). Of 22 mutations previously identified in LHR seven have been shown to have impaired trafficking to the plasma membrane (Tao, 2006). Another pituitary gonadotrophin receptor, the human follicle-stimulating hormone receptor also carries mutations that show a lack of receptor function due to intracellular retention (Beau *et al.*, 1998; Rannikko *et al.*, 2002). The human V2 vasopressin receptor carries over 190 mutations linked with the disease nephrogenic diabetes insipidus. Of these over 70% of the functionally characterised mutants show intracellular retention. Other examples of human receptors known to contain mutations that cause intracellular retention include the thyroid-stimulating hormone receptor, the melanocortin-1 receptor, melanocortin-3 receptor, melanocortin-4 receptor and the C-C chemokine receptor type 5 (Tao, 2006).

The mechanism by which the dTas2r1$_{V14E}$, dTas2r1$_{G100E}$ and dTas2r1$_{G132E}$ variants might cause intracellular retention was not investigated as part of this study. In the case of human rhodopsin, many mutations are related to the disruption of a disulphide bond between ECL1 and ECL2 (Stojanovic *et al.*, 2002). However all three dTas2r1 variations found here occur within the transmembrane helices. Both valine and glycine are non-polar amino acids without electrically charged side chains. Glutamic acid has a negatively charged side chain, which could disrupt helix packing and hydrophobic interactions within the transmembrane region.

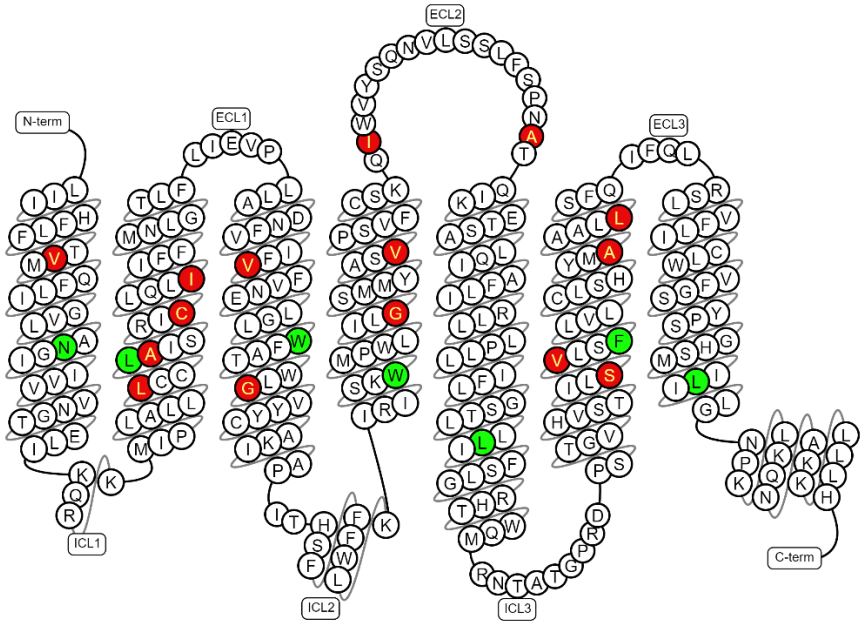

Figure 4.13: 2D representation of dTas2r1 generated with GPCRdb (Pandy-Szekeres et al., 2018)
Variations identified as part of this project are highlighted in red. The most conserved residues for Tas2rs as identified by Singh *et al.* (2011) are highlighted in green. Conserved residues are identical to those for hTas2r1 except for TM4 where the human sequence has a leucine residue.

Two other variants caused minor modulation of the receptor response. The dTas2r1$_{A52T}$ (g156a) variant located in TM2 resulted in a slightly suppressed E_{max} value in the calcium mobilisation assay. This change from a non-polar alanine residue to a polar threonine residue appears to impact the efficacy with which 6-nitrosaccharin activates the receptor. The dTas2r1$_{S227F}$ (c680t) variant located in TM6 also appeared to impact E_{max}, but in this case a slight increase in the efficacy with which 6-nitrosaccharin appeared to activate the receptor was observed. In this case, the change from serine to phenylalanine was a polar amino acid to a non-polar amino acid change.

The structural elements comprising the binding site for Tas2rs have been proposed to be different for different Tas2r receptors. In the case of hTAS2R1 Upadhyaya *et al.* (2010) proposed TM1, 2, 3 and 7 and ECL-1 and ECL-2 to be implicated in ligand

binding. Alternatively Dai *et al.* (2011) proposed TM3, 5, 6 and 7 as the regions associated with ligand binding, with a role for ICL2 in receptor activation. The binding site for hTAS2R10 has been proposed to involve TM3 to 7 (Born *et al.*, 2013). In humans, the primary receptor for 6-nitrosaccharin was shown to be hTAS2R43 using a GTPγS based assay using receptor expressed in Sf9 insect cell membranes and transducin. Variations between hTAS2R43 and hTAS2R31(44) in the region of TM2-TM5 were shown to harbour residues important for 6-nitrosaccharin interaction (Pronin *et al.*, 2004). In this context, a change within TM2 or TM6 of dTas2r1 could have a functional impact on receptor function, indicating both dTas2r1$_{A52T}$ and dTas2r1$_{S227F}$ can be reconciled with the published data.

The other variants tested had no impact on receptor function in response to 6-nitrosaccharin. The variant dTas2r1$_{L48F}$ (g146t) showed a change where both versions have non-polar amino acids, although leucine does have a positively charged side chain whilst that of phenylalanine is hydrophobic. The dTas2r1$_{C57G}$ (t169g) version of the receptor is an example where both cysteine and glycine are non-polar uncharged amino acids. All other remaining tested variants, namely dTas2r1$_{I61V}$ (a181g), dTas2r1$_{V86M}$ (g256a), dTas2r1$_{V139I}$ (g415a), dTas2r1$_{A164V}$ (c491t), dTas2r1$_{V228F}$ (g682t), dTas2r1$_{A241V}$ (c722t) and dTas2r1$_{L245M}$ (t730a) represent changes within the group of non-polar, neutrally charged amino acids with hydrophobic side chains, which would appear to be in line with their lack of impact on receptor responses.

4.5.2. Distribution and expression of d*Tas2r1* variants

While the DBVDC was an invaluable resource in the course of this work, the database does currently have some limitations. In particular, the low representation of many breeds makes assessment of the prevalence of some of the identified variations impossible to determine. For example the dTas2r1$_{V14E}$ variant that resulted in reduced cell surface expression of the receptor *in vitro* was found as a homozygote only once in the database in 1 of 2 Friesian Stabyhouns. Without genotypes for more dogs of this breed it not possible to speculate on the impact of this on the taste perception of this breed. It is also not clear if the receptor would be expressed

normally in a native taste receptor cell. Intracellular retention is often a problem in heterologous cell models, but for the Tas2rs the use of export tags like the rat Sstr3 tag used here have largely solved this problem. Using this tag, it was previously shown that all human Tas2rs were expressed at the cell membrane successfully (Meyerhof *et al.*, 2010).

Further research could investigate if other strategies might be more applicable when studying the impact of receptor variations. The rSstr3 tag certainly is useful for studying Tas2r receptor function, but other strategies have been explored. Some class A GPCRs require the co-expression of accessory proteins to translocate correctly in HEK based cell models. For example, *in vitro* expression of some receptors from the class A GPCR olfactory receptor family can be achieved only with the co-expression of accessory proteins such as receptor transporting protein 1 (RTP1), RTP2, resistance to inhibitors of cholinesterase 8 homolog B (Ric8b) and RTP1S or a combination thereof (Saito *et al.*, 2004; Zhuang *et al.*, 2007; Zhuang *et al.*, 2008). Members of the RTP and receptor expression enhancing protein (REEP) families were shown to enhance expression of some hTAS2Rs *in vitro* when no rSstr3 or other export tag was included (Behrens *et al.*, 2006). Co-immunostaining with subcellular markers showed that some hTAS2Rs with poor expression were localised within the trans-Golgi compartment, indicating that they had passed the quality control mechanisms of the ER. This suggests that lack of expression was due to poor localisation rather than misfolding (Behrens *et al.*, 2006). It was also found that some hTAS2Rs would express well in HEK293T cells without the addition of an export tag or an exogenous accessory protein, while other hTAS2Rs did not. This was explained by the discovery that some members of the REEP family were expressed endogenously in HEK293T cells. They were also found to be expressed in human circumvallate papillae and testis, two sites of hTAS2R expression (Behrens *et al.*, 2006). It may be interesting to observe the impact of sequence variants in Tas2rs in a system where exogenous (or endogenous) accessory proteins are used without the influence of an export tag, although the conditions may need to be different for each Tas2r tested. It is also likely that some Tas2rs will not express well without an export tag, regardless of the accessory proteins used.

It is not clear if individual dogs in the DBVDC are closely related as family pedigree records are not included within the metadata distributed with the .vcf file. Several of the identified variants showed evidence of increased prevalence in one or more dog breeds. In particular, the dTas2r1$_{I148M}$ (c491t) variant was common in the Leonberger breed, but almost completely absent in the other breeds within the DBVDC. The dTas2r1$_{I148M}$ variant did not impact on the function of the receptor with 6-nitrosaccharin and coded for a change to an amino acid with similar properties to the reference isoleucine. This variant is likely to have become prevalent in this breed due to the effects of selective breeding within a small population of related individuals. The Leonberger breed was created in the mid-1800's, but is reported to have been reduced to only a handful of individuals over the course of the first and second world wars (Lusby *et al.*, 2005). With such a small population it is easy to imagine how seemingly harmless variations may have become common in the breed. Even deleterious variations can accumulate in some dog breeds, leading to a high incidence of particular diseases (Donner *et al.*, 2018).

The majority of the identified variants in d*Tas2r1* occurred as heterozygotes. Differences in allelic expression have been linked to bitter taste sensitivity. It was previously shown that in human TAS2R38 PAV/AVI heterozygotes, expression of each version of the gene varied widely between individuals, but bitter taste perception was correlated with expression of the "taster" PAV version (Lipchock *et al.*, 2013). Therefore, heterozygous individuals are still of interest, but taste perception may be more aligned with expression level of the most sensitive haplotype than with genotype alone. Of course haplotype plays an important role, but as a high impact functional variation for dTas2r1 was not identified here, the haplotype of the dogs was not explored further.

4.5.3. Summary

Without prior knowledge of an existing phenotype with regards to bitter perception in dogs of different breeds, *in vitro* analysis such as that conducted here could lead to useful insights into variation in bitter taste perception in dogs. Testing all coding

variants in all deorphanised dog bitter receptors was beyond the scope of this Chapter. However, this is not an unreasonable objective given that instruments with much higher throughput for calcium mobilisation assays than the FlexStation are available (Chapter 2).

In the cell model used here, several naturally occurring variants in d*Tas2r1* caused a loss of receptor expression at the cell surface, presumably because they were retained intra-cellularly. Two of the variants were very rare, appearing in only one of 65 Yorkshire Terriers or in the ancestor of the dog, the Grey Wolf. One of the variants was somewhat more common in dogs, with 9 breeds showing at least one carrier. The Standard Poodle in particular showed a higher incidence of this variation with 4 of 15 individuals being heterozygous. The Friesian Stabyhoun was the only breed to show a homozygous individual for the variant, but this was only one of two individuals of this breed in the database, and hence the prevalence of this variation in the breed as a whole cannot be predicted. Whether these variants are expressed normally in vivo is unclear. Further work in this area might include gathering genotype data for a larger sample of Friesian Stabyhouns to confirm the prevalence of this variant in that breed. If significant numbers of variant homozygotes were seen, it would also be interesting to test for dTas2r1 expression in native taste receptor cells of this breed. If disruption of dTas2r1 expression was observed, a further experiment with a taste panel of these dogs might confirm specific bitter taste perception deficiencies.

In Chapter 2 nine ligands for dTas2r1 were identified. Only 6-nitrosaccharin was tested with the variants identified here. Further testing with other ligands of dTas2r1 may reveal other consequences of these variations. In many cases testable ligand concentrations in the calcium mobilisation assay were limited by compound solubility or by the occurrence of non-specific responses in the mock-transfected cells. Variant induced changes in ligand affinity or efficacy would be easier to identify if the assay was more sensitive. As discussed in Chapter 2 the sensitivity of the assay system used here was slightly lower than that used in other studies for some receptor-compound combinations. It is not clear if this is due to receptor expression,

G protein coupling or a combination of these, and other factors. Further optimisation of the expression vector or the assay protocol might help improve responses and make the impact of receptor variants easier to study.

Another option might be to remove dependency of the assay readout on successful G protein coupling by using an assay format that measures direct ligand binding. This would only be applicable where receptor variants were known to impact ligand binding, and not G protein coupling. There are many options for a binding assay of this type, all of which utilise a labelled ligand with either a radioactive, fluorescent or bioluminescent label (Stoddart *et al.*, 2016).

Phenotypic variation in dog breeds has accompanied their selection for other traits such as tameness, size and their ability to perform useful tasks. In some cases this selection has resulted in undesirable consequences such as increased susceptibility to disease. The impact on the sensory systems of the dog has only be studied in a few cases, and is often focused on the olfactory system. However, the taste system of dogs is also of interest and in particular the bitter taste receptors contain gene variability between breeds. As resources like the DBVDC expand it will become easier to identify interesting variants quickly. Also, expansion of the testing done here with more dog Tas2rs and a wider selection of receptor agonists may reveal many more interesting variations. A high impact functional variant equivalent to the PAV haplotype found in hTAS2R38 was not identified here, but only dTas2r1 was assessed. Such variation may be present in other dTas2rs and only a comprehensive analysis of all dog Tas2rs can answer the question of how much bitter taste variability exists in dogs completely.

Chapter 5. Final discussion

In this thesis, the repertoire of bitter taste receptors in the dog, their function, expression and their variation in different dog breeds was explored. Taste sensitivity in companion animals is of interest in the field of pet food manufacture. The creation and supply of commercially-prepared pet food offers a reliable, affordable and convenient option for pet owners who wish to feed a nutritionally-complete diet to their pets. However, there are many pressures on the formulation of commercial pet foods. The question of sustainability in relation to owning and feeding pet dogs and cats has been raised. Generally cats and dogs consume a higher proportion of their energy requirements from animal-derived material (33%) when compared to humans (19%) (Okin, 2017). This is associated with the greater environmental impact of animal protein consumption. A large amount of the animal protein used in the manufacture of pet food comes from by-products of the human food chain. However, ingredient selection varies widely for pet foods in different product categories, with premium or super-premium diets often containing higher quality meat products that can result in some competition for resources with the human food chain. Other factors such as pet obesity due to overfeeding and the selection of specific ingredients for pet foods also contribute to the environmental impact of the pet food industry (Swanson *et al.*, 2013). In response to this, and other factors such as volatile commodity prices, pet food manufacturers have an interest in the use of novel sources of protein, innovation in recipe formulation and flexibility in raw material use. Such changes can impact on the performance of a pet food product, and of particular interest is any negative impact on the palatability of the product. In contrast to humans, where detailed sensory information can be obtained about why one food is preferred over another, pets can only indicate their preference for a food product through their behaviour. Their behaviour around food, preference for one diet over another, and ultimately how much of a diet they want to consume can give information on their liking, but gives no information on why one diet is preferred over another. While some studies have shown that nutritional factors like macronutrient composition can influence preference (Hewson-Hughes *et al.*, 2013; Hewson-Hughes *et al.*, 2016), these require exposure to the diet over an extended

time period, and do not explain preferences on first exposure to new diets. In this case, it is most likely a combination of the flavour and texture of the diet that influences liking. Bitter tastes are usually associated with reduced liking or rejection. Knowing how sensitive dogs are to specific sources of bitterness, or being able to assess pet food products for sources of bitterness could be of benefit in the pet food manufacturing industry.

The second area where flavour, and specifically bitter taste, is of interest in pet dogs is the area of pet safety. Accidental poisoning of pet dogs is not uncommon, and in some cases bitter-tasting deterrents are used in an attempt to deter ingestion. The chemical agent used for this is denatonium benzoate because of its known strong bitter taste to humans. It is included in some brands of ethylene glycol-containing automotive antifreeze as a deterrent to ingestion by both humans and pets. However, some animals are known to be less sensitive to the taste of denatonium benzoate than humans, and so the efficacy of this strategy for dogs is not clear. Sensitivity to denatonium benzoate is governed in part by the sensitivity of the bitter taste receptors to this compound.

In both of these examples, a fundamental understanding of bitter taste receptor function in dogs provides useful information on the similarity in bitter taste perception between humans and dogs, which particular receptors are responsive to which compounds, and which compounds might be more or less bitter-tasting for dogs. This was one of the primary aims of this thesis, along with assessing expression of putative dog Tas2rs and identifying levels of functional variation in different dog breeds.

There are several studies that surveyed the dog reference genome to identify candidate bitter taste receptors (Go *et al.*, 2006; Dong *et al.*, 2009; Hu *et al.*, 2013; Shang *et al.*, 2017). In this study, the genome was also searched, but in addition to this the DBVDC database of dog genomes was analysed to make sure that no rare variants appeared in the reference sequence. A total of 16 putative bitter receptors were identified, which fits well with the semi-carnivorous nature of dogs, when

compared to a related obligate carnivore like the domestic cat (13 Tas2rs) or a classic omnivore like the human (25 TAS2Rs). As a result of work done to confirm the reference sequences, dTas2r4, which at the time was a pseudogene in the dog reference genome sequence, was found to be putatively functional, with a full length coding sequence. Screening of the receptor in the calcium mobilisation assay proved that this receptor could function as a bitter receptor (Gibbs *et al.*, 2017).

Confirmed gene sequences were used in testing of all 16 putative dog bitter receptors in the cell-based calcium mobilisation assay. In some cases, this revealed functional differences in ligand binding between dog and human orthologues, while in other cases common ligands were active with both dog, and the equivalent human receptor. Differences in sensitivity of orthologous receptors to the same compound were also identified, as were differences in tuning breadth between them. These data suggest that dogs have a well-developed sense of bitter taste, but that it is not directly equivalent to that of humans. Recognition of, and sensitivity to, certain bitter stimuli will vary between species while other stimuli may be perceived as similar. This work, and previous work comparing human and mouse receptors (Lossow *et al.*, 2016), show that at least part of this is due to differences in receptor ligand binding profiles and sensitivity. This highlights the potential pitfalls of extrapolating human taste perception of pet food products to the pets themselves. The dog-specific data generated here helps to reinforce the message that human sensory testing may be excellent for pet food product quality control purposes, but does not necessarily indicate how the product will perform with its eventual consumers.

The calcium mobilisation assay used here employed a novel G protein chimera, as opposed to the $G_{\alpha16/gust44}$ chimera that is most often used in the published literature. One of the main aims of this project was to validate the use of this system and expand upon the limited data that was available on its performance. The novel $G_{\alpha16/gust/o}$ chimera retained the first and the last 6 amino acids of the $G_{\alpha gust}$ sequence, which relate to the regions preceding the β6 sheet, and the C terminal region after the α5 helix (Ueda *et al.*, 2003). The rest of the sequence was substituted with the

corresponding $G_{\alpha o}$ sequence. The testing performed was partly intended to build a more comprehensive data set for this system, but was primarily aimed at discovering ligands for dog Tas2rs. Human receptors were also tested to allow comparison of responses with published data. In most cases ligands seen to activate human receptors here were in agreement with published ligands where the information was available. There was, however, a trend for thresholds of activation for human receptors to be slightly higher in concentration. There were also some instances where known ligands for human Tas2rs did not elicit an identifiable response here.

In order to address some of these inconsistencies, permission to use the $G_{\alpha 16/gust44}$-expressing cell line was obtained for the scope of this work only. Testing of all compounds in the library with dog and human Tas2r1 was performed and the data compared to that obtained with the $G_{\alpha 16/gust/o}$ cell line. The data were similar to that generated with the $G_{\alpha 16/gust/o}$ cell line, with no improvement in sensitivity and no additional ligands identified. This would point to some other factors in the assay as a source for the sensitivity issues experienced here. Many different factors might be the cause of this, including vector design, transfection procedures, instrument sensitivity or cell culture procedures. One obvious difference between the work conducted here and much of the published work was the instrument used for reading the calcium signal. Here a FlexStation or Hamamatsu FDSS/µCELL system was used, while much of the published work was conducted using a FLIPR system. Given these differences, the question of what impact the novel $G_{\alpha 16/gust/o}$ chimera might have on assay sensitivity cannot be fully addressed by the data collected here. In order to answer this question it would be necessary to conduct further experiments using both G protein chimeras in parallel, with a wider range of receptors and ligands. This would identify if differences in the G protein chimera, or the assay conditions were responsible for the differences seen between data generated here, and that published elsewhere.

Throughout all of the testing conducted here, only two instances were identified where a human receptor-ligand interaction with the $G_{\alpha 16/gust/o}$ cell line was not supported by the published data. Human TAS2R1 was previously reported not to

respond to (-)-α-thujone (Meyerhof *et al.*, 2010) and this was discussed in detail in Chapter 2. Also a response of hTAS2R7 was seen to the compound 6α-methylprednisolone. This combination was previously tested, but no response was seen (Li *et al.*, 2008). The rarity of this occurrence in the data suggest that the two different G protein chimeras are similar in their interactions with the receptors. This also indicates that responses seen with the dog Tas2r receptors and the $G_{\alpha16/gust/o}$ cell line would be replicated in the $G_{\alpha16/gust44}$ cell line, although further confirmation of this in future work would be reassuring.

The work conducted here indicated that while dog Tas2r10 was functioning and responsive to the human TAS2R10 ligand cucurbitacin B, it was not activated by denatonium benzoate. This was especially interesting given the use of denatonium benzoate as a bitter deterrent in automotive antifreeze and other products. Only one dog Tas2r was found to respond to this compound, dTas2r4, with a threshold of 400µM. Previously-generated *in vivo* data for dogs shows aversion to, but not complete rejection of, 100µM denatonium benzoate. These data suggest that the reduced sensitivity of dogs to denatonium benzoate is at least partly based on the relative insensitivity of their bitter receptors to this compound. While recommended concentrations of 67-111.5µM (30-50ppm) (ABA_Act, 2005) may be sufficient for deterring children from consuming a toxic household product, a higher level might be more effective for dogs.

Alternatively, if deterring ingestion by pet dogs was the primary concern, then some chemicals may prove to be more effective deterrents at low concentrations. In this study the naturally-occurring compound cucurbitacin B had the lowest threshold of activation of any positive compound. Cucurbitacin B is a member of a family of ~20 tetracyclic terpenes which are found in pumpkins, gourds and cucumbers. Toxicity among the family varies, but this has not prevented the exploration of these compounds as drugs, particularly in the field of cancer therapy (Alghasham, 2013). In mice 14mg/kg is listed as the LD50 for an oral dose of cucurbitacin B, while denatonium benzoate has a LD50 of 560mg/kg. However, cucurbitacin E has an oral

LD50 of 340mg/kg, which is not dissimilar to that of denatonium benzoate. The response of dog bitter receptors to cucurbitacin E was not evaluated here, but the sensitivity of *in vitro* mouse and human Tas2rs to cucurbitacin E and B has previously been published (Meyerhof *et al.*, 2010; Lossow *et al.*, 2016). This showed similar activation thresholds for cucurbitacin E and B within species, with mTas2r105 responding to 10µM and 30µM respectively, and mTas2r114 responding to 3µM in both cases. Human TAS2R10 responded to lower concentrations of 0.01µM in both cases while hTAS2R14 responded to 100µM concentrations of cucurbitacin B only. In comparison, the most sensitive human Tas2r for denatonium benzoate, TAS2R47, shows a threshold concentration of 0.03µM (Meyerhof *et al.*, 2010). In the experiments conducted here with cucurbutacin B, human and dog Tas2r10 had a common threshold concentration of 0.69µM, which would indicate that dogs might be more sensitive than mice to this compound, and perhaps as sensitive as humans. Further work could be undertaken to establish if a member of the cucurbitacin family might act as a potent bittering agent, useful in deterring accidental ingestion of toxic household substances by both humans and pets equally, at a concentration low enough to maintain an acceptably low risk of any toxicity. Such work should be approached with caution, as toxicity can vary greatly between species.

In order to determine if all putatively-identified dog *Tas2r* genes were in fact expressed in the taste papillae of the tongue, RNA-seq analysis was carried-out in dog fungiform taste papillae. Positive identification of expression in these samples proved to be challenging, as has been the case in other studies. The combination of low numbers of taste receptor cells, low levels of receptor expression and variation in expression levels between different papillae all contributed to this observation. However, in this study, it was essential to take a minimally-invasive approach to papillae sampling. Sampling of circumvallate papillae is much more difficult, due to the accessibility of the taste bud-containing papillae wall. It was not deemed possible to sample circumvallate papillae within the ethical constraints of animal care at Waltham.

Receptor expression was confirmed in many cases, regardless of the low expression levels observed. Perhaps most interestingly, receptor expression was shown not to be distributed uniformly in fungiform papillae from different areas of the tongue. Overall, *Tas2r* expression levels were significantly lower at the front of the tongue. While the perception of bitter taste is often associated with the back of the tongue, where the circumvallate papillae house many more *Tas2r*-expressing taste buds, there is less information on how bitter taste varies across the anterior portion of the tongue. One study looked at threshold responses to quinine from human fungiform papillae at different locations, and found a reduced sensitivity at the front (Collings, 1974), which would be in alignment with the data generated here. However, other studies are not in agreement with this (Doty *et al.*, 2016) and differences in methodology may be related to the lack of consensus (Colvin *et al.*, 2018). Replication of the work done here in humans or another model species, a larger sample set, or both may help to clarify this area. A targeted approach using qRT-PCR would be less costly, although pre-amplification techniques may make detection easier, as was the case for this study.

Selective breeding of dogs has had a major impact on their development as a species. However, the impact on their chemical senses has not been well-defined. Breed characteristics are sometimes associated with the sense of smell, with some breeds suggested to have a keener sense of smell due to their performance in olfactory-based tasks (Polgar *et al.*, 2016) . However, performance in such tasks can be related to breed temperament and performance in reward-based training, and is not necessarily related to their olfactory sensitivity (Hall *et al.*, 2015; Lazarowski *et al.*, 2020). Impacts of breeding on taste have not been previously described. This project aimed to establish if functional polymorphisms in bitter taste receptors of dogs might be present, as is the case for humans, and if there were any breed-associated differences in their distribution.

Testing all identified variants in all dog Tas2rs was not possible within the scope of this study. Instead, all identified coding polymorphisms in dTas2r1 were tested for their impact on the response of the receptor to the ligand 6-nitrosaccharin.

Surprisingly, three of the variants resulted in a near complete lack of expression, presumably as the receptor was retained intracellularly. Such variants are relatively common in GPCRs, and when present in other receptors can result in various medical conditions. Here, these variants were present mostly as heterozygotes, with only a few cases of homozygous variants being found. Still, it is intriguing that such variants were identified and further work to characterise the occurrence, frequency and impact of such variation should be conducted.

Other variants having an impact on the receptor response to 6-nitrosaccharin were identified, but the impact was subtle. A high-impact functional variant was not identified as part of this study, but may well exist in other dog Tas2rs. The work done here has the potential to be expanded, incorporating more ligands for dTas2r1 and more dog Tas2rs, particularly the ones deorphanised here. A better understanding of variation in dog bitter taste perception could help when trying to prevent accidental poisoning of dogs, and it would also reveal if dogs, like humans, show individual or breed-associated differences in their taste perception.

While research on the Tas2rs has progressed greatly since their discovery, one area where progress has not been as swift is the development of structural models. To date no Tas2r crystal structure has been determined, and due to their limited homology with other GPCR families existing models are considered to be low resolution (Di Pizio *et al.*, 2017; Behrens *et al.*, 2020). The possible reasons for this are varied. Until recently, Tas2rs were not considered to be drug targets, although they now represent a promising candidate for the development of new asthma medications. Also their low expression in anatomical structures containing a mixture of cell types makes their purification from these sources unattractive. They have also proved difficult to express in cellular models, and these factors have most likely contributed greatly to the current absence of a crystal structure.

Due to these limitations in structural modelling, a focus has remained on supporting analysis from homology models with *in vitro* data and mutagenesis experiments. The *in vitro* data generated as part of this study will certainly be a useful resource in

future modelling studies with dog Tas2rs, enabling initial model verification and refinement. A recently developed resource named BitterPredict (Dagan-Wiener *et al.*, 2017) demonstrates what can be achieved with the currently-available information on bitter tasting compounds contained within the BitterDB (Wiener *et al.*, 2012; Dagan-Wiener *et al.*, 2018). Here, a machine learning approach was combined with existing data derived partly from *in vitro* studies, to generate the BitterPredict classifier, a machine learning algorithm which achieved 70-90% correct classification of molecules as bitter. Although this approach was only able to classify molecules as bitter, with no indication of the level of bitterness, such approaches may become valuable in the food and drug industries in the future. Should one or more Tas2r crystal structures become available, structural models will become even more valuable sources of information.

Dogs have maintained their position as one of the preferred companion animals of man for many centuries, during which time they have transitioned from scavenging around human settlements to feeding on specialised diets designed to completely satisfy their nutritional needs. How dogs are fed will continue to change, and a better understanding of the sensory capabilities of dogs in relation to feeding will enable further innovation in the formulation and manufacture of dog food diets.

Appendices

Appendix 1.1: Dog *Tas2r* sequences used for primer design and gene synthesis.

d*Tas2r1*

atgttagagttttaccttattatccattttcttttcacagtgatgcaatttctcatcggggttttagcaaatggcatcattgtg
gtggtgaatggcactgagttgatcaagcagagaaagatgattcccttggctctccttctttgctgtctggcgatttccagga
tttgtctacaattgatcatcttcttcatgaatctgggtactctcttcttgattgaagtccccctacttgctgataattttgtaat
tttcgtgtttgtaaatgaattgggactttggttcgccacatggcttggggtttactactgtgccaagatcgcccccataactc
actcattctttttctggttgaagataaggatatccaagtggatgccatggctgatcctcgggtccatgatgtatgcatccgt
cccttctgttttctgcagcaaacagatatgggtttattcccaaaacgttttgtccagccttttttccccaaacgcaactcaaa
tcaaagaaacatctgctttacagattgcctttcttattaggttattattgccactgcttatctttctcggttccaccctacttttt
gatattttccctggggagacacacctggcagatgagaaacacagcaacaggccccagggaccctagcacaggtgtcca
cgtgagcacgatcctgtccgttctatccttcctggtcctctgcctctcccactacatggcagctgctttgctctcttttcagat
ctttcagctcagaagcctcgtctttctgatctgtctctgggtgtttgggtcctatccttctggacactctatgatcttaatttta
ggaaatcctaaattgaaacaaaatgcaaagaagctcctcctccacgggaagtgctgccagtga

d*Tas2r2*

atgatctccttttttgtcagctcttcctcatgttattgttatgtcagcagaatttatcacagggattacagtaaatggatttctt
atcatcatgaactgtaaagaattgatcaaaagcagaaagccaacaccagtgcaactccttttcatatgtatagggatgtc
gagatttggtctgctcatggtgttaatgatacaaagtttttttctctgtgttatttccactcttttataaggtaaacatttttggt
acagcaatgttgttcttttggatgtttttagctctgtcagtttctggtttgccacctgcctttctgtattttactgcctcaagat
agcaggcttcactcaatcctgttttctttggctgaaattcaggatctcgaagttaatgccttggctacttctgggaagtttgc
tggcctccatgagcattgcagctctgtgtattgaagcagattaccctaaaaaggtggatgatgatgccctcaagaatgcc
acattgaagaggactgaacccaagataaggcaaattagtgaaatgctgcttgtcaacttggcattactatttcctctagcc
atatttgtgatgtgcacttttatgttattcatttctctctataagcacactcatcggatgcaaaatggatctcatggtgttaga
aatgccagcacaaaagcccatataaatgcattaaaaacagtgataacattcttttgcttctttatttcttattttgctgcctt
catggcaaatatgacattcagtattccttatggaagtcattgcttctttgtagtaaaggacataatggcagcatttccctct
ggtcattcaattataatcctcctgagtaattctaaataccaacaacctttcaggagacttctctgcttcaaaaagaatcaat
ga

d*Tas2r3*

atgtcagggctggggaaatccgtgttcctggttctgtctgtcactcagttcattctggggatgctggggaatggtttcatag
tgttggtcaatggcagcagctggttcaagaacaagacagtctctttgtctgacgttatcatcactaacctggctctctccag
gattgttctgctgtggattctcttggttgatggtgttttaatggtcttcttttccaaagtacatgatgaagggacagtaatgg
aaattattgatattttctggacatttacgaaccacctgagcatttggcttgccacctgtctcagtgtcctctactgcctgaaa
attgccagtttctcccatccgacgttcctctggctcaagtggagagtttccagagtggtcgtacagatgattttgggtgcac
tgctcttatcgtgtgccagtgccatgtctctggtccatgaatttaagatctattctattctcagtggaattgctggtacaggg
aatgtgaccgagcactttagaaagaagagaaatgactataaagtggcccatgttcttgggactctgtggaacctccctcc
cctaattgtttctctggcctcctactttctgctcatcttctccctgggaaggcacacacagcagatgaagcacagtggcacc
agctccagagatctgagcacggaggcccaccagagagccatcaaaatcatcgtctctttcctctttctcttcctgctttact
ttcttgccttttaattacatcatccagttatttcataccagaaactgagatggttaagagagttggagtagttgttacaatg
ttttaccctgccagccactcattcgttatcattctgggaaacaataagctgaagcagatgtttacggagatgctgtgctgtg
agcctggttatctgaagcctggattcaaaagacctttgccccataa

d*Tas2r4*

atgcttcagatattctttttatctgccattattttctcagcaattttgaattttgtgggactcattgtaaatctgtttattgcagt
ggtcagttataggacttggctcaaaagccatagaatttcctcttctaattggatcctcttcagcttgggcatcaccagattt
cttatgctgggactgtttctactcaacatcatctacttcttcatctctccaaaaatggaaaggtcggtgcacctatcccactt
tttcctgtcgtgttggatgtttttggactctaatagtctctggtttgtaaccttgctcaatgccttgtactgcgtgaagattac
ggacttccaacttggagtatttctcctgctgaagcgaaatctctccccaaagatccccaggctgttgctagcctgtgtactg
atttctgccttcaccactctcctgtatgttgtgctcaaacagacatcatcccttcctgaatttgtgactcagagaaatggtac
aggatgtggcatccatgggagtgtcttgtctttggtgacctctttggtcttgcgctcagttctccagtttatcattaatgtgac
ttctgcttccttgttgatacattccttgaggagacatatacagaagatgcagaaaaacaccactatttttttggaatcctcag
actgaagctcatgtgggcgctatgaagctgatgatctgtttcctcatcctgtacattccttactcagttgctaccttgctaca
ttatttcccttatggtgggatggatttgagaaccagatccatctgtttggttatttccagcttttaccctccaggacattctat
tctcattatcctcacacatcctaaactgaaaacaaaagcaaagaagattctttgtttcaacaaatag

d*Tas2r5*

atgctgactgctgccctaccactgctgatggtggtggcagtggttgaatttctcattggcttggtgggaaatggagtcctta
tggtctggagttttggtgaatgggtcagaaaattcaacgggtcctcatacaacctcattgtcctgggcctggctgtctgccg
atttctcctgcagtgtctgattatgatggacttaagcctgtttccatttttccagagtagccgttggcttcactatctcagtat
cttctggatcctggtaagccaggccagcctgtggtttgccactttcctcagcgtcttctactgcaggaagatcatgaccctt
gaacatcctgtctgcttgtggctgaagcagagggcctattgcctgagtctctggtgccttctggtgtacctcatgatcagttt

gttacttgtagcacacattggcttaaagccctataatccttctcaaggcaacagcagcattctgtacccccttaaaagctg
gcactacctgtatatagtaaagctcaacgcaggaagtggattgcctctcatggtgtttcttgtttcttctgggatgctgattg
tctctttgtatagacaccacaagaagatggaggtacatacagctggtaggagagatgctcaggccaaggctcacatcac
tgtactgaagtccttgggctgcttccttatccttcatgtgatttatatcctggccagccccttttccattacctccaagtcttct
gctgatctcctcgttgtcttcatctctgagacagtcatggctgcctatccttctcttcattctgtcattctgatcctggggaatc
ccaggatgaagcagacttgtcagagaattctgtggaagacagtgtgtgcttggaaatcctag

d*Tas2r7*

atgccggataaagtggagagcatcttaatgctcgtagcagctggagaattttcaatggggattttagggaatacattcatt
ggattggtaaactgcataggctggatcaagaagaggaagattgcctccattgatttaatcctcacaagtctggccatatc
cagaatttgtctattatgtataatactattagattgttttatattggtgctgtatccagatgtctatgctaccggtaaacaaat
gagaataattgacttcttctggacactaaccaaccatttaagtgtctggtttgccacctgtctcagcattttctatttcctca
agattgcgaatttcttccatccccttttcctctggatgaagtggagaattgacagtgcgattcctaggatcctgctgggatg
cttggccctttctgtgtttattagccttgttgtcactgagaatttgaatgatgatttcagatgttgtgttaggacaaagaaga
aaacaaacttaactgtgagatgcagagtaaagaaagctaaatattcttccatcaagatttgcctcaacctgttaacgcta
ttcccctttctgtgtccctgatctcatttctcctcttgatcctctccctctggagacataccaggcagatgaagttcaatgcc
acagggtgtagagacttcagcatagaagcccacatgggagccatgaaagctgtcatctcctttctcctccttttcatcgcc
tactatttggcctttcttgtagccacctctagctactttatgccagagactgaattagctgtgatcattggtgagttgatagc
tctaatctatccctcgagccattcgtttatcctaattctggggagcaataaattaagacaggcatctctaagggtactatgg
aaagtaaaatatgtcttaaaaagaagaaacttctaa

d*Tas2r10*

atgctaagcatactggaaggcctcctcatttttatagctgttagtgaatcaatactgggagttttagggaatggatttattg
gacttgtcaattgtattgactgtgtgaagaacaaaaagttttctatggttggctttattctcactggcttagctacttccaga
atttgtctgatattgataataattacagatggatttataaagatattctctccagatatgtattcctctggtaacttaattgat
tatattagttacctatgggtaattatcaatcaatcaagtatctggtttgccaccagcctcagcatcttctatttcctgaagat
agcaaatttttcccaccacatttttctctggctgaagggtagaatcaatagcgttcttcccccttctgatgggatccttgtttat
ttcatggttatttacttttccacaaattgtgaagattattaatgataatagaatgaagagtagaaatacaacctggcagct
caacatgcagaaaagtgaattctttactaagcagattttactcaacctaggagtcattcttctctttactctatgcctgatta
catgtttcttgctaatcgtttccctttggagacacaacaggcacatgcaattgaatgtcactggactccgagaccccagta
cagaagcacatgtgaaagcaatgaaaattttggtatcttttatcatcctctttatcttgtattttataggcattgccatagaa
atatcatgtttcattctgccagaaaacaaactgctgtttatttttggtatgatgaccacagccatctatccctggggtcattc

atttatcctaattctaggaaacagcaagctaaagcaagcttctttgaagaccctgcagcaactcaagtgcgaggcaagg
agactgctcacagctgcacagatccatgtgggggaaatggatgttccaggagaataatctag

d*Tas2r12*

atggcaggcacaatgaagaatgtatttatgatgatttttgccggagaattcataatagggattttgggaaatggattcatt
atattggttaactgtatcgattggatcaggagctggaagttcttcctgattgactttattcttacctgcttagccatttccagg
atatttctgctgtgcataataatgttaggcataggtctagatataatttgtaaggaaatatggtacaatgataatcaactg
ataacctttgaagtcctctggacaggatgcaattatttctgcacaatctgtactgtgtgcctcagtgtcttctacttcctcaa
gatagccaactcttccaatcccattttcttctggctaaaacggagaattcacagactgcttctcattattgtcctgggagca
gtcttctatttctgcttgtccctgcttttgaaggatatagtatttaagaacatgatcaaaaccaaggtaaacactgaaagca
atgtgacattaaatttcacagcgagaaaatatgatttactaacttctaatatattcctgaacatgctattcgtcatccccttt
gcagtgtctctggcttcctttgtccttttgatccattccttatggaaccataccaggcggatgaagggcattgattctgggg
atcttatcacagaggcccatgtaagagccatgaagtttatgatttcattcctgctattcttctttatatactatttgagcaat
attataatatattttgcctatgttgttctggatagtctggtggcaaaaatttttgctaatatattagtattttcctatccttctg
gccatccatttcttctgattttatggaactgcaaattgaaacaggcttctctctatgtcctgaggaagctgaagtggtgcat
gaatctaaggaaacccgcatacataaagcatacctga

d*Tas2r38*

atgttggctctgactcctgttataactgtgtcctatgaagtcaagagtgcatttatgttcctttcagtactggagctcgcagt
ggggatcctgaccaatgccttcattttcttggtgaatttttgggatgtggtgaggaggcagccactgagcaactgcgatctt
atccttctgagtctcagcctcactcgacttttcctgcatgggctgctgtttctggatgccatccagcttacatacttccagcg
gatgaaagacccactgagcctcagctaccagaccatcatcatgctctggatgatcacaaaccaagctgggctctggctc
accacctgtctcagtcttttctactgctccaagattgtccgtttctctcataccctccttctctgcttggcaaactgggtctcc
aggaaggcaccccagatgctcctgggtgccatgcttttctcttctgcctgcactctcctctgtttgggggacttctttagtag
atctggctttgcattcacaactgtgctactcatgaataatacagaatttaattcacaaattgtaaaactcaatttctattatt
cctccatcttctgtaccctggggtcaatccctcctttcatgtttttttctggtttcttctggggtgctgattatctctctgggaag
gcacatgagaacaatgaaggccaacaccaaagactccggtgaccccagcctggaggcccatatcaaagcactcatatc
tctcatctcctttctctgcctctatgtggtgtcattctgtgttgcccttatctcagtgcctttaaccatggtgtggcacaacaa
gatcggggtaatgatctgtgtagggatcctagcagcttgtccctctatacatgcagccatcctgatctcaggcaatgccaa
gctgaggagagctgtggagaccattctactctgggttcagagcagccttaaggtaagggcaggccacagggcagatctc
aggactccagatctatgttga

d*Tas2r39*

atgatggaaacctgcaatcccccagaaaatgaattgtcaccatttggcatcctctcgattttaacaattacaggcactgaa
tgcatcgttggtatcattgcaaatgggttcatcatggctataaatgcggctgaatggattaaaaataagacagtttccaca
agtggcagagtcctgtttttcttgagtgcatccagaatagctctccaaagcttcacaatgctagaaattaccttcagttcaa
catccccacgtttttataatgaagatgttatgtatgacacattcaaagtaagtttcatgttcttaaatcattgtagcctctgg
tttgctgcttggctcagtttcttctacttcgtgaagattgctgatttctcccacccccttttttctcaagctgaagtggagaattt
ccagactgatgccctggcttctgtggctttcagtgcttatttccttgggctacagtatgctcctctccaatgacatctacact
gtgtattgtaacaattcttctatcccctcttccaactccactaagaaaaaatacttcactaagaccaatgtggtcaacctgg
ttcttctctataacctggggatcttcattcctctaatcatgttcatcctttcggccaccctgctgatcatctctctcaagagac
atacactacacatggaaagcaatgccactggctgcagggaccccagcatggaggctcacataggggccatcagagcga
ccagctactttctcattctctatattttcaattcagttgctctatttctctatatgtccaacatctttgatatcaacagctcctg
gaatattttgtgcaaattcatcatggctgcctaccctgctggtcactccattctgctgattcaggacaaccctgggttgaga
agagcctggaagcggcttcagcctcaagttcatttttacctaaaagagcagactccatga

d*Tas2r40*

atggccacagtgagcacagatgccacggatagagacatgtccaggtttaaaatcgtcctcaccttggtggtccccggaat
agagtgcctcactggcatcgttgggaatggcttcatcacaatcatccatggggccaagtgggccagaggcaaaaggctc
ccggtcactgactgcattctgctgatgctcagcttttccaggctcttactgcagatctggatgatgctggagaatatttaca
gtctactattccgggtcacttacaaccaaagcacagtgtttatagtcttcaaagtcactgtcattttcctgaactatttcaac
ctctggcttgctgcctggctcaacatcttctattgtctgagaatcacaaacttggctcaccatgtgttcttcatgatgaagag
gaaaatcacggagctgatgcctcggcttctgggactgtcactgttcatctccttatgcttcagctttcctttctctacagata
tcttccatgtgtacgtaaacagttccatccctatccgttcctccaataccaccgagaagaagtacttctctgagaccaatgt
ggtcaacctggttcttctctataacctggggatcttcattcctctgatcatgttcatcctttcggccaccctgctgatcatctc
tctcaagagacacacactacacatggaaagcaatgccactggctgcagggaccccagcatggaggctcactttggggcc
atcagagcgaccagctactttctcattctctacattttcaatgcagttgctctatttctttccatgtccaacatcttcgacatc
aacagctcctggaatattttgtgcaaaattgtcatggccgcctacccagctagccactcagtgctactgatcttgggtaac
cctgggctgagaagagcctggaagaggtttcagcaccatgttcctcttcacctgtaa

d*Tas2r41*

atgcagcccgccgtgtccgccttcttcatgctgctctttgtcctgctgtgtgtcctggggatcctggccaacggcttcatcgt
gctggtgctgagcagggagaggatgcggcgggggaggctgctcccctccgacgtgatcctccttagcctgggcgcctccc
gcttctgcctgcagtgcattgggatgatgaacaacttttactactacctccacctggaggagtacagcacgggcccggctc
ggcaattctttggcctccactgggacttcctgaactcggccaccttctggttcggctcttggctcagcgtcctcttctgcatg

aagatcgccagcttcacccaccccaccttcctctggctgaggtggcggctcccaggctcggtgccctggctcctcggggct
tccctcctgatctccttcctcgtcaccctgctcttcttttggggaaaccatgccgtgtatcaaggattcctaatcagaaaata
ccccgggaacatgaccttccagcagtggagcaggaggctggaaattcactatttcttgcccctgaaattcatcaccttgtc
agtgccttgctctgtcttcctggtgtccatcgcactgttgattaattccctgaggcgacacaggggaggatgcggcgcag
tggccacggcctgcaggaccccagcagccaggctcacaccagggctctgaagtccctcgtctccttcctcattctgtatgc
tctgtcctttgcgtccctggtcatcgatgctgcgggtttcttctgctcgcagagtgactggtactggccctggcagattttaa
tctacctgtgcacctctgtccatccctatatcctcatcctcagcaacctccggctccgaggggggtgcaggcagctacttct
gttggtcaggggctcccagctggcctag

d*Tas2r42*

atgttagctggattggatataatctttcttacactgtcaacagcagaattcataattggaatgttggggaatgcgttcattg
gactggtaaactgctctgaatgggtcaagaaccggaaaatctctttagctgacttcattctcatctgcttggctatctccag
aatcgctcagctgttggtgtcatggtttgaatcatttatgatgggactatctccacttttcttttccacttataaactggcaaa
atctattactttgctttggagaataactcatcatttggctacgtggtttagtacctgcctaagcattttctacctccttaagat
agctcagttctctcattccctttcctctggctgaggtggagaatgaacagagtggttcttgcaattcttgtattttctttgttc
tttctactgtttgactttctaatgctagaaacattcaatgatctcttctcgaatgtcgatgcaatggatgaaagtaatctgac
tttatatatatatgaaagtaaaacttttatgttaaaaccttgattcttcttagtttttcctatatcattcctattattctgtccc
tgacctcattgctccttttatttctgtccttggtaaaacacatcagaaatttgcagctcaactccatgggctccagggattcc
agcacacaggcccataaaaaagccattaaaatggtgatgtctttcctcttcctttcacagttcacttttttccatacaatt
gtcaaattggatgttttttttatttggaacaagaagatcacaaagtttatcatgttggccgtttatgtctttccttcaagcca
ctcactaattttgattctgggaaacagcaagctgagacagacagccttgaaggtactgtggcatcttaaaagctccctga
aaagagaaaaaccaaattcatctttaccgatagactttccagaatctttccaatga

d*Tas2r43*

atgctacctttactacagagcatttttccatcctagtaatgacagaatttgttctaggaaattttgccaatggcttcatagt
gctggtgaactacattgcatgggtcaagagacaaaagatctcctcagctgatcaaattctcactggtctggctgtctccag
aattggtttactctgggtaatattaataaattggtatgcaactctgttgaatccagctttatatagcttagaagtaaggcttc
ttgttcatattgcctggacagcgaacaatcattttagcatctggcttgctactagcctcagtgtattttatttgttcaaaatag
ccaatttctctaaccttatttttcttcgcctaaagtggagagttaaaagtgtagtttttgtgatgctgttggggtctttgttctt
tttggtttttcatgttgcagtggtaagcatatatgagcaaatgcagatgaaggaatatgaaggaaacatcactaggcaga
ccaaactgagggacattgcacagcttatgaatatgactgtattcacgctaatgaactttgtacccttgctatatccctaac
atcttttctgctgttaatcttttccctgtggaaacatctcaagaagatgcgatccggtggtaaaagatatcaagattccagc

accaaggtccacataaaagccatgcagactgtgatctcttttcttttgttattagtttgttacttcctgactttaattgccata
gtttggagttctaataggctgcagaacaagttgatcttcttgctttgcaaggctattggaatcctgtatccttcaagccactc
atttatcctgatttggggaaacaagaagctcagagaggactttctgtcatttctgtggcagctgaagggctggctgaaaa
aaggatataagaggagcatcatgtgtcttctaggagaaaacaaattgatggagtctgtaatatttttttcttctacttctttt
tctaatgagtatgtaattgagcaatttccaaagatttacctaaaaaagtcttttctctga

d*Tas2r62*

atgtcctcctcacctacattgatcttcatggtcatcttcttcctggagtcgttggctgcaatgctgcagaatggcttcatggtt
actgtgttgggcagggagtgggtgcgacgccggacgctgcctgcaggtgacatgattgtggcctccctggctgcctcctg
gttctgcctgcatggggtggccatcctgaacaacctcttgatcttctttggttttcacttcgtaagggattattacaacaccc
tctggcactttgtcaacactctcactctctggctcactgcctggcttgctgtcttctactgtgtgaaggtcgccgtcttctctc
acccggtcttcttctggctgaaatggaggatttctcggttagtgcccaggctgctgctgggctccctggtcttagttggcctg
acagtcatctcatcagccattgtgactggaattctgaaacagatgattgcctccaagagttcccaaggaaacagcacctg
ggctgagagagtacaggccttctataggtcttttcatctatttgatgtaatgcttatgtggtcagttccattcctcctgttctt
ggtgtccatgctcttgcttgtgttctcactgtgccggcatttggggttgatgaggaactatagacaggacccatgtgatcct
agcacccgggttcacacgatggccctgaagtcacttgtcttcttccttgtcttctacacaccatatttcctgtctctggttgtt
gttgctatagaaataacaaacttccagagtcactggtactgggcctgggaagtggtaacctatgcgagcatctgtctgca
ctccagcatgctggtgctaagcagccccaaactgagaaaggtcctgatgaccaggctttggaaagctctggacaaaggc
tga

d*Tas2r67*

atgccatctagaattgaaaatgcttttctggtagcagcagcaggagaactcataactggaatgttggggaacggtttcatt
gtactagttaactgcattgacttggtgaagaatctaaagctctctactgctgactgcatcctcaccagcctggctctttcca
gaatcattcttctttgtataatactacttgattcacttttaatggtgttttggcaacatctttatgccattgataagctagcaa
aattcattagtgtttttggacactaagcaatcacctaactacctggattgttacctgtctaaatgttttctacttctttaaaa
tagccaatttttcccacccctgtttcacctggctgaggtggagaattagcagagtgctacttgtgcttccactggggtcttta
ttcttactgtttttcaactttgaattattagatacatttacgaatttctgggttaatctctatcaaagacatgaaagaaactc
aatttggtccctagatgtaagtaaaactctgtatcttaacagcttgattgttttcagtttcatctacttaatccccttttcttctg
tccctggcctctttgctccttttatttctttccttaatgagacatatcaggaatgtgcaacggaactccagctctagggactt
cagaacagaggcccataaaagggccatgaaaatggtgatgtcttctcttttttctttccatggttaattttacttccatcctat
taacaggatggttttccctttactgcagaatcatcaggccaatttggctgtcctgttattatcgactcttgtaccctcaggc

cactcatttattctaattttgggaaacaacaagttgagacaagctgcgttaggtctactgtggcatcttaattgccacctga
aaatggtgaagcctttcgcttcctag

Appendix 2.1: Comound details for the screening library.

Compound	**Supplier**	**Product ID**	**CAS Number**
1, 10-Phenanthroline	Sigma	131377-25G	66-71-7
4-Benzylpiperidine	Sigma	142360-25G	31252-42-3
6-Nitrosaccharin	CarboSynth	FN15866	22952-24-5
Acetaminophen	Sigma	A7085-100G	103-90-2
6α-Methylprednisolone	Sigma	M0639-100MG	83-43-2
Aloin	Sigma	B6906-25MG	1415-73-2
(-)-α-Thujone	Sigma	89231-5ML	546-80-5
Aristolochic acid I	Sigma	A5512-100MG	313-67-7
Brucine sulphate salt hydrate	Sigma	B0378-25G	652154-10-4
(-)-Camphor	Sigma	21293-1G	464-48-2
Chloramphenicol	Sigma	C0378-5G	56-75-7
Chlorhexidine	Sigma	282227-5G	55-56-1
Chloroquine diphosphate salt	Sigma	C6628-25G	50-63-5
Colchicine	Sigma	C9754-1G	64-86-8
Cucurbitacin B hydrate	Sigma	C8499-25MG	6199-67-3
Cycloheximide	Sigma	01810-5G	66-81-9
Denatonium benzoate	Sigma	D5765-10G	3734-33-6
Dextromethorphan hydrobromide monohydrate	Sigma	D2531-5G	6700-34-1
1,1-Dimethylbiguanide hydrochloride	Sigma	D150959-5G	1115-70-4

1,1-Diphenyl-4-piperidino-1-butanol hydrochloride (Diphenidol)	Tokyo Chemical Industry (TCI)	D2062	3254-89-5
Doxepin hydrochloride	Sigma	D4526-1G	1229-29-4
Ethylpyrazine	Sigma	250384-5G	13925-00-3
Flavone	Sigma	F2003-1G	525-82-6
N-(3-Oxooctanoyl)-L-homoserine lactone	Sigma	O1764-100MG	147795-39-9
Aurintricarboxylic acid	Sigma	A1895-25G	4431-00-9
L-Menthol	Sigma	W266523-100G	2216-51-5
Ofloxacin	Sigma	O8757-10G	82419-36-1
Oleuropein	Sigma	12247-50MG	32619-42-4
Omeprazole	Sigma	O104-100MG	73590-58-6
Oxybutynin chloride	Sigma	O2881-5G	1508-65-2
Oxyphenonium bromide	Sigma	O5501-5G	50-10-2
Papaverine hydrochloride	Sigma	P3510-5G	61-25-6
Parthenolide	Sigma	P0667-5MG	20554-84-1
Picrotoxin	Sigma	P1675-5G	124-87-8
Pirenzepine dihydrochloride	Sigma	P7412-1G	29868-97-1
Prednisone	Sigma	P6254-10G	53-03-2
6-Propyl-2-thiouracil (PROP)	Sigma	P3755-10G	51-52-5
N-Phenylthiourea (PTC)	Sigma	P7629-10G	103-85-5

Quinacrine dihydrochloride	Sigma	Q3251-25G	69-05-6
Quinine hydrochloride dihydrate	Sigma	Q1125-5G	6119-47-7
Resveratrol	Sigma	R5010-100MG	501-36-0
Sucralose	Sigma	69293-100G	56038-13-2
D-(-)-Salicin	Sigma	S0625-25G	138-52-3
Sinigrin hydrate	Sigma	85440-1G	3952-98-5
Strychnine hydrochloride	Sigma	S8753-25G	1421-86-9
Thiamine hydrochloride	Sigma	T4625-5G	67-03-8
Trimethoprim	Sigma	92131-5G	738-70-5
Yohimbine	Sigma	Y3125-10G	65-19-0

Appendix 3.1: All code used for edgeR analysis of RNAseq data.

```
#Script for expression analysis of STAR aligned data with featureCounts processing

#Set wd
setwd("C:/Users/gibbsmat/OneDrive - Mars Inc/Documents/Taste and Olfactory Receptors/PhD/Taste papillae sampling/star-featcount_results/edgeR")

#Read in the group data
targets <-read.delim('groups.tsv', stringsAsFactors = FALSE)

#Set groups
group <- paste(targets$location, targets$Status, sep=".")
group <- factor(group)
table(group)

#Read in the raw count data
raw_counts <- read.delim('raw_counts_2.tsv', stringsAsFactors = FALSE, row.names = 1)
raw_counts <- raw_counts[!apply(is.na(raw_counts),1,all),]

#Convert it to a matrix
raw_counts_matrix <- as.matrix(raw_counts)

#Read in count_results
count_results <- read.delim('count_results.tsv', stringsAsFactors = FALSE)

#Visualise count_results
library(ggplot2)
stats <-data.frame(count_results[, -1], row.names = count_results[, 1])
stats <- stats[apply(stats, 1, function(x) any(x > 0)),]
stats <- reshape2::melt(t(stats))
```

```
stats$name <- targets[stats$Var1, 'Name']

ggplot(stats, aes(x = name, y = value, fill = Var2)) +
 geom_bar(stat = "identity", position = 'fill') +
 theme_bw() +
 theme(axis.text.x = element_text(angle = 90), legend.title = element_blank()) +
 xlab("Sample") +
 ylab(NULL)

#Read in the gtf file information
gtf_file <- ('Canis_familiaris.CanFam3.1.96.2.gtf')
library(rtracklayer)
gtf_content <- import(gtf_file, feature.type = 'gene')
annotation <- data.frame(elementMetadata(gtf_content), stringAsFactors = FALSE)
rownames(annotation) <- annotation$gene_id

#Order rows and columns of expression matrix to match gene and sample tables
raw_counts_matrix
raw_counts_matrix <- raw_counts_matrix[rownames(annotation), gsub("\\-
",".",targets[,1])]

#Load edgeR
library(edgeR)

#Build DGE list
dgList<- DGEList(counts = raw_counts_matrix, samples = targets, genes = annotation,
group = targets$location)

#Calculate normalisation factors
dgList <- calcNormFactors(dgList)

#Output TMM normalised counts
```

```
tmm <- cpm(dgList)

#Multi-dimensional scaling plot
plotMDS(
  dgList,
  gene.selection = 'pairwise',
  col = as.integer(dgList$samples$group), # specifics the sample attribute that will colour the points
  labels = dgList$samples$ID #  specifics the sample attribute that will label the points
)

#Remove the outlying samples
dgList2 <- dgList[, which(dgList$samples$ID != "S20, S35, S28, S25")]

#Make a PCA plot
library(ggplot2)
library(ggrepel)

pca_plot <- function(inputDgList,labels,color,shape,PC1,PC2){

  ## PCA analysis
  dgList <- inputDgList
  pcavals <- log2(dgList$counts + 1)   # log transforming the counts makes it easy to compare very high and very
  # low levels of expression. Adding 1 is necessary to avoid log transforming zeros.
  pcavals_var <- pcavals[apply(pcavals, 1, function(x) length(unique(x))) > 1, ]  # remove genes that have the same expression in every sample
  pcavals_t <- t(pcavals_var)                    # transpose  (swap row and columns) the data frame
  pcavals_m <- as.matrix(pcavals_t, scale =T)       # convert the data frame to a matrix
  pca <- prcomp(pcavals_m)             #  Perform the principle components analysis
```

```
  fraction_explained <- round((pca$sdev)^2/sum(pca$sdev^2), 3) * 100 # Get the
fraction of variance explained by each princple component

  guides <- guides(shape=FALSE)
  if(PC2=="PCA2"){guides <- guides(shape=FALSE,color=FALSE)}
  plotdata <- as.data.frame(pca$x)
  plotdata$label = dgList$samples[[labels]]        # Make a list of labels for each point
  plotdata$color <-as.factor(dgList$samples[[color]])     # Make a list of factors to
determine the color of each point
  plotdata$shape <-as.factor(dgList$samples[[shape]])  # Make a list of factors to
determine the shape of each point
  pcaplot <- ggplot(plotdata, aes_string(PC1, PC2, color = 'color', shape = 'shape',
label = 'label')) +
    geom_point(size = 3) + # change this number to alter the size of the points
    geom_text_repel(size = 3, segment.size = 0.1, nudge_y = 0.05, nudge_x = 0.05,
point.padding = unit(0.5, 'lines'), force = 2, max.iter = 10000)+
    theme(
      axis.text.x=element_text(size=14),
      axis.text.y=element_text(size=14),
      axis.title.x=element_text(size=16),
      axis.title.y=element_text(size=16),
      legend.text = element_text(size=12),
      legend.title = element_text(size=14),
      legend.position="bottom"
    )+
    scale_x_continuous(limits=c(-1,1)*max(abs(plotdata$PC1)),name = paste0("PC1
(",round(summary(pca)$importance[2,1]*100),"%"))+ #These two lines added by
Ruth to scale plot correctly and add % to axis labels
    scale_y_continuous(limits=c(-1,1)*max(abs(plotdata$PC2)),name = paste0("PC2
(",round(summary(pca)$importance[2,2]*100),"%"))
```

```
 #By addgng `geom_text_repel` the labels will be added in sensible places, join to the point with a line if necessary.


 ## make a scree plot
 variance<- pca$sdev^2               # get the variance for each principle component.
 variance <- variance[1:(length(variance)-1)]    # Miss the last one because it's 0 and makes the plot look weird
 pev <- (cumsum(variance)/sum(variance))*100      # Calculate the culmative variance explained by increasing numbers of principle components.
 plotdata <- data.frame(
   PC = c(1:length(pev)),
   pev = pev,
   type = 'scree'
 )

 origin_line <- data.frame(PC = c(0, 1), pev = c(0, pev[1]), type = 'orign')
 screeplot <-  ggplot(rbind(plotdata, origin_line), aes(PC, pev,color = type, linetype = type)) +
   geom_point(size = 3) + geom_path()  + scale_color_manual(values = c('black', 'grey'))+
   ylab('Cumulative variance explained (%)') + xlab('Principal component') + theme_bw() + theme(legend.position="none") +
   theme ()

 list(
   pca = pca,
   pcaplot = pcaplot,
   screeplot  = screeplot
 )

}
```

```
pca_output <- pca_plot(dgList, labels = 'ID', color = 'group', shape
='Breed','PC1','PC2')

#Output pca and scree plots
print(pca_output$pcaplot)
print(pca_output$screeplot)

#Test for associations between principle components and variables
pca_pvals<-function(pca,variables,this_dgList)
{
 pcameta<-this_dgList$samples[,variables]  # Variables to test for association with
principle components
 last_pc<-10 # Number of principle components to include

 ## create an empty matrix (columns are experimental variables, rows are principle
components)
 pvals <- matrix(
  data = NA,
  ncol = ncol(pcameta),
  nrow = last_pc,
  dimnames = list(as.character(1:last_pc), colnames(pcameta))
 )

 # Fill the matrix with anova p values

 for (i in 1:ncol(pcameta)) {
  for (j in 1:last_pc) {
   fit <- aov(pca$x[, j] ~ as.factor(pcameta[, i]))
   if ("Pr(>F)" %in% names(summary(fit)[[1]])) {
    pvals[j, i] <- summary(fit)[[1]][["Pr(>F)"]][[1]]
   }
```

```
  }
 }

 # Calculate the percent variance explained by each component
 fraction_explained <- round((pca$sdev)^2/sum(pca$sdev^2), 3) * 100
 names(fraction_explained) <- colnames(pca$x)
 rownames(pvals) <- paste(paste('PC', 1:last_pc, sep = ""), " (",
fraction_explained[1:last_pc],  "%)", sep = "" )
 pvals
}

#Use this function
pca_pvals(pca_output$pca,c('group','Breed','dog'),dgList) # arguments are results of
PCA analysis and list of
# experimental variables to test, and the dgList object

#Filter the data on cpm threshold
dgList <- dgList[rowSums(cpm(dgList)>=0.0001) >= 1, , keep.lib.sizes=FALSE]
dgList <- calcNormFactors(dgList)

#Model the experimental design
design <- model.matrix(~ 0 + location + dog, data = dgList$samples)
design

#Estimate dispersion
dgGlm <- estimateDisp(dgList, design, robust = TRUE)
plotBCV(dgGlm)

#Fit GLMs
fit <- glmQLFit(dgGlm, design, robust = TRUE)

#Set up contrasts
```

```
contrast_name <- "locationBack-locationFront"
contrast_matrix <- makeContrasts(contrasts=contrast_name, levels=design)

#Test for De with first contrast
de <- glmQLFTest(fit, contrast=contrast_matrix)

#Top genes
top_genes <- topTags(de, n=20)
top_genes

#Code for plot_gene
plot_gene <- function(gene_id, inputDgList){

  expr <- cpm(inputDgList)

  plot_data <- cbind(inputDgList$samples, expression = expr[gene_id,]) # Add
expression
  #data for the top gene to a copy of the sample info
  plot_data <- plot_data[order(plot_data$group),] # Re-order so we show cancer/
non-cancer
  #samples in different groups
  plot_data$sample <- factor(rownames(plot_data), levels=rownames(plot_data)) #
Create a
  #variable to be used as a sample label

  p <- ggplot(plot_data, aes(x=Name, y=expression, fill=group)) +
    geom_bar(stat = "identity") +  theme_bw() +
    theme(axis.text.x = element_text(angle = 90, hjust = 1)) +
    ggtitle(paste(gene_id, annotation$gene_name[match(gene_id,
annotation$gene_id)], sep=": "))
  print(p)
}
```

```
#Run the plot_gene function for one gene
plot_gene('ENSCAFG00000011075', dgList)

#Plot the top genes expression profile
plot_gene(rownames(top_genes)[1], dgList)
plot_gene(rownames(top_genes)[2], dgList)
plot_gene(rownames(top_genes)[3], dgList)

#Plot heatmap
plot_heatmap <- function(plot_genes, title='', inputDgList){

 library(pheatmap)

 # Pick sample variables to plot
 annotation_col <- inputDgList$samples[with(inputDgList$samples,
order(group,location)),
                          c( 'location','Breed')]     # you will need change or remove
'Gender'
 # according the variables in your experiment

 # Take out any genes not in the matrix
 plot_genes <- plot_genes[plot_genes %in% rownames(inputDgList)]

 # Make an expression mratix by calculating cpm and pulling out the selected genes,
 #ordering by the sample annotation

 expression <- cpm(inputDgList)[plot_genes,rownames(annotation_col)]
 plotmatrix <- log2(expression + 0.1)

 rownames(plotmatrix) <- annotation[rownames(plotmatrix), 'gene_name']
```

```
 grid::grid.newpage()
 pheatmap(
  plotmatrix,
  show_rownames = T,
  annotation_col = annotation_col,
  border_color = NA,
  legend = FALSE,
  cluster_cols = FALSE, # change o TRUE to get a dendrogram of samples
  cluster_rows = TRUE,
  scale = 'row',
  color = colorRampPalette(rev(RColorBrewer::brewer.pal(n = 7, name =
"RdYlBu")))(100),
  main = title
 )
}
#Order and plot top genes
plot_heatmap(rownames(top_genes), inputDgList = dgList)

#p-values for all genes
results <- topTags(de, n=nrow(dgList), sort.by='none')$table

#write to file
write.csv(results, file='differential_results.csv')

#Check overall genes matching threshold FDR and fold change
fdr_threshold <- 0.05
fc_threshold <- 2

diffexp_genes <- rownames(results)[abs(results$logFC) >= log2(fc_threshold) &
                                   results$FDR <= fdr_threshold ]
print(paste(length(diffexp_genes), 'genes are differentially expressed at
```

```
        a fold change of at least',fc_threshold, 'and a maximum FDR of',
fdr_threshold))

#MA plots
plotMD(de, status = decideTestsDGE(de, p.value=0.05),cex=0.3) # 'cex' dictates the
size of the points
abline(h=c(-1,1),col='blue')

#MA plot in ggplot
ma_plot<- function(results_table, fc_threshold, fdr_threshold){

 results_table$significant <- 'no'
 results_table$significant[ results_table$FDR <= fdr_threshold  ] <- 'yes'
 ggplot(results_table, aes(logCPM, logFC,  color=significant )) +
  geom_point(alpha = 0.2) +     # This alters the transparency of the points
  scale_colour_manual(name = 'significant',   # provides the label
                      values = setNames(c('red','grey'),c('yes', 'no'))) +
  geom_hline(yintercept=log2(fc_threshold), linetype= "dashed") +
  geom_hline(yintercept=-1*log2(fc_threshold), linetype= "dashed") +
  theme_bw()
}

ma_plot(results,2, 0.05) #  The arguments are: results table, fold change threshold,
FDR threshold

#Volcano plot
volcano_plot<- function(results_table, fc_threshold, fdr_threshold, log=FALSE){

 results_table$significant <- 'no'
 results_table$significant[ abs(results_table$logFC) >= log2(fc_threshold) &
                            results_table$FDR <= fdr_threshold  ] <- 'yes'
```

```
 # Un-log the values if necessary

 if(! log){
  results_table$logFC <- sign(results_table$logFC)*2**abs(results_table$logFC)
 }
 ggplot(results_table, aes(logFC, -log10(FDR), color=significant )) +
  geom_point(alpha = 0.2) +     # This alters the transparency of the points
  scale_colour_manual(name = 'significant',
                      values = setNames(c('red','grey'),c('yes', 'no'))) +
  theme_bw()
}

volcano_plot(results, fc_threshold, fdr_threshold) #  The arguments are : results
table, fold change threshold, FDR threshold
volcano_plot(results, fc_threshold, fdr_threshold,log=TRUE) # Arguments are results
table, fold change threshold, FDR threshold

#Write cpm to file
cpm_list <- (cpm(dgList, normalized.lib.sizes = FALSE, log = FALSE))
write.csv(cpm_list, file ='cpm_list.csv')
```

Appendix 3.2: Raw count and TMM data used for dTas2r expression analysis.

edgeR TMM Values

	S1	S2	S3	S4	S5	S6	S7	S8	S9	S10	S11	S12	S13	S14	S15	S16	S17	S18	S19	S21	S22	S23	S24	S26	S27	S29	S30	S31	S32	S33	S34		
	Front	Mid	Back	Back	Front	Front	Mid	Mid	Back	Back	Front	Mid	Front	Mid	Mid	Back	Back	Front	Front	Mid	Back	Mid	Back	Back	Back	Mid	Back	Back	Front	Front	Mid		
dTAS2R1	0	0	0	0	0	0	0	0	0	0	0	0	0	0	0	0	0	0	0	0	0	0	0	0	0	0	0	0	0	0	0		
dTAS2R2	0	0	0	0	0	0	0	0	0.3633557	0	0	0	0	0	0	0	0	0	0	0	0	0.04870926	0	0	0.56800259	0.3278791	0	0	0	0	0		
dTAS2R3	0	0	0	0	0	0	0	0	0	0	0	0	0	0	0	0	0	0	0	0	0	0.21919169	0	0	0	0	0	0	0	0	0		
dTAS2R4	0	0	0	0	0	0	0	0	0	0	0	0	0	0	0	0	0	0	0	0	0	0	0	0	0	0.2341993	0	0	0	0	0		
dTAS2R5	0	0	0	0	0	0	0	0	0	0	0	0	0	0	0	0	0	0	0	0	0	0	0	0.0354563	0	0.1170997	0	0	0	0	0		
dTAS2R7	0	0	0	0	0	0	0	0	0	0	0	0	0	0	0	0.2540675	0	0	0	0	0	0	0	0	0	0	0	0	0	0	0		
dTAS2R10	0	0	0	0.19823021	0	0	0	0	0	0	0	0	0	0	0	0.05007395	0	0	0	0	0	0	0	0	0.11833387	0	0	0	0	0	0		
dTAS2R12	0	0	0	0	0	0	0	0	0	0	0	0	0	0	0	0	0	0	0	0	0	0	0	0.1772815	0	0	0	0	0	0	0		
dTAS2R38	0	0	0	0	0	0	0	0	0	0	0	0	0	0	0	0.2253328	0	0	0	0	0	0	0	0	0	0	0	0	0	0	0		
dTAS2R39	0	0.09106922	0	0	0	0	0	0	0	0	0	0	0	0	0	0	0	0	0	0	0	0	0	0	0	0.0702598	0	0	0	0	0		
dTAS2R40	0.0561938	0	0.79177974	0.14867266	0	0	0	0	0	0	0	0	0	0.0549924	0.38369951	0.2253328	0.91266637	0	0	0.0757559	0	0.65757506	0	0.3191068	0	0	0	0.2280045	0	0	0		
dTAS2R41	0	0	0	0	0	0	0	0	0	0	0	0	0	0	0	0.30044373	0	0	0.0358744	0	0	0.0730639	0	0.0709126	0	0	0	0.4180083	0	0	0		
dTAS2R42	0.0280969	0.06830191	0	0.0991151	0	0	0.0501461	0	0	0	0	0	0	0	0.05481422	0.05007395	0	0	0.0358744	0.9090708	0.21818911	0.02435463	0	0.0354563	0.30766807	0.3044591	0.38315888	0.0760015	0	0	0		
dTAS2R43	0	0	0	0	0	0.0399672	0	0	0	0	0	0	0	0	0	0.10014791	0	0	0.0358744	0.1515118	0.03116987	0	0.8206441	0	0	0.0702598	0	0.0380008	0	0	0		
dTAS2R62	0.0842907	0	0	0.17345143	0	0	0	0.1214456	0.1816776	1.5018479	0	0	0.04185609	0.3574506	0.08222132	0	0.5475998	0.4119275	0.1076233	0	0	0	1.1283856	0.7091262	0.26033452	0.2107794	0	0.3420068	0.17370913	0	1.35917847	>0	
dTAS2R67	0	0	0	0	0	0	0	0	0	0	0	0.4198554	0	0	0.16444265	0	0	0	0	0	0	0	0	0	0.0946671	0.351299	0	0	0	0	0	>=0.25	

star+fc raw counts

	S1	S2	S3	S4	S5	S6	S7	S8	S9	S10	S11	S12	S13	S14	S15	S16	S17	S18	S19	S21	S22	S23	S24	S26	S27	S29	S30	S31	S32	S33	S34		
	Front	Mid	Back	Back	Front	Front	Mid	Mid	Back	Back	Front	Mid	Front	Mid	Mid	Back	Back	Front	Front	Mid	Back	Mid	Back	Back	Back	Mid	Back	Back	Front	Front	Mid		
dTAS2R1	0	0	0	0	0	0	0	0	0	0	0	0	0	0	0	0	0	0	0	0	0	0	0	0	0	0	0	0	0	0	0		
dTAS2R2	0	0	0	0	0	0	0	0	12	0	0	0	0	0	0	0	0	0	0	0	0	2	0	0	24	14	0	0	0	0	0		
dTAS2R3	0	0	0	0	0	0	0	0	0	0	0	0	0	0	0	0	0	0	0	0	0	9	0	0	0	0	0	0	0	0	0		
dTAS2R4	0	0	0	0	0	0	0	0	0	0	0	0	0	0	0	0	0	0	0	0	0	0	0	0	0	10	0	0	0	0	0		
dTAS2R5	0	0	0	0	0	0	0	0	0	0	0	0	0	0	0	0	0	0	0	0	0	0	0	1	0	5	0	0	0	0	0		
dTAS2R7	0	0	0	0	0	0	0	0	0	0	0	0	0	0	0	11	0	0	0	0	0	0	0	0	0	0	0	0	0	0	0		
dTAS2R10	0	0	0	8	0	0	0	0	0	0	0	0	0	0	0	2	0	0	0	0	0	0	0	0	5	0	0	0	0	0	0		
dTAS2R12	0	0	0	0	0	0	0	0	0	0	0	0	0	0	0	0	0	0	0	0	0	0	0	5	0	0	0	0	0	0	0		
dTAS2R38	0	0	0	0	0	0	0	0	0	0	0	0	0	0	0	9	0	0	0	0	0	0	0	0	0	0	0	0	0	0	0		
dTAS2R39	0	4	0	0	0	0	0	0	0	0	0	0	0	0	0	0	0	0	0	0	0	0	0	0	0	3	0	0	0	0	0		
dTAS2R40	2	0	23	8	0	0	0	0	0	0	0	0	0	4	14	9	16	0	0	1	0	28	0	10	0	0	0	6	0	0	0		
dTAS2R41	0	0	0	0	0	0	0	0	0	0	0	0	0	0	0	12	0	0	1	0	0	3	0	2	0	0	0	10	0	0	0		
dTAS2R42	1	3	0	4	0	0	2	0	0	0	0	0	0	0	2	2	0	2	1	12	8	1	0	1	13	13	8	3	0	0	0		
dTAS2R43	0	0	0	0	0	1	0	0	0	0	0	0	0	0	0	4	0	0	1	2	1	0	8	0	0	3	0	1	0	0	0		
dTAS2R62	3	0	0	7	0	0	0	3	6	19	0	0	1	13	3	0	9	8	3	0	0	0	11	20	11	9	0	9	5	0	24	>0	
dTAS2R67	0	0	0	0	0	0	0	0	0	0	0	11	0	0	6	0	0	0	0	0	0	0	0	0	4	15	0	0	0	0	0	>=10	

Appendix 4.1: Responses of variant dTas2r1 receptors compared to wild type with 6-nitrosaccharin not presented in Chapter 4.

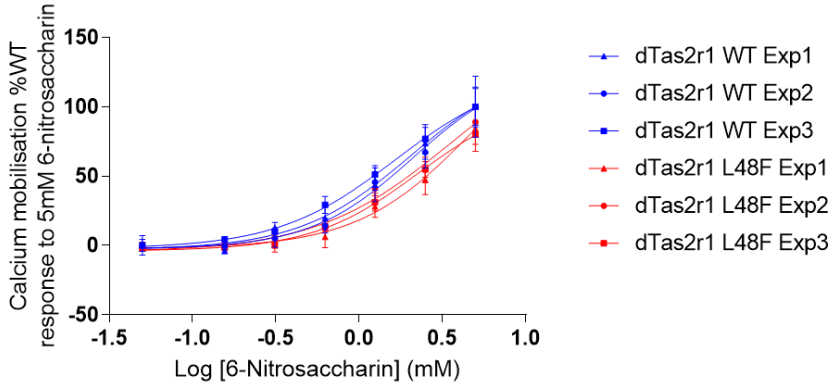

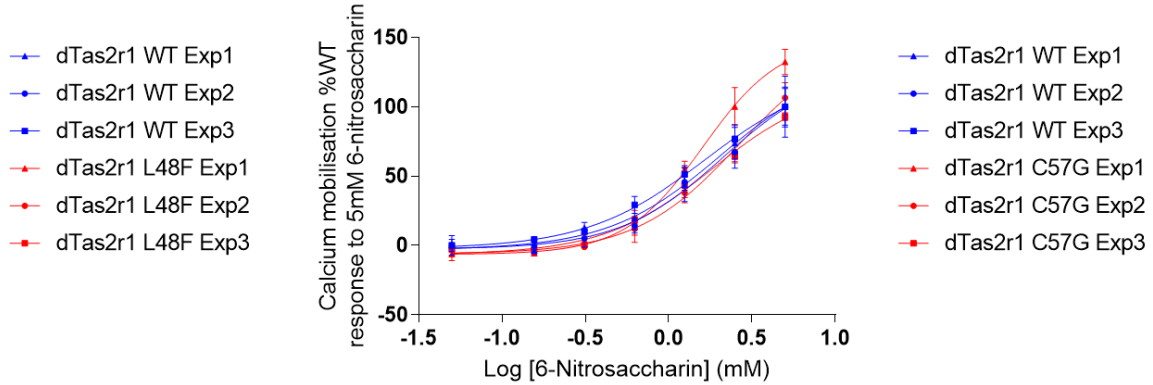

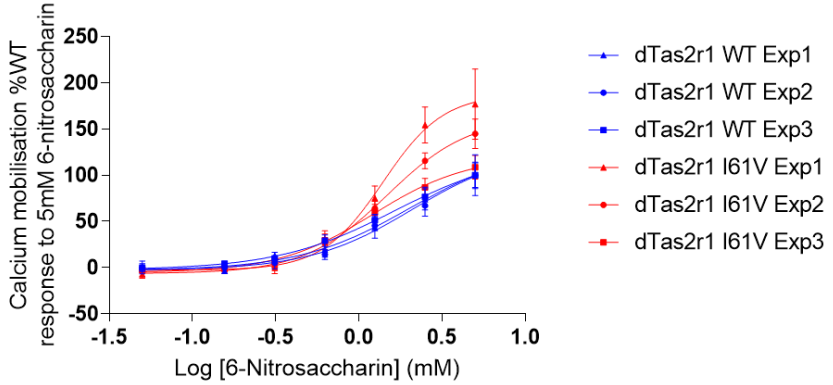

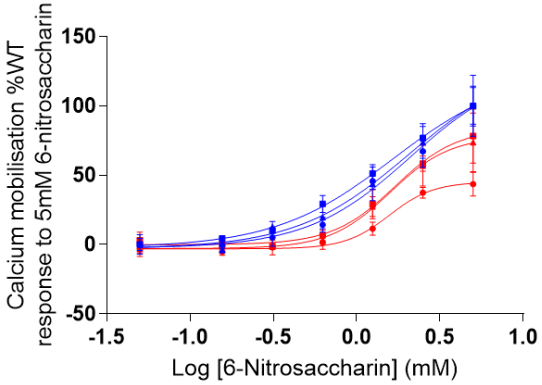

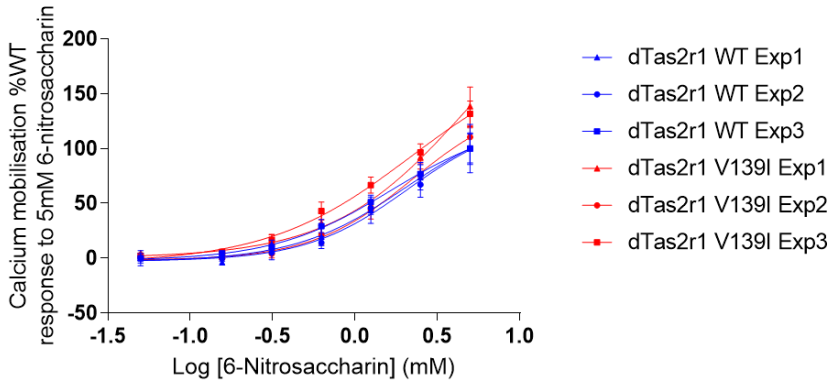
Calcium mobilisation %WT response to 5mM 6-nitrosaccharin
200
150
100
50
0
-50
-1.5
-1.0
-0.5
0.0
0.5
1.0
Log [6-Nitrosaccharin] (mM)
dTas2r1 WT Exp1
dTas2r1 WT Exp2
dTas2r1 WT Exp3
dTas2r1 V139I Exp1
dTas2r1 V139I Exp2
dTas2r1 V139I Exp3

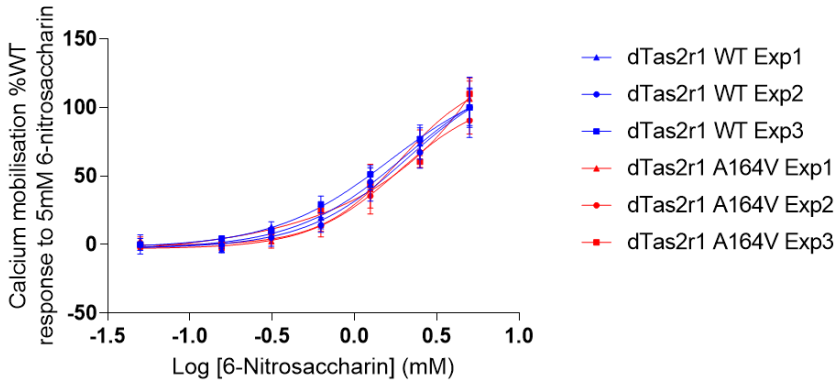
Calcium mobilisation %WT response to 5mM 6-nitrosaccharin
150
100
50
0
-50
-1.5
-1.0
-0.5
0.0
0.5
1.0
Log [6-Nitrosaccharin] (mM)
dTas2r1 WT Exp1
dTas2r1 WT Exp2
dTas2r1 WT Exp3
dTas2r1 A164V Exp1
dTas2r1 A164V Exp2
dTas2r1 A164V Exp3

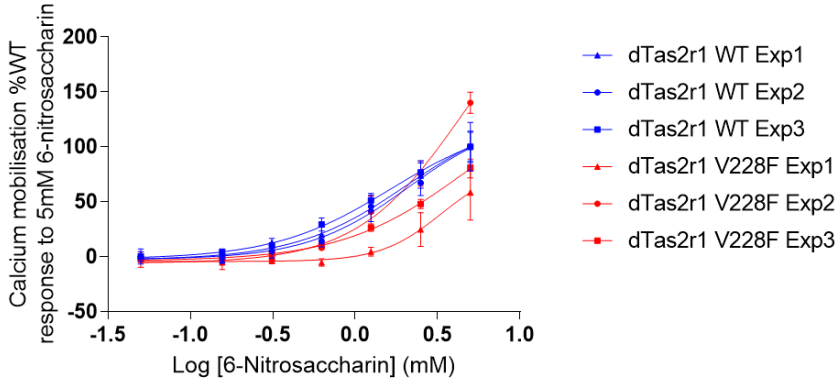
Calcium mobilisation %WT response to 5mM 6-nitrosaccharin
200
150
100
50
0
-50
-1.5
-1.0
-0.5
0.0
0.5
1.0
Log [6-Nitrosaccharin] (mM)
dTas2r1 WT Exp1
dTas2r1 WT Exp2
dTas2r1 WT Exp3
dTas2r1 V228F Exp1
dTas2r1 V228F Exp2
dTas2r1 V228F Exp3

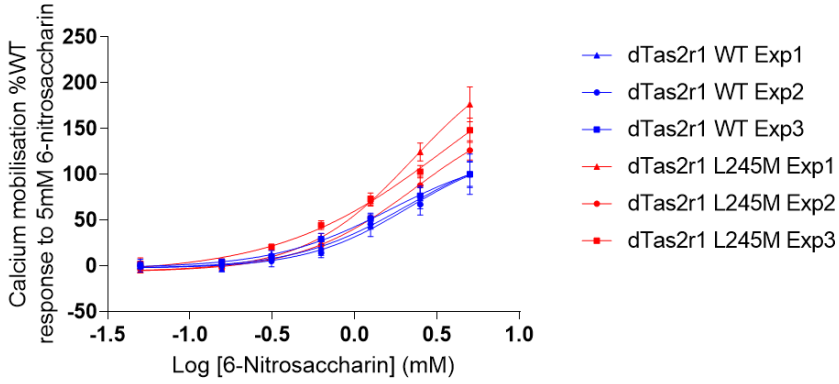
Calcium mobilisation %WT response to 5mM 6-nitrosaccharin
250
200
150
100
50
0
-50
-1.5
-1.0
-0.5
0.0
0.5
1.0
Log [6-Nitrosaccharin] (mM)
dTas2r1 WT Exp1
dTas2r1 WT Exp2
dTas2r1 WT Exp3
dTas2r1 L245M Exp1
dTas2r1 L245M Exp2
dTas2r1 L245M Exp3

References

(2005). Antifreeze Bittering Agent Act of 2005, S. 1110. *109th Congress*.

Adler E, Hoon MA, Mueller KL, Chandrashekar J, Ryba NJ, Zuker CS (2000). A novel family of mammalian taste receptors. *Cell* **100**(6)**:** 693-702.

Alghasham AA (2013). Cucurbitacins - a promising target for cancer therapy. *International journal of health sciences* **7**(1)**:** 77-89.

Ammon C, Schafer J, Kreuzer OJ, Meyerhof W (2002). Presence of a plasma membrane targeting sequence in the amino-terminal region of the rat somatostatin receptor 3. *Arch Physiol Biochem* **110**(1-2)**:** 137-145.

An SS, Liggett SB (2018). Taste and smell GPCRs in the lung: Evidence for a previously unrecognized widespread chemosensory system. *Cellular signalling* **41:** 82-88.

Arvidson K, Friberg U (1980). Human taste: response and taste bud number in fungiform papillae. *Science* **209**(4458)**:** 807-808.

Athanasiou D, Aguila M, Bellingham J, Li W, McCulley C, Reeves PJ*, et al.* (2018). The molecular and cellular basis of rhodopsin retinitis pigmentosa reveals potential strategies for therapy. *Progress in retinal and eye research* **62:** 1-23.

Axelsson E, Ratnakumar A, Arendt ML, Maqbool K, Webster MT, Perloski M*, et al.* (2013). The genomic signature of dog domestication reveals adaptation to a starch-rich diet. *Nature* **495**(7441)**:** 360-364.

Bai B, Zhao WM, Tang BX, Wang YQ, Wang L, Zhang Z*, et al.* (2015). DoGSD: the dog and wolf genome SNP database. *Nucleic Acids Res* **43**(Database issue)**:** D777-783.

Ballesteros JA, Weinstein H (1995). [19] Integrated methods for the construction of three-dimensional models and computational probing of structure-function relations in G protein-coupled receptors. **25:** 366-428.

Bartel DL, Sullivan SL, Lavoie EG, Sevigny J, Finger TE (2006). Nucleoside triphosphate diphosphohydrolase-2 is the ecto-ATPase of type I cells in taste buds. *J Comp Neurol* **497**(1)**:** 1-12.

Beau I, Touraine P, Meduri G, Gougeon A, Desroches A, Matuchansky C*, et al.* (1998). A novel phenotype related to partial loss of function mutations of the follicle stimulating hormone receptor. *The Journal of clinical investigation* **102**(7)**:** 1352-1359.

Behrens M, Bartelt J, Reichling C, Winnig M, Kuhn C, Meyerhof W (2006). Members of RTP and REEP gene families influence functional bitter taste receptor expression. *The Journal of biological chemistry* **281**(29)**:** 20650-20659.

Behrens M, Brockhoff A, Kuhn C, Bufe B, Winnig M, Meyerhof W (2004). The human taste receptor hTAS2R14 responds to a variety of different bitter compounds. *Biochemical and biophysical research communications* **319**(2)**:** 479-485.

Behrens M, Foerster S, Staehler F, Raguse JD, Meyerhof W (2007). Gustatory expression pattern of the human TAS2R bitter receptor gene family reveals a heterogenous population of bitter responsive taste receptor cells. *The Journal of neuroscience : the official journal of the Society for Neuroscience* **27**(46)**:** 12630-12640.

Behrens M, Gunn HC, Ramos PC, Meyerhof W, Wooding SP (2013). Genetic, functional, and phenotypic diversity in TAS2R38-mediated bitter taste perception. *Chemical senses* **38**(6)**:** 475-484.

Behrens M, Korsching SI, Meyerhof W (2014). Tuning properties of avian and frog bitter taste receptors dynamically fit gene repertoire sizes. *Molecular biology and evolution* **31**(12)**:** 3216-3227.

Behrens M, Ziegler F (2020). Structure-Function Analyses of Human Bitter Taste Receptors-Where Do We Stand? *Molecules* **25**(19).

Beidler LM, Fishman I, Hardiman C (1955). Species differences in taste responses. *American Journal of Physiology--Legacy Content* **181**(2)**:** 235-239.

Belitz HD, Wieser H (1985). Bitter compounds: Occurrence and structure-activity relationships. *Food Reviews International* **1**(2)**:** 271-354.

Berning C, Griffith J, Wild J (1982). Research on the effectiveness of denatonium benzoate as a deterrent to liquid detergent ingestion by children. *Fundamental and Applied Toxicology* **2**(1)**:** 44-48.

Bhattacharya S, Hall SE, Vaidehi N (2008). Agonist-induced conformational changes in bovine rhodopsin: insight into activation of G-protein-coupled receptors. *J Mol Biol* **382**(2)**:** 539-555.

Bjornerfeldt S, Webster MT, Vila C (2006). Relaxation of selective constraint on dog mitochondrial DNA following domestication. *Genome research* **16**(8)**:** 990-994.

Blakeslee AF (1932). Genetics of Sensory Thresholds: Taste for Phenyl Thio Carbamide. *Proceedings of the National Academy of Sciences of the United States of America* **18**(1)**:** 120-130.

Born S, Levit A, Niv MY, Meyerhof W, Behrens M (2013). The human bitter taste receptor TAS2R10 is tailored to accommodate numerous diverse ligands. *The Journal of neuroscience : the official journal of the Society for Neuroscience* **33**(1)**:** 201-213.

Botigue LR, Song S, Scheu A, Gopalan S, Pendleton AL, Oetjens M*, et al.* (2017). Ancient European dog genomes reveal continuity since the Early Neolithic. *Nat Commun* **8:** 16082.

Bray NL, Pimentel H, Melsted P, Pachter L (2016). Near-optimal probabilistic RNA-seq quantification. *Nat Biotechnol* **34**(5)**:** 525-527.

Brockhoff A, Behrens M, Massarotti A, Appendino G, Meyerhof W (2007). Broad tuning of the human bitter taste receptor hTAS2R46 to various sesquiterpene lactones, clerodane and labdane diterpenoids, strychnine, and denatonium. *Journal of agricultural and food chemistry* **55**(15)**:** 6236-6243.

Brockhoff A, Behrens M, Niv MY, Meyerhof W (2010). Structural requirements of bitter taste receptor activation. *Proceedings of the National Academy of Sciences of the United States of America* **107**(24)**:** 11110-11115.

Bufe B, Breslin PA, Kuhn C, Reed DR, Tharp CD, Slack JP*, et al.* (2005). The molecular basis of individual differences in phenylthiocarbamide and propylthiouracil bitterness perception. *Curr Biol* **15**(4)**:** 322-327.

Bufe B, Hofmann T, Krautwurst D, Raguse JD, Meyerhof W (2002). The human TAS2R16 receptor mediates bitter taste in response to beta-glucopyranosides. *Nat Genet* **32**(3)**:** 397-401.

Bustin S, Nolan T (2004). Pitfalls of Quantitative Real-Time Reverse-Transcription Polymerase Chain Reaction. *J Biomol Tech* **15**(3)**:** 155-166.

Caicedo A, Pereira E, Margolskee RF, Roper SD (2003). Role of the G-Protein Subunit α-Gustducin in Taste Cell Responses to Bitter Stimuli. *The Journal of Neuroscience* **23**(30)**:** 9947-9952.

Chandrashekar J, Hoon MA, Ryba NJ, Zuker CS (2006). The receptors and cells for mammalian taste. *Nature* **444**(7117)**:** 288-294.

Chandrashekar J, Kuhn C, Oka Y, Yarmolinsky DA, Hummler E, Ryba NJ*, et al.* (2010). The cells and peripheral representation of sodium taste in mice. *Nature* **464**(7286)**:** 297-301.

Chandrashekar J, Mueller KL, Hoon MA, Adler E, Feng L, Guo W*, et al.* (2000). T2Rs Function as Bitter Taste Receptors. *Cell* **100**(6)**:** 703-711.

Chandrashekar J, Yarmolinsky D, von Buchholtz L, Oka Y, Sly W, Ryba NJ*, et al.* (2009). The taste of carbonation. *Science* **326**(5951)**:** 443-445.

Chaudhari N, Landin AM, Roper SD (2000). A metabotropic glutamate receptor variant functions as a taste receptor. *Nat Neurosci* **3**(2)**:** 113-119.

Chaudhari N, Roper SD (2010). The cell biology of taste. *The Journal of cell biology* **190**(3)**:** 285-296.

Chen J, Larson ED, Anderson CB, Agarwal P, Frank DN, Kinnamon SC*, et al.* (2019). Expression of Bitter Taste Receptors and Solitary Chemosensory Cell Markers in the Human Sinonasal Cavity. *Chemical senses* **44**(7)**:** 483-495.

Cheng LHH, Robinson PP (1991). The distribution of fungiform papillae and taste buds on the human tongue. *Archives of Oral Biology* **36**(8)**:** 583-589.

Chesnoy S, Huang L (2000). Structure and function of lipid-DNA complexes for gene delivery. *Annual review of biophysics and biomolecular structure* **29:** 27-47.

Clapham DE, Neer EJ (1997). G protein beta gamma subunits. *Annual review of pharmacology and toxicology* **37:** 167-203.

Clapp TR, Stone LM, Margolskee RF, Kinnamon SC (2001). Immunocytochemical evidence for co-expression of Type III IP3 receptor with signaling components of bitter taste transduction. *BMC Neuroscience* **2**(1)**:** 6.

Collings VB (1974). Human taste response as a function of locus of stimulation on the tongue and soft palate. *Perception & psychophysics* **16**(1)**:** 169-174.

Colvin JL, Pullicin AJ, Lim J (2018). Regional Differences in Taste Responsiveness: Effect of Stimulus and Tasting Mode. *Chemical senses* **43**(8)**:** 645-653.

Conesa A, Madrigal P, Tarazona S, Gomez-Cabrero D, Cervera A, McPherson A*, et al.* (2016). A survey of best practices for RNA-seq data analysis. *Genome Biol* **17:** 13.

Conklin BR, Farfel Z, Lustig KD, Julius D, Bourne HR (1993). Substitution of three amino acids switches receptor specificity of Gq alpha to that of Gi alpha. *Nature* **363**(6426)**:** 274-276.

Conte C, Ebeling M, Marcuz A, Nef P, Andres-Barquin PJ (2003). Evolutionary relationships of the Tas2r receptor gene families in mouse and human. *Physiol Genomics* **14**(1)**:** 73-82.

Dagan-Wiener A, Di Pizio A, Nissim I, Bahia MS, Dubovski N, Margulis E*, et al.* (2018). BitterDB: taste ligands and receptors database in 2019. *Nucleic Acids Res*.

Dagan-Wiener A, Nissim I, Ben Abu N, Borgonovo G, Bassoli A, Niv MY (2017). Bitter or not? BitterPredict, a tool for predicting taste from chemical structure. *Sci Rep* **7**(1)**:** 12074.

Dai W, You Z, Zhou H, Zhang J, Hu Y (2011). Structure-function relationships of the human bitter taste receptor hTAS2R1: insights from molecular modeling studies. *Journal of receptor and signal transduction research* **31**(3)**:** 229-240.

Damak S, Rong M, Yasumatsu K, Kokrashvili Z, Varadarajan V, Zou S*, et al.* (2003). Detection of sweet and umami taste in the absence of taste receptor T1r3. *Science* **301**(5634)**:** 850-853.

Davies MN, Secker A, Halling-Brown M, Moss DS, Freitas AA, Timmis J*, et al.* (2008). GPCRTree: online hierarchical classification of GPCR function. *BMC research notes* **1:** 67.

Davis SF, Hoskinson KJ, Wilder KA, Sander JA, Larsen RK, Knapp M (1988). A cross-species analysis of the aversiveness of denatonium saccharide and quinine. *Bulletin of the Psychonomic Society* **26**(5)**:** 419-422.

DeFazio RA, Dvoryanchikov G, Maruyama Y, Kim JW, Pereira E, Roper SD*, et al.* (2006). Separate populations of receptor cells and presynaptic cells in mouse taste buds. *The Journal of neuroscience : the official journal of the Society for Neuroscience* **26**(15)**:** 3971-3980.

Di Pizio A, Kruetzfeldt LM, Cheled-Shoval S, Meyerhof W, Behrens M, Niv MY (2017). Ligand binding modes from low resolution GPCR models and mutagenesis: chicken bitter taste receptor as a test-case. *Sci Rep* **7**(1)**:** 8223.

Di Pizio A, Levit A, Slutzki M, Behrens M, Karaman R, Niv MY (2016). Comparing Class A GPCRs to bitter taste receptors: Structural motifs, ligand interactions and agonist-to-antagonist ratios. *Methods in cell biology* **132:** 401-427.

Di Pizio A, Niv MY (2014). Computational Studies of Smell and Taste Receptors. *Israel Journal of Chemistry* **54**(8-9)**:** 1205-1218.

Dillies MA, Rau A, Aubert J, Hennequet-Antier C, Jeanmougin M, Servant N*, et al.* (2013). A comprehensive evaluation of normalization methods for Illumina high-throughput RNA sequencing data analysis. *Brief Bioinform* **14**(6)**:** 671-683.

Dinehart ME, Hayes JE, Bartoshuk LM, Lanier SL, Duffy VB (2006). Bitter taste markers explain variability in vegetable sweetness, bitterness, and intake. *Physiol Behav* **87**(2)**:** 304-313.

Dobin A, Davis CA, Schlesinger F, Drenkow J, Zaleski C, Jha S*, et al.* (2013). STAR: ultrafast universal RNA-seq aligner. *Bioinformatics* **29**(1)**:** 15-21.

Dong D, Jones G, Zhang S (2009). Dynamic evolution of bitter taste receptor genes in vertebrates. *BMC Evol Biol* **9:** 12.

Donner J, Anderson H, Davison S, Hughes AM, Bouirmane J, Lindqvist J*, et al.* (2018). Frequency and distribution of 152 genetic disease variants in over 100,000 mixed breed and purebred dogs. *PLoS genetics* **14**(4)**:** e1007361.

Dotson CD, Zhang L, Xu H, Shin YK, Vigues S, Ott SH*, et al.* (2008). Bitter taste receptors influence glucose homeostasis. *PloS one* **3**(12)**:** e3974.

Doty RL, Dziewit JA, Marshall DA (2006). Antifreeze ingestion by dogs and rats: influence of stimulus concentration. *The Canadian Veterinary Journal* **47**(4)**:** 363.

Doty RL, Heidt JM, MacGillivray MR, Dsouza M, Tracey EH, Mirza N*, et al.* (2016). Influences of age, tongue region, and chorda tympani nerve sectioning on signal detection measures of lingual taste sensitivity. *Physiol Behav* **155:** 202-207.

Downes GB, Gautam N (1999). The G protein subunit gene families. *Genomics* **62**(3)**:** 544-552.

Dror RO, Pan AC, Arlow DH, Borhani DW, Maragakis P, Shan Y*, et al.* (2011). Pathway and mechanism of drug binding to G-protein-coupled receptors. *Proceedings of the National Academy of Sciences of the United States of America* **108**(32)**:** 13118-13123.

Einhauer A, Jungbauer A (2001). The FLAG™ peptide, a versatile fusion tag for the purification of recombinant proteins. *Journal of Biochemical and Biophysical Methods* **49**(1-3)**:** 455-465.

Ewels P, Magnusson M, Lundin S, Kaller M (2016). MultiQC: summarize analysis results for multiple tools and samples in a single report. *Bioinformatics* **32**(19)**:** 3047-3048.

Fagerberg L, Hallstrom BM, Oksvold P, Kampf C, Djureinovic D, Odeberg J*, et al.* (2014). Analysis of the human tissue-specific expression by genome-wide integration of transcriptomics and antibody-based proteomics. *Molecular & cellular proteomics : MCP* **13**(2)**:** 397-406.

Farbman AI (1980). Renewal of Taste Bud Cells in Rat Circumvallate Papillae. *Cell Proliferation* **13**(4)**:** 349-357.

Feeney E, O'Brien S, Scannell A, Markey A, Gibney ER (2011). Genetic variation in taste perception: does it have a role in healthy eating? *The Proceedings of the Nutrition Society* **70**(1)**:** 135-143.

Felgner PL, Gadek TR, Holm M, Roman R, Chan HW, Wenz M*, et al.* (1987). Lipofection: a highly efficient, lipid-mediated DNA-transfection procedure. *Proceedings of the National Academy of Sciences* **84**(21)**:** 7413-7417.

Finger TE, Danilova V, Barrows J, Bartel DL, Vigers AJ, Stone L*, et al.* (2005). ATP signaling is crucial for communication from taste buds to gustatory nerves. *Science* **310**(5753)**:** 1495-1499.

Finger TE, Kinnamon SC (2011). Taste isn't just for taste buds anymore. *F1000 Biol Rep* **3:** 20.

Fleige S, Pfaffl MW (2006). RNA integrity and the effect on the real-time qRT-PCR performance. *Mol Aspects Med* **27**(2-3)**:** 126-139.

Flock T, Hauser AS, Lund N, Gloriam DE, Balaji S, Babu MM (2017). Selectivity determinants of GPCR-G-protein binding. *Nature* **545**(7654)**:** 317-322.

Floriano WB, Hall S, Vaidehi N, Kim U, Drayna D, Goddard WA, 3rd (2006). Modeling the human PTC bitter-taste receptor interactions with bitter tastants. *Journal of molecular modeling* **12**(6)**:** 931-941.

Fox AL (1932). The Relationship between Chemical Constitution and Taste. *Proceedings of the National Academy of Sciences of the United States of America* **18**(1)**:** 115-120.

Frantz LA, Mullin VE, Pionnier-Capitan M, Lebrasseur O, Ollivier M, Perri A*, et al.* (2016). Genomic and archaeological evidence suggest a dual origin of domestic dogs. *Science* **352**(6290)**:** 1228-1231.

Fredriksson R, Lagerstrom MC, Lundin LG, Schioth HB (2003). The G-protein-coupled receptors in the human genome form five main families. Phylogenetic analysis, paralogon groups, and fingerprints. *Mol Pharmacol* **63**(6)**:** 1256-1272.

Garcia-Nafria J, Tate CG (2019). Cryo-EM structures of GPCRs coupled to Gs, Gi and Go. *Mol Cell Endocrinol* **488:** 1-13.

Garcia J, Hankins W (1975). The Evolution of Bitter and the Acquisition of Toxiphobia. 39-45.

Garneau NL, Nuessle TM, Sloan MM, Santorico SA, Coughlin BC, Hayes JE (2014). Crowdsourcing taste research: genetic and phenotypic predictors of bitter taste perception as a model. *Front Integr Neurosci* **8:** 33.

Geng Y, Mosyak L, Kurinov I, Zuo H, Sturchler E, Cheng TC*, et al.* (2016). Structural mechanism of ligand activation in human calcium-sensing receptor. *Elife* **5**.

GfK (2016). GfK Pet Ownership Survey 2016.

Gibbs M, Horsfall, A., O'Flynn, C., Desforges, N., Forman, O.,, Winnig M, Holliday, N., McGrane, S., Logan, D. (2017). Bitterness and Breeding: Bitter taste receptors in the domestic dog (Canis familiaris). *XXVIIth Annual Meeting of the European Chemoreception Research Organization*.

Glendinning JI (1994). Is the bitter rejection response always adaptive? *Physiology & Behavior* **56**(6)**:** 1217-1227.

Glendinning JI, Yiin YM, Ackroff K, Sclafani A (2008). Intragastric infusion of denatonium conditions flavor aversions and delays gastric emptying in rodents. *Physiol Behav* **93**(4-5)**:** 757-765.

Go Y, Investigators ST-NY (2006). Proceedings of the SMBE Tri-National Young Investigators' Workshop 2005. Lineage-specific expansions and contractions of the bitter taste receptor gene repertoire in vertebrates. *Molecular biology and evolution* **23**(5)**:** 964-972.

Grace J, Russek M (1969). The influence of previous experience on the taste behavior of dogs toward sucrose and saccharin. *Physiology & Behavior* **4**(4)**:** 553-558.

Graf R, Mattera R, Codina J, Evans T, Ho YK, Estes MK*, et al.* (1992). Studies on the interaction of alpha subunits of GTP-binding proteins with beta gamma dimers. *European journal of biochemistry* **210**(2)**:** 609-619.

Grassin-Delyle S, Abrial C, Fayad-Kobeissi S, Brollo M, Faisy C, Alvarez JC*, et al.* (2013). The expression and relaxant effect of bitter taste receptors in human bronchi. *Respiratory research* **14:** 134.

Haddad S, Noreldin AE, Kamal B, Abdeen A, Farouk SM, Abbott LC*, et al.* (2019). Morphological and functional comparison of lingual papillae in suckling and adult feral cats: Forensic evidence. *Anat Histol Embryol*.

Hall NJ, Glenn K, Smith DW, Wynne CD (2015). Performance of Pugs, German Shepherds, and Greyhounds (Canis lupus familiaris) on an odor-discrimination task. *J Comp Psychol* **129**(3)**:** 237-246.

Hansen S, Janssen C, Beasley V (1993). Denatonium benzoate as a deterrent to ingestion of toxic substances: toxicity and efficacy. *Veterinary and human toxicology* **35**(3)**:** 234-236.

Hass N, Schwarzenbacher K, Breer H (2007). A cluster of gustducin-expressing cells in the mouse stomach associated with two distinct populations of enteroendocrine cells. *Histochemistry and cell biology* **128**(5)**:** 457-471.

Hayes JE, Feeney EL, Allen AL (2013). Do polymorphisms in chemosensory genes matter for human ingestive behavior? *Food Qual Prefer* **30**(2)**:** 202-216.

Hewson-Hughes AK, Colyer A, Simpson SJ, Raubenheimer D (2016). Balancing macronutrient intake in a mammalian carnivore: disentangling the influences of flavour and nutrition. *R Soc Open Sci* **3**(6)**:** 160081.

Hewson-Hughes AK, Hewson-Hughes VL, Colyer A, Miller AT, McGrane SJ, Hall SR*, et al.* (2013). Geometric analysis of macronutrient selection in breeds of the domestic dog,

Canis lupus familiaris. *Behavioral Ecology* **24**(1)**:** 293-304.

Higgins MJ, Hayes JE (2019). Regional variation of bitter taste and aftertaste in humans. *Chemical senses*.

Hoeppner MP, Lundquist A, Pirun M, Meadows JR, Zamani N, Johnson J*, et al.* (2014). An improved canine genome and a comprehensive catalogue of coding genes and non-coding transcripts. *PloS one* **9**(3)**:** e91172.

Hofmann KP, Scheerer P, Hildebrand PW, Choe HW, Park JH, Heck M*, et al.* (2009). A G protein-coupled receptor at work: the rhodopsin model. *Trends in biochemical sciences* **34**(11)**:** 540-552.

Holland VF, Zampighi GA, Simon SA (1989). Morphology of fungiform papillae in canine lingual epithelium: location of intercellular junctions in the epithelium. *J Comp Neurol* **279**(1)**:** 13-27.

Holliday JC (1940). Total distribution of taste buds on the tongue of the pup.

Hopp TP, Prickett KS, Price VL, Libby RT, March CJ, Pat Cerretti D*, et al.* (1988). A Short Polypeptide Marker Sequence Useful for Recombinant Protein Identification and Purification. *Bio/Technology* **6**(10)**:** 1204-1210.

Horn F, Bettler E, Oliveira L, Campagne F, Cohen FE, Vriend G (2003). GPCRDB information system for G protein-coupled receptors. *Nucleic Acids Res* **31**(1)**:** 294-297.

Hu LL, Shi P (2013). Smallest bitter taste receptor (T2Rs) gene repertoire in carnivores. *Dongwuxue Yanjiu* **34**(E3)**:** E75-81.

Huang AL, Chen X, Hoon MA, Chandrashekar J, Guo W, Trankner D*, et al.* (2006). The cells and logic for mammalian sour taste detection. *Nature* **442**(7105)**:** 934-938.

Huang L, Shanker YG, Dubauskaite J, Zheng JZ, Yan W, Rosenzweig S*, et al.* (1999). Ggamma13 colocalizes with gustducin in taste receptor cells and mediates IP3 responses to bitter denatonium. *Nat Neurosci* **2**(12)**:** 1055-1062.

Huang YA, Maruyama Y, Stimac R, Roper SD (2008). Presynaptic (Type III) cells in mouse taste buds sense sour (acid) taste. *J Physiol* **586**(12)**:** 2903-2912.

Ibarra-Soria X, Levitin MO, Saraiva LR, Logan DW (2014). The olfactory transcriptomes of mice. *PLoS genetics* **10**(9)**:** e1004593.

Imai H, Suzuki N, Ishimaru Y, Sakurai T, Yin L, Pan W*, et al.* (2012). Functional diversity of bitter taste receptor TAS2R16 in primates. *Biol Lett* **8**(4)**:** 652-656.

Ishimaru Y, Inada H, Kubota M, Zhuang H, Tominaga M, Matsunami H (2006). Transient receptor potential family members PKD1L3 and PKD2L1 form a candidate sour taste receptor. *Proceedings of the National Academy of Sciences of the United States of America* **103**(33)**:** 12569-12574.

Itoigawa A, Hayakawa T, Suzuki-Hashido N, Imai H (2019). A natural point mutation in the bitter taste receptor TAS2R16 causes inverse agonism of arbutin in lemur gustation. *Proc Biol Sci* **286**(1904)**:** 20190884.

Jackson M, Payne H (1995). Bittering agents: their potential application in reducing ingestions of engine coolants and windshield wash. *Vet Hum Toxicol.* **Aug;37(4):323-6.**

Jagannathan V, Drogemuller C, Leeb T, Dog Biomedical Variant Database C (2019). A comprehensive biomedical variant catalogue based on whole genome sequences of 582 dogs and eight wolves. *Anim Genet* **50**(6)**:** 695-704.

Jang HJ, Kokrashvili Z, Theodorakis MJ, Carlson OD, Kim BJ, Zhou J*, et al.* (2007). Gut-expressed gustducin and taste receptors regulate secretion of glucagon-like peptide-1. *Proceedings of the National Academy of Sciences of the United States of America* **104**(38)**:** 15069-15074.

Janssen S, Laermans J, Verhulst PJ, Thijs T, Tack J, Depoortere I (2011). Bitter taste receptors and alpha-gustducin regulate the secretion of ghrelin with functional effects on food intake and gastric emptying. *Proceedings of the National Academy of Sciences of the United States of America* **108**(5)**:** 2094-2099.

Jeon TI, Seo YK, Osborne TF (2011). Gut bitter taste receptor signalling induces ABCB1 through a mechanism involving CCK. *Biochem J* **438**(1)**:** 33-37.

Jiang P, Cui M, Zhao B, Snyder LA, Benard LM, Osman R*, et al.* (2005). Identification of the cyclamate interaction site within the transmembrane domain of the human sweet taste receptor subunit T1R3. *The Journal of biological chemistry* **280**(40)**:** 34296-34305.

Jiang P, Ji Q, Liu Z, Snyder LA, Benard LM, Margolskee RF*, et al.* (2004). The cysteine-rich region of T1R3 determines responses to intensely sweet proteins. *The Journal of biological chemistry* **279**(43)**:** 45068-45075.

Jiang P, Josue J, Li X, Glaser D, Li W, Brand JG*, et al.* (2012). Major taste loss in carnivorous mammals. *Proceedings of the National Academy of Sciences of the United States of America* **109**(13)**:** 4956-4961.

Jobson MA, Hogan SL, Maxwell CS, Hu Y, Hladik GA, Falk RJ*, et al.* (2015). Clinical Features of Reported Ethylene Glycol Exposures in the United States. *PloS one* **10**(11)**:** e0143044.

Jones DT, Reed RR (1987). Molecular cloning of five GTP-binding protein cDNA species from rat olfactory neuroepithelium. *Journal of Biological Chemistry* **262**(29)**:** 14241-14249.

Kaji I, Karaki S, Fukami Y, Terasaki M, Kuwahara A (2009). Secretory effects of a luminal bitter tastant and expressions of bitter taste receptors, T2Rs, in the human and rat large intestine. *American journal of physiology. Gastrointestinal and liver physiology* **296**(5)**:** G971-981.

Kanazawa H (1993). Fine Structure of the Canine Taste Bud with Special Reference to Gustatory Cell Functions. *Archives of Histology and Cytology* **56**(5)**:** 533-548.

Kare M (1971). Comparative study of taste. In. *Taste*, edn: Springer. p^pp 278-292.

Katragadda M, Maciejewski MW, Yeagle PL (2004). Structural studies of the putative helix 8 in the human beta(2) adrenergic receptor: an NMR study. *Biochim Biophys Acta* **1663**(1-2)**:** 74-81.

Kaukeinen DE, Buckle AP (1992). Evaluations of aversive agents to increase the selectivity of rodenticides, with emphasis on denatonium benzoate (Bitrex®) bittering agent.

Kim D, Woo JA, Geffken E, An SS, Liggett SB (2017). Coupling of Airway Smooth Muscle Bitter Taste Receptors to Intracellular Signaling and Relaxation Is via Galphai1,2,3. *American journal of respiratory cell and molecular biology* **56**(6)**:** 762-771.

Kim KS, Egan JM, Jang HJ (2014). Denatonium induces secretion of glucagon-like peptide-1 through activation of bitter taste receptor pathways. *Diabetologia* **57**(10)**:** 2117-2125.

Kim MR, Kusakabe Y, Miura H, Shindo Y, Ninomiya Y, Hino A (2003). Regional expression patterns of taste receptors and gustducin in the mouse tongue. *Biochemical and biophysical research communications* **312**(2)**:** 500-506.

Kim U, Wooding S, Ricci D, Jorde LB, Drayna D (2005). Worldwide haplotype diversity and coding sequence variation at human bitter taste receptor loci. *Hum Mutat* **26**(3)**:** 199-204.

Kinnamon SC (2016). G Protein–Coupled Taste Transduction. 271-285.

Kirkness EF, Bafna V, Halpern AL, Levy S, Remington K, Rusch DB*, et al.* (2003). The dog genome: survey sequencing and comparative analysis. *Science* **301**(5641)**:** 1898-1903.

Kishi M, Emori Y, Tsukamoto Y, Abe K (2001). Primary culture of rat taste bud cells that retain molecular markers for taste buds and permit functional expression of foreign genes. *Neuroscience* **106**(1)**:** 217-225.

Kitchell R (1963). Comparative anatomical and physiological studies of gustatory mechanisms. *Olfaction and taste I***:** 235-255.

Kitchell R (1978). Taste perception and discrimination by the dog. *Advances in veterinary science and comparative medicine* **22:** 287.

Kohl S, Behrens M, Dunkel A, Hofmann T, Meyerhof W (2013). Amino acids and peptides activate at least five members of the human bitter taste receptor family. *Journal of agricultural and food chemistry* **61**(1)**:** 53-60.

Kok BP, Galmozzi A, Littlejohn NK, Albert V, Godio C, Kim W*, et al.* (2018). Intestinal bitter taste receptor activation alters hormone secretion and imparts metabolic benefits. *Molecular Metabolism*.

Krafts K, Hempelmann E, Skorska-Stania A (2012). From methylene blue to chloroquine: a brief review of the development of an antimalarial therapy. *Parasitol Res* **111**(1)**:** 1-6.

Kuhn C, Bufe B, Winnig M, Hofmann T, Frank O, Behrens M*, et al.* (2004). Bitter taste receptors for saccharin and acesulfame K. *The Journal of neuroscience : the official journal of the Society for Neuroscience* **24**(45)**:** 10260-10265.

Kumazawa T, Nakamura M, Kurihara K (1991). Canine taste nerve responses to umami substances. *Physiology & Behavior* **49**(5)**:** 875-881.

Lalonde ER, Eglitis JA (1961). Number and distribution of taste buds on the epiglottis, pharynx, larynx, soft palate and uvula in a human newborn. *The Anatomical Record* **140**(2)**:** 91-95.

Landau WM, Liu P (2013). Dispersion estimation and its effect on test performance in RNA-seq data analysis: a simulation-based comparison of methods. *PloS one* **8**(12)**:** e81415.

Latronico AC, Chai Y, Arnhold IJ, Liu X, Mendonca BB, Segaloff DL (1998). A homozygous microdeletion in helix 7 of the luteinizing hormone receptor associated with familial testicular and ovarian resistance is due to both decreased cell surface expression and impaired effector activation by the cell surface receptor. *Mol Endocrinol* **12**(3)**:** 442-450.

Lawton DM, Furness DN, Lindemann B, Hackney CM (2000). Localization of the glutamate-aspartate transporter, GLAST, in rat taste buds. *European Journal of Neuroscience* **12**(9)**:** 3163-3171.

Lazarowski L, Krichbaum S, DeGreeff LE, Simon A, Singletary M, Angle C*, et al.* (2020). Methodological Considerations in Canine Olfactory Detection Research. *Frontiers in veterinary science* **7:** 408.

Lee RJ, Xiong G, Kofonow JM, Chen B, Lysenko A, Jiang P*, et al.* (2012). T2R38 taste receptor polymorphisms underlie susceptibility to upper respiratory infection. *The Journal of clinical investigation* **122**(11)**:** 4145-4159.

Lei W, Ravoninjohary A, Li X, Margolskee RF, Reed DR, Beauchamp GK*, et al.* (2015). Functional Analyses of Bitter Taste Receptors in Domestic Cats (Felis catus). *PloS one* **10**(10)**:** e0139670.

Letunic I, Bork P (2019). Interactive Tree Of Life (iTOL) v4: recent updates and new developments. *Nucleic Acids Res* **47**(W1)**:** W256-W259.

Li D, Zhang J (2014). Diet shapes the evolution of the vertebrate bitter taste receptor gene repertoire. *Molecular biology and evolution* **31**(2)**:** 303-309.

Li X, Staszewski L, Xu H, Durick K, Zoller M, Adler E (2002). Human receptors for sweet and umami taste. *Proceedings of the National Academy of Sciences of the United States of America* **99**(7)**:** 4692-4696.

Li X, Xu H, Li Q, Tang H, Pronin A (2008). Identification of bitter ligands that specifically activate human t2r receptors and related assays for identifying human bitter taste modulators. *US20080038739A1***:** 1-82.

Liao Y, Smyth GK, Shi W (2014). featureCounts: an efficient general purpose program for assigning sequence reads to genomic features. *Bioinformatics* **30**(7)**:** 923-930.

Liggett SB (2013). Bitter taste receptors on airway smooth muscle as targets for novel bronchodilators. *Expert opinion on therapeutic targets* **17**(6)**:** 721-731.

Lindblad-Toh K, Wade CM, Mikkelsen TS, Karlsson EK, Jaffe DB, Kamal M*, et al.* (2005). Genome sequence, comparative analysis and haplotype structure of the domestic dog. *Nature* **438**(7069)**:** 803-819.

Linden RW (1993). Taste. *British dental journal* **175**(7)**:** 243-253.

Lipchock SV, Mennella JA, Spielman AI, Reed DR (2013). Human bitter perception correlates with bitter receptor messenger RNA expression in taste cells. *Am J Clin Nutr* **98**(4)**:** 1136-1143.

Liu Z, Liu G, Hailer F, Orozco-terWengel P, Tan X, Tian J*, et al.* (2016). Dietary specialization drives multiple independent losses and gains in the bitter taste gene repertoire of Laurasiatherian Mammals. *Front Zool* **13:** 28.

Lossow K, Hubner S, Roudnitzky N, Slack JP, Pollastro F, Behrens M*, et al.* (2016). Comprehensive Analysis of Mouse Bitter Taste Receptors Reveals Different Molecular Receptive Ranges for Orthologous Receptors in Mice and Humans. *The Journal of biological chemistry* **291**(29)**:** 15358-15377.

Lusby M, Trafford M (2005). *Leonberger*. edn. Kennel Club Books.

Mahdi A, Van der Merwe D (2013). Dog and cat exposures to hazardous substances reported to the Kansas State Veterinary Diagnostic Laboratory: 2009-2012. *J Med Toxicol* **9**(2)**:** 207-211.

Mainland JD, Keller A, Li YR, Zhou T, Trimmer C, Snyder LL*, et al.* (2014). The missense of smell: functional variability in the human odorant receptor repertoire. *Nat Neurosci* **17**(1)**:** 114-120.

Marchiori A, Capece L, Giorgetti A, Gasparini P, Behrens M, Carloni P*, et al.* (2013). Coarse-grained/molecular mechanics of the TAS2R38 bitter taste receptor: experimentally-validated detailed structural prediction of agonist binding. *PloS one* **8**(5)**:** e64675.

Marshall D, Doty R (1990). Taste responses of dogs to ethylene glycol, propylene glycol, and ethylene glycol-based antifreeze. *J Am Vet Med Assoc.* **15;197(12):1599-602.**

Maruyama Y, Yasuda R, Kuroda M, Eto Y (2012). Kokumi substances, enhancers of basic tastes, induce responses in calcium-sensing receptor expressing taste cells. *PloS one* **7**(4)**:** e34489.

Matsunami H, Montmayeur JP, Buck LB (2000). A family of candidate taste receptors in human and mouse. *Nature* **404**(6778)**:** 601-604.

Mattes RD (2009). Is there a fatty acid taste? *Annu Rev Nutr* **29:** 305-327.

McLaren W, Gil L, Hunt SE, Riat HS, Ritchie GR, Thormann A*, et al.* (2016). The Ensembl Variant Effect Predictor. *Genome Biol* **17**(1)**:** 122.

McLaughlin SK, McKinnon PJ, Margolskee RF (1992). Gustducin is a taste-cell-specific G protein closely related to the transducins. *Nature* **357**(6379)**:** 563-569.

Mennella JA, Spector AC, Reed DR, Coldwell SE (2013). The bad taste of medicines: overview of basic research on bitter taste. *Clin Ther* **35**(8)**:** 1225-1246.

Meyerhof W, Batram C, Kuhn C, Brockhoff A, Chudoba E, Bufe B*, et al.* (2010). The molecular receptive ranges of human TAS2R bitter taste receptors. *Chemical senses* **35**(2)**:** 157-170.

Miller IJ, Jr. (1986). Variation in human fungiform taste bud densities among regions and subjects. *Anat Rec* **216**(4)**:** 474-482.

Miller IJ, Reedy FE (1990a). Quantification of fungiform papillae and taste pores in living human subjects. *Chemical senses* **15**(3)**:** 281-294.

Miller IJ, Reedy FE (1990b). Variations in human taste bud density and taste intensity perception. *Physiology & Behavior* **47**(6)**:** 1213-1219.

Mistretta CM, Baum, B.J. (1984). Quantitative study of taste buds in fungiform and circumvallate papillae of young and aged rats. *J. Anat.* **138:** 323-332.

Miyoshi MA (2001). IP3 receptor type 3 and PLCbeta2 are co-expressed with taste receptors T1R and T2R in rat taste bud cells. *Chemical senses* **26**(3)**:** 259-265.

Mueller KL, Hoon MA, Erlenbach I, Chandrashekar J, Zuker CS, Ryba NJ (2005). The receptors and coding logic for bitter taste. *Nature* **434**(7030)**:** 225-229.

Munch F (1896). Die Topographie der Papillen der Zunge des Menschen und der Sauge tiere. *Morph. Arb* **6:** 605-690.

Nayak AP, Shah SD, Michael JV, Deshpande DA (2019). Bitter Taste Receptors for Asthma Therapeutics. *Frontiers in physiology* **10:** 884.

Nelson G, Chandrashekar J, Hoon MA, Feng L, Zhao G, Ryba NJ*, et al.* (2002). An amino-acid taste receptor. *Nature* **416**(6877)**:** 199-202.

Nelson G, Hoon MA, Chandrashekar J, Zhang Y, Ryba NJP, Zuker CS (2001). Mammalian Sweet Taste Receptors. *Cell* **106**(3)**:** 381-390.

Nelson SL, Sanregret JD (1997). Response of pigs to bitter-tasting compounds. *Chemical senses* **22**(2)**:** 129-132.

Niimura Y, Matsui A, Touhara K (2014). Extreme expansion of the olfactory receptor gene repertoire in African elephants and evolutionary dynamics of orthologous gene groups in 13 placental mammals. *Genome research* **24**(9)**:** 1485-1496.

Niimura Y, Nei M (2005). Comparative evolutionary analysis of olfactory receptor gene clusters between humans and mice. *Gene* **346:** 13-21.

Nyakatura K, Bininda-Emonds OR (2012). Updating the evolutionary history of Carnivora (Mammalia): a new species-level supertree complete with divergence time estimates. *BMC biology* **10:** 12.

Nygaard R, Frimurer TM, Holst B, Rosenkilde MM, Schwartz TW (2009). Ligand binding and micro-switches in 7TM receptor structures. *Trends in pharmacological sciences* **30**(5)**:** 249-259.

O'Neil MJ (2014). The Merck Index (15th edition)2014 307 Edited by Maryadele J. O'Neil and others The Merck Index (15th edition) London Royal Society of Chemistry 2013 xiv + 1896 pp. 9781849736701 £99.99. *Reference Reviews* **28**(8)**:** 38-39.

Offermanns S, Simon MI (1995). G 15 and G 16 Couple a Wide Variety of Receptors to Phospholipase C. *Journal of Biological Chemistry* **270**(25)**:** 15175-15180.

Ohsu T, Amino Y, Nagasaki H, Yamanaka T, Takeshita S, Hatanaka T*, et al.* (2010). Involvement of the calcium-sensing receptor in human taste perception. *The Journal of biological chemistry* **285**(2)**:** 1016-1022.

Oka Y, Butnaru M, von Buchholtz L, Ryba NJ, Zuker CS (2013). High salt recruits aversive taste pathways. *Nature* **494**(7438)**:** 472-475.

Okin GS (2017). Environmental impacts of food consumption by dogs and cats. *PloS one* **12**(8)**:** e0181301.

Oldham WM, Hamm HE (2008). Heterotrimeric G protein activation by G-protein-coupled receptors. *Nat Rev Mol Cell Biol* **9**(1)**:** 60-71.

Ostrander EA, Wayne RK (2005). The canine genome. *Genome research* **15**(12)**:** 1706-1716.

Ozdener H, Yee KK, Cao J, Brand JG, Teeter JH, Rawson NE (2006). Characterization and long-term maintenance of rat taste cells in culture. *Chemical senses* **31**(3)**:** 279-290.

Ozdener MH, Rawson NE (2013). Primary culture of mammalian taste epithelium. *Methods in molecular biology* **945:** 95-107.

Pandy-Szekeres G, Munk C, Tsonkov TM, Mordalski S, Harpsoe K, Hauser AS*, et al.* (2018). GPCRdb in 2018: adding GPCR structure models and ligands. *Nucleic Acids Res* **46**(D1)**:** D440-D446.

Parker HG, Dreger DL, Rimbault M, Davis BW, Mullen AB, Carpintero-Ramirez G*, et al.* (2017). Genomic Analyses Reveal the Influence of Geographic Origin, Migration, and Hybridization on Modern Dog Breed Development. *Cell Rep* **19**(4)**:** 697-708.

Perez CA, Huang L, Rong M, Kozak JA, Preuss AK, Zhang H*, et al.* (2002). A transient receptor potential channel expressed in taste receptor cells. *Nat Neurosci* **5**(11)**:** 1169-1176.

PetFoodIndustry (accessed 2017). https://www.petfoodindustry.com/pet-food-market-data/US-pet-market-sales-by-category-2011-14.

Pirrone F, Pierantoni L, Mazzola SM, Vigo D, Albertini M (2015). Owner and animal factors predict the incidence of, and owner reaction toward, problematic behaviors in companion dogs. *Journal of Veterinary Behavior: Clinical Applications and Research* **10**(4)**:** 295-301.

Plassais J, Kim J, Davis BW, Karyadi DM, Hogan AN, Harris AC*, et al.* (2019). Whole genome sequencing of canids reveals genomic regions under selection and variants influencing morphology. *Nat Commun* **10**(1)**:** 1489.

Polgar Z, Kinnunen M, Ujvary D, Miklosi A, Gacsi M (2016). A Test of Canine Olfactory Capacity: Comparing Various Dog Breeds and Wolves in a Natural Detection Task. *PloS one* **11**(5)**:** e0154087.

Premont RT, Gainetdinov RR (2007). Physiological roles of G protein-coupled receptor kinases and arrestins. *Annual review of physiology* **69:** 511-534.

Pronin AN, Tang H, Connor J, Keung W (2004). Identification of ligands for two human bitter T2R receptors. *Chemical senses* **29**(7)**:** 583-593.

Pronin AN, Xu H, Tang H, Zhang L, Li Q, Li X (2007). Specific alleles of bitter receptor genes influence human sensitivity to the bitterness of aloin and saccharin. *Curr Biol* **17**(16)**:** 1403-1408.

Purba LH, Widayati KA, Tsutsui K, Suzuki-Hashido N, Hayakawa T, Nila S*, et al.* (2017). Functional characterization of the TAS2R38 bitter taste receptor for phenylthiocarbamide in colobine monkeys. *Biol Lett* **13**(1).

Pydi SP, Singh N, Upadhyaya J, Bhullar RP, Chelikani P (2014). The third intracellular loop plays a critical role in bitter taste receptor activation. *Biochim Biophys Acta* **1838**(1 Pt B)**:** 231-236.

Raffan E, Dennis RJ, O'Donovan CJ, Becker JM, Scott RA, Smith SP*, et al.* (2016). A Deletion in the Canine POMC Gene Is Associated with Weight and Appetite in Obesity-Prone Labrador Retriever Dogs. *Cell Metab* **23**(5)**:** 893-900.

Rannikko A, Pakarinen P, Manna PR, Beau I, Misrahi M, Aittomaki K*, et al.* (2002). Functional characterization of the human FSH receptor with an inactivating Ala189Val mutation. *Mol Hum Reprod* **8**(4)**:** 311-317.

Rasmussen SG, Choi HJ, Rosenbaum DM, Kobilka TS, Thian FS, Edwards PC*, et al.* (2007). Crystal structure of the human beta2 adrenergic G-protein-coupled receptor. *Nature* **450**(7168)**:** 383-387.

Robinson MD, McCarthy DJ, Smyth GK (2010a). edgeR: a Bioconductor package for differential expression analysis of digital gene expression data. *Bioinformatics* **26**(1)**:** 139-140.

Robinson MD, Oshlack A (2010b). A scaling normalization method for differential expression analysis of RNA-seq data. *Genome Biol* **11**(3)**:** R25.

Roland WS, van Buren L, Gruppen H, Driesse M, Gouka RJ, Smit G*, et al.* (2013). Bitter taste receptor activation by flavonoids and isoflavonoids: modeled structural requirements for activation of hTAS2R14 and hTAS2R39. *Journal of agricultural and food chemistry* **61**(44)**:** 10454-10466.

Roland WS, Vincken JP, Gouka RJ, van Buren L, Gruppen H, Smit G (2011). Soy isoflavones and other isoflavonoids activate the human bitter taste receptors hTAS2R14 and hTAS2R39. *Journal of agricultural and food chemistry* **59**(21)**:** 11764-11771.

Rondard P, Pin JP (2015). Dynamics and modulation of metabotropic glutamate receptors. *Current opinion in pharmacology* **20:** 95-101.

Rossler P (2000). G Protein betagamma Complexes in Circumvallate Taste Cells Involved in Bitter Transduction. *Chemical senses* **25**(4)**:** 413-421.

Rössler P, Kroner C, Freitag J, Noè J, Breer H (1998). Identification of a phospholipase C β subtype in rat taste cells. *European Journal of Cell Biology* **77**(3)**:** 253-261.

Roudnitzky N, Behrens M, Engel A, Kohl S, Thalmann S, Hubner S*, et al.* (2015). Receptor Polymorphism and Genomic Structure Interact to Shape Bitter Taste Perception. *PLoS genetics* **11**(9)**:** e1005530.

Rowland J (1987). Incidence of ethylene glycol intoxication in dogs and cats seen at Colorado State University Veterinary Teaching Hospital. *Vet Hum Toxicol.* **Feb;29(1):41-4.**

Ruiz CJ, Wray K, Delay E, Margolskee RF, Kinnamon SC (2003). Behavioral evidence for a role of alpha-gustducin in glutamate taste. *Chemical senses* **28**(7)**:** 573-579.

Sainz E, Cavenagh MM, Gutierrez J, Battey JF, Northup JK, Sullivan SL (2007). Functional characterization of human bitter taste receptors. *Biochem J* **403**(3)**:** 537-543.

Saito H, Kubota M, Roberts RW, Chi Q, Matsunami H (2004). RTP family members induce functional expression of mammalian odorant receptors. *Cell* **119**(5)**:** 679-691.

San Gabriel A, Uneyama H, Yoshie S, Torii K (2005). Cloning and characterization of a novel mGluR1 variant from vallate papillae that functions as a receptor for L-glutamate stimuli. *Chemical senses* **30 Suppl 1:** i25-26.

Sandal M, Behrens M, Brockhoff A, Musiani F, Giorgetti A, Carloni P*, et al.* (2015). Evidence for a Transient Additional Ligand Binding Site in the TAS2R46 Bitter Taste Receptor. *J Chem Theory Comput* **11**(9)**:** 4439-4449.

Sandall L (1896). "an Overdose of Strychnine.". *The Lancet* **147**(3787)**:** 887.

Sandau MM, Goodman JR, Thomas A, Rucker JB, Rawson NE (2015). A functional comparison of the domestic cat bitter receptors Tas2r38 and Tas2r43 with their human orthologs. *BMC Neurosci* **16:** 33.

Sanger F, Coulson AR (1975). A rapid method for determining sequences in DNA by primed synthesis with DNA polymerase. *Journal of Molecular Biology* **94**(3)**:** 441-448.

Sanger F, Nicklen S, Coulson AR (1977). DNA sequencing with chain-terminating inhibitors. *Proceedings of the National Academy of Sciences of the United States of America* **74**(12)**:** 5463-5467.

Schachter JB, Sromek SM, Nicholas RA, Harden TK (1997). HEK293 human embryonic kidney cells endogenously express the P2Y1 and P2Y2 receptors. *Neuropharmacology* **36**(9)**:** 1181-1187.

Schiffman SS, Gatlin LA, Frey AE, Heiman SA, Stagner WC, Cooper DC (1994). Taste perception of bitter compounds in young and elderly persons: Relation to lipophilicity of bitter compounds. *Neurobiology of Aging* **15**(6)**:** 743-750.

Schneider EH, Schnell D, Strasser A, Dove S, Seifert R (2010). Impact of the DRY motif and the missing "ionic lock" on constitutive activity and G-protein coupling of the human histamine H4 receptor. *J Pharmacol Exp Ther* **333**(2)**:** 382-392.

Schroeder A, Mueller O, Stocker S, Salowsky R, Leiber M, Gassmann M*, et al.* (2006). The RIN: an RNA integrity number for assigning integrity values to RNA measurements. *BMC Mol Biol* **7:** 3.

Sclafani A (2004). The sixth taste? *Appetite* **43**(1)**:** 1-3.

Semack A, Sandhu M, Malik RU, Vaidehi N, Sivaramakrishnan S (2016). Structural Elements in the Galphas and Galphaq C Termini That Mediate Selective G Protein-coupled Receptor (GPCR) Signaling. *The Journal of biological chemistry* **291**(34)**:** 17929-17940.

Shan L, Wu Q, Wang L, Zhang L, Wei F (2018). Lineage-specific evolution of bitter taste receptor genes in the giant and red pandas implies dietary adaptation. *Integr Zool* **13**(2)**:** 152-159.

Shang S, Wu X, Chen J, Zhang H, Zhong H, Wei Q*, et al.* (2017). The repertoire of bitter taste receptor genes in canids. *Amino Acids*.

Sharkey DJ, Scalice ER, Christy KG, Jr., Atwood SM, Daiss JL (1994). Antibodies as thermolabile switches: high temperature triggering for the polymerase chain reaction. *Biotechnology (N Y)* **12**(5)**:** 506-509.

Shearin AL, Ostrander EA (2010). Leading the way: canine models of genomics and disease. *Disease models & mechanisms* **3**(1-2)**:** 27-34.

Shen Y, Li R, Tian F, Chen Z, Lu N, Bai Y*, et al.* (2018). Impact of RNA integrity and blood sample storage conditions on the gene expression analysis. *Onco Targets Ther* **11:** 3573-3581.

Shi P, Zhang J (2006). Contrasting modes of evolution between vertebrate sweet/umami receptor genes and bitter receptor genes. *Molecular biology and evolution* **23**(2)**:** 292-300.

Shi P, Zhang J, Yang H, Zhang YP (2003). Adaptive diversification of bitter taste receptor genes in Mammalian evolution. *Molecular biology and evolution* **20**(5)**:** 805-814.

Simeone A, Acampora D, Mallamaci A, Stornaiuolo A, D'Apice MR, Nigro V*, et al.* (1993). A vertebrate gene related to orthodenticle contains a homeodomain of the bicoid class and demarcates anterior neuroectoderm in the gastrulating mouse embryo. *The EMBO Journal* **12**(7)**:** 2735-2747.

Singh N, Pydi SP, Upadhyaya J, Chelikani P (2011). Structural basis of activation of bitter taste receptor T2R1 and comparison with Class A G-protein-coupled receptors (GPCRs). *The Journal of biological chemistry* **286**(41)**:** 36032-36041.

Slack JP, McCluskey TS (2005). Chimeric alpha q-gustducin g-proteins. *EP1581555B1* **EP1581555B1:** 1-21.

Soares S, Kohl S, Thalmann S, Mateus N, Meyerhof W, De Freitas V (2013). Different phenolic compounds activate distinct human bitter taste receptors. *Journal of agricultural and food chemistry* **61**(7)**:** 1525-1533.

Soave O, Brand C (1991). Coprophagy in animals: a review. *The Cornell veterinarian* **81**(4)**:** 357-364.

Soranzo N, Bufe B, Sabeti PC, Wilson JF, Weale ME, Marguerie R*, et al.* (2005). Positive selection on a high-sensitivity allele of the human bitter-taste receptor TAS2R16. *Curr Biol* **15**(14)**:** 1257-1265.

Spielman AI, Pepino MY, Feldman R, Brand JG (2010). Technique to collect fungiform (taste) papillae from human tongue. *J Vis Exp*(42).

Stähler F, Riedel K, Demgensky S, Neumann K, Dunkel A, Täubert A*, et al.* (2008). A Role of the Epithelial Sodium Channel in Human Salt Taste Transduction? *Chemosensory Perception* **1**(1)**:** 78-90.

Stark R, Grzelak M, Hadfield J (2019). RNA sequencing: the teenage years. *Nature reviews. Genetics* **20**(11)**:** 631-656.

Stevens DR, Seifert R, Bufe B, Muller F, Kremmer E, Gauss R*, et al.* (2001). Hyperpolarization-activated channels HCN1 and HCN4 mediate responses to sour stimuli. *Nature* **413**(6856)**:** 631-635.

Stevens RC, Cherezov V, Katritch V, Abagyan R, Kuhn P, Rosen H*, et al.* (2013). The GPCR Network: a large-scale collaboration to determine human GPCR structure and function. *Nat Rev Drug Discov* **12**(1)**:** 25-34.

Stoddart LA, White CW, Nguyen K, Hill SJ, Pfleger KD (2016). Fluorescence- and bioluminescence-based approaches to study GPCR ligand binding. *British journal of pharmacology* **173**(20)**:** 3028-3037.

Stojanovic A, Hwa J (2002). Rhodopsin and Retinitis Pigmentosa: Shedding Light on Structure and Function. *Receptors and Channels* **8**(1)**:** 33-50.

Suku E, Fierro F, Giorgetti A, Alfonso-Prieto M, Carloni P (2017). Multi-scale simulations of membrane proteins: The case of bitter taste receptors. *Journal of Science: Advanced Materials and Devices* **2**(1)**:** 15-21.

Sukumaran SK, Lewandowski BC, Qin Y, Kotha R, Bachmanov AA, Margolskee RF (2017). Whole transcriptome profiling of taste bud cells. *Sci Rep* **7**(1)**:** 7595.

Swanson KS, Carter RA, Yount TP, Aretz J, Buff PR (2013). Nutritional sustainability of pet foods. *Advances in nutrition* **4**(2)**:** 141-150.

Syed AS, Korsching SI (2014). Positive Darwinian selection in the singularly large taste receptor gene family of an 'ancient' fish, Latimeria chalumnae. *BMC genomics* **15:** 650.

Tao YX (2006). Inactivating mutations of G protein-coupled receptors and diseases: structure-function insights and therapeutic implications. *Pharmacology & therapeutics* **111**(3)**:** 949-973.

Tao YX, Conn PM (2018). Pharmacoperones as Novel Therapeutics for Diverse Protein Conformational Diseases. *Physiol Rev* **98**(2)**:** 697-725.

Taruno A, Vingtdeux V, Ohmoto M, Ma Z, Dvoryanchikov G, Li A*, et al.* (2013). CALHM1 ion channel mediates purinergic neurotransmission of sweet, bitter and umami tastes. *Nature* **495**(7440)**:** 223-226.

Teng B, Wilson CE, Tu Y-H, Joshi NR, Kinnamon SC, Liman ER (2019). Cellular and Neural Responses to Sour Stimuli Require the Proton Channel Otop1. *Current Biology*.

Thalmann O, Shapiro B, Cui P, Schuenemann VJ, Sawyer SK, Greenfield DL*, et al.* (2013a). Complete mitochondrial genomes of ancient canids suggest a European origin of domestic dogs. *Science* **342**(6160)**:** 871-874.

Thalmann S, Behrens M, Meyerhof W (2013b). Major haplotypes of the human bitter taste receptor TAS2R41 encode functional receptors for chloramphenicol. *Biochemical and biophysical research communications* **435**(2)**:** 267-273.

Toledo SP, Brunner HG, Kraaij R, Post M, Dahia PL, Hayashida CY*, et al.* (1996). An inactivating mutation of the luteinizing hormone receptor causes amenorrhea in a 46,XX female. *The Journal of clinical endocrinology and metabolism* **81**(11)**:** 3850-3854.

Tomchik SM, Berg S, Kim JW, Chaudhari N, Roper SD (2007). Breadth of tuning and taste coding in mammalian taste buds. *The Journal of neuroscience : the official journal of the Society for Neuroscience* **27**(40)**:** 10840-10848.

Topin J, Bouysset C, Kim Y, Rhyu M, Fiorucci S, Golebiowski J (2020).

Trut L, Oskina I, Kharlamova A (2009). Animal evolution during domestication: the domesticated fox as a model. *Bioessays* **31**(3)**:** 349-360.

Tsutsui K, Otoh M, Sakurai K, Suzuki-Hashido N, Hayakawa T, Misaka T*, et al.* (2016). Variation in ligand responses of the bitter taste receptors TAS2R1 and TAS2R4 among New World monkeys. *BMC Evol Biol* **16**(1)**:** 208.

Tuckerman F (1890). On the gustatory organs of some of the mammalia. *Journal of Morphology* **4**(2)**:** 151-193.

Ueda T, Ugawa S, Yamamura H, Imaizumi Y, Shimada S (2003). Functional interaction between T2R taste receptors and G-protein α subunits expressed in taste receptor cells. *The Journal of neuroscience* **23**(19)**:** 7376-7380.

Uhlen M, Fagerberg L, Hallstrom BM, Lindskog C, Oksvold P, Mardinoglu A*, et al.* (2015). Proteomics. Tissue-based map of the human proteome. *Science* **347**(6220)**:** 1260419.

Unger VM, Schertler GF (1995). Low resolution structure of bovine rhodopsin determined by electron cryo-microscopy. *Biophysical Journal* **68**(5)**:** 1776-1786.

Upadhyaya J, Pydi SP, Singh N, Aluko RE, Chelikani P (2010). Bitter taste receptor T2R1 is activated by dipeptides and tripeptides. *Biochemical and biophysical research communications* **398**(2)**:** 331-335.

Weis WI, Kobilka BK (2018). The Molecular Basis of G Protein-Coupled Receptor Activation. *Annual review of biochemistry* **87:** 897-919.

Wheeler DL, Barrett T, Benson DA, Bryant SH, Canese K, Chetvernin V*, et al.* (2007). Database resources of the National Center for Biotechnology Information. *Nucleic Acids Res* **35**(Database issue)**:** D5-12.

Widayati KA, Yan X, Suzuki-Hashido N, Itoigawa A, Purba LHPS, Fahri F*, et al.* (2019). Functional divergence of the bitter receptor TAS2R38 in Sulawesi macaques. *Ecology and Evolution*.

Wiener A, Shudler M, Levit A, Niv MY (2012). BitterDB: a database of bitter compounds. *Nucleic Acids Res* **40**(Database issue)**:** D413-419.

Winnig M, Bufe B, Kratochwil NA, Slack JP, Meyerhof W (2007). The binding site for neohesperidin dihydrochalcone at the human sweet taste receptor. *BMC structural biology* **7:** 66.

Witt M, Reutter K (2015). Anatomy of the Tongue and Taste Buds. 637-664.

Wolfe BL, Trejo J (2007). Clathrin-dependent mechanisms of G protein-coupled receptor endocytosis. *Traffic* **8**(5)**:** 462-470.

Wong GT, Gannon KS, Margolskee RF (1996). Transduction of bitter and sweet taste by gustducin. *Nature* **381**(6585)**:** 796-800.

Wooding S (2006). Phenylthiocarbamide: a 75-year adventure in genetics and natural selection. *Genetics* **172**(4)**:** 2015-2023.

Wooding S, Bufe B, Grassi C, Howard MT, Stone AC, Vazquez M*, et al.* (2006). Independent evolution of bitter-taste sensitivity in humans and chimpanzees. *Nature* **440**(7086)**:** 930-934.

Wooding S, Gunn H, Ramos P, Thalmann S, Xing C, Meyerhof W (2010). Genetics and bitter taste responses to goitrin, a plant toxin found in vegetables. *Chemical senses* **35**(8)**:** 685-692.

Wooding S, Kim UK, Bamshad MJ, Larsen J, Jorde LB, Drayna D (2004). Natural selection and molecular evolution in PTC, a bitter-taste receptor gene. *Am J Hum Genet* **74**(4)**:** 637-646.

Xu X, Kaindl J, Clark MJ, Hubner H, Hirata K, Sunahara RK*, et al.* (2020). Binding pathway determines norepinephrine selectivity for the human beta1AR over beta2AR. *Cell research*.

Yan W, Sunavala G, Rosenzweig S, Dasso M, Brand JG, Spielman AI (2001). Bitter taste transduced by PLC-β 2-dependent rise in IP 3 and α-gustducin-dependent fall in cyclic nucleotides. *American Journal of Physiology-Cell Physiology* **280**(4)**:** C742-C751.

Yang N, Lei Z, Li X, Zhao J, Liu T, Ning N*, et al.* (2014). Chloroquine stimulates Cl- secretion by Ca2+ activated Cl- channels in rat ileum. *PloS one* **9**(1)**:** e87627.

Yasumatsu K, Manabe T, Yoshida R, Iwatsuki K, Uneyama H, Takahashi I*, et al.* (2015). Involvement of multiple taste receptors in umami taste: analysis of gustatory nerve responses in metabotropic glutamate receptor 4 knockout mice. *J Physiol* **593**(4)**:** 1021-1034.

Yasumatsu K, Ohkuri T, Yoshida R, Iwata S, Margolskee RF, Ninomiya Y (2020). Sodium-glucose cotransporter 1 as a sugar taste sensor in mouse tongue. *Acta Physiol (Oxf)***:** e13529.

Ye J, Coulouris G, Zaretskaya I, Cutcutache I, Rozen S, Madden TL (2012). Primer-BLAST: a tool to design target-specific primers for polymerase chain reaction. *BMC Bioinformatics* **13:** 134.

Yoshida R, Horio N, Murata Y, Yasumatsu K, Shigemura N, Ninomiya Y (2009). NaCl responsive taste cells in the mouse fungiform taste buds. *Neuroscience* **159**(2)**:** 795-803.

Zhang GH, Zhang HY, Wang XF, Zhan YH, Deng SP, Qin YM (2009). The relationship between fungiform papillae density and detection threshold for sucrose in the young males. *Chemical senses* **34**(1)**:** 93-99.

Zhang J, Jin H, Zhang W, Ding C, O'Keeffe S, Ye M*, et al.* (2019). Sour Sensing from the Tongue to the Brain. *Cell*.

Zhang Y, Hoon MA, Chandrashekar J, Mueller KL, Cook B, Wu D*, et al.* (2003). Coding of Sweet, Bitter, and Umami Tastes. *Cell* **112**(3)**:** 293-301.

Zhao H, Li J, Zhang J (2015). Molecular evidence for the loss of three basic tastes in penguins. *Curr Biol* **25**(4)**:** R141-142.

Zhu YY, Machleder EM, Chenchik A, Li R, Siebert PD (2001). Reverse transcriptase template switching: a SMART approach for full-length cDNA library construction. *Biotechniques* **30**(4)**:** 892-897.

Zhuang H, Matsunami H (2007). Synergism of accessory factors in functional expression of mammalian odorant receptors. *The Journal of biological chemistry* **282**(20)**:** 15284-15293.

Zhuang H, Matsunami H (2008). Evaluating cell-surface expression and measuring activation of mammalian odorant receptors in heterologous cells. *Nat Protoc* **3**(9)**:** 1402-1413.

Zuniga JR, Davis SH, Englehardt RA, Miller IJ, Schiffrman SS, Phillips C (1993). Taste performance on the anterior human tongue varles with fungiform taste bud density. *Chemical senses* **18**(5)**:** 449-460.